

CONTRACTOR FINAL REPORT

TEST #

127

NRD 12
R Eppinger

NHTSA Technical Report
DOT-HS-805 889

127 AFS

SIDE IMPACT SLED & PADDING DEVELOPMENT

February 1981



Prepared by
U.S. DEPARTMENT OF TRANSPORTATION
National Highway Traffic Safety Administration
Safety Research Laboratory
Washington, D.C. 20590

This document is disseminated under the sponsorship of the Department of Transportation in the interest of information exchange. The United States Government assumes no liability for its contents or use thereof.

Technical Report Documentation Page

1 Report No DOT-HS-805-889		2 Government Accession No		3 Recipient's Catalog No	
4 Title and Subtitle SIDE IMPACT SLED & PADDING DEVELOPMENT				5 Report Date February 1981	
				6 Performing Organization Code NRD-52	
7 Author(s) Michael W. Monk, Lisa K. Sullivan				8 Performing Organization Report No SRL-17	
				10 Work Unit No. (TRAIS)	
9 Performing Organization Name and Address Safety Research Laboratory National Highway Traffic Safety Administration P.O. Box 37 East Liberty, Ohio 43319				11 Contract or Grant No	
				13 Type of Report and Period Covered FINAL June 1979 - February 1981	
12 Sponsoring Agency Name and Address U.S. Department of Transportation National Highway Traffic Safety Administration Washington, D.C. 20590				14 Sponsoring Agency Code	
				15 Supplementary Notes	
16 Abstract <p>A study was conducted to devise and fabricate a HYG E sled buck which could be used to simulate oblique side impact collisions. Once completed the buck was demonstrated by simulating the occupant and side door interactions of two separate laboratory car-to-car impacts. The degree of success of these two simulations is discussed.</p> <p>Following the simulations, the sled buck was used to select padding materials which appeared promising for occupant protection in side impact collisions. The selection criteria and results are presented.</p>					
17 Key Words Side Impact HYGE Sled Simulations Padding			18 Distribution Statement Document is available to the U.S. public through the National Technical Information Service, Springfield, Virginia 22161		
19 Security Classif (of this report) Unclassified		20 Security Classif (of this page) Unclassified		21. No. of Pages 295	22 Price

TABLE OF CONTENTS

	<u>Page</u>
LIST OF TABLES	iii
LIST OF FIGURES	iv
LIST OF APPENDICES	vi
1.0 BACKGROUND	1
2.0 OBJECTIVES	1
3.0 PROJECT ELEMENT SUMMARY	2
4.0 PROJECT ELEMENT OVERVIEW	3
5.0 SIDE IMPACT SLED & PADDING DEVELOPMENT	9
5.1 RICSAC and Budd Cars and Data	9
5.2 New Dummy Computer Software	10
5.3 Prototype Side Impact Dummy	13
5.4 Analysis of RICSAC and Budd Test Data	14
5.5 Interior Door Crush Devices	26
5.6 Interior Door Crush Tests	37
5.7 Analysis of Dynamic Science Test	42
5.8 Definition of Interior Door Stiffness	49
5.9 Design and Fabrication of Sled Buck	52
5.10 HYGE Sled Simulation of Budd Test #11	56
5.11 HYGE Sled Simulation of Dynamic Science Test #8330-2	66
5.12 Review of Prior Padding Studies	77
5.13 Padding Component Tests	82
5.14 Padding Evaluation: HYGE Sled Tests	98
5.15 Tarrriere Drop Tests	104
6.0 CONCLUSIONS AND RECOMMENDATIONS	105
REFERENCES	107
APPENDICES	

LIST OF FIGURES

<u>Figure No.</u>		<u>Page</u>
1	Project Element Flow Chart	4
2	HSRI Data Processing Flow Chart	11
3	Budd Test No. 12 - Upper Door Acceleration	15
4	Crash Tests/Rigid Wall Comparison	17
5	Calspan Baseline Crash Test #5	18
6	Vehicle Accelerometer Placement Schematic	21
7	Force Direction By Film Analysis	22
8	RICSAC #2 Force Direction	23
9	Budd #7 Force Direction	23
10	Budd #4 Force Direction - Front	24
11	Budd #4 Force Direction - Rear	24
12	Budd #6 Force Direction - Front	25
13	Budd #6 Force Direction - Rear	25
14	Car-to-Car Impact Layout	27
15	Car-to-Car Holding Fixture	28
16	Upper Torso Body Form Drawing	30
17	Pelvis Body Form Drawing	31
18	Whole Body Form Drawing	32
19	Upper Torso Body Form - Photo	33
20	Pelvis Body Form - Photo	34
21	Whole Body Form - Photo	35
22	Static Crush Test Fixture	36
23	Dynamic Crush Test #7	39
24	Static Crush Test #17	39
25	DySci No. 8330-2 Upper Door/Thorax Acceleration	43
26	DySci No. 8330-2 Lower Door/Pelvis Acceleration	43
27	DySci No. 8330-2 Upper Door Velocity	44
28	DySci No. 8330-2 Lower Door Velocity	45
29	DySci No. 8330-2 Upper Door/Thorax Velocity	47

Appendices

- A - Interior Door Crush Test Results
- B - Interior Door Stiffness Trend Curves
- C - Discussion of Roller Tape Mechanisms
- D - Occupant/Door Comparisons from Budd #11 Simulation
- E - Body Form Responses from Dynamic Science
Test #8330-2 Simulation
- F - Force vs. Deflection Curves for Phase I Padding
Component Tests
- G - Force vs. Deflection Curves for Phase II Padding
Component Tests
- H - Body Form Responses from HYGE Sled Padding
Evaluation Tests
- I - Drawing & Description of Fluid Impact Accelerator
- J - Tarriere Drop Tests

ACKNOWLEDGMENTS

The views and findings of this report are those of the authors and do not necessarily reflect the policy of the NHTSA. The authors are grateful to the following for technical support in the fabrication of special hardware and the successful conduct of experiments:

Herb Litteral
Ed McGhee
Harvey Witter
Harry Mullins
Bob Esser

The authors wish to thank Mr. Richard M. Morgan for assistance in formulating the project objectives and Mr. Lee Stucki for coordination of the project with other NHTSA research efforts.

Also, special thanks go to Reva Blaker and Susan Weiser for the preparation of the manuscript.

1.0 Background:

Lateral accidents are responsible for an estimated 30 percent of motor vehicle occupant fatalities each year. Within the past 5 years, efforts have greatly increased toward understanding the side impact environment and interpreting side impact data. These studies form the basis for current efforts to provide improvements to the level of crash survivability of passenger cars.

Accident data gathered under the National Crash Severity Study indicates head and thoracic injuries caused by side rails and door contact are a major problem in side impact collisions.

As part of a larger effort to mitigate the deaths and injuries caused by door contact, the Agency initiated the search for producible, energy-absorbing interiors for installation into structurally modified vehicles. This report reviews the approach used in selecting a side impact cushioning material.

2.0 Objectives:

There were two main objectives to the overall project. The first objective was to design and fabricate a sled buck which accurately reproduced the environment of a modified Rabbit in a side impact collision. The test mode in which the Rabbit was evaluated was a 60 degree impact, with the impacting vehicle traveling at 30 mph and the Rabbit traveling at 15 mph. The second objective was to develop a suitable padding material for installation into the modified Rabbit structure.

4.0 Project Element Overview

The following is a brief description of each project element. A flow chart, providing easy reference to the sequence of the project elements, is shown in Figure 1.

Project Element 1 - Order and Receive RICSAC Cars

Project Element 2 - Order and Receive RICSAC Data

Project Element 3 - Order and Receive Budd Cars

The purpose of obtaining the RICSAC^{(1)*} and Budd⁽²⁾ cars and data was to aid the SRL in defining the side impact environment for HYGE sled testing.

Project Element 4 - New Dummy Computer Software

The purpose of installing the new dummy computer software was to provide a means of estimating the injury level to a human thorax based on the responses of the dummy during impact. The software provided as output the Abbreviated Injury Scale (AIS) based on four methods: B parameter of the left upper rib signal, Q parameter of the left upper rib signal, average power of the upper spine and average power of the lower spine.

Project Element 5 - Acquire New Side Impact Dummy

A new side impact dummy was developed for the Agency under Contract No. DOT-HS-4-00921. The production version of the dummy was desired for this project. However, only the prototype version was available for use during component level and HYGE sled testing.

*Numbers in parenthesis refer to references at the end of the text.

Project Element 6 - RICSAC and Budd Crash Test Analysis

The RICSAC⁽¹⁾ and Budd⁽²⁾ Crash Test data were analyzed to determine the necessary parameters for HYGE sled simulation of the side impact environment. The Budd tests utilized Part 572 dummies in a stationary VW Rabbit. The RICSAC tests utilized Part 572 dummies in two-car-moving side impacts.

Project Element 7 - Interior Door Crush Device

Two interior door crush test devices were devised to statically and dynamically impact the door interiors of previously impacted VW Rabbits obtained during project elements 1 and 3. The torso, pelvic and whole body regions of a 50th percentile male were represented by three rigid body forms fabricated for the interior door stiffness tests.

Project Element 8 - Interior Door Crush Tests

The purpose of the interior door crush tests was to determine the force-deflection properties of the Rabbit door interior. The stiffness that was desired was that experienced by the occupant when the door was pushed into him by an impacting vehicle. General trends in vehicle stiffness were investigated using several different VW Rabbits.

Project Element 9 - Dynamic Science 214 Mode Crash Test Analysis

Dynamic Science Test No. 8330-2⁽³⁾ was performed under conditions being considered as candidate in the upgrade of the FMVSS No. 214 test procedure (60 degree side impact, both cars moving), using the prototype side impact dummy. The test data were analyzed to determine test conditions (dummy positioning, peak accelerations, etc) for HYGE sled simulation prior to conducting padding evaluation tests on the HYGE sled.

Project Element 14 - Review of Prior Padding Studies

A limited literature search was conducted which identified only four studies directly related to the project. The four studies dealt with padding used in interior vehicle applications and were reviewed.

Project Element 15 - Component Level Padding Tests

The main purposes of the component level padding tests were (1) to identify padding materials viable for thorax protection and (2) to eliminate performing extensive HYGE sled tests using undesirable padding materials.

The padding materials were evaluated for their desirability as a thoracic restraint by three main criteria: (1) padding force-deflection properties, (2) body form AIS calculated from the B(LUR) parameter and (3) peak spinal acceleration.

The component level tests were performed in two phases. Phase I consisted of impacting the prototype SID thorax laterally into 5 inch padding samples at 15 mph. A number of the less desirable padding materials were eliminated during Phase I testing. Phase II consisted of impacting 3 inch padding samples at 15 mph. Those padding materials which passed the criteria during Phase II testing were then evaluated on the HYGE sled buck.

Project Element 16 - HYGE Sled Padding Evaluation Tests

Those padding materials which had been deemed viable candidates for thoracic protection, based on component level test results, were tested on the HYGE sled. The series of 17 tests, using the prototype SID, was performed to evaluate the protective capability of the padding materials. The door contacted the dummy at an impact velocity of 23.5 mph.

5.0 Side Impact Sled and Padding Development

5.1 RICSAC and Budd Cars and Data

The tentative test mode for the FMVSS No. 214 upgrade is as follows:

Bullet (striking) car velocity - 30 mph

Target (struck) car velocity - 15 mph

Impact angle - 60 degrees into vehicle compartment

Two previous side impact collision studies were chosen to be analyzed. The first study, "Research Input for Computer Simulation of Automobile Collisions"⁽¹⁾ (RICSAC), developed a library of experimental data to validate computer reconstruction techniques. In the study, four 60 degree side impact collisions with both cars moving were conducted. The second study, "Lightweight Subcompact Vehicle Side Structure Program"⁽²⁾, (the Budd Study), included a number of 60 degree side impact collisions with only the bullet vehicle moving and the target vehicle stationary.

The films and hard copy reports from the four RICSAC tests and selected Budd tests were ordered and received. The two Rabbits, two Pintos and three Malibus crashed in the RICSAC Study were shipped from Buffalo, New York to the VRTC in East Liberty, Ohio. The purpose of obtaining the seven vehicles was to (1) help in the definition of the side impact environment (Section 5.4) and (2) provide vehicle interiors for interior stiffness testing (Section 5.6). Five Rabbits, crashed during the Budd Study, were also shipped from Buffalo to the VRTC. The purpose of obtaining these vehicles was (1) for use in the interior crush tests (Section 5.6) and (2) to help in designing the energy-absorbing material to fit the structurally modified Rabbits.

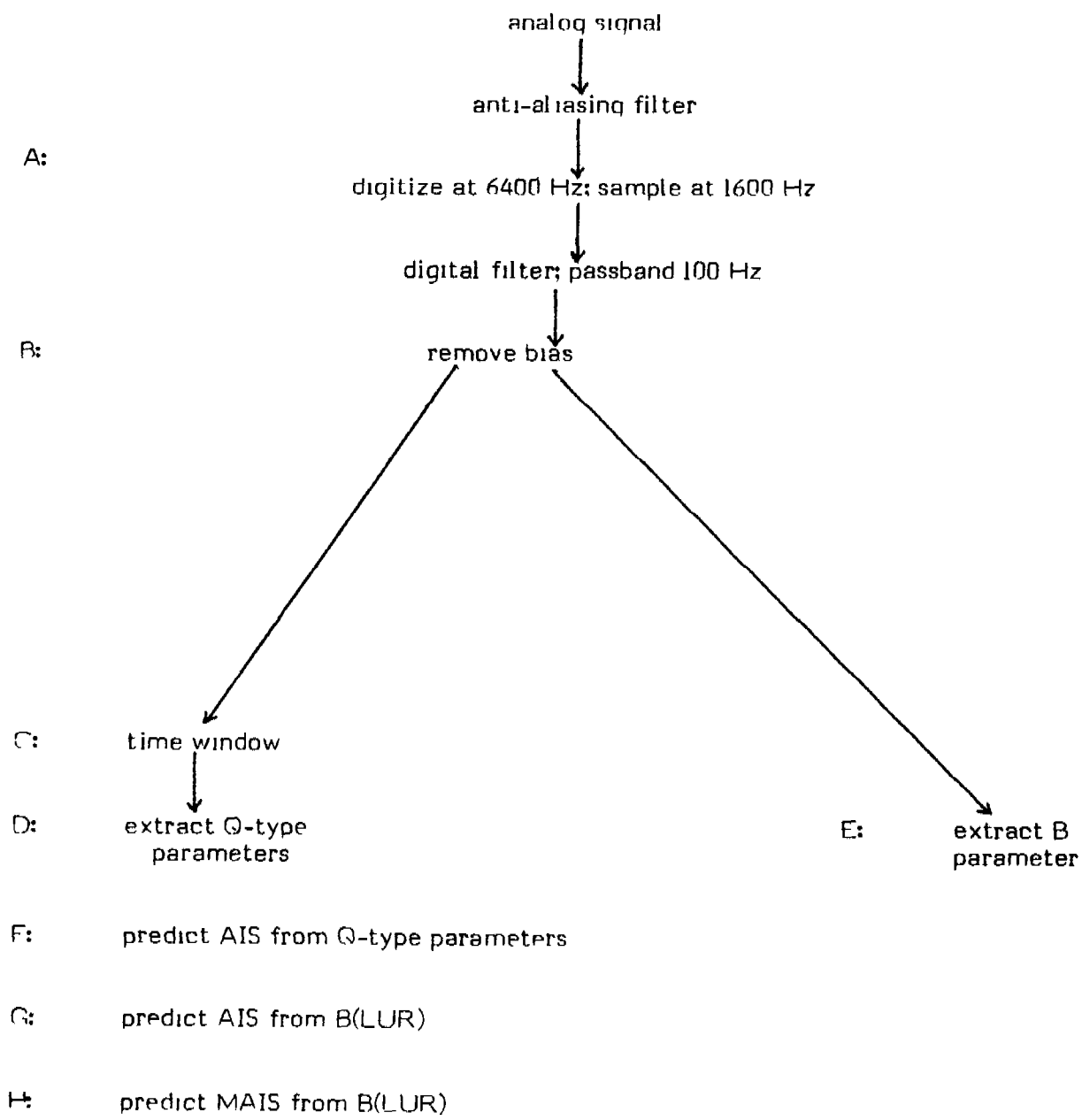
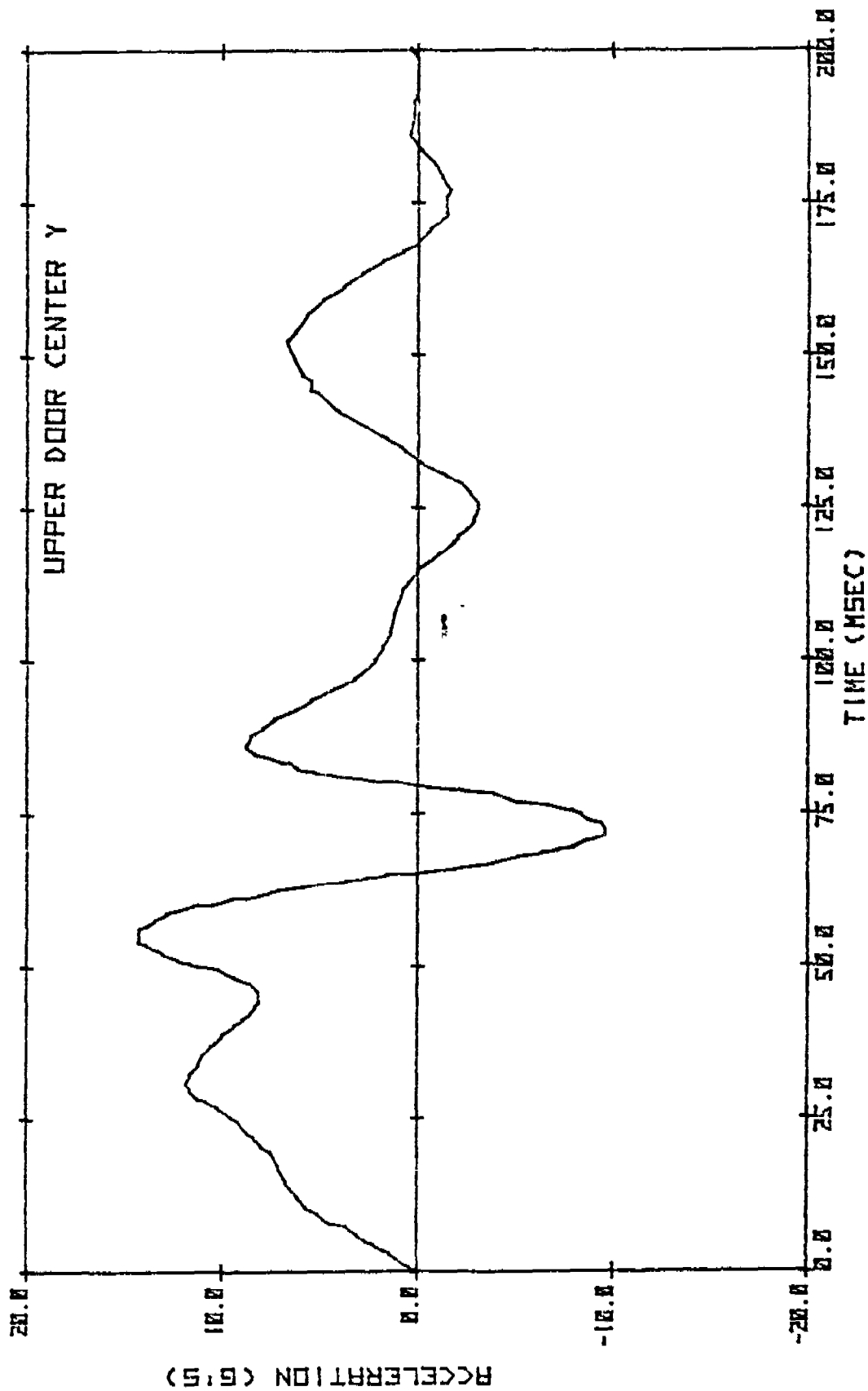


FIGURE 2
HSRI Data Processing Flow Chart

5.3 Prototype Side Impact Dummy

Under Contract No. DOT-HS-4-00921 with the HSRI, the Side Impact Dummy (SID) was developed for the Agency. Only a prototype version of the dummy was completed at the time of this project's initiation. This prototype was used in the second portion of the HYGE sled tests and a prototype thorax was used throughout the mini sled component tests.

During the final stages of this project, a production version of the SID became available and was utilized for HYGE sled simulations.

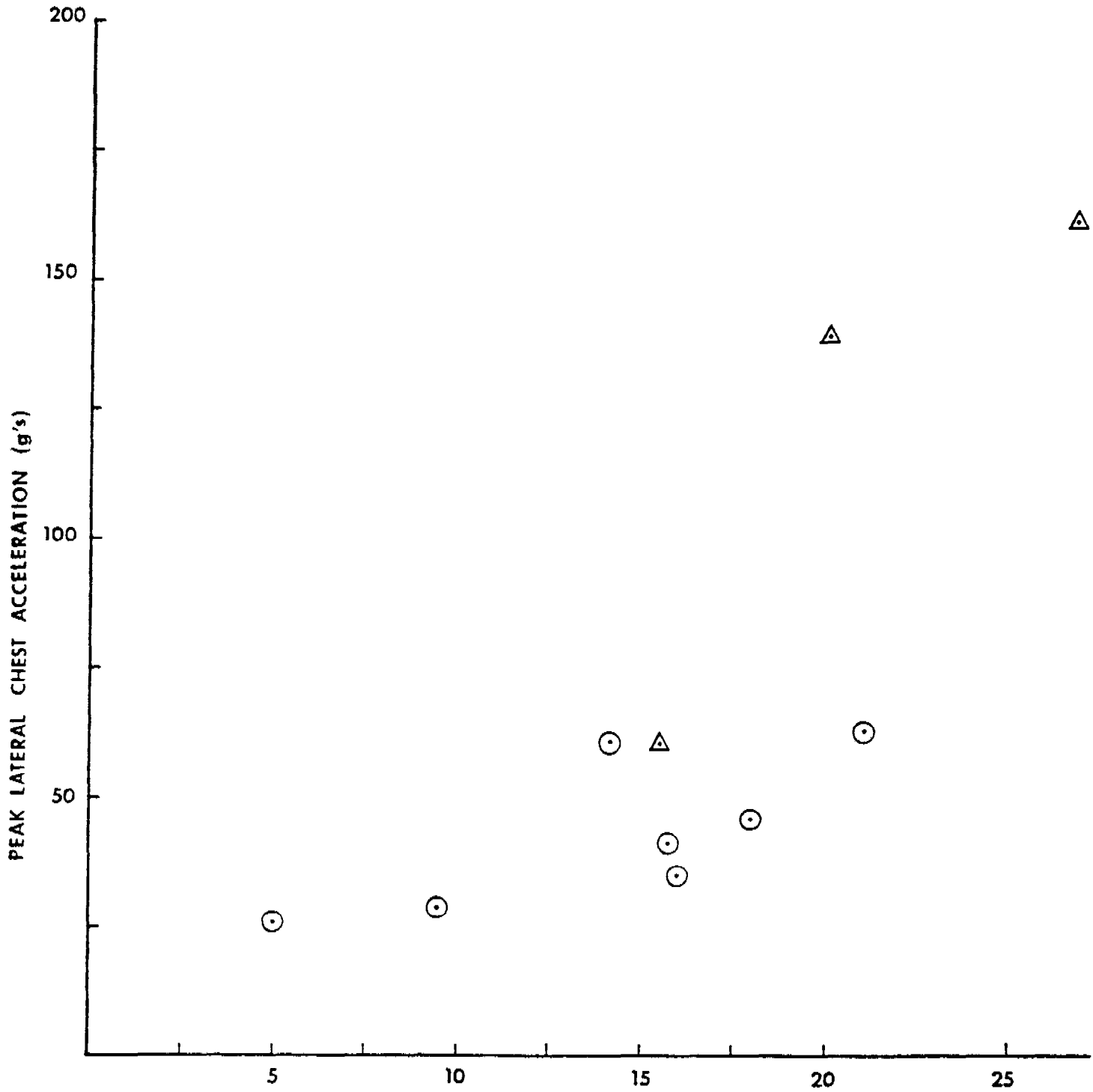


BUDD MOD RABBIT TEST #12 15HZ

FIGURE 3
Budd Test No. 12 - Upper Door Acceleration

○ CALSPAN CRASH TESTS WITH DOOR PANEL (1975)

△ HSRI SLED TESTS WITH RIGID WALL (1976)



LATERAL VELOCITY OF PANEL AT TIME OF 572 DUMMY CONTACT (mph)

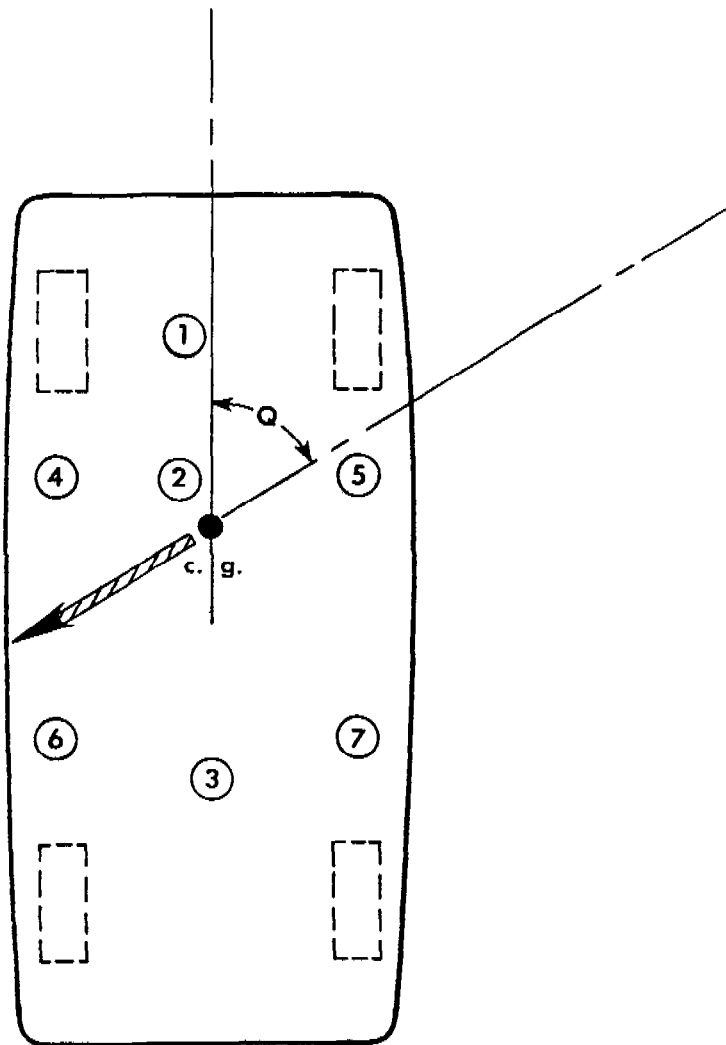
FIGURE 4 - Crash Tests/Rigid Wall Comparison

the crash the dummy impacts the struck door interior.

The door velocity does not continue to rise [after the 24 msec point] and approach the bumper velocity. The dummy impacts the door; and force builds up to interrupt the velocity rise. While it is believed that the primary source of this force is the dummy impacting the door, other structural effects (such as the seat structure) may be contributing. The door was within 2 mph of V_f at the instant of dummy contact.

At 35 msec, the occupant's chest experiences it's maximum lateral acceleration of about 46 G [3 msec duration]. Assuming that the 50th percentile's upper body has an effective weight of 80 pounds, the dummy would be producing a decelerating force on the door of about 3700 pounds at this time.

At 40 msec the dummy and the door reach a common velocity of about 12 mph. By computing the area between the occupant and door velocity curves between 24 and 40 msec we can determine the extent of door padding penetration and dummy chest compliance. This calculation yields a prediction of 3 inches. The vehicle which is being tested has very little padding [less than one inch]. Therefore, it is likely that the upper door structure [the window sill area] is functioning essentially like padding, attenuating chest lateral G-levels by deforming under the inertial force of the dummy upper body. That is, the dummy may be making beneficial use of the full upper door depth to substitute for the padding that is not there. Note that at about 50 msec the interior door velocity again increases, indicating that the interior door has now bottomed out (stiffness increases) against the striking vehicle.



1. FIREWALL ACCELEROMETER
2. DRIVE TUNNEL ACCELEROMETER
3. REAR DECK ACCELEROMETER
4. LEFT FRONT COMPARTMENT ACCELEROMETER
5. RIGHT FRONT COMPARTMENT ACCELEROMETER
6. LEFT REAR COMPARTMENT ACCELEROMETER
7. RIGHT REAR COMPARTMENT ACCELEROMETER

FIGURE 6

VEHICLE ACCELEROMETER PLACEMENT SCHEMATIC

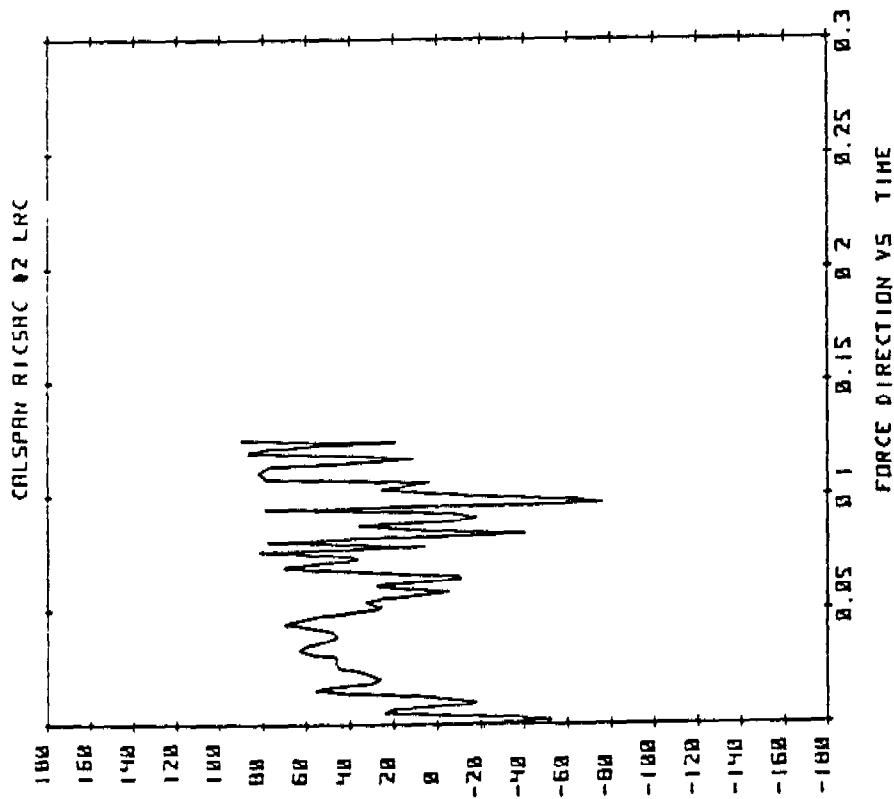


FIGURE 8
RICSAC #2 Force Direction

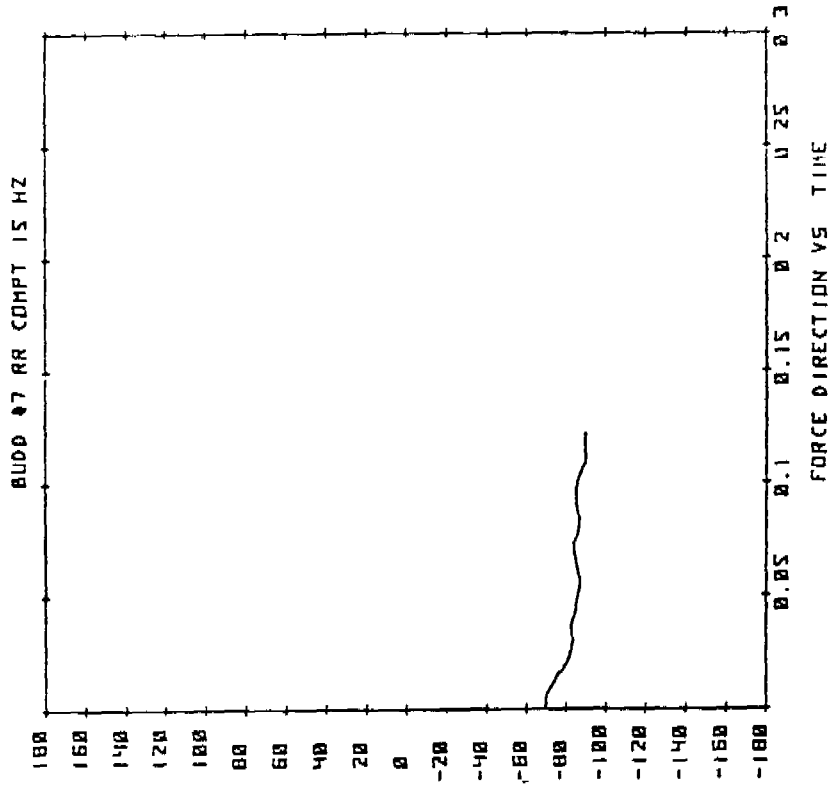


FIGURE 9
Budd #7 Force Direction - Rear

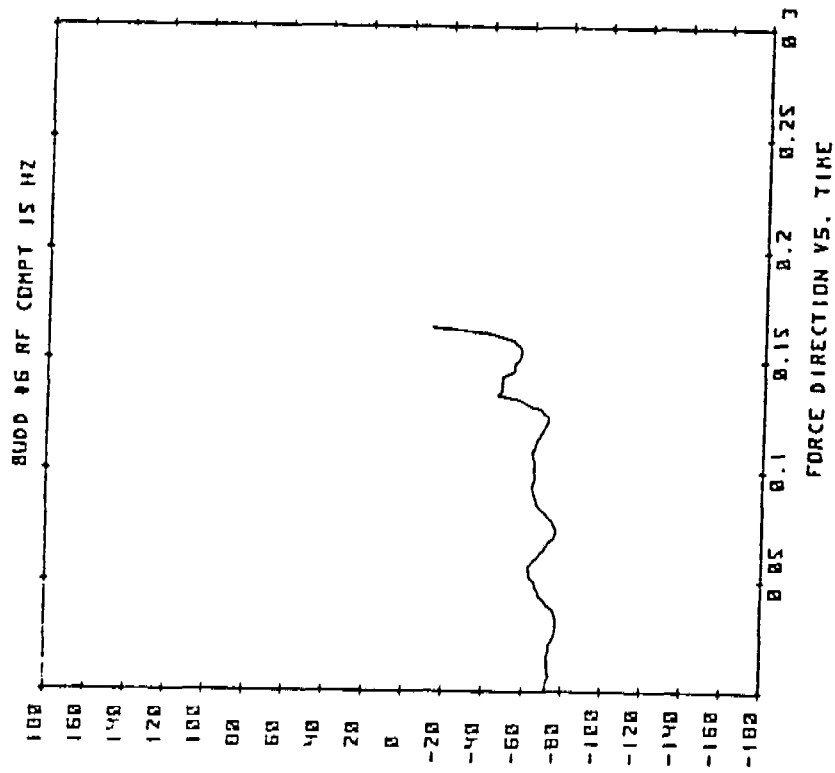


FIGURE I2

Budd #6 Force Direction - Front

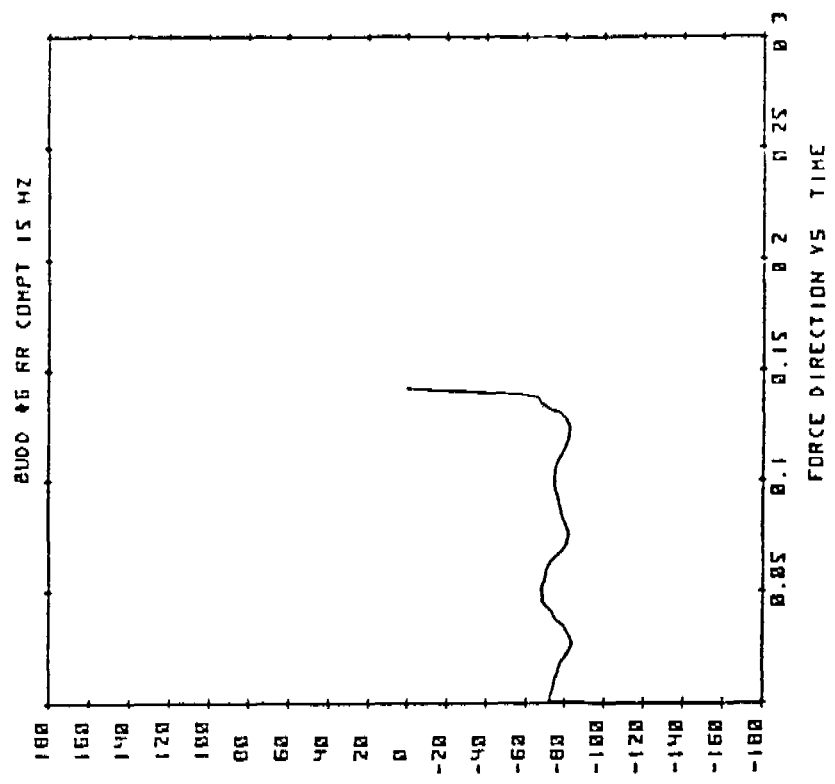


FIGURE I3

Budd #6 Force Direction - Rear

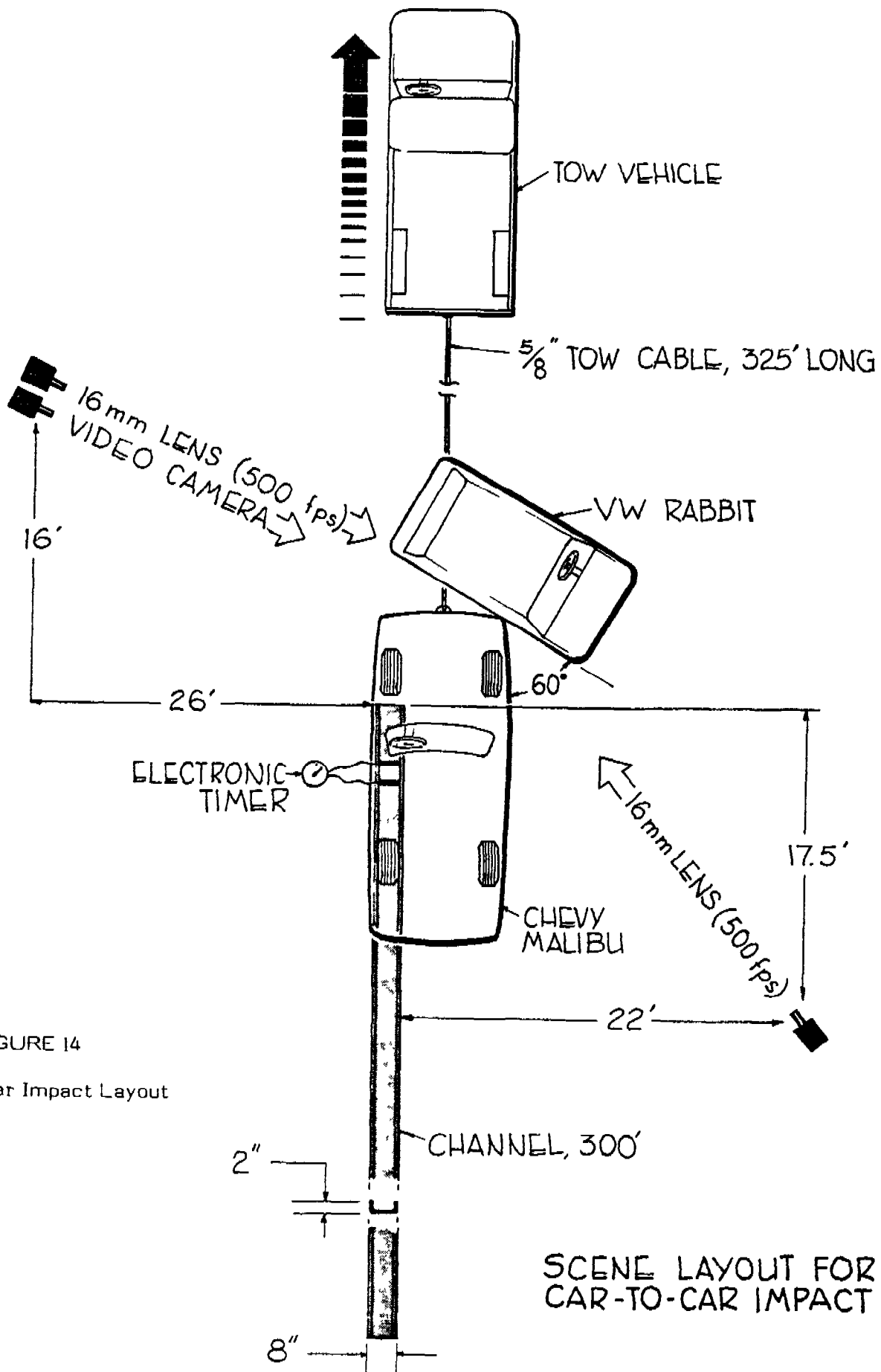
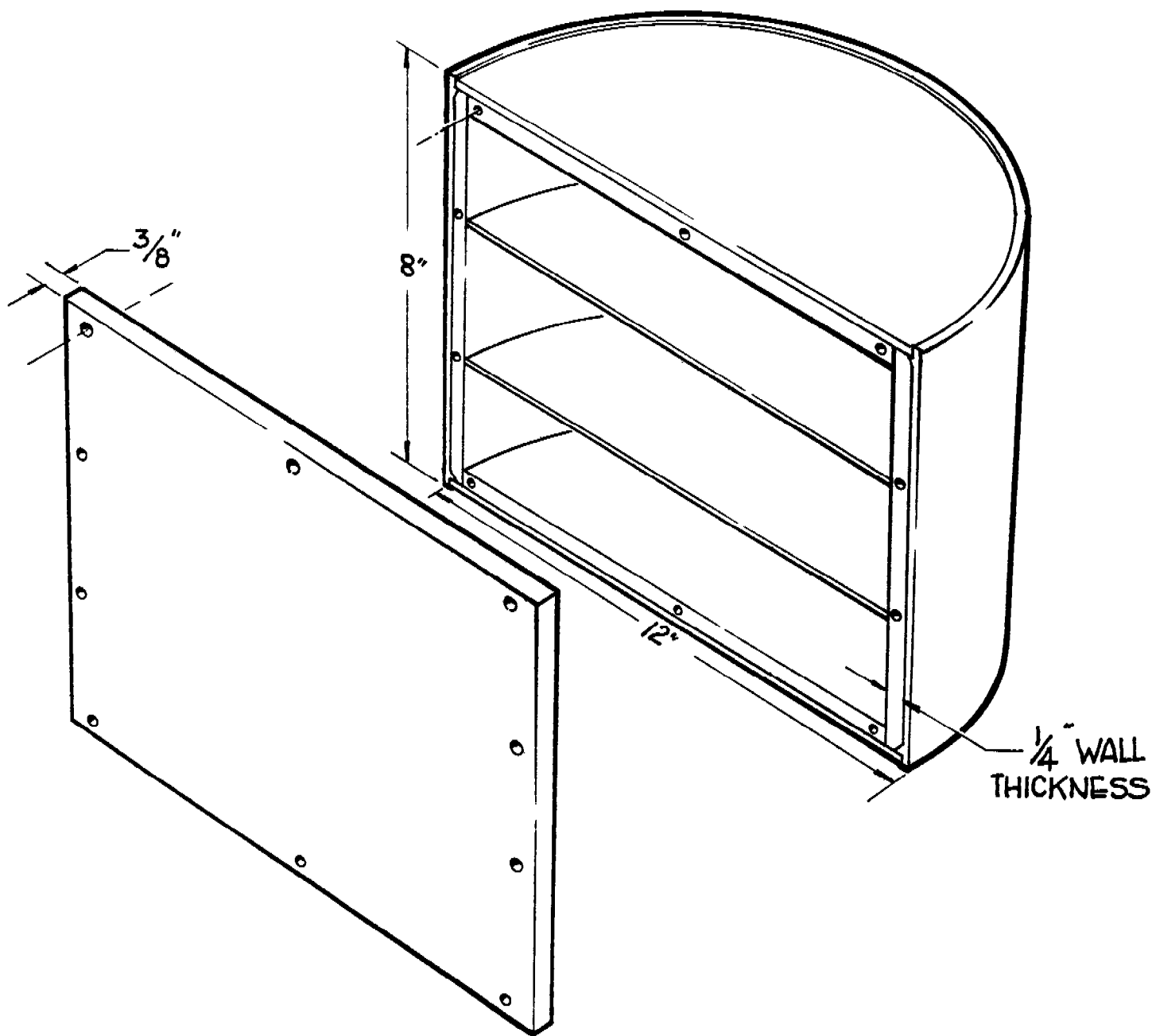


FIGURE 14
 Car-to-Car Impact Layout

The interior stiffness tests were performed using a rigid body form which represented the approximate surface area of a 50th percentile male. Three body forms were fabricated; an upper body form representing the torso area, a lower body form to represent the pelvic region, and a whole body form to represent the combined torso and pelvic areas. Figures 16 through 18 contain drawings of the body forms and photos are shown in Figures 19 through 21.

The static interior stiffness tests were performed by mounting the body forms on a static crush test fixture (Figure 22). The fixture consisted of a frame, a 10-ton hydraulic hand jack, and a 10,000 pound load cell. The frame was designed to be attached to a forklift. The fixture was designed to measure forces over a static deflection of around 2.0".

The dynamic crush tests were performed with the pedestrian impact device⁽⁷⁾, utilizing the same body forms. The impact velocities were around 20 mph. The acceleration data was used to compute force and the displacement potentiometer gave the corresponding displacement.



FORM No. 2

FIGURE 17
Pelvis Body Form

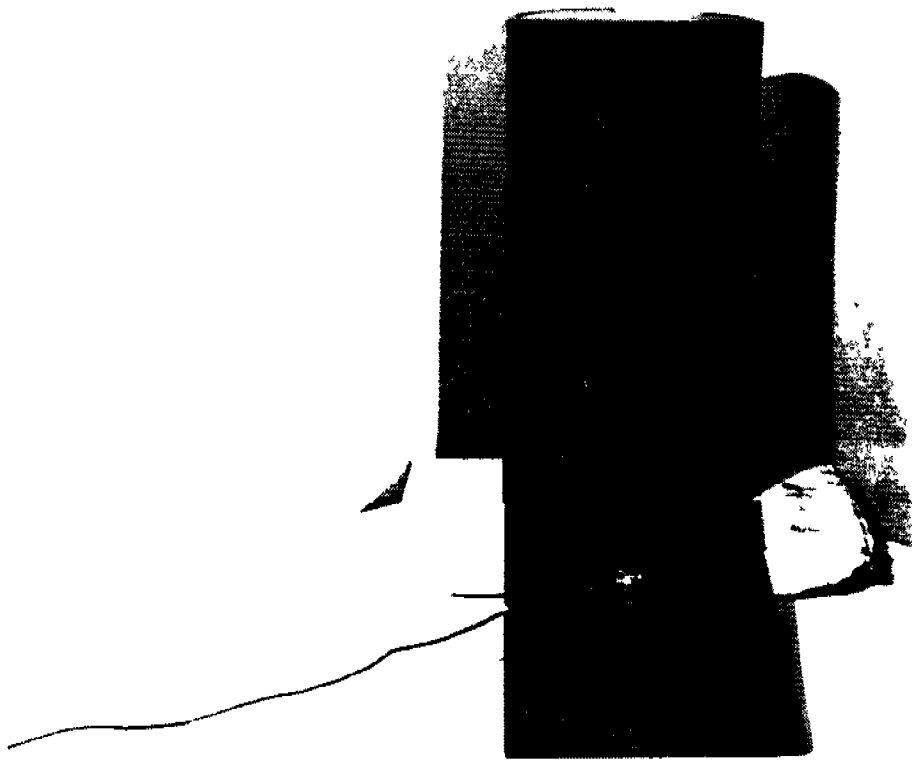


FIGURE 19
Upper Torso Body Form

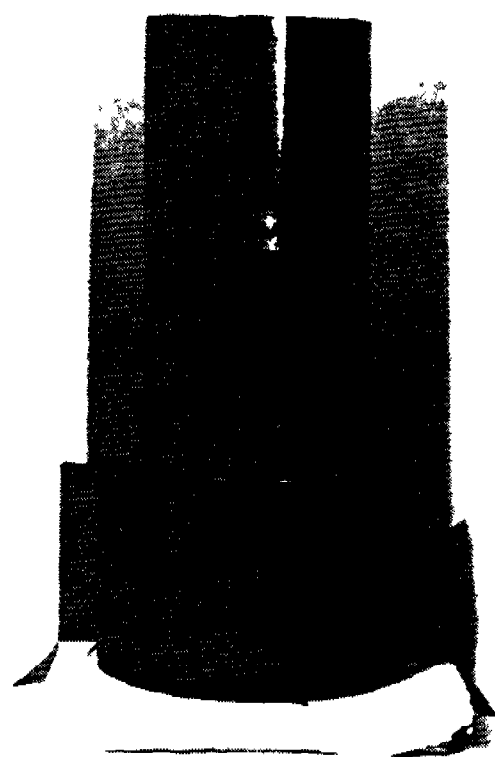


FIGURE 21
Whole Body Form

5.6 Interior Door Crush Tests

The purpose of the interior door crush tests was to determine the force-deflection properties of the Rabbit door interior.

Interior crush tests were conducted during October 1979. Table I is the test matrix. Tests No. 2 through No. 9 were performed using the pedestrian impact device to dynamically impact the door interior with the rigid body forms. Most of the vehicles had been previously impacted from the outside and the door was deformed into the compartment. The amount of this intrusion was noted with each test. Tests No. 4, No. 5 and No. 10 used the whole body form at 20 mph. All other tests were conducted with an upper and a lower body form separately, i.e., two tests on each door. Therefore, tests No. 2 & No. 3, No. 6 & No. 7 and No. 8 & No. 9 were pairs of impacts on the same doors with the separate body forms. The body forms' acceleration data and the displacement data were reduced to force-deflection curves using the Hewlett-Packard 9830 Calculator. Figure 23 is a photograph of the post test setup of test No. 7, which was a lower body form into the lower door area with the impacting car engaged near the D.O.R. point.

Tests No. 1 and No. 11 through No. 15 were car-to-car crash tests at 60 degrees. A Chevrolet Malibu was towed into the undeformed sides of the VW Rabbits at various impact speeds. The purpose of the crash tests was to pre-crush the doors of the Rabbits prior to conducting the static interior crush tests. Speeds of 10, 15 and 20 mph were arbitrarily chosen to provide 3 typical levels of penetration. This enabled the stiffness of the inner panel to be correlated with the amount of crush of the door caused by the impacting car. Some impacts were at the door opening reference point and some were at the occupant hip point as noted.

Tests No. 16 through No. 25 were static crush tests performed with the static crush fixture. Again, the tests were conducted using the three body forms and engaging the impacting car at one of the two points. Figure 24 is a photo of

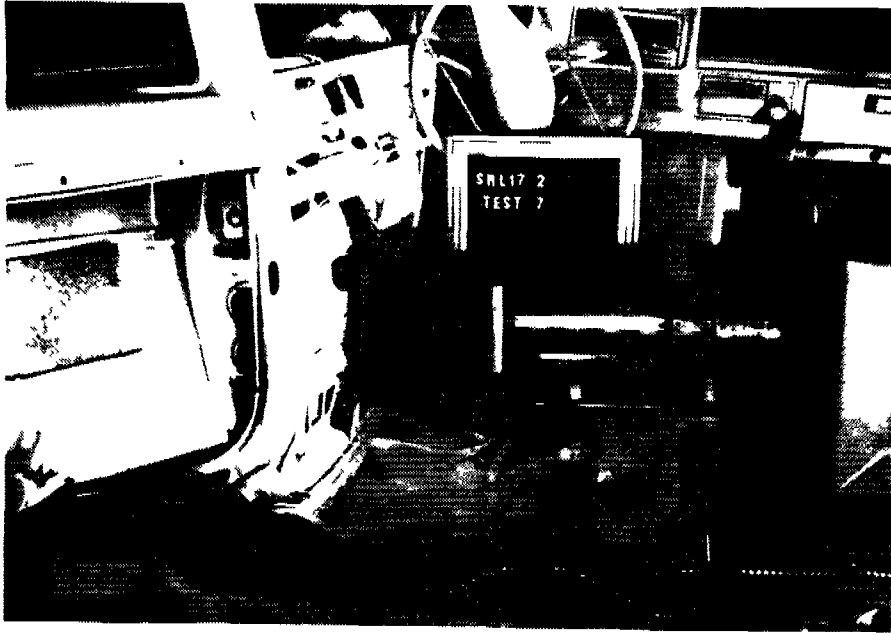


FIGURE 23
Dynamic Crush Test #7

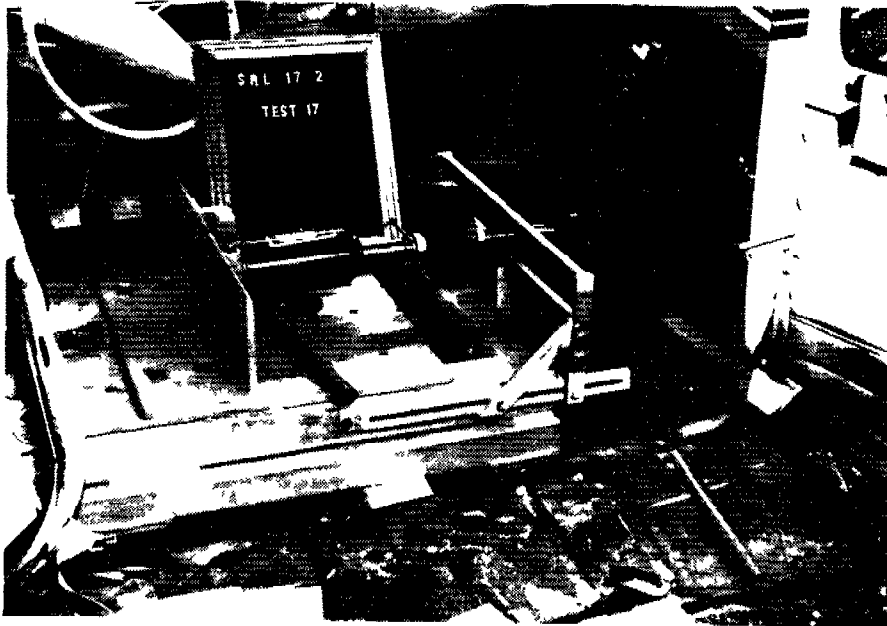


FIGURE 24
Static Crush Test #17

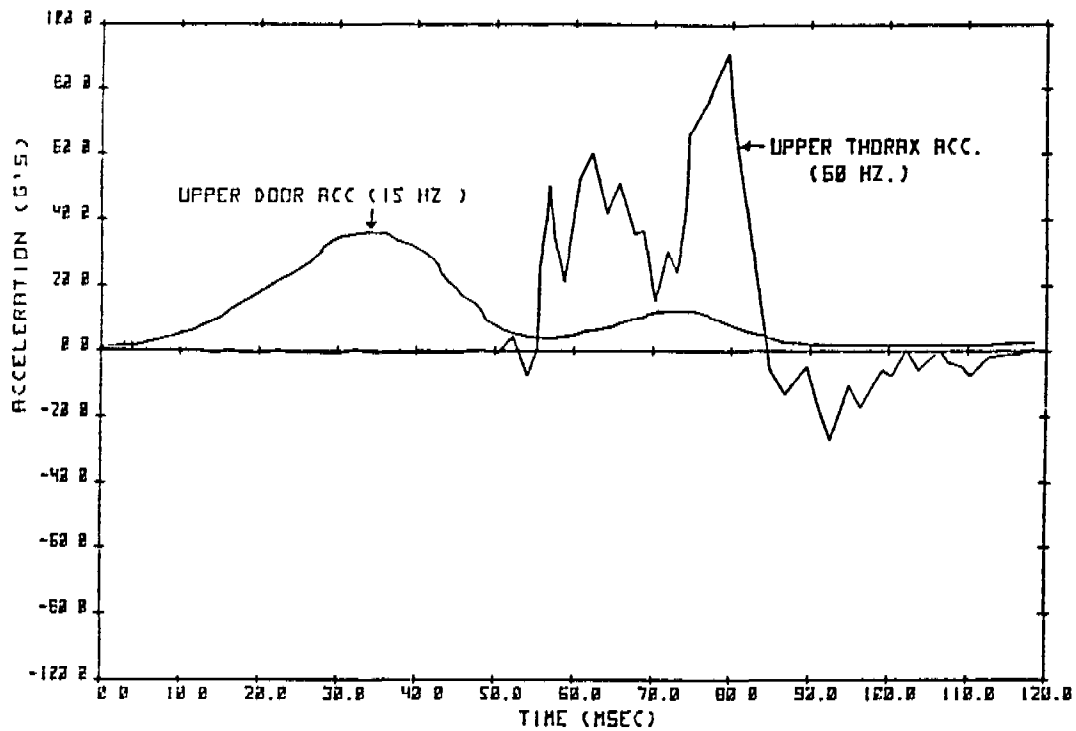
Three symbols were used in Appendix B to designate the type of door used. The type of door and its corresponding symbol are as follows:

- Baseline door
- Revised lightweight door
- Revised middleweight door

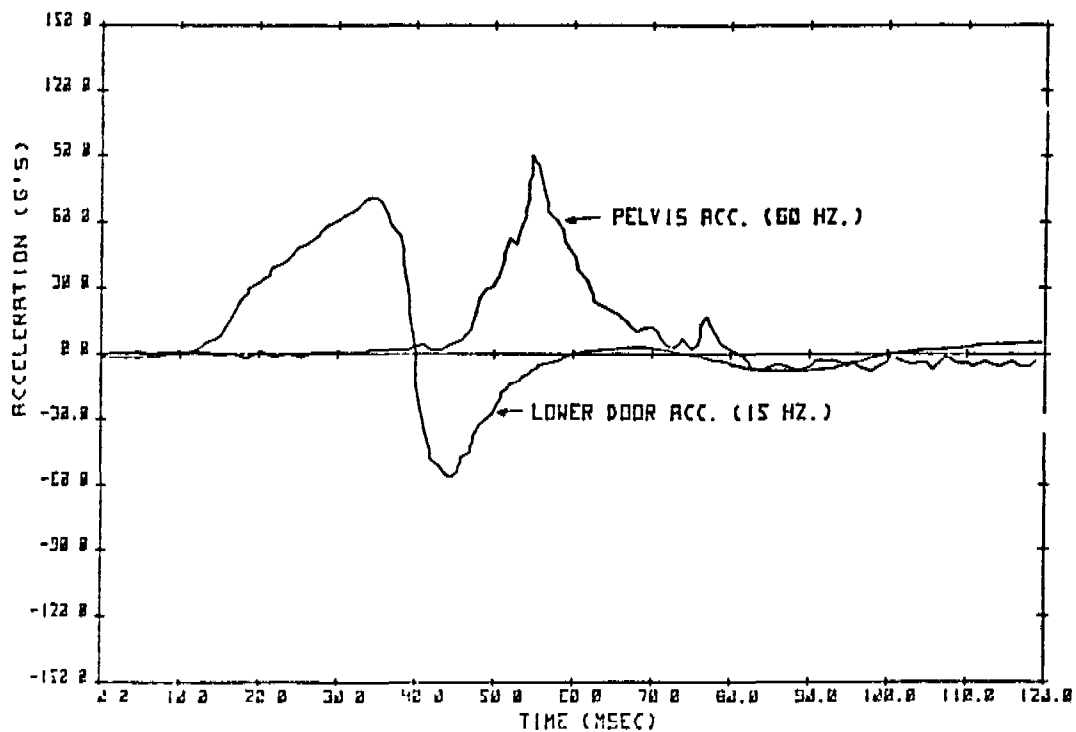
On each graph, the symbols designate specific points of data used in analysis. On certain graphs, a "?" appears. This is to signify our doubts about the validity of the data and to refer the reader to the preceding paragraph.

The majority of test results exhibited the door properties that were believed to be present: larger forces with larger vehicle penetration, and larger forces on the lower body form than on the upper body form under the same test conditions.

The results showed that the lower door interior is much stiffer than the upper door during the collision. Lower door interior stiffness was seen to increase with increased penetration of the striking vehicle. The upper door sheet metal was established to be a relatively yielding surface for an occupant to interact with. Trends regarding variations in interior door stiffness due to the structural modifications or to the impact point are not felt to be conclusive.



TEST NO 8330-2 60 DEG. IMPACT
 FIGURE 25 - Upper Door/Thorax Acceleration



TEST NO 8330-2 60 DEG IMPACT
 FIGURE 26 - Lower Door/Pelvis Acceleration

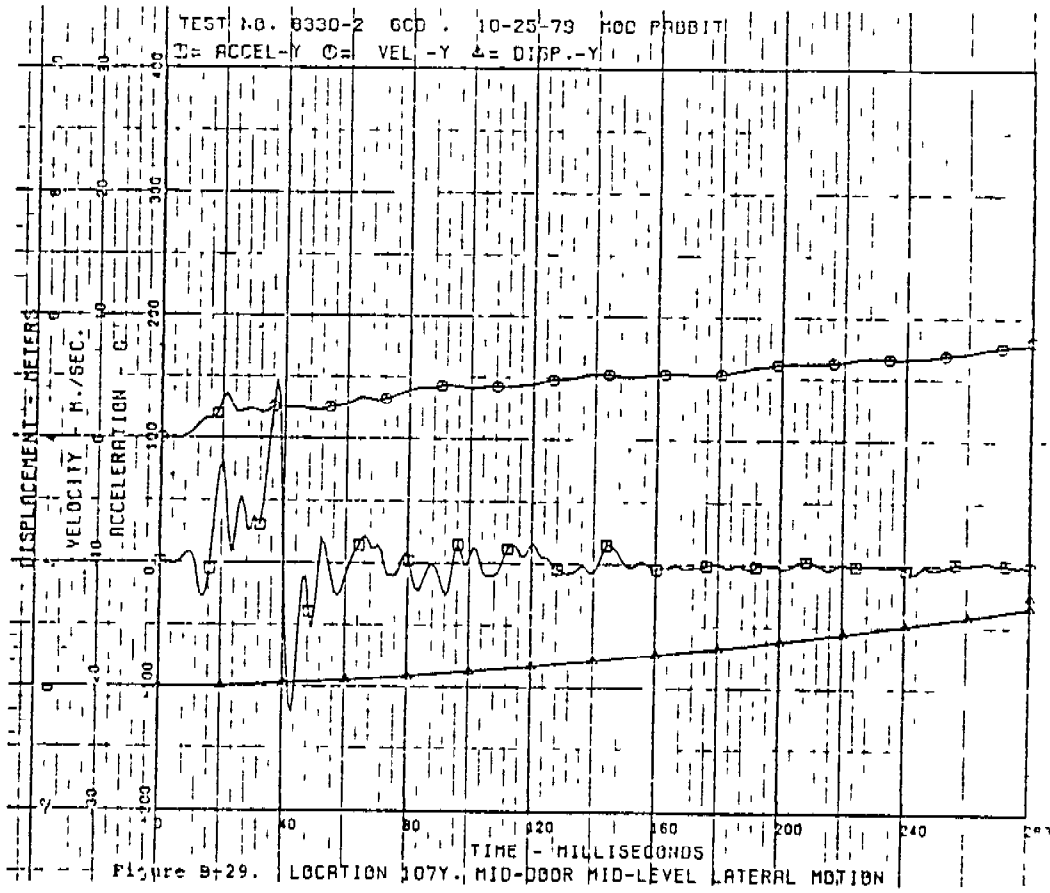
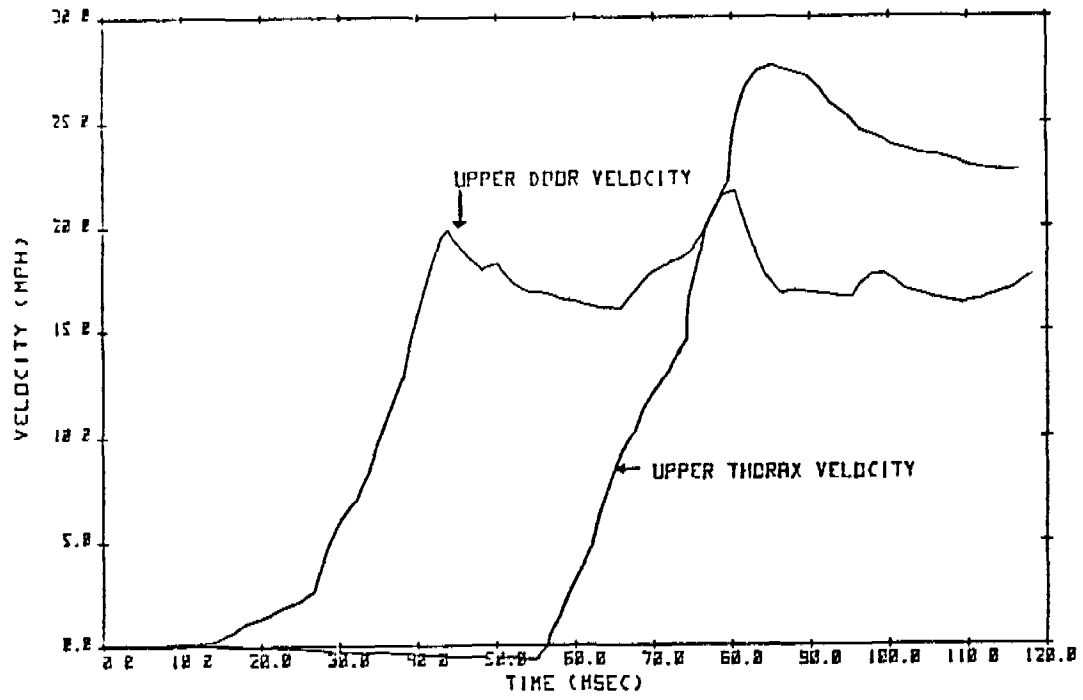


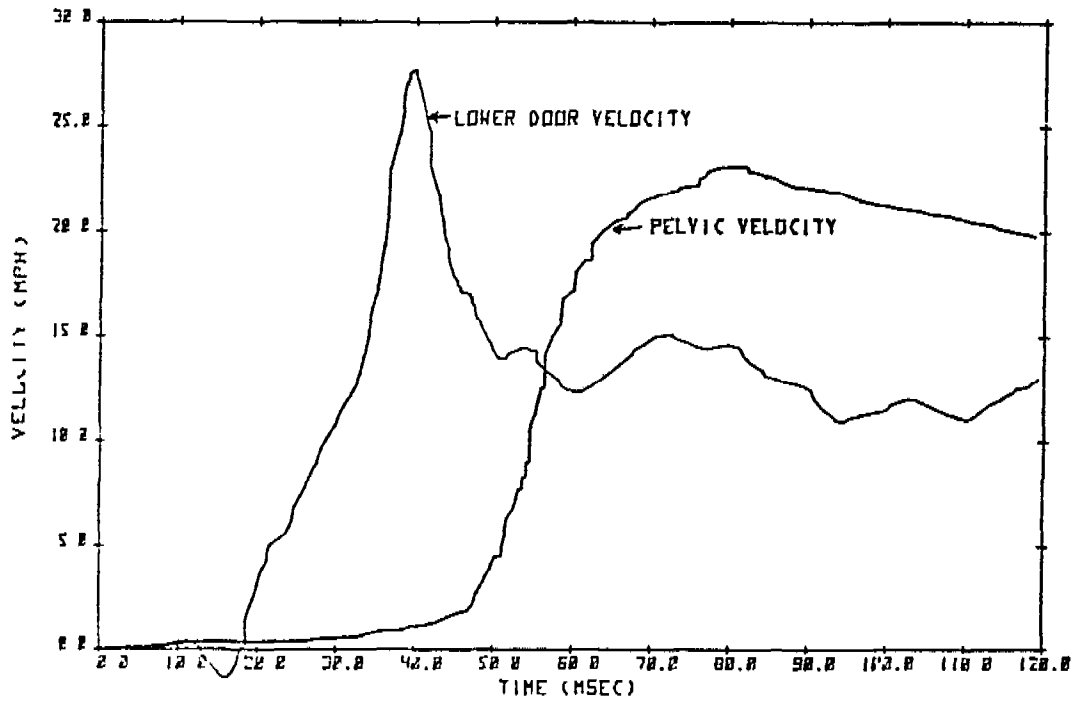
FIGURE 28

DySci No. 8330-2 Lower Door Velocity



TEST NO. 8330-2 60 DEG. IMPACT

FIGURE 29 - Upper Door/Thorax Velocity



TEST NO. 8330-2 60 DEG. IMPACT

FIGURE 30 - Lower Door/Pelvis Velocity

5.8 Definition of Interior Door Stiffness

As mentioned in the previous section, the sled buck was to be demonstrated by reproducing two separate laboratory collisions. The first was to be of a stationary struck VW Rabbit with a Part 572 dummy in the front seat. The second was described in Section 5.7. Budd test No. II⁽²⁾ was selected as the first because the revised middleweight door modification was tested and because the data appeared consistent. The stiffness of the interior door was to be determined from the information gathered in Section 5.6.

It was found from looking at the Budd data that the impacting vehicle intruded 12.4 inches into the compartment. The Part 572 dummy contacted the door at 50 msec into the event and the peak dummy-door interaction occurred at 60 msec. At 75 msec, the far side dummy contacted the near side dummy, preventing further analysis. The impacting car, at 60 msec, approached the seated position (hip point) of the dummy and intruded to near the maximum amount.

Figure 32 shows the force vs. deflection that was derived for the upper door panel on the HYGE sled and Figure 33 shows the lower door panel properties. Figures 32 and 33 reflect static properties of the door. Both static and dynamic force-vs-deflection data were derived for the VW interiors. It was judged to be more reliable to match the static properties of the door panels on the HYGE sled to the static properties of the actual vehicle, since static measurements were more easily made. It was understood that these were only starting points which could be adjusted during HYGE testing.

STATIC CRUSH PROPERTIES

TEST 21
LOWER BODY FORM
13.5 IN. CRUSH AT
THE HIP POINT
BASELINE DOOR

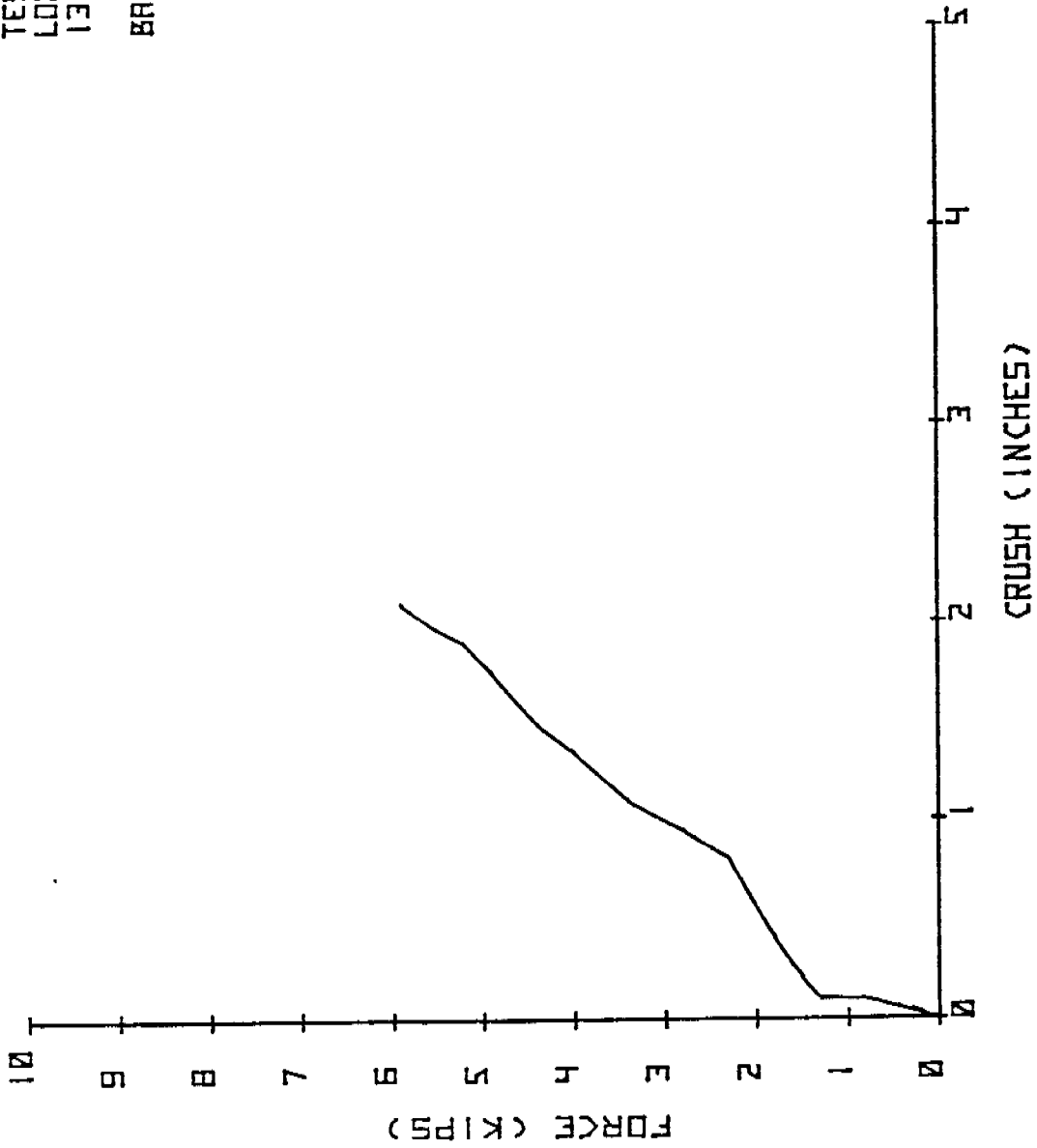


FIGURE 33

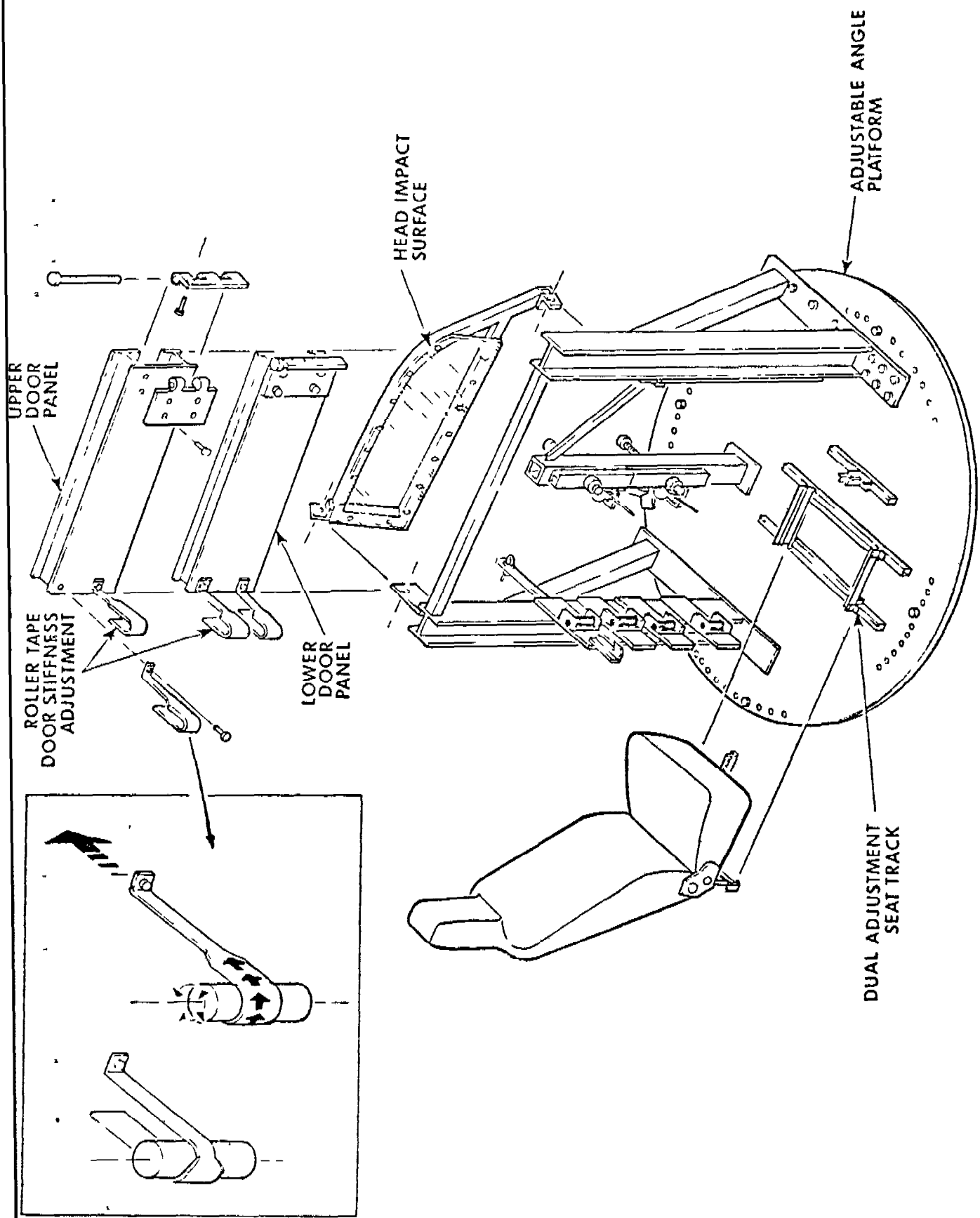
Static Crush Test No. 21

The roller tape mechanisms provided achievement of separate force levels for each panel. A roof rail was positioned above the door panels. A left-front seat was positioned on the buck, with the seat track adjustable in the X and Y directions. The seat back was reinforced to the buck frame to prevent lateral motion of the seat.

The sled buck platform was designed to be adjustable to any desired angle. For our purpose, the buck was angled 15 degrees off of pure lateral to approximate the force direction of the 60 degree impact. The sled buck was instrumented to measure accelerations in the X, Y and Z directions. Accelerometers were mounted on each contact panel to measure its lateral acceleration. Potentiometers were also mounted behind each panel to measure the panel's relative displacement. Three high speed camera mounts were positioned on the buck in the following manner: on the front of the buck, outboard to the left, and directly overhead of the dummy.

Toward the end of the padding component testing, a sheet of Lexan was angled outboard from the door panels to simulate the impacting car's hood, which the dummy's head contacted during the Dynamic Science test⁽³⁾.

Figure 34 is an assembled view of the sled buck. An exploded view is shown in Figure 35.

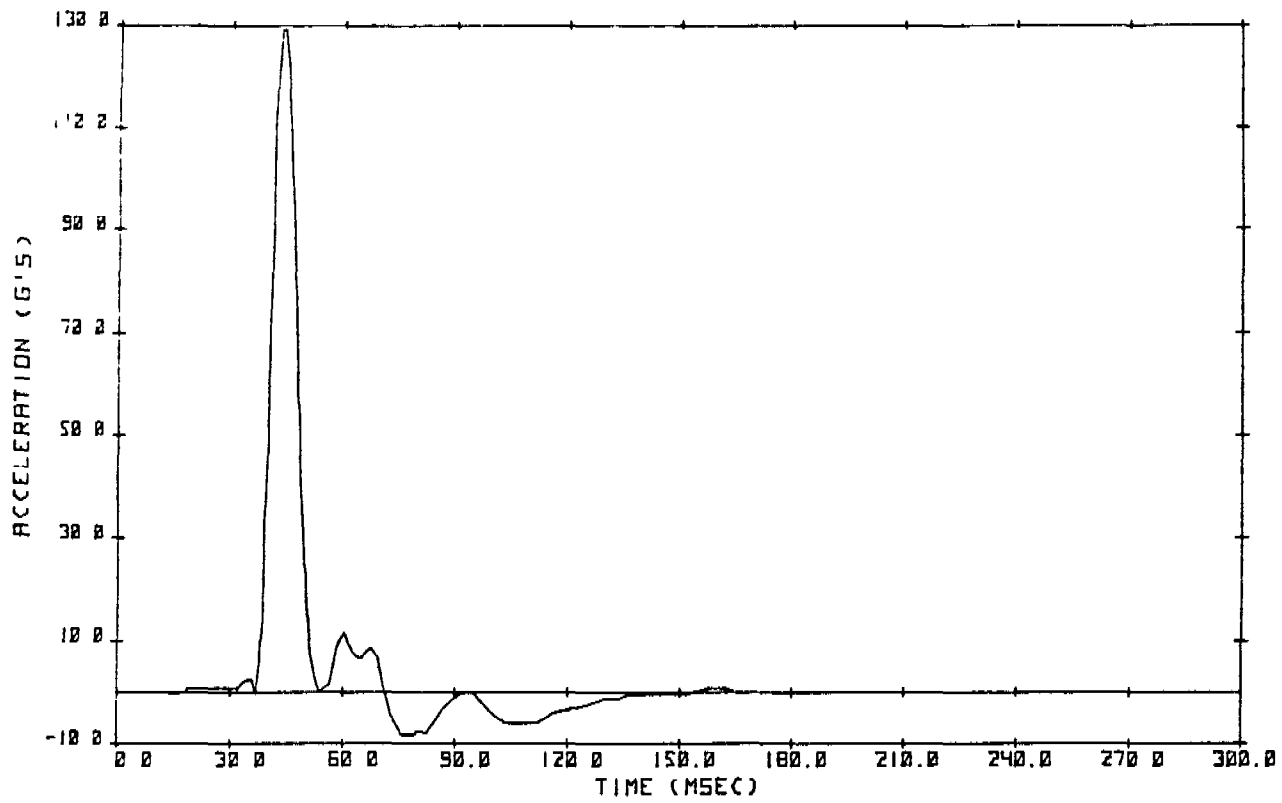


SIDE IMPACT SLED BUCK-EXPLODED VIEW

FIGURE 35

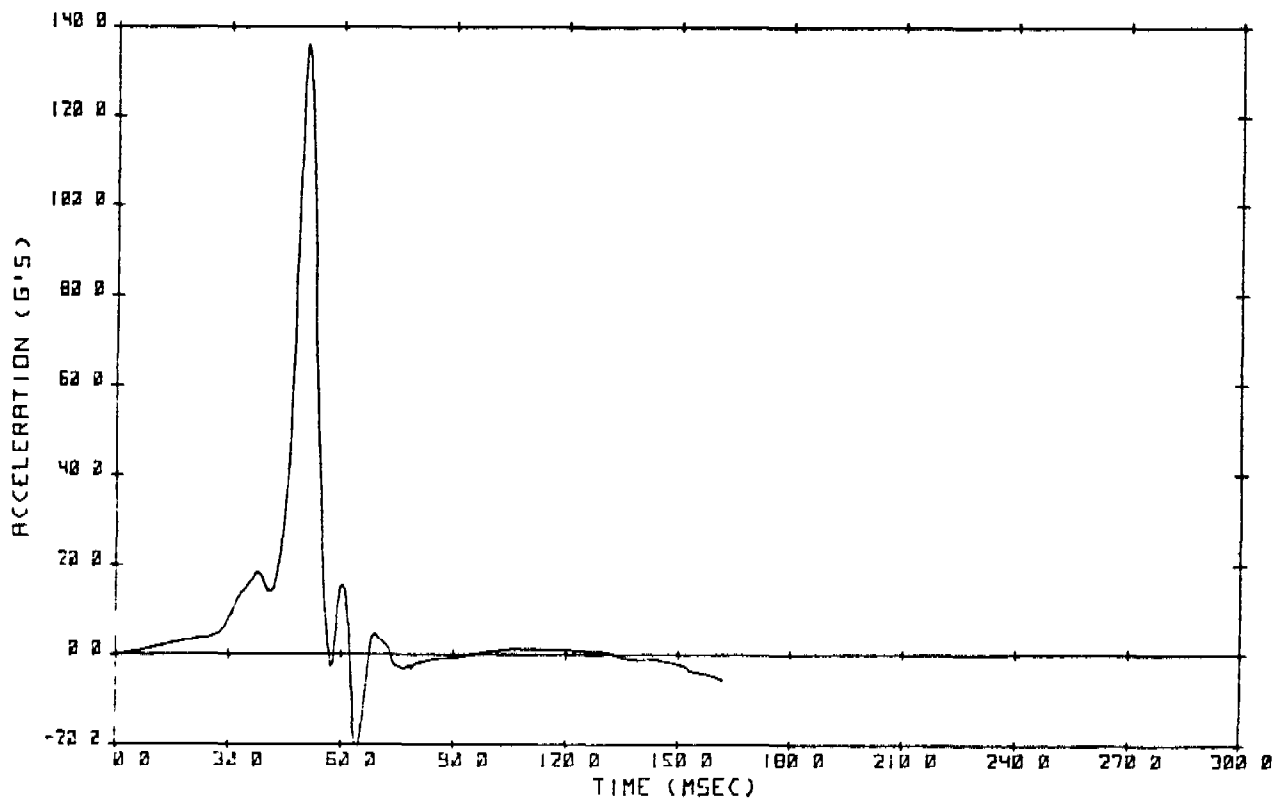
TABLE 2
Test Buck Parameter Variations Matrix for Budd Simulation

Test #	Door Reference Position	Bottom Panel Offset	Max. Force Upper Panel (lbs)	Max. Force Lower Panel (lbs)	Upper Panel Max. Force Per Tape	Lower Panel Max. Force Per Tape	Length of Tape Profile	Min. Force Upper Panel (lbs)	Min. Force Lower Panel (lbs)	Unit, Arr. to Door Distance
1	0	0.75"	1160	5640	#1 - 580 lbs #2 - 580 lbs	#3 - 2820 lbs #4 - 2820 lbs	3.0"	753	1176	4.65"
2	1.0"	1.5"	3000	6459	#1 - 2000 lbs #2 - 1000 lbs	#3 - 3760 lbs #4 - 2699 lbs	3.0"	753	2321	4.5"
3	1.0"	2.5"	3000	6459	#1 - 2250 lbs #2 - 750 lbs	#3 - 3760 lbs #4 - 2699 lbs	2.0"	753	2909	4.5"
4	1.0"	1.625"	3000	6459	#1 - 2499 lbs #2 - 501 lbs	#3 - 3760 lbs #4 - 2699 lbs	2.0"	753	2909	4.5"
5	1.0"	2.625"	3000	6459	#1 - 2499 lbs #2 - 501 lbs	#3 - 3760 lbs #4 - 2699 lbs	2.0"	753	2909	5.0"
6	1.0"	2.375"	3000	6459	#1 - 2499 lbs #2 - 501 lbs	#3 - 3760 lbs #4 - 2699 lbs	2.0"	753	2909	5.0"
7	1.0"	2.625"	3000	6459	#1 - 2499 lbs #2 - 501 lbs	#3 - 3760 lbs #4 - 2699 lbs	2.0"	753	2909	5.0"
8	1.0"	2.437"	(NO TAPES)	-	-	-	-	-	-	5.0"
9	1.0"	2.437"	(NO TAPES)	-	-	-	-	-	-	5.0"



CHEST ACCELERATION (SRL 17-5 #9)

FIGURE 36



PELVIS ACCELERATION (SRL 17-5 #9)

FIGURE 37



0 ms



30 ms



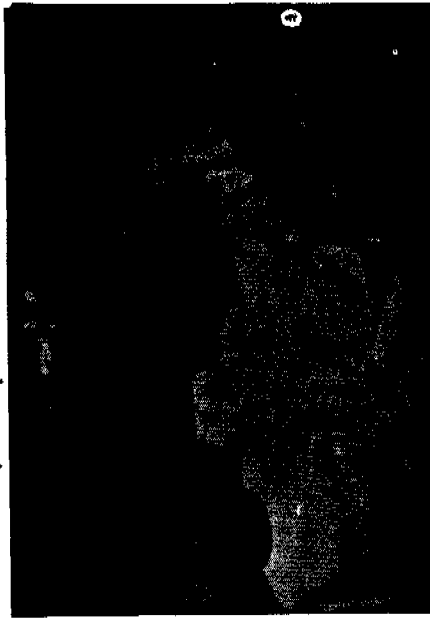
10 ms



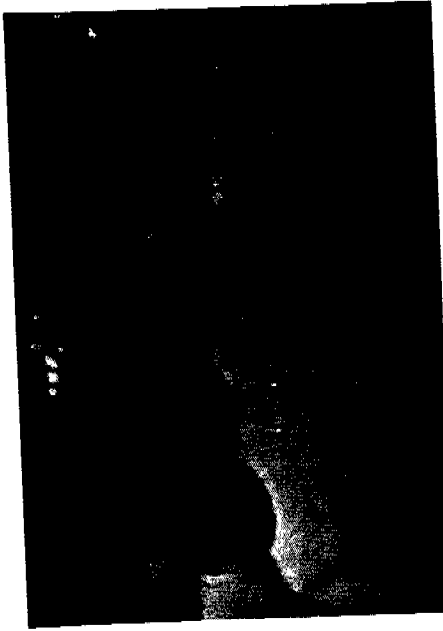
40 ms



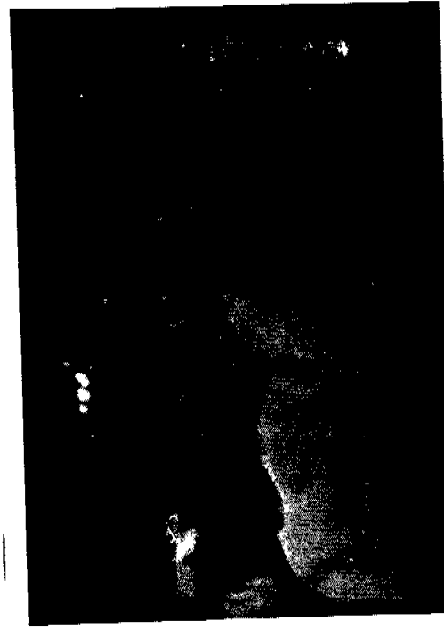
70 ms



20 ms

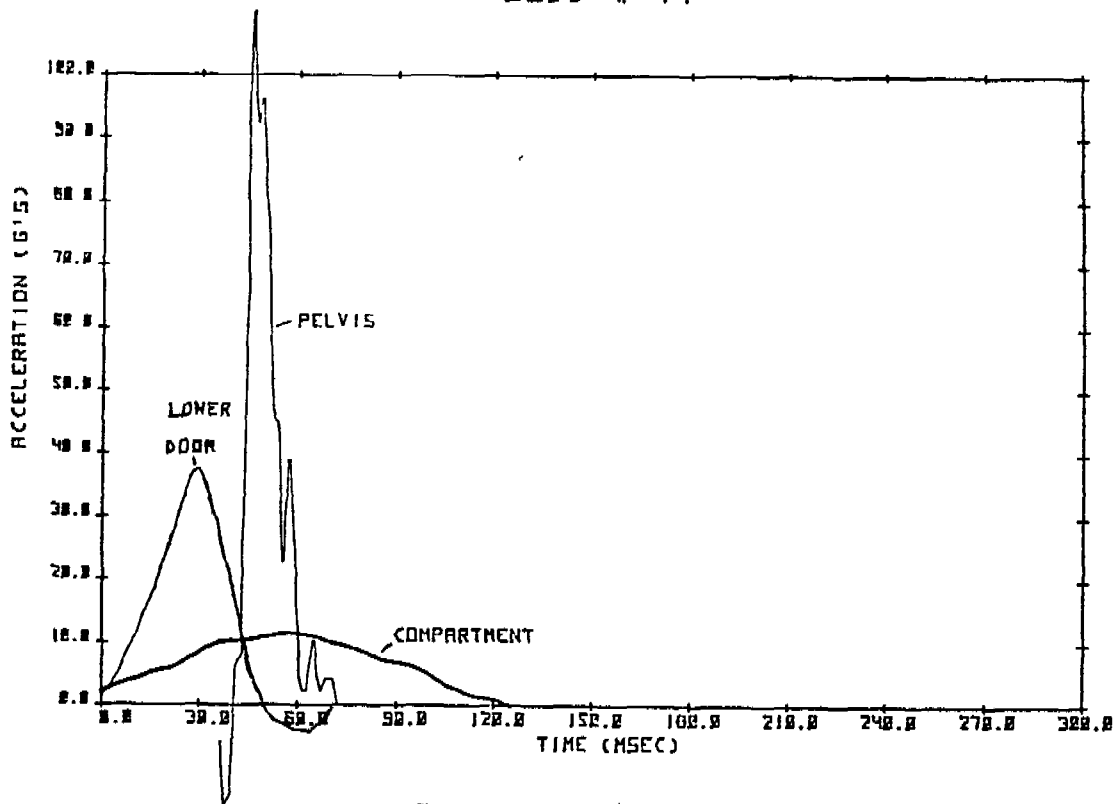


50 ms



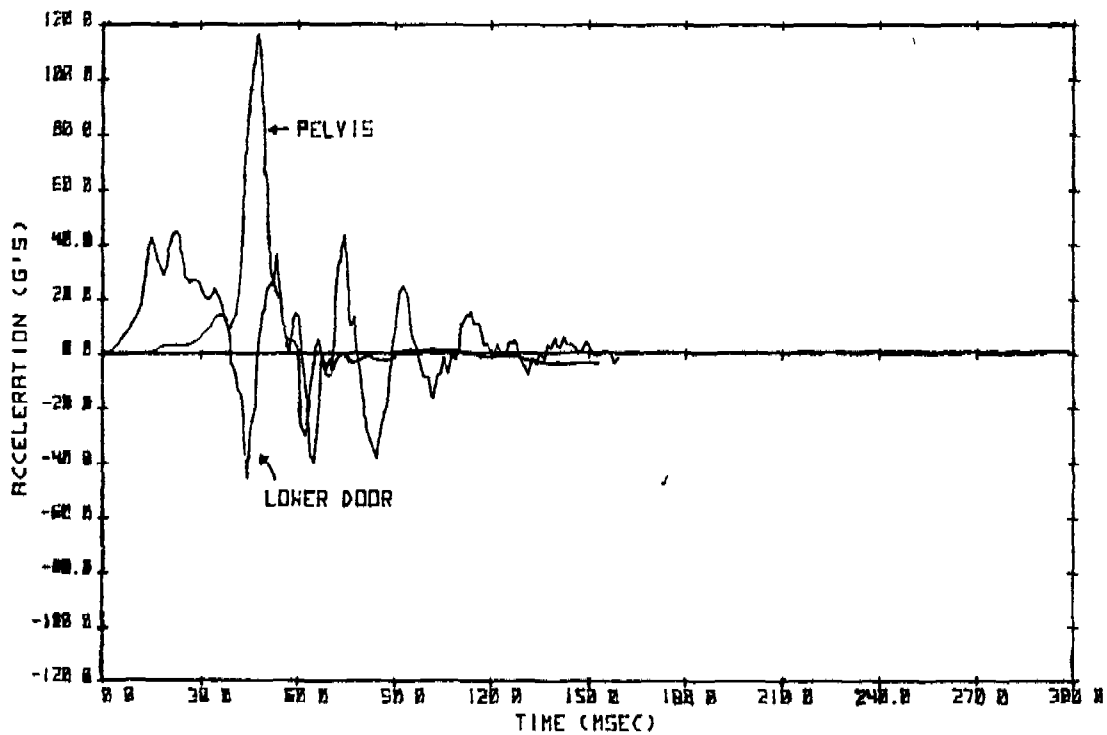
80 ms

FIGURE 38 - Budd Test No 11



VEHICLE/OCCUPANT-PELVIS ACCELERATIONS

FIGURE 40
SRL 17-5 TEST #6



LOWER DOOR/OCCUPANT-PELVIS ACCELERATIONS

FIGURE 41

in the car event. Also, the early inertial spike on the chest acceleration was higher in the simulation. The inertial spike indicated that the effective mass of the door was too high, but the doors could not be significantly lightened without losing needed strength. The roller tape profile was adjusted to accomplish an approximate match (average magnitude and pulse width) of the car event. The chest response of Figure 43 was felt to be a reasonable approximation of that of Figure 42.

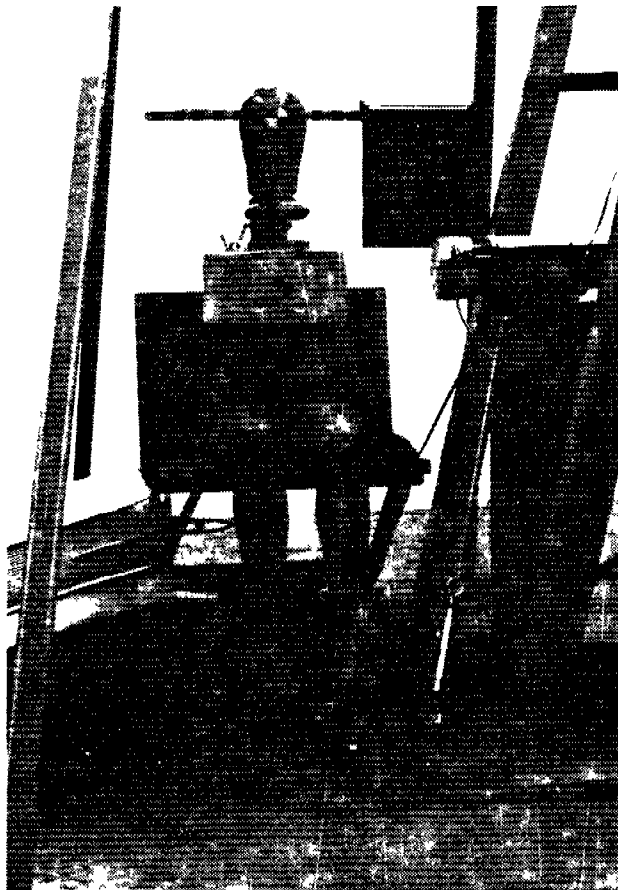
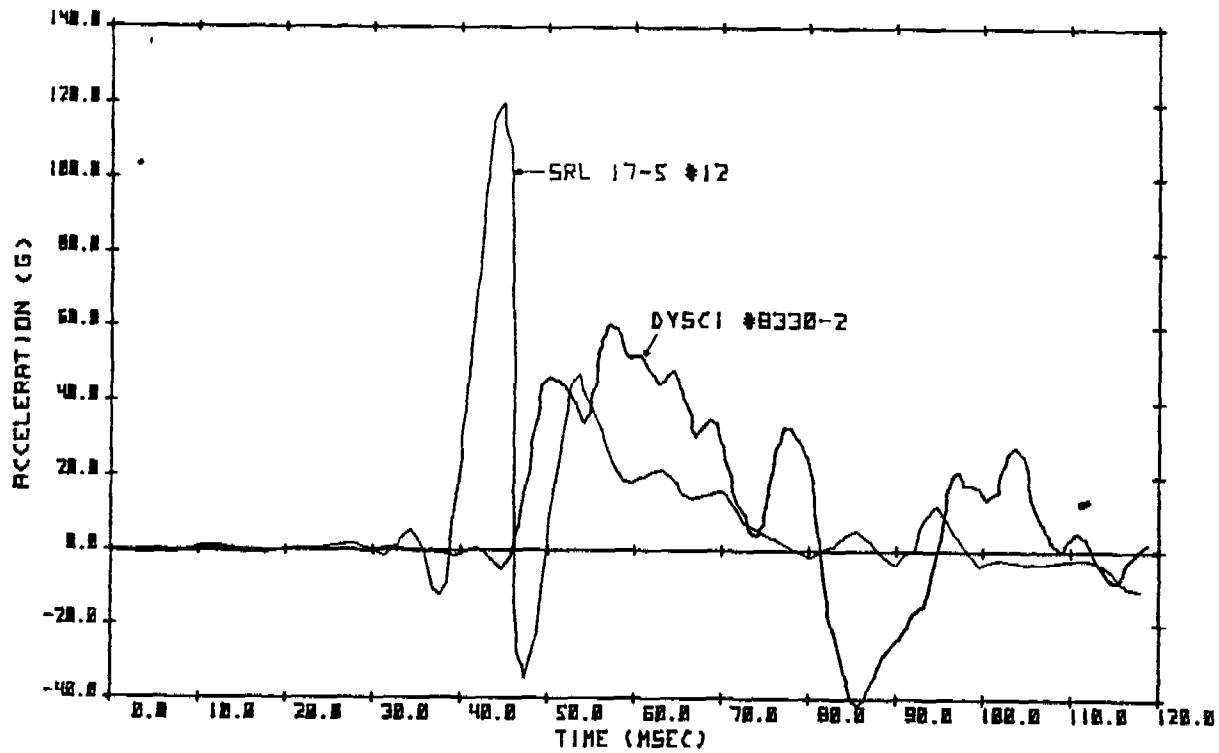


FIGURE 44

Pendulum Calibration Test Set-up

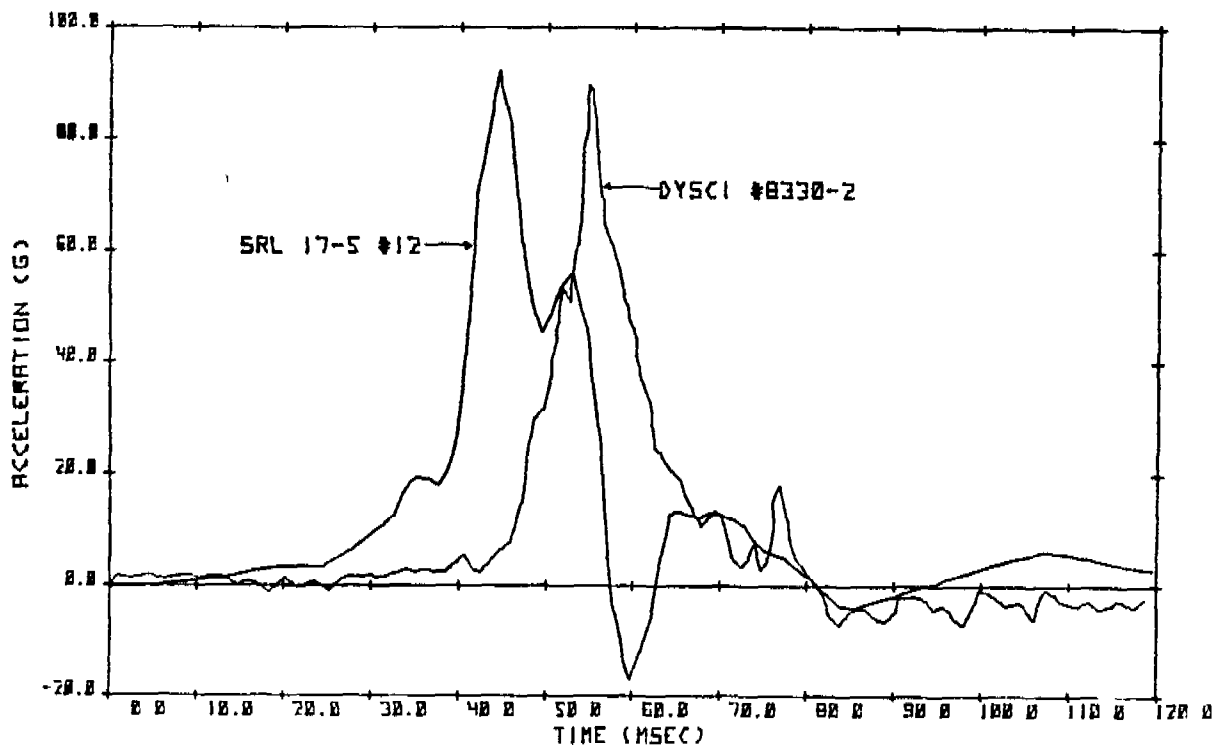
Test Buck Parameter Variations Matrix for
DySci No. 8330-2 Simulation

Test #	Bottom Panel Offset	Max. Force Upper Panel (lbs)	Max. Force Lower Panel (lbs)	Upper Panel Max. Force Per Tape	Lower Panel Max. Force Per Tape	Length of Tape Profile	Min. Force Panel (lbs)		Min. Force Lower Panel (lbs)	Dummy Arm to Door Distance	Dummy Pelvis to Door Distance
							Upper Panel (lbs)	Lower Panel (lbs)			
10	1.25"	3000	6459	#1 - 2499 #2 - 501	#3 - 3760 #4 - 2699	2.0"	753	2909	6.0"	5.5"	
11	1.75"	3500	6459	#1 - 2917 #2 - 583	#3 - 3760 #4 - 2699	2.0"	753	2909	6.5"	5.5"	
12	1.75"	3500	5347	#1 - 2917 #2 - 583	#3 - 2673.5 #4 - 2673.5	2.0"	753	2374	6.5"	5.5"	
13	0"	3500	5347	#1 - 2917 #2 - 583	#3 - 2673.5 #4 - 2673.5	2.0"	753	2374	6.5"	6.5"	
14	1.0"	3500	4812.4	#1 - 2917 #2 - 583	#3 - 2406.2 #4 - 2406.2	2.0"	753	2139	6.5"	7.25"	
15	1.0"	3724.6	4812.4	#1 - 2994.4 #2 - 730.2	#3 - 2406.2 #4 - 2406.2	1.0"	753	2139	6.5"	7.25"	
16	1.0"	3671.1	4812.4	#1 - 2940.9 #2 - 730.2	#3 - 2406.2 #4 - 2406.2	1.0"	1020.7	2139	6.5"	7.25"	
1	1.0"	3671.1	4812.4	#1 - 2940.9 #2 - 730.2	#3 - 2406.2 #4 - 2406.2	1.0"	1020.7	2139	6.5"	7.25"	



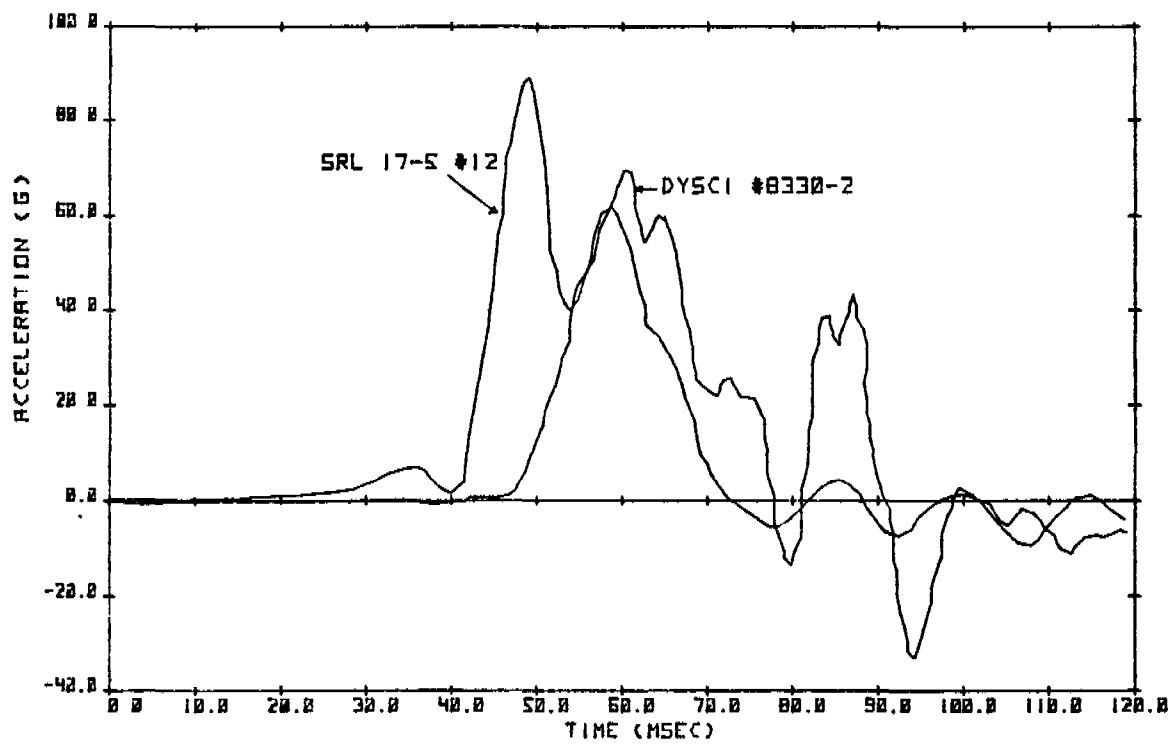
L. UPPER RIB ACCELERATION

FIGURE 45



PELVIS ACCELERATION

FIGURE 46



LOWER SPINE ACCELERATION

FIGURE 49



0 ms



70 ms



20 ms



30 ms



40 ms



50 ms



40 ms



70 ms



80 ms

FIGURE 50 - DySci Test No 8330-2

5.12 Review of Prior Padding Studies

The purpose of reviewing the literature on previous padding studies was to discover possible experiments with direct application to side impact thorax protection.

The literature on the mechanical and chemical properties of various foams is extensive. However, many of these studies involve specific paddings in special tests. As concluded by William R.S. Fan in his paper, "A Simulation of the Dynamic Properties of Energy Absorbing Materials,"⁽⁸⁾ the dynamic behavior of various foams varies, depending on the test performed. A material judged favorably in one test might not perform well in another test. Therefore, in choosing previous padding studies to review, only those dealing with padding used in interior vehicle applications were considered. The four studies reviewed were James E. Greene's, "Basic Research in Crashworthiness II -- Development and Testing of Vehicle Side Structure Modifications"⁽⁹⁾ and "Occupant Survivability in Lateral Collisions"⁽⁵⁾, Mark Haffner's, "Dynamic Characteristics of Energy-Absorbing Materials" (study was not published), and L.S. Paul's "Energy Absorption and Shock Attenuation Characteristics of School Bus Padding Materials"⁽¹⁰⁾.

James Greene's (Calspan), "Basic Research in Crashworthiness II - Development and Testing of Vehicle Side Structure Modifications"⁽⁹⁾ dealt with the progressive structural modifications made on 1968(69) mid-sized Fords. However, some consideration was given to interior padding. Styrofoam, a IPCF polystyrene, was tested in a 4 inch thickness with and without 1 inch diameter holes drilled to reduce the density. Also, a 3 inch thick sample of styrofoam with holes, covered with ensolite, and a 3 inch sample of ethafoam were tested.

The ethafoam static test results indicated poor energy absorption, and ethafoam was eliminated. The remaining three (3) combinations were tested dynamically at 10 mph using a 430 pound flat-bottomed impact weight. The

tests showed that the padding and structural modifications did lower the acceleration levels of the dummies. However, the extent of the improvement due specifically to the padding and specifically to the structural modifications could not be clearly distinguished from these tests alone.

As pointed out in this study, the usefulness of paper Honeycomb in automotive applications is questionable. Prolonged exposure to high humidity reduces the crush strength up to 50 percent, water deteriorates the paper, the paper is readily flammable if not treated, and production tolerances allow a 20 percent range in crush strength values. Furthermore, the application of Honeycomb as an interior door padding is probably not compatible with current mass production techniques.

In 1977, Mark Haffner at the NHTSA, SRL, began a study entitled "The Dynamic Characterization of Energy Absorbing Materials". In this study, Haffner reviewed previous literature on energy absorbing materials, ran five tests to determine the effect of temperature on ethafoam (polyethylene) 220, and setup an experiment matrix with 15 experiments for 3 different thicknesses.

Unfortunately, prior to running the 15 experiments at 3 thicknesses of foam, the SRL was moved to Ohio and the group working on the project was separated. The project was never completed.

"Energy Absorption and Shock Attenuation Characteristics of School Bus Padding Materials"⁽¹⁰⁾ was the most recent and informative study. The study evaluated seatback, side wall, and ceiling paddings. Various materials were judged in several areas: flammability, smoke emissions, toxicity, environmental resistiveness, and maintainability.

Based on results from the above methods of testing, five materials were chosen as core materials:

- Honeycomb ACG-I-.003 - an aluminum product

In conclusion, it was found that experiments directly applicable to side impact thorax protection (i.e., using current injury criteria and surrogate design) have not been performed. Although L.S. Pauls' school bus padding study did consider or test a large number of paddings, those materials chosen for extensive testing (paper honeycomb, etc.) generally are not well suited for the current mass production techniques used to fabricate such components for interior doors. These findings indicated a need for a padding study that focused on the specific application required.

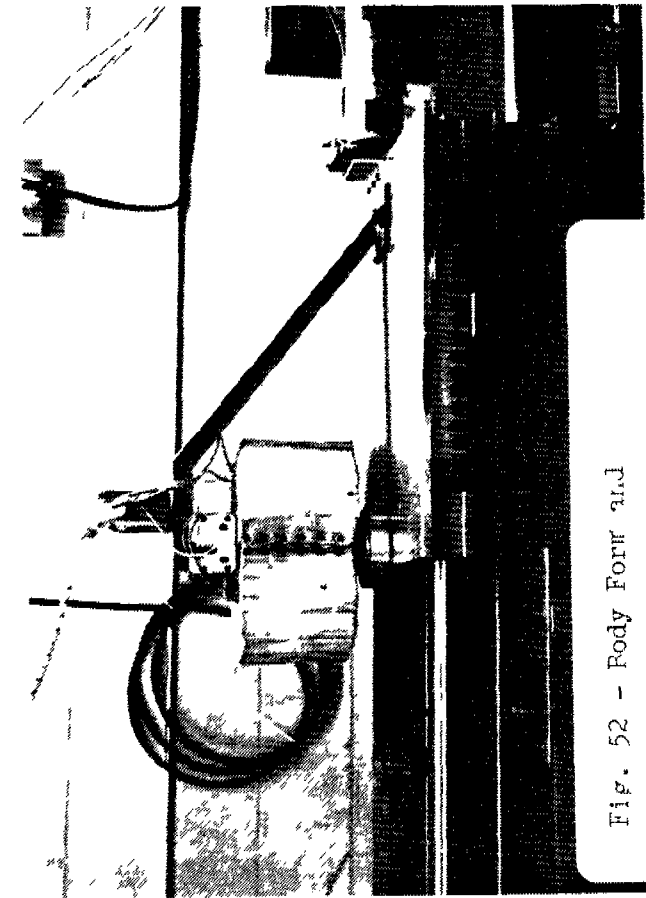


Fig. 52 - Body Four and
Sled Platform



Fig. 53 - View from Accelerator
to Strike Plate

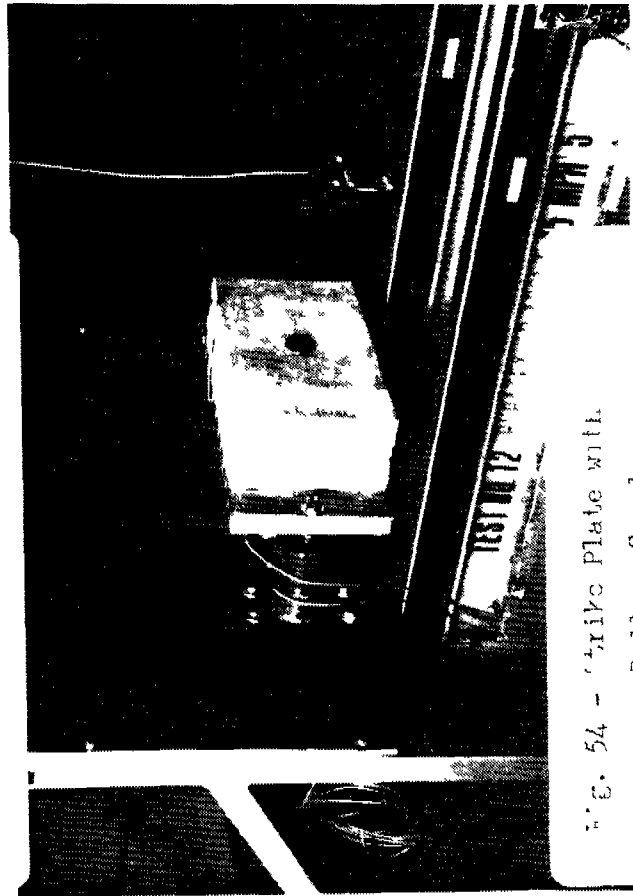


Fig. 54 - Strike Plate with
Padding Sample

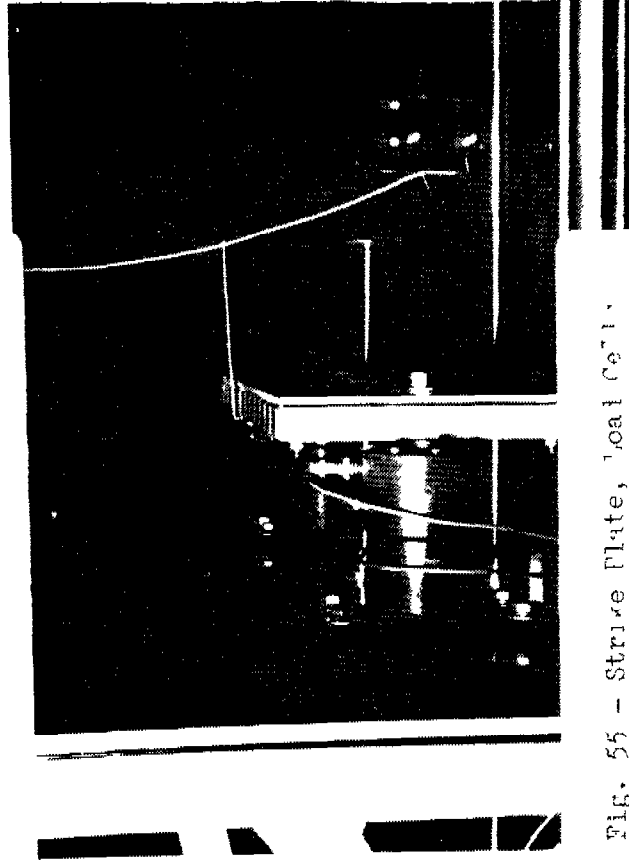


Fig. 55 - Strike Plate, Load Cell,
and Displacement Rod

of each material with the least amount of breakage. Upon completion of Phase I, many of the less desirable paddings were identified and were not used in more severe testing. Phase II testing consisted of impacting those paddings that passed Phase I criteria. The tests were performed using 3 inch padding samples with an impact velocity of 15 mph.

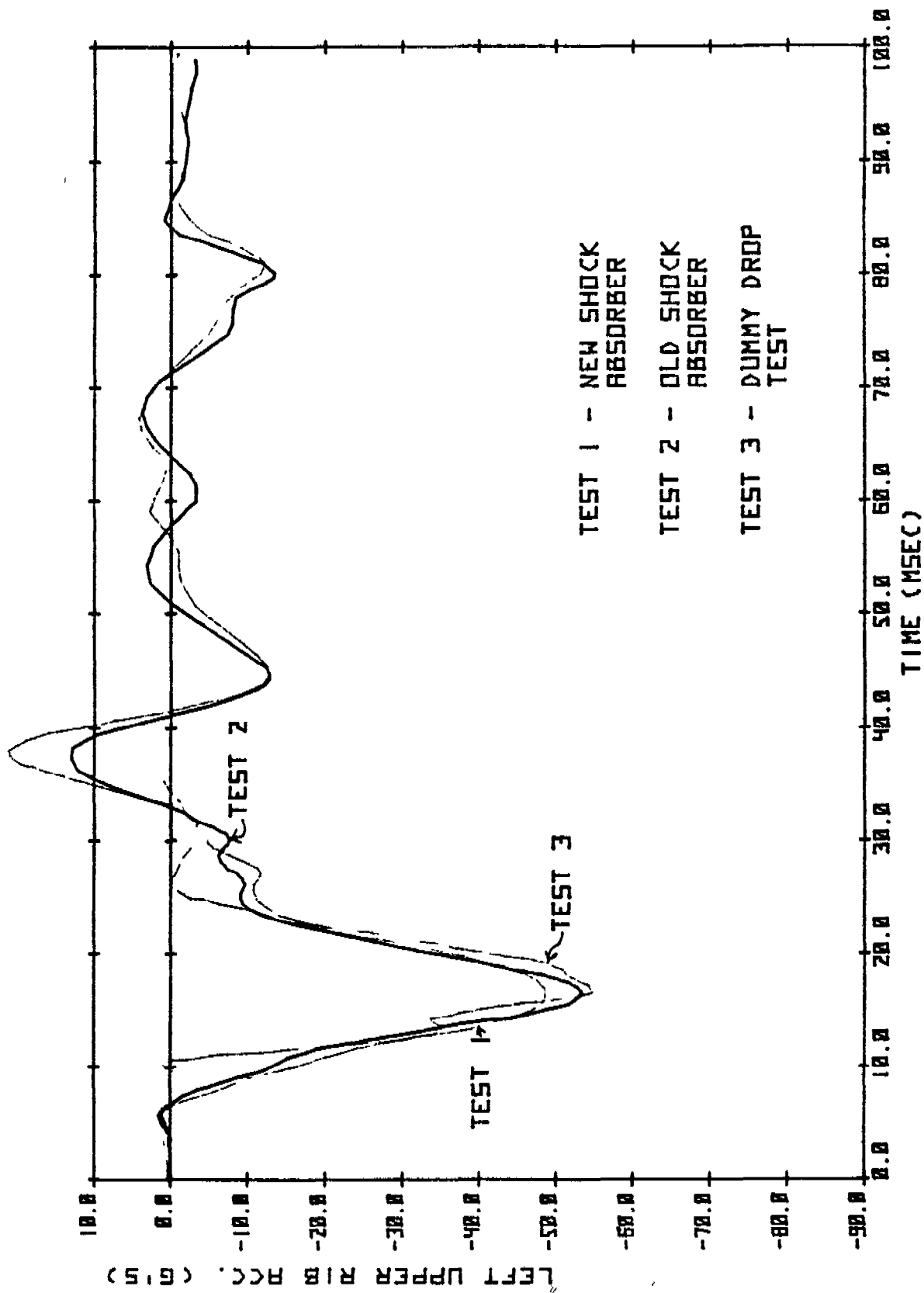
The paddings were judged as to their desirability for a thoracic restraint by three main criteria. These criteria were (1) the padding force-deflection properties, (2) the body form AIS calculated from the B(LUR) parameter, and (3) the peak spinal acceleration.

Data Recording: The data that were recorded included lateral accelerations of the left upper rib, right upper rib, and upper and lower spine; forward acceleration of the lower sternum; load cell readings for both load cells; sled velocity; and padding and thorax displacement. All data was recorded on FM tape except thorax displacement which was recorded on a strip chart. The thorax displacement measured was simply the displacement of the shock absorber in the thorax.

An overhead camera recorded 1000 fps movie coverage of the padding and thorax crush and provided a double check of the electronic data.

Data Processing: As stated in Element 4, the SRL used 2-pole Butterworth filters (100Hz cutoff) using an 8:1 reduction in play back and a 3200 Hz digitizing rate to maintain uniformity with data processing done by the HSRI.

All data processing (AIS calculations and plots) was performed on the PDP-11 minicomputers located at the VRTC. The two load cell readings and the displacement potentiometer reading for each test were digitized and combined to obtain force-deflection curves.



RIGID DUMMY DROP VS. 10 MPH MINISLED TESTS

FIGURE 57

The criteria for Phase I padding acceptance were as follows:

- (1) AIS measurement less than or equal to 3.
- (2) Peak upper spine (3 msec duration) acceleration less than or equal to 40 G's.
- (3) Padding peak force of 3200 pounds or less.

Table 6 is a list of all materials tested in this Phase I. Table 7 summarizes test results for each material tested (duplicate tests on the materials are not shown). Appendix F contains the force vs. deflection plots for Phase I.

Rubatex R-310-V, Ensolite AAC and the APR padding were the more effective materials observed in Phase I testing. Table 8 shows the best 5 paddings within each of the 3 individual approaches. It was felt that each of these materials, coupled with the flexibility in the door structure, would provide protection up to the 20 mph range of occupant-door interaction. Table 9 shows the paddings that were selected for Phase II testing. (Subsequent to the Phase I testing, other materials and other variations of Phase I materials were supplied to the VRTC. These were tested in Phase II only.)

Phase II Testing (3" material samples; 15 mph; minisled)

Additional (those not on Table 9) materials and variations of materials included in the Phase II testing include the following:

- Fiberglass honeycomb (custom made by Owens Corning as per SRL's request)(called Fiberglass H_{BC}).
- Polyurethane foam supplied by General Tire and Rubber Co., in varying densities (called GTREM -" ").
- A layered variation of Ensolite consisting of 2 inches of Ensolite AAC fronted with 1 inch of Ensolite BCR (the composite was called Ensolite ABC).
- A layered variation of Rubatex consisting of 2 inches of Rubatex R-310-V fronted with 1 inch of R-8407-S (the composite was called Rubatex R-2VS).

TABLE 7

Component Level Phase I Test Results

Test No.	Padding Type	Thickness (in.)	Velocity (mph)	Temp.	Peak Spinal Accel	AIS B	Chest Deflection	Padding Deflection (in.)	Load (Cells) (lbs.)
10	Tarriere	5.625	14.99	640F	30.8	2.5	1.7"	3.27	2383
7	Ensolite AAC	5.625	14.99	630F	33.2	2.3	1.9"	2.99	2739
13	Rubatex R-4991-T	5.25	15.15	640F	34.2	2.7	1.7"	3.81	2700
15	Rubatex R-310-V	5.25	14.99	670F	30.7	2.3	1.7"	3.03	2295
23	Ensolite HCR	5.25	14.76	640F	34.5	2.6	1.625"	2.76	2955
25	Fiberglas Type G	5.25	14.99	640F	49.0	3.2	1.7"	2.90	4110
26	Neoprene LS-200	5.0	14.82	690F	59.0	3.1	1.85"	4.69	5466
28	Neoprene UDRP	5.0	15.15	700F	59.5	3.3	1.75"	4.8	5339
30	Ethafoam (220)	5.0	14.99	710F	37.2	2.5	1.65"	3.85	3398
32	Ethafoam (600)	5.13	14.92	720F	39.0	2.9	1.55"	2.0	3643

TABLE 7 (Cont.)

Component Level Phase I Test Results

Test No.	Padding Type	Thickness (in.)	Velocity (mph)	Temp.	Peak Spinal Accel	AIS B	Chest Deflection	Padding Deflection (in.)	Load (Cells) (lbs.)
57	Fiberglass Dual Density	4.25	14.20	700F	45.5	3.0	1.5"	3.60	3486
58	Fiberglass Type L	4.75	15.25	690F	51.5	3.2	1.4"	1.75	4561
59	Fiberglass Type Q	4.625	15.25	700F	62.6	3.3	1.275"	1.45	6021
64	Ensollite MLC (white)	5.5"	14.75	700F	44.0	2.8	1.65"	4.50	3613
65	Ensollite MLC White (20 mil)	5.5	14.75	700F	44.4	2.9	1.50"	4.32	3940
68	Ensollite MLC (Blk)	5.5	14.75	670F	42.6	2.9	1.575"	4.30	4287
69	Ensollite MLC (B-20)	5.5	15.15	660F	46.9	3.0	1.75"	3.74	3774
72	Ensollite LPC	5.25	15.37	630F	41.5	2.9	1.80"	3.84	3037
73	Ensollite LPC (20)	5.25	15.25	660F	43.8	2.9	1.75"	3.79	3218
74	Ensollite FBC	5.25	15.25	670F	45.1	3.0	1.65"	4.0	3931
75	Ensollite FBC (20)	5.25	15.25	670F	46.8	3.0	1.65"	3.96	3774

TABLE 9

Padding Materials for Component
Level Phase II Tests

Ensolite AAC

Rubatex R-310-V

Rubatex R-4991-T

Ethafoam 400

Durafoam C222A

Durafoam C111A

APR

TABLE 10

Component Level Phase II Test Results

TEST NO	PADDING TYPE	THICKNESS (IN)	VELOCITY (MPH)	TEMP (°F)	PEAK SPINAL ACCEL(G)	AIS B Para- meter	CHEST DEFLECTION (IN)	PADDING DEFLECTION (IN)	LOAD CELLS (LBS)
60	Ensolite AAC	3.5	15.15	68	44.0	2.7	1.7	2.42	3579
61	Ensolite BCR	3.8	15.15	68	41.6	2.6	1.51	1.59	3320
62	Ensolite HCR	3.4	15.15	66	46.3	2.8	1.53	2.31	3682
63	Ethafoam 600	3.0	15.32	66	46.3	2.7	1.55	1.74	3740
77	Rubatex R-310-V	3.06	15.08	70	44.9	2.9	1.6	2.39	4209
78	Durafoam C111A	3.0	15.15	69	48.0	3.2	1.8	2.41	3476
79	Durafoam C222A	3.0	15.32	71	44.0	3.0	1.73	2.16	3433
80	Rubatex 2VS	3.0	15.08	70	47.9	2.9	1.63	1.65	3906
81	Ensolite ABC	3.0	15.15	69	40.1	2.7	1.75	2.25	3311
82	Fiberolas HBC	3.75	15.15	69	45.4	3.0	1.65	3.30	3857
84	Fiberglas HEC	3.19	15.32	67	46.5	3.0	1.4	2.75	3232
87	GTRM C41104	3.0	15.32	67	42.9	2.9	1.4	2.41	3305
88	GTRM C41101	3.0	15.15	69	46.5	3.1	1.33	2.0	3906
89	Ensolite AEC	3.0	15.22	65	41.6	2.8	1.60	2.70	2953
90	Rubatex R-310-V	3.19	15.15	68	50.6	3.1	1.53	2.83	3545
91	Parriere APR	3.0	15.22	68	48.4	3.0	1.65	2.8	3916
92	Rubatex 2VS	3.0	15.15	67	52.5	3.0	1.45	2.13	4004
93	Fiberglas H3BC	3.5	14.82	78	39.3	2.5	---	3.25	3804

TABLE 11

HYD. Seated Landing Evaluation Test Results

TEST NO.	FILE NAME	PADDING: UPPER PANEL	PADDING: LOWER PANEL	ATS B PARAM.	PEAK UPPER SPINE (G)	PEAK LOWER SPINE (G)	PEAK PELVIS (G)	DAMPER DISPLACEMENT (IN)
18	S17318	-	-	4.0	66.6	76.3	90.6	1.6
19	S17319	Ensolute ABC-3"	Ensolute BCR-1"	3.2	46.5	59.0	83.0	1.6
20	S17320	Fiberqlas H2BC-3 13"	Ensolute BCR-1"	3.6	46.0	63.4	79.4	1.55
21	S17321	GTREM- 3.0"	GTREM- 3.0"	3.4	45.6	66.9	85.9	1.42
22	S17322	Rubatex 2VS-3"	Rubatex R-8407-S-1"	3.3	53.0	63.4	78.0	1.59
23	S17323	Fiberqlas H3BC-3.5"	Ensolute BCR-1.0"	3.3	42.5	61.8	96.9	1.53
24	S17324	Durafoam C111A-3.0"	Durafoam C111A-1.0"	3.9	52.0	55.5	80.6	1.56
25	S17325	Durafoam C222A-3"	Durafoam C222A-1"	3.5	40.1	53.0	79.7	1.43
26	S17326	Rubatex R-310-V-3"	Rubatex R-310-V-1"	3.8	44.8	55.5	81.6	1.49
27	S17327	GTREM- 3.0"	GTREM- 3.0"	3.5	56.0	77.2	130.0	1.39
28	S17328	APR- 3.0"	APR- 2.0"	3.5	44.5	59.6	67.4	1.53
29	S17329	Durafoam C311A-3.0"	Durafoam C111A-3.0"	3.6	48.0	73.1	70.6	1.47
30	S17330	Ethafoam 60C-3"	Ethafoam 400-3"	3.5	48.5	70.6	78.8	1.53
31	S17331	Rubatex R-310-V-3.25"	Rubatex R-310-V-3.25"	3.4	76.9	58.5	77.7	1.51
32	S17332	Ensolute AAC-3.0"	Ensolute AAC-3.0"	3.7	43.1	62.4	69.8	1.44
33	S17333	Fiberqlas H4BC-3.5"	Fiberqlas H2BC-3.5"	3.3	43.0	66.4	86.9	1.47
34	S17334	-	-	3.8	78.4	82.2	71.5	1.47

Tests No. 35 and No. 36 were baseline (unpadded) tests. The presence of the molded arms on the dummy raised the question whether to keep the original door positioning (used in Tests No. 18 through No. 34) the same or to keep the door to dummy distances the same. The change in dummy geometry made it impossible to do both. In Test No. 35, all test parameters, except the door panels' offset, remained the same as those in Tests No. 18 through No. 34. The offset was reduced from 1.5 inches to 1.0 inch. The dummy arm-to-door distance was 6.5 inches and the dummy pelvis-to-door distance was 7.75 inches. In Test No. 36, the door panels' offset was returned to the original position, decreasing the dummy arm-to-door distance to 4.75 inches. AIS (Blur) for Test No. 35 was 4.03 and for Test No. 36, AIS (Blur) was 4.12. Test No. 35 configuration was chosen for the padding tests due to the fact that its AIS was closest to that of Test No. 18 (4.01).

The paddings tested were GTREM, Fiberglas H2BC, Ensolite ABC and APR. The Rubatex and Fiberglas H3BC were temporarily out of stock. Each set of paddings was positioned in the same configuration as tested with the prototype dummy. The parameters used to make the comparisons were: AIS (Blur), peak (3 msec) upper spine acceleration, peak (3 msec) lower spine acceleration and peak (3 msec) pelvis acceleration. In all tests it was observed that the final version dummy predicts higher injury measures than did the prototype dummy in an identical test condition. As can be seen from Table 12, the only "acceptable" (AIS less than 3.5) injury reading on the production version dummy came from the "B" parameter on the left upper rib.

This test series finalized the HYGE sled testing.

Although it was intended that the best of the available paddings be selected after the HYGE sled testing, this final selection was not done. The reasons were as follows:

- The surrogate, which had changed mid-way through this study, was still not in final production form (not only was the SID

still under refinement, but discussions with headquarters personnel indicated that a dummy developed by the APR of France might be selected over the SID).

- The feasibility of actually molding or fabricating finished door components from the materials was unknown. The effect of such a procedure on the protective capability was also unknown.
- The final selection was judged to require other factors besides the protective capability (such as cost, weight, flammability, etc. of the finished panels).

It was decided to invite all six of the suppliers to participate in a study entitled "Side Impact Padding Integration Study". It was hoped that the surrogate would be finalized during the interim.

6.0 Conclusions and Recommendations

From this study, the following was concluded:

- A method of controlled component level testing was developed to identify padding materials that are suitable candidates for thoracic protection.

Materials that were identified:

Fiberglass Honeycomb	(supplied by Owens Corning)
GTR	(supplied by General Tire & Rubber Co.)
Rubatex R-310-V	(supplied by Rubatex Corp.)
Ethafoam 600	(supplied by Dow Chemical)
Ensolite AAC, & BCR	(supplied by Uniroyal)
Durafoam C111A, & C222A	(supplied by Monmouth Rubber)

- A simple sled buck was developed which mimics the crash environment experienced by an occupant of a struck vehicle in an oblique side collision. The sled buck incorporates the following features:
 - upper and lower door panels with adjustable stiffness properties
 - adjustable base angle for oblique impact simulations
 - HYGE acceleration capability to mimic the door acceleration pulse from a car-to-car impact
- Testing was conducted using the Part 572 dummy on the side impact sled buck which showed that a "rigid wall" impact is not a reasonable approximation of a car side impact environment. The rigid wall environment increased the chest acceleration from 75 g's to 130 g's at the same impact velocity.
- Using the prototype SID, in a simulation of an oblique side impact at impacting speeds of 30 mph and 15 mph for the striking and struck vehicles respectively, 3 inches of padding yielded thoracic injury levels of less than AIS 3.5 and upper spinal accelerations less than 53 g's (goals selected for the study).

References

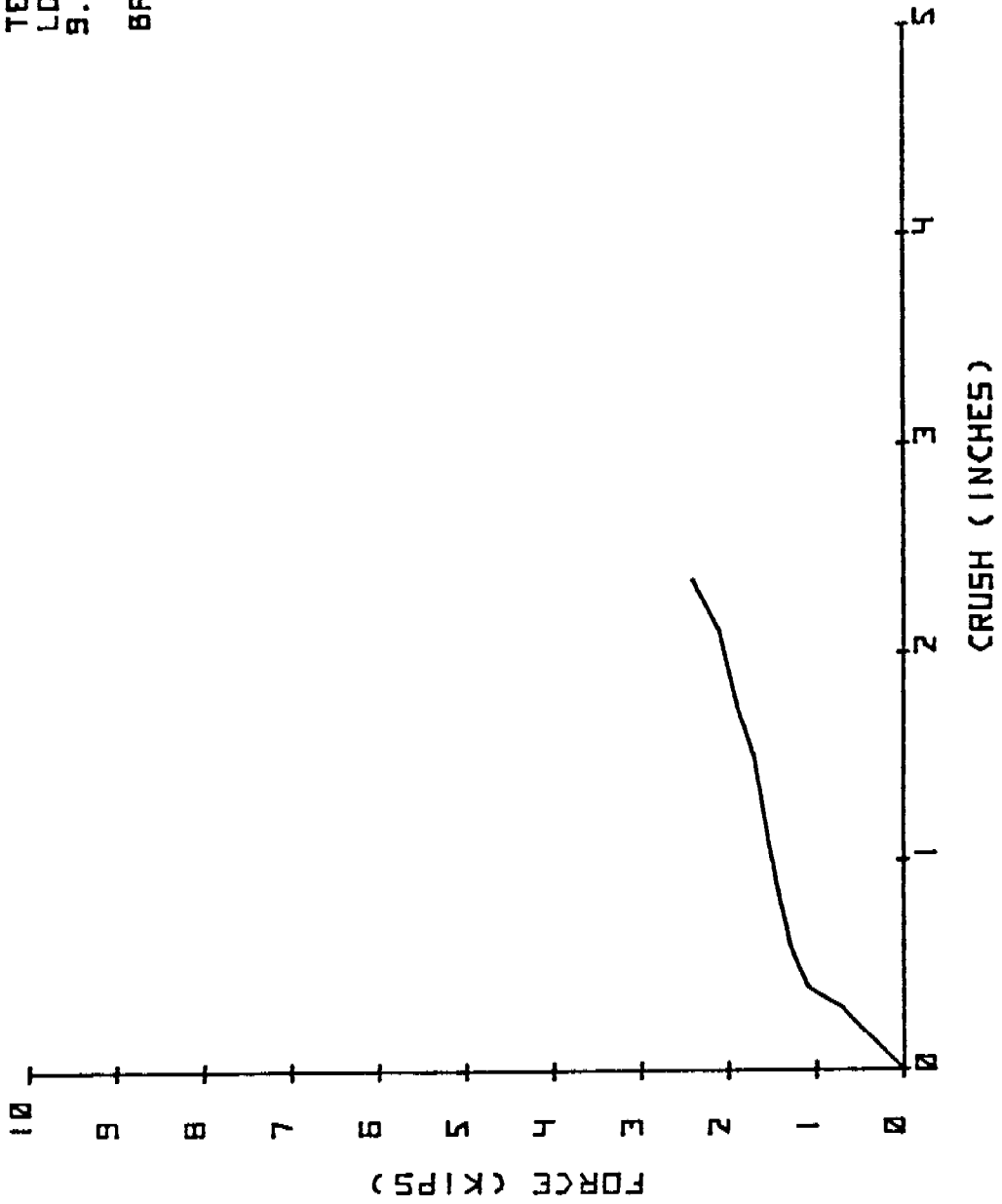
1. Shoemaker, N.E., "Research Input for Computer Simulation of Automobile Collisions," Final Report for NHTSA Contract DOT-HS-7-01511, 1978
2. "Lightweight Subcompact Vehicle Side Structure Program," Monthly Progress Reports under NHTSA Contract DOT-HS-7-01588.
3. "Countermeasures for Side Impact," Monthly Progress Reports under NHTSA Contract DOT-HS-9-02177
4. Tarriere, C., et. al., "Synthesis of Human Tolerances Obtained From Lateral Impact Simulations", Proceedings of 7th International Technical Conference on Experimental Safety Vehicles, Paris, 1979.
5. Greene, J.E., "Occupant Survivability in Lateral Collisions," Volumes I and II, Report Nos. DOT-HS-801 801 and DOT-HS-801 802, January 1976.
6. Melvin, J.W., et al., "Side Impact Response and Injury," Sixth International Technical Conference on Experimental Safety Vehicles, October 1976.
7. Eppinger, R.H., and Pritz, H.B., "Development of a Simplified Vehicle Performance Requirement for Pedestrian Injury Mitigation", Seventh International Technical Conference on Experimental Safety Vehicles, DOT-HS-805-199, December 1979.
8. Fan, William R.S., "A Simulation of the Dynamic Properties of Energy Absorbing Material," SAE Report No. 700425, 1970.
9. Greene, J., "Basic Research in Crashworthiness II -- Development and Testing of Vehicle Side Structure Modifications," Final Report of Contract No. DOT-HS-800-879.
10. Paul, L.S., "Energy Absorption and Shock Attenuation Characteristics of School Bus Padding Materials Volume III - Appendices," Report No. DOT-HS-805-272, January 1980.

APPENDIX A

Interior Door Crush Tests Results

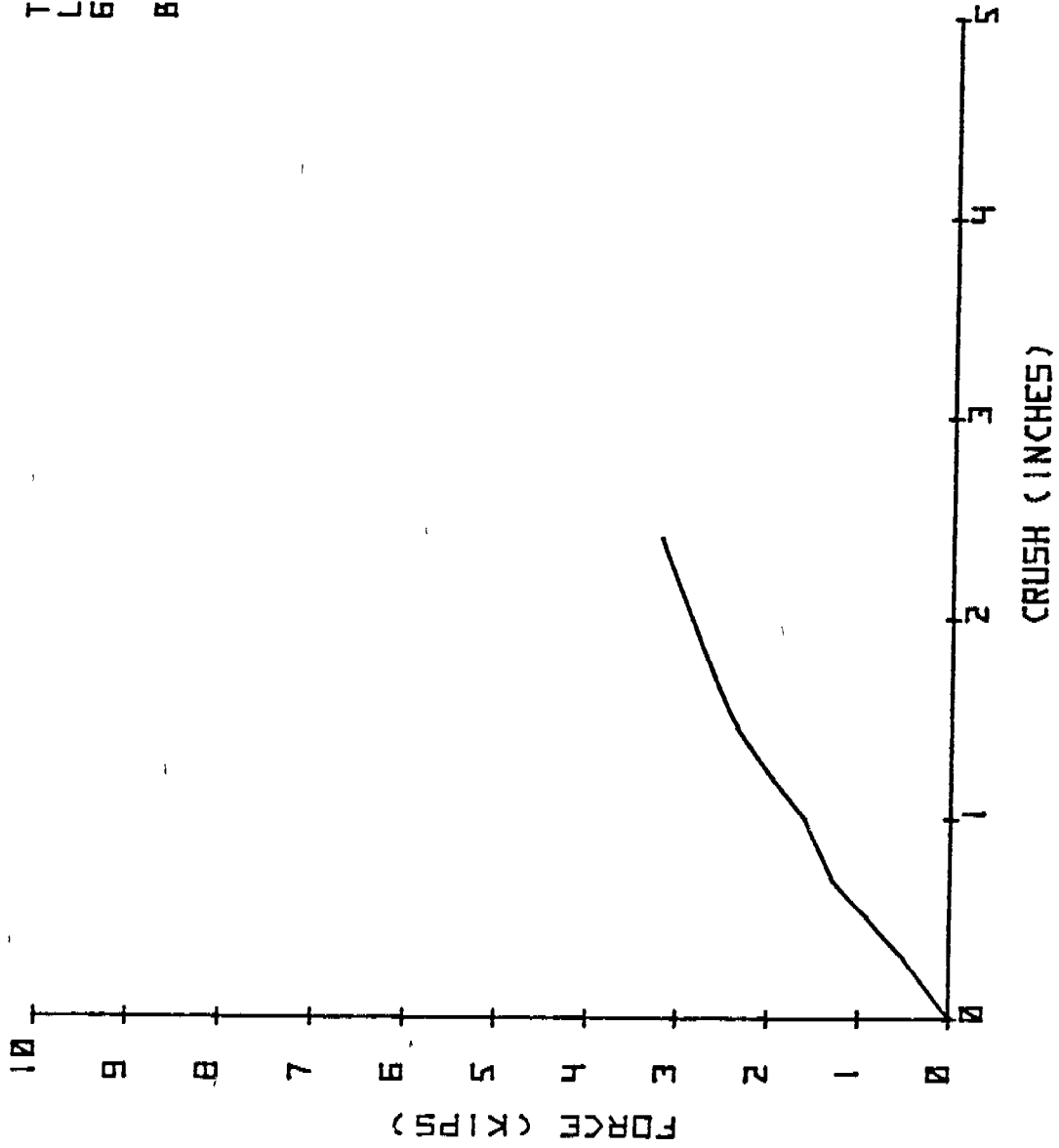
STATIC CRUSH PROPERTIES

TEST 17
LOWER BODY FORM
9.75 IN. CRUSH AT
THE HIP POINT
BASELINE DOOR



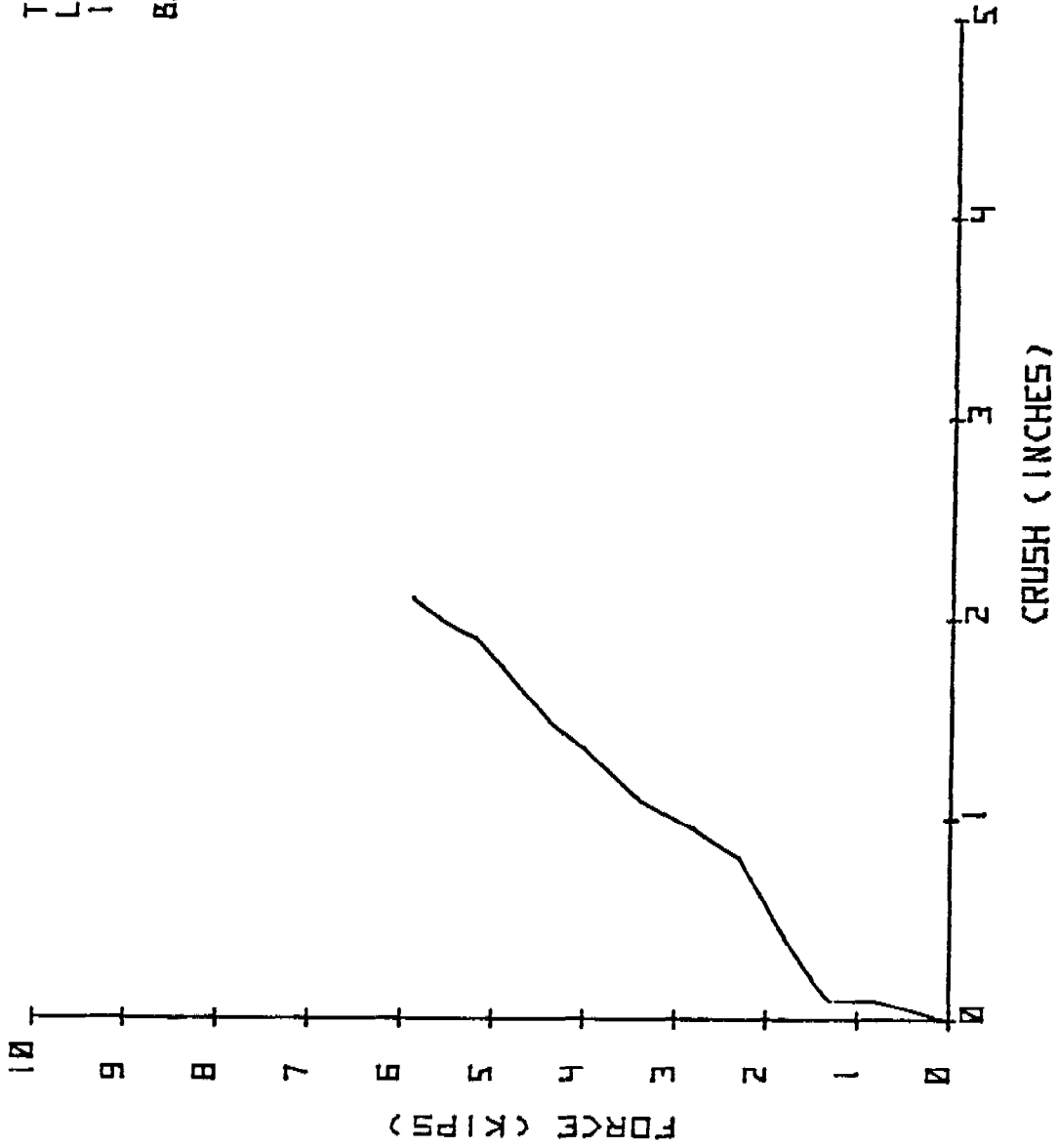
STATIC CRUSH PROPERTIES

TEST 19
LOWER BODY FORM
6.8 IN. CRUSH AT
THE HIP POINT
BASELINE DOOR



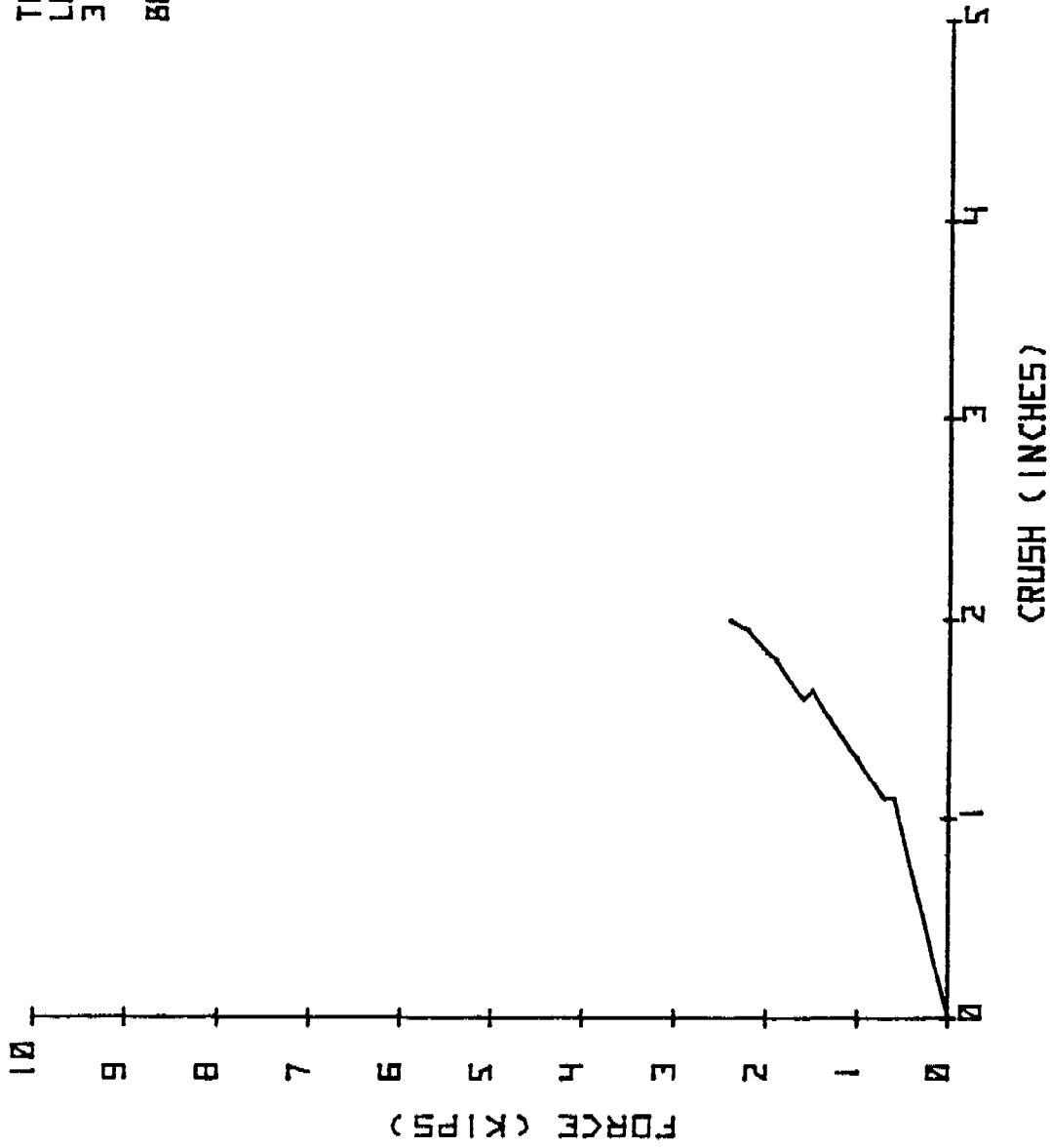
STATIC CRUSH PROPERTIES

TEST 21
LOWER BODY FORM
13.5 IN. CRUSH AT
THE HIP POINT
BASELINE DOOR



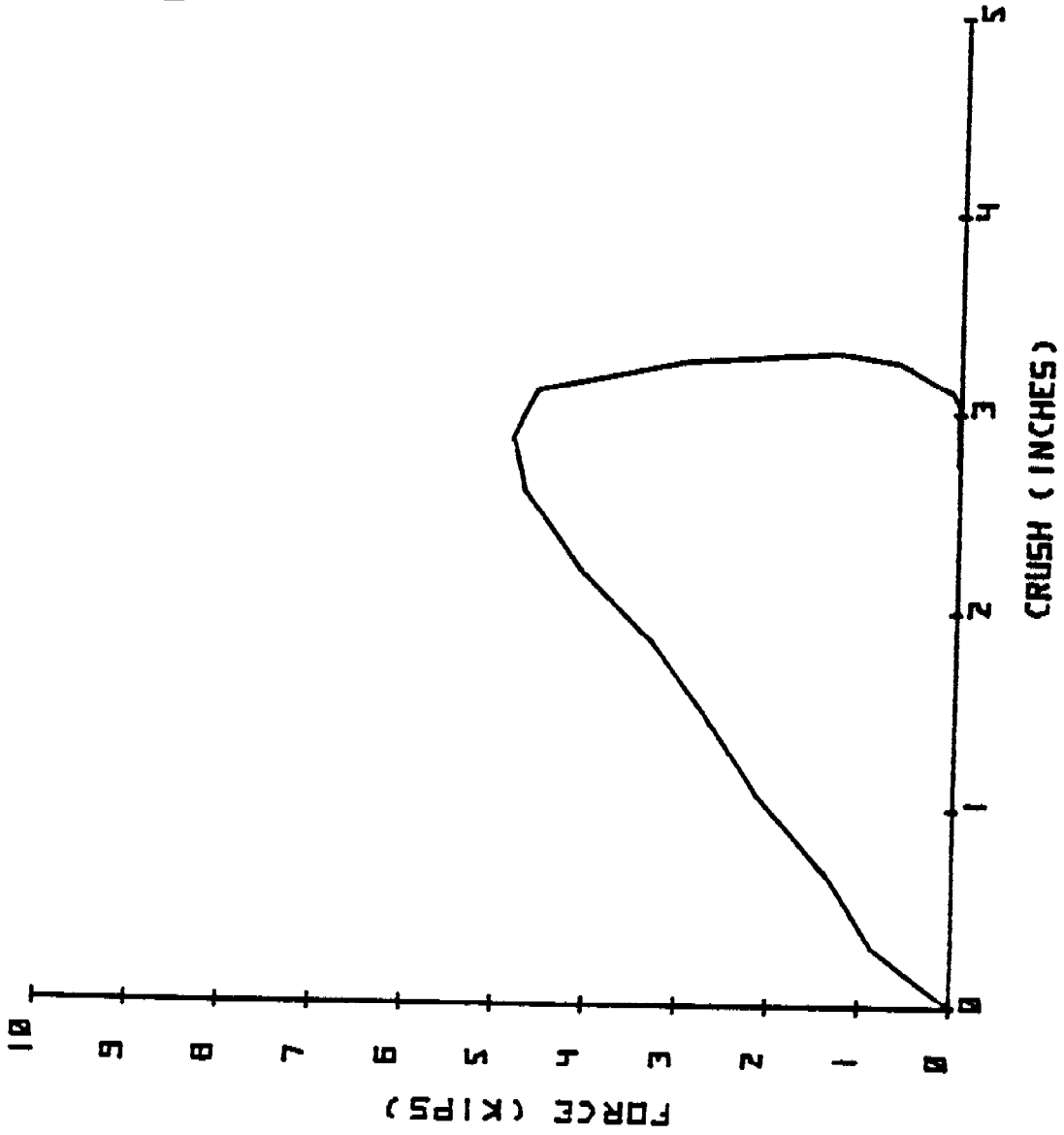
STATIC CRUSH PROPERTIES

TEST 23
LOWER BODY FORM
3.0 IN. CRUSH AT
THE D.O.R.
BASELINE DOOR



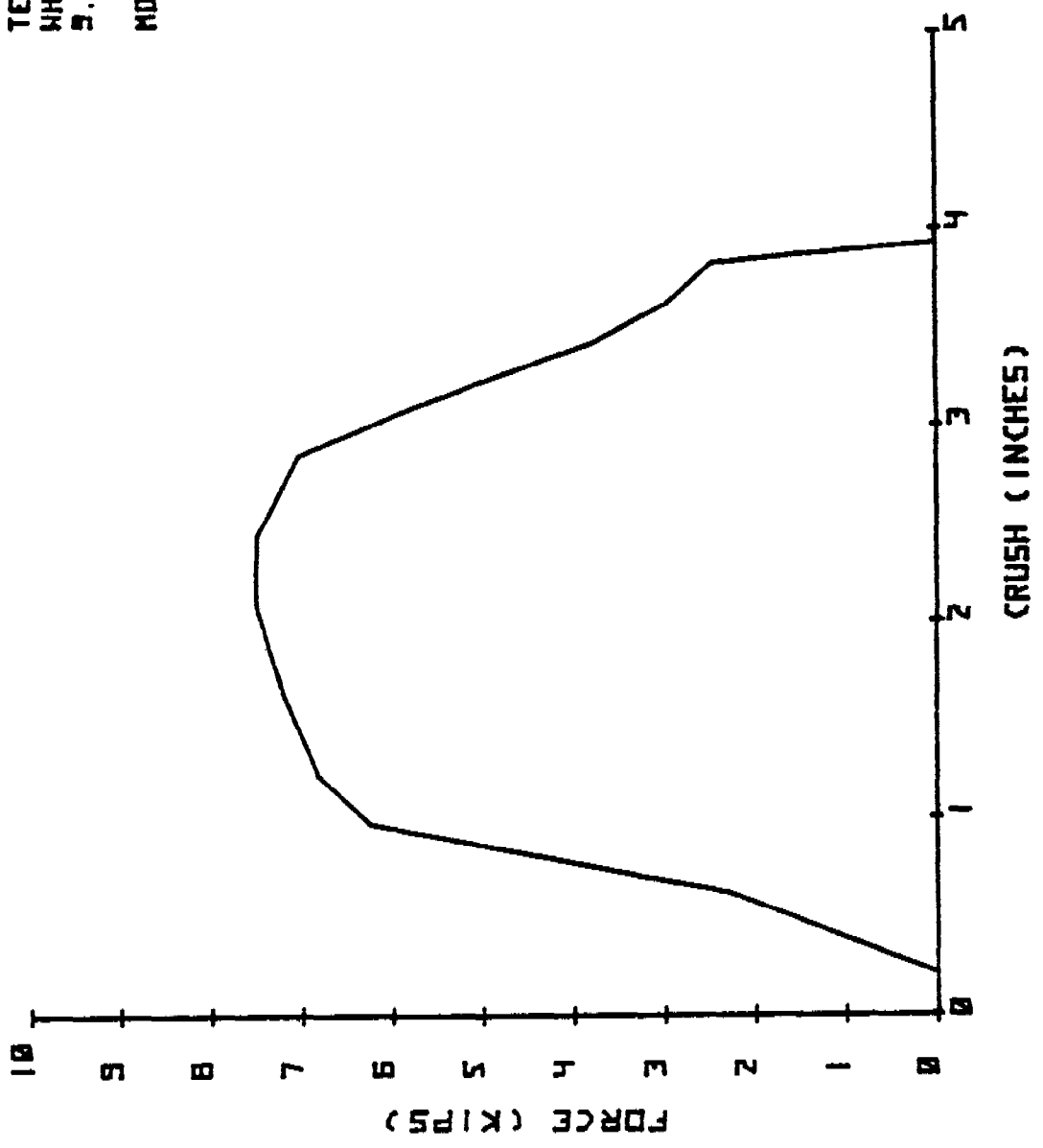
DYNAMIC CRUSH PROPERTIES

TEST 2
LOWER BODY FORM
13 IN. CRUSH AT
THE HIP POINT
BASELINE DOOR



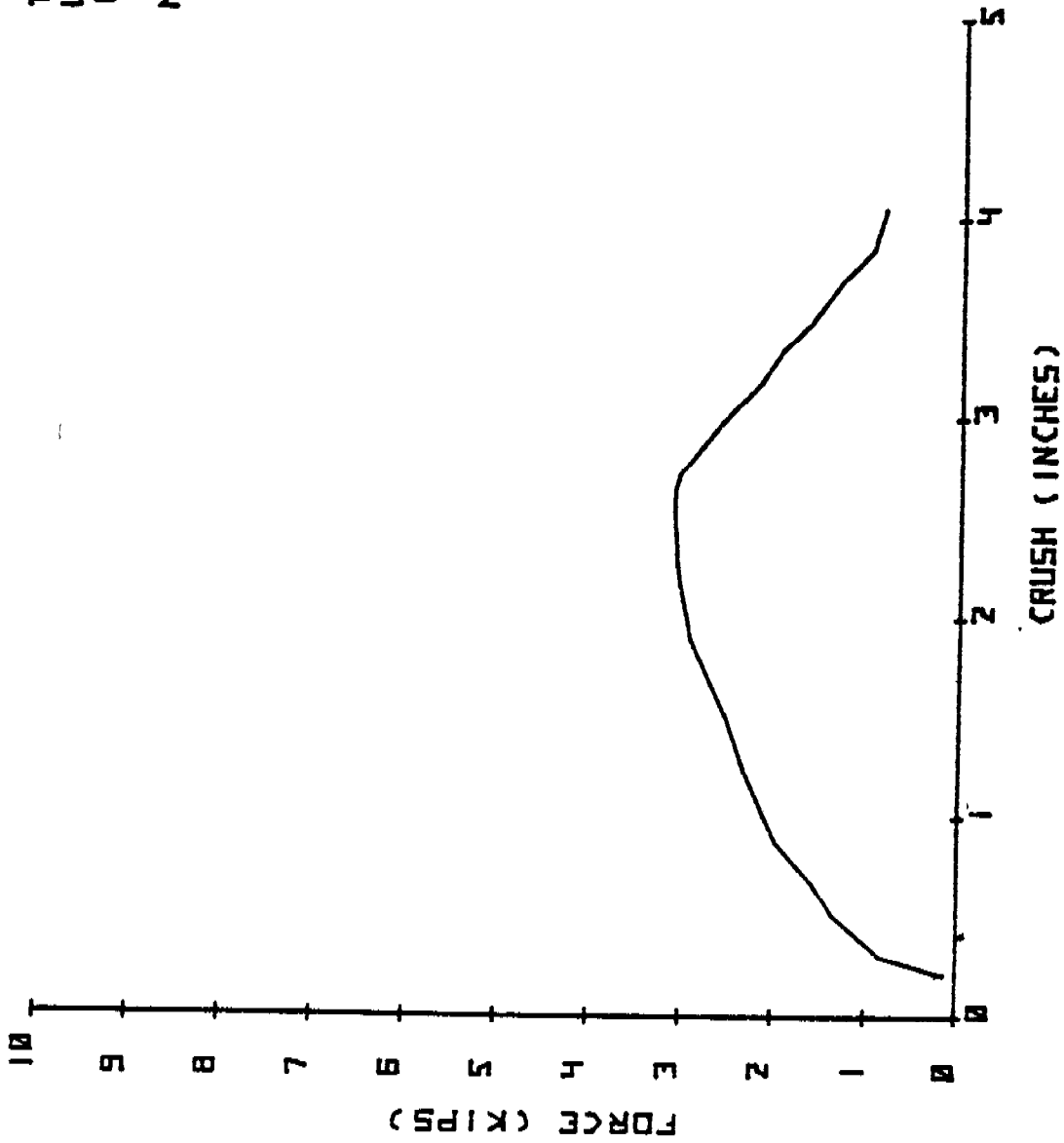
DYNAMIC CRUSH PROPERTIES

TEST 4
WHOLE BODY FORM
5.4 IN. CRUSH AT
THE D.O.R.
MOD. (RLK) DOOR



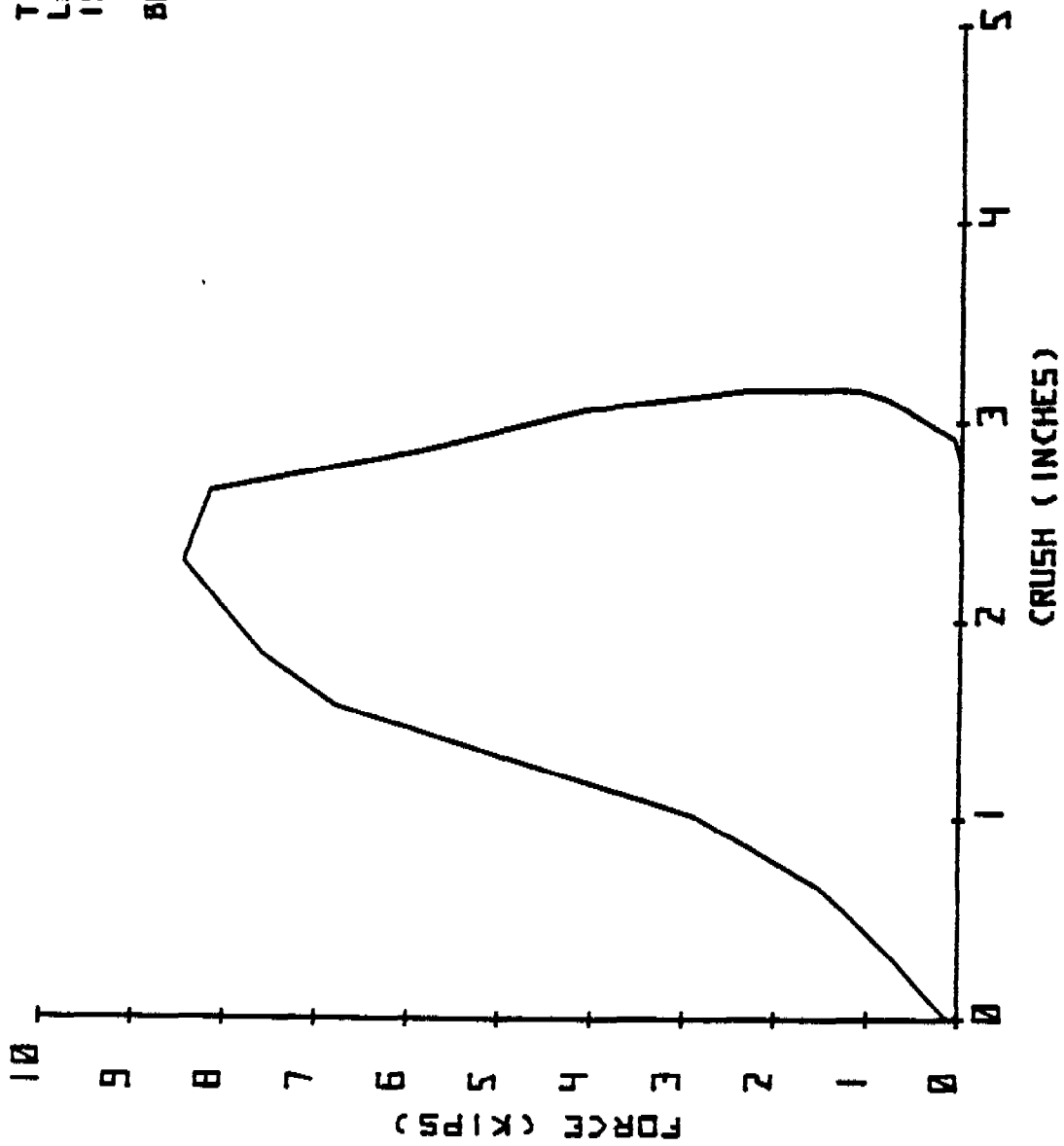
DYNAMIC CRUSH PROPERTIES

TEST 6
UPPER BODY FORM
15.8 IN. CRUSH AT
THE D.D.R.
MOD. (RLH) DDDR



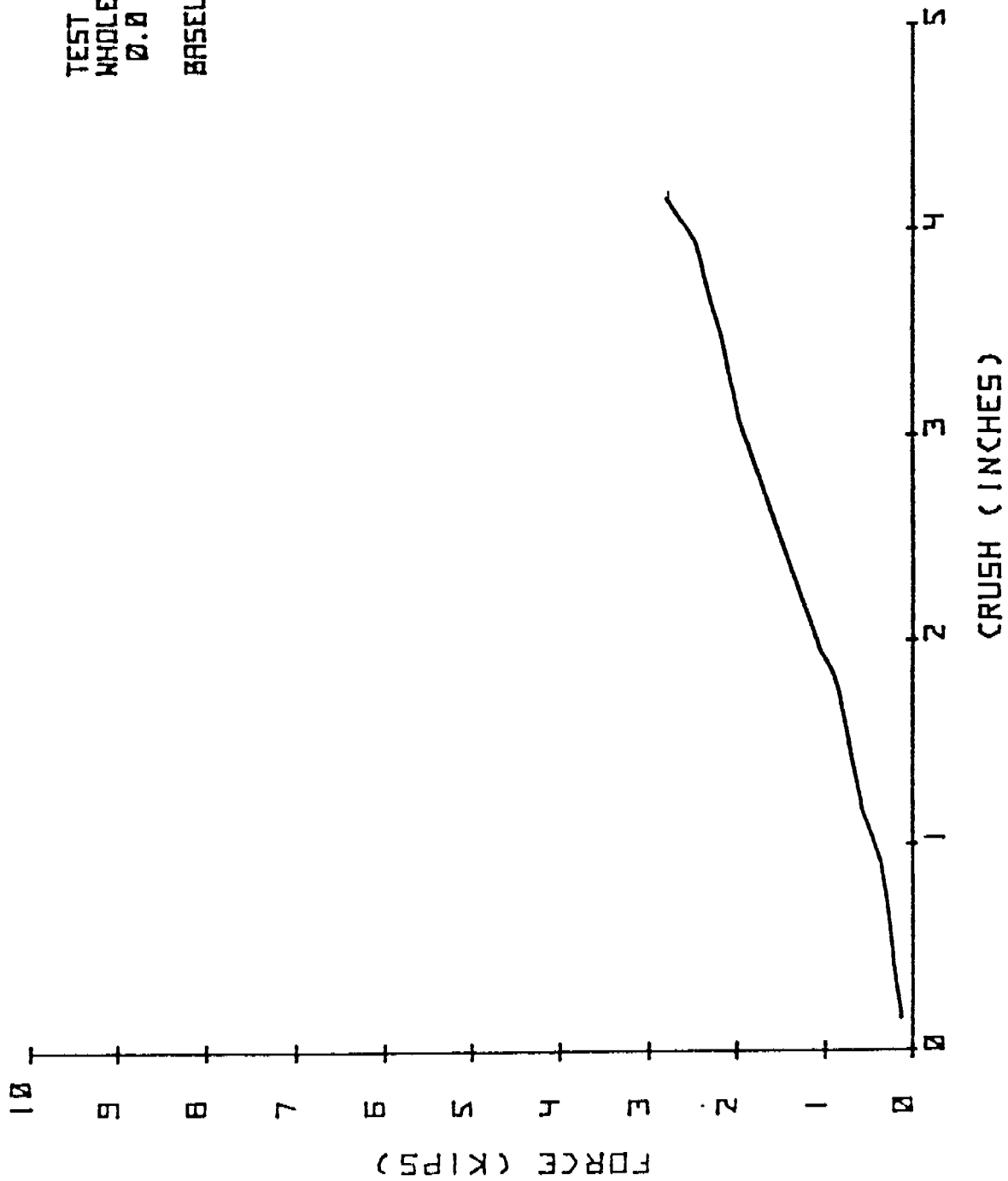
DYNAMIC CRUSH PROPERTIES

TEST #
LOWER BODY FORM
19.0 IN. CRUSH AT
THE HIP POINT
BASELINE DOOR



DYNAMIC CRUSH PROPERTIES

TEST 10
WHOLE BODY FORM
Ø.Ø IN. CRUSH
BASELINE DOOR

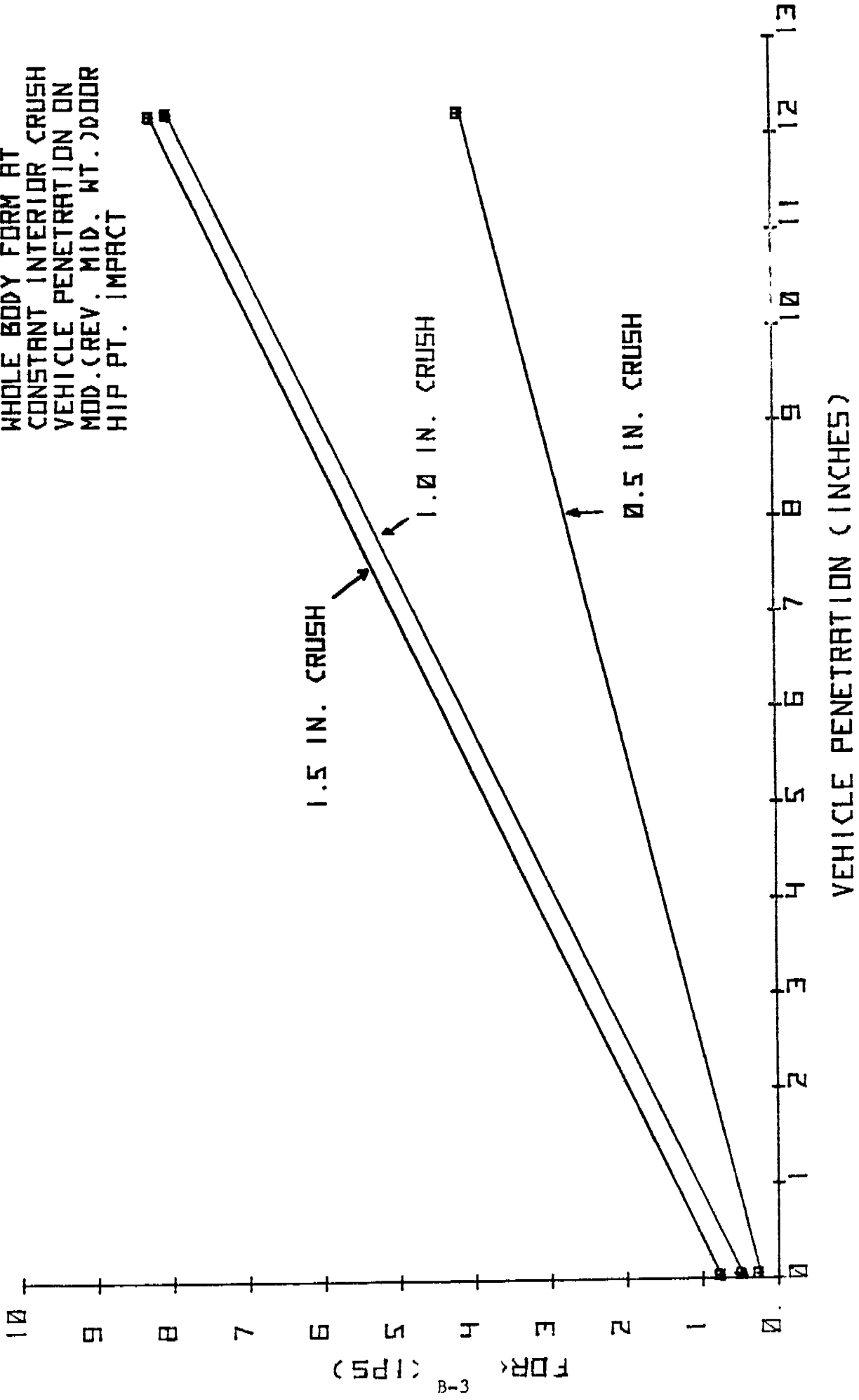


APPENDIX B

Interior Door Stiffness Trend Curves

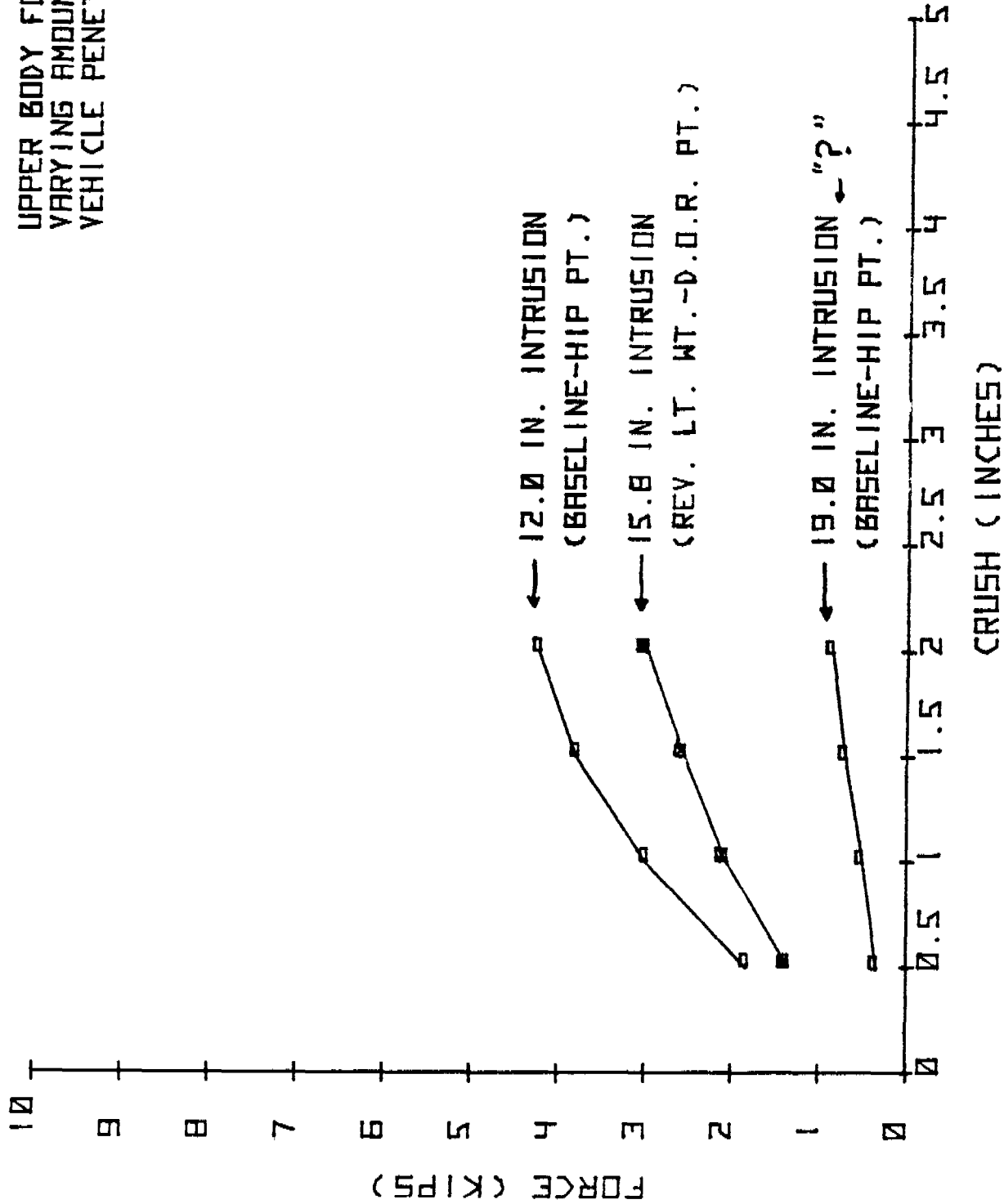
DYNAMIC CRUSH PROPERTIES

WHOLE BODY FORM AT
CONSTANT INTERIOR CRUSH
VEHICLE PENETRATION ON
MOD. (REV. MID. WT.) DOOR
HIP PT. IMPACT



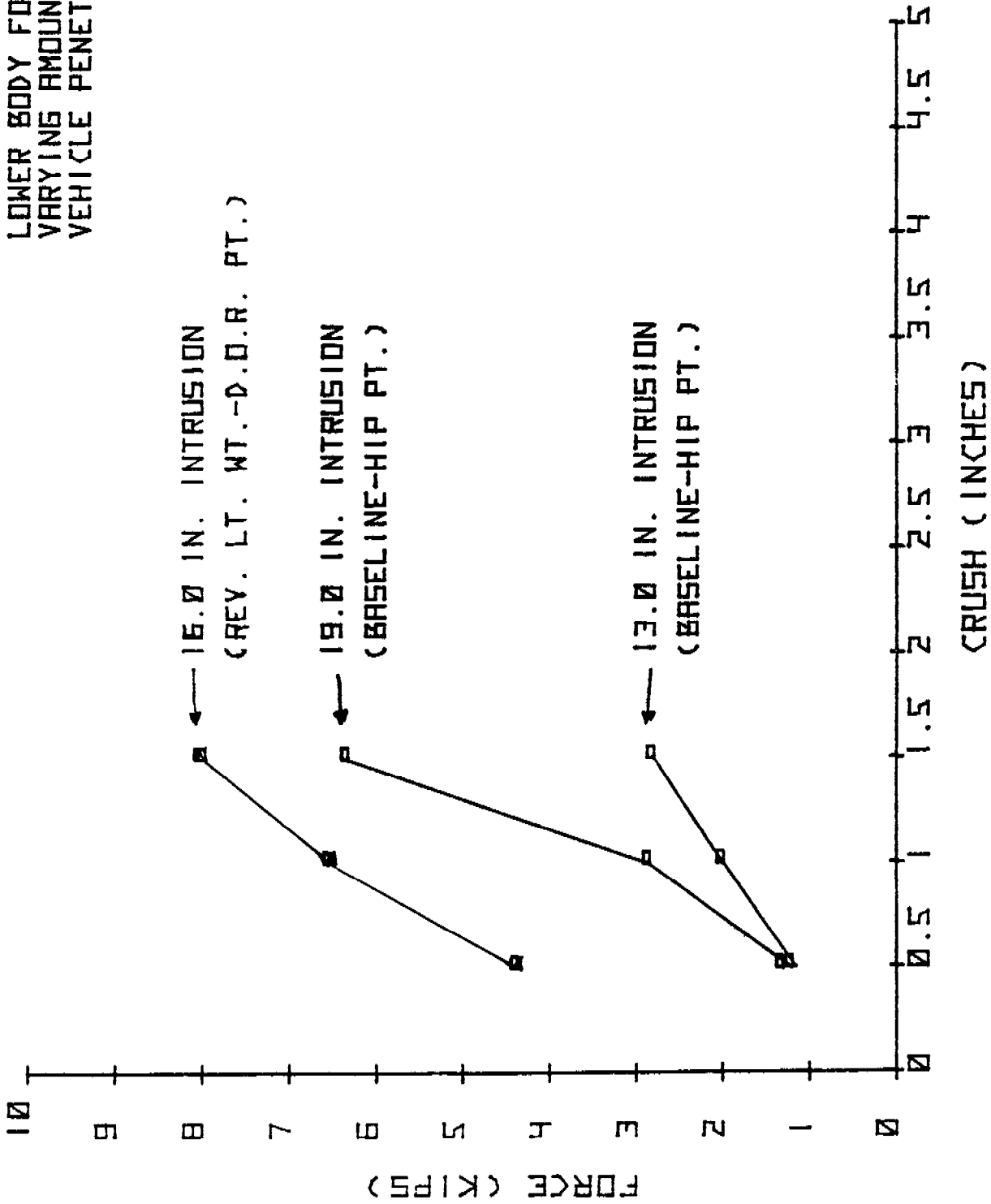
DYNAMIC CRUSH PROPERTIES

UPPER BODY FORM AT
VARYING AMOUNTS OF
VEHICLE PENETRATION



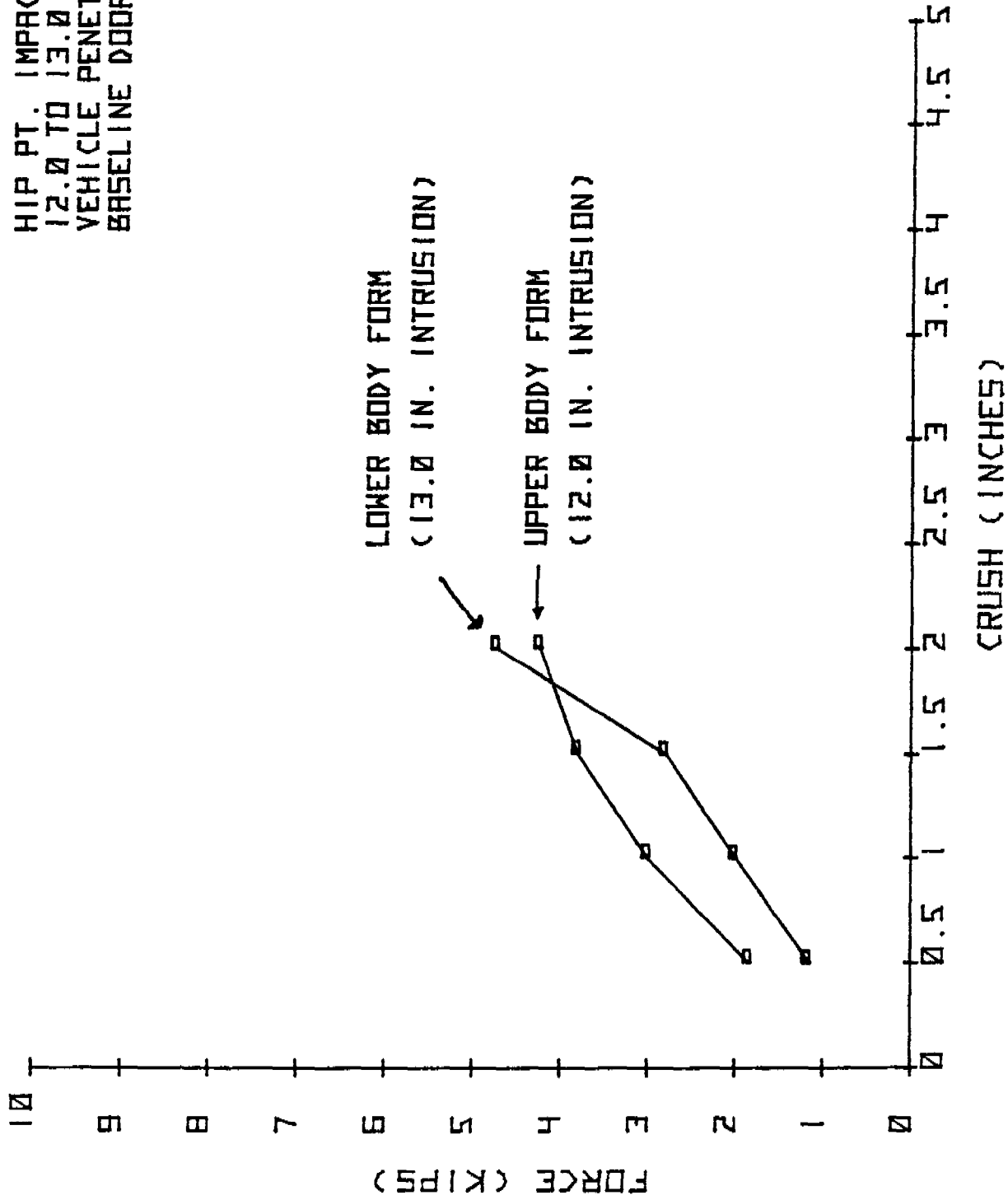
DYNAMIC CRUSH PROPERTIES

LOWER BODY FORM AT
VARYING AMOUNTS OF
VEHICLE PENETRATION



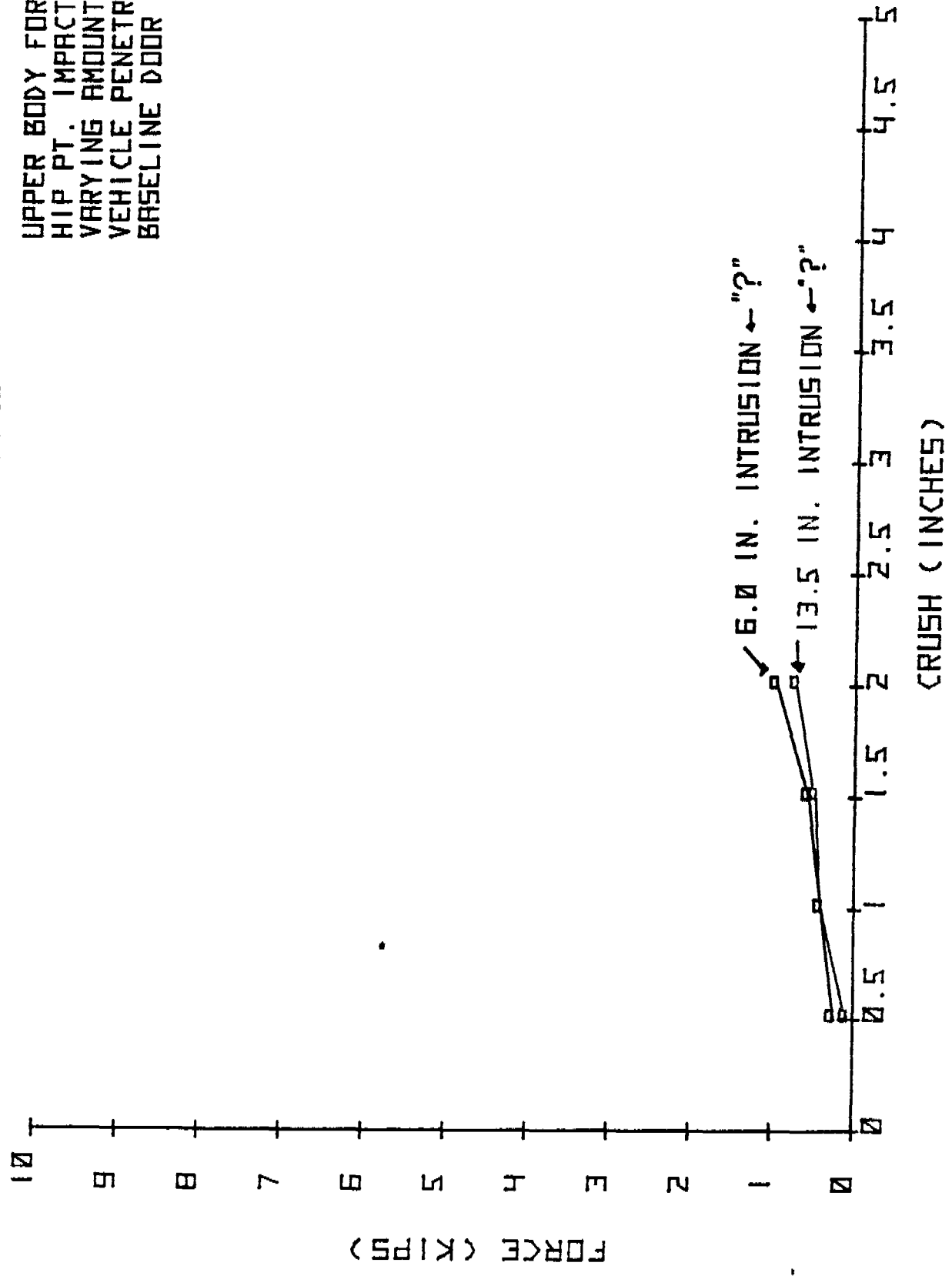
DYNAMIC CRUSH PROPERTIES

HIP PT. IMPACT AT
12.0 TO 13.0 INCHES OF
VEHICLE PENETRATION
BASELINE DOOR



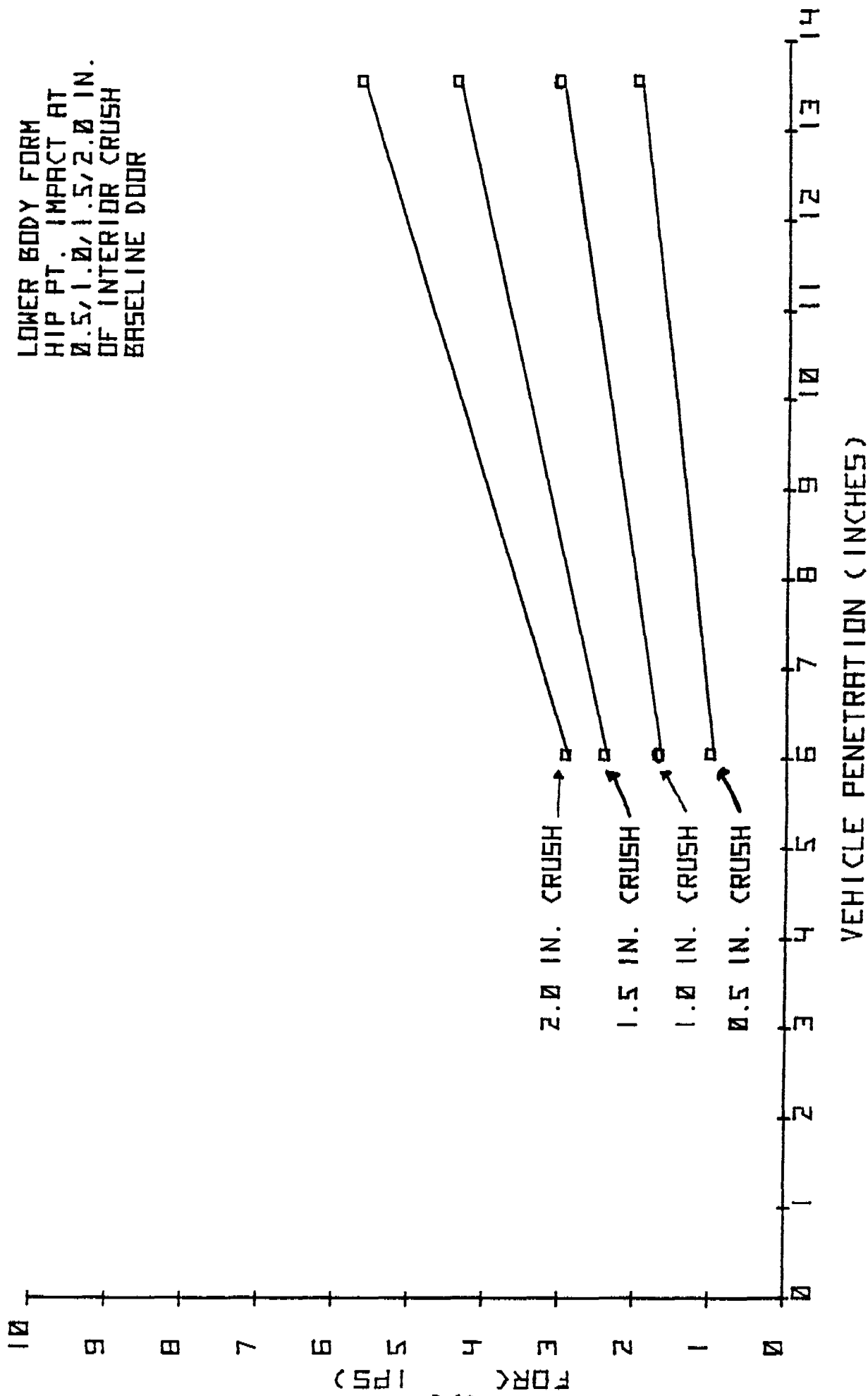
STATIC CRUSH PROPERTIES

UPPER BODY FORM
HIP PT. IMPACT AT
VARYING AMOUNTS OF
VEHICLE PENETRATION
BASELINE DOOR



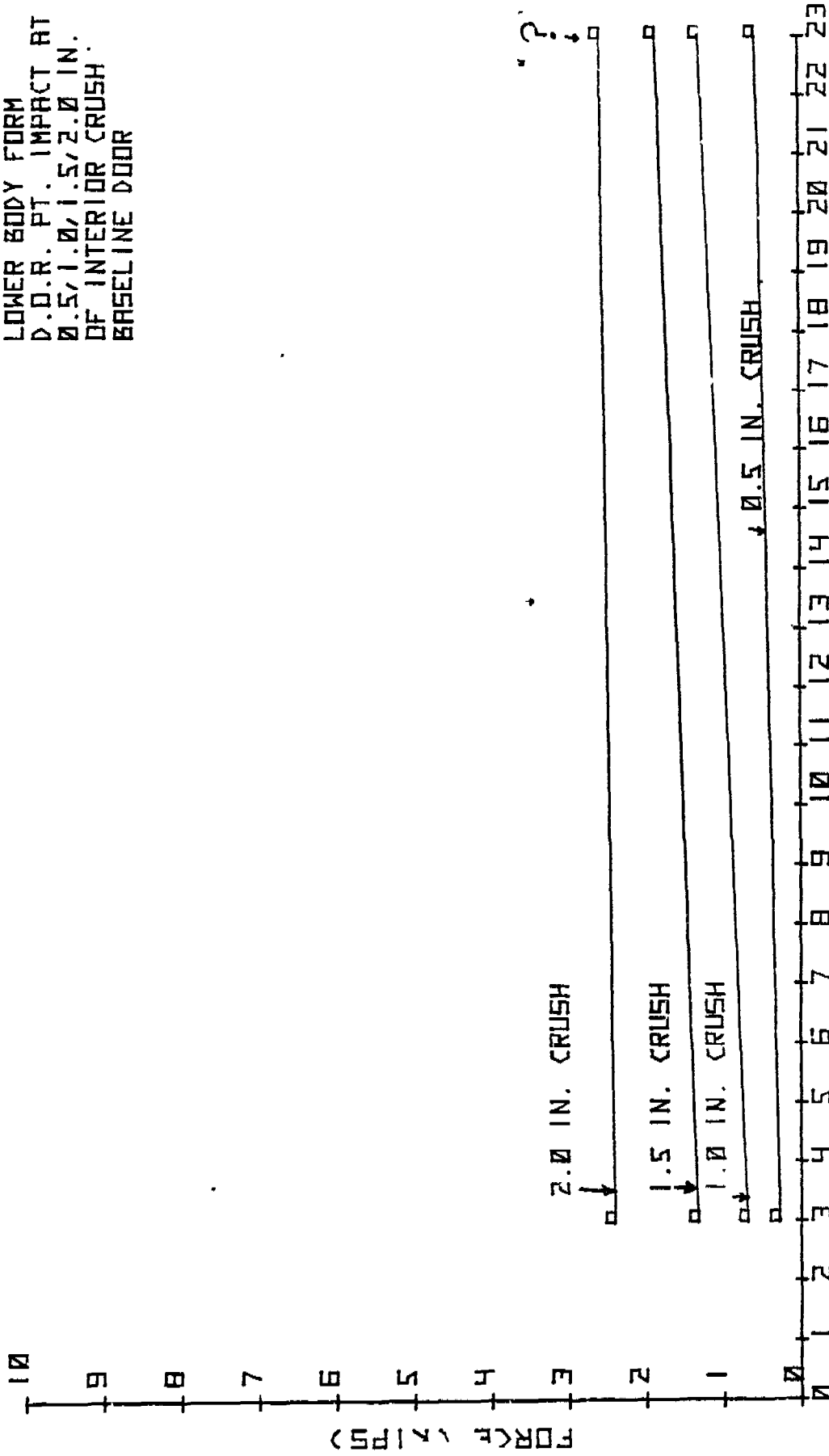
STATIC CRUSH PROPERTIES

LOWER BODY FORM
HIP PT. IMPACT AT
Ø.5/1.Ø/1.5/2.Ø IN.
OF INTERIOR CRUSH
BASELINE DOOR



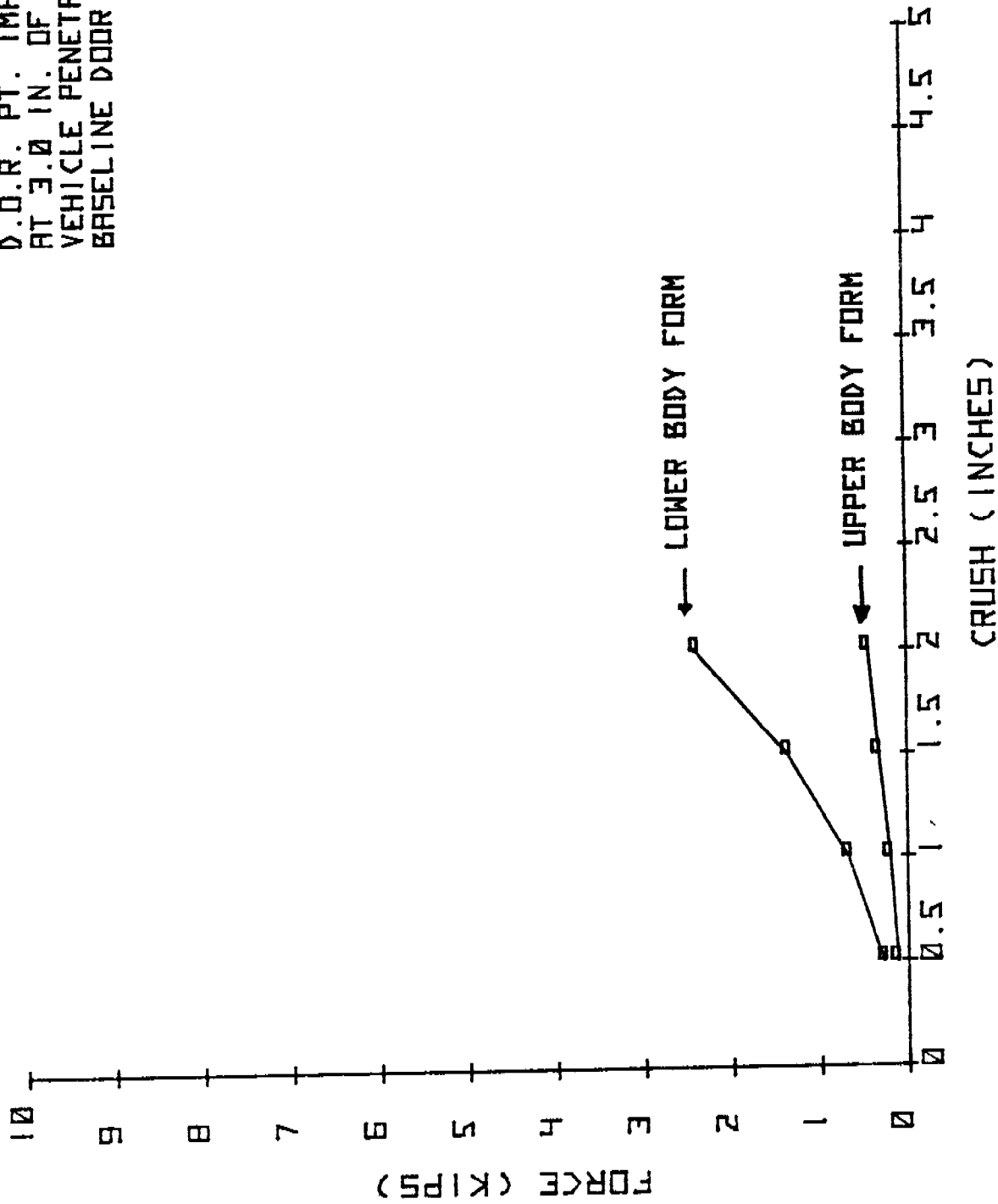
STATIC CRUSH PROPERTIES

LOWER BODY FORM
 D.O.R. FT. IMPACT AT
 0.5/1.0/1.5/2.0 IN.
 OF INTERIOR CRUSH.
 BASELINE DOOR



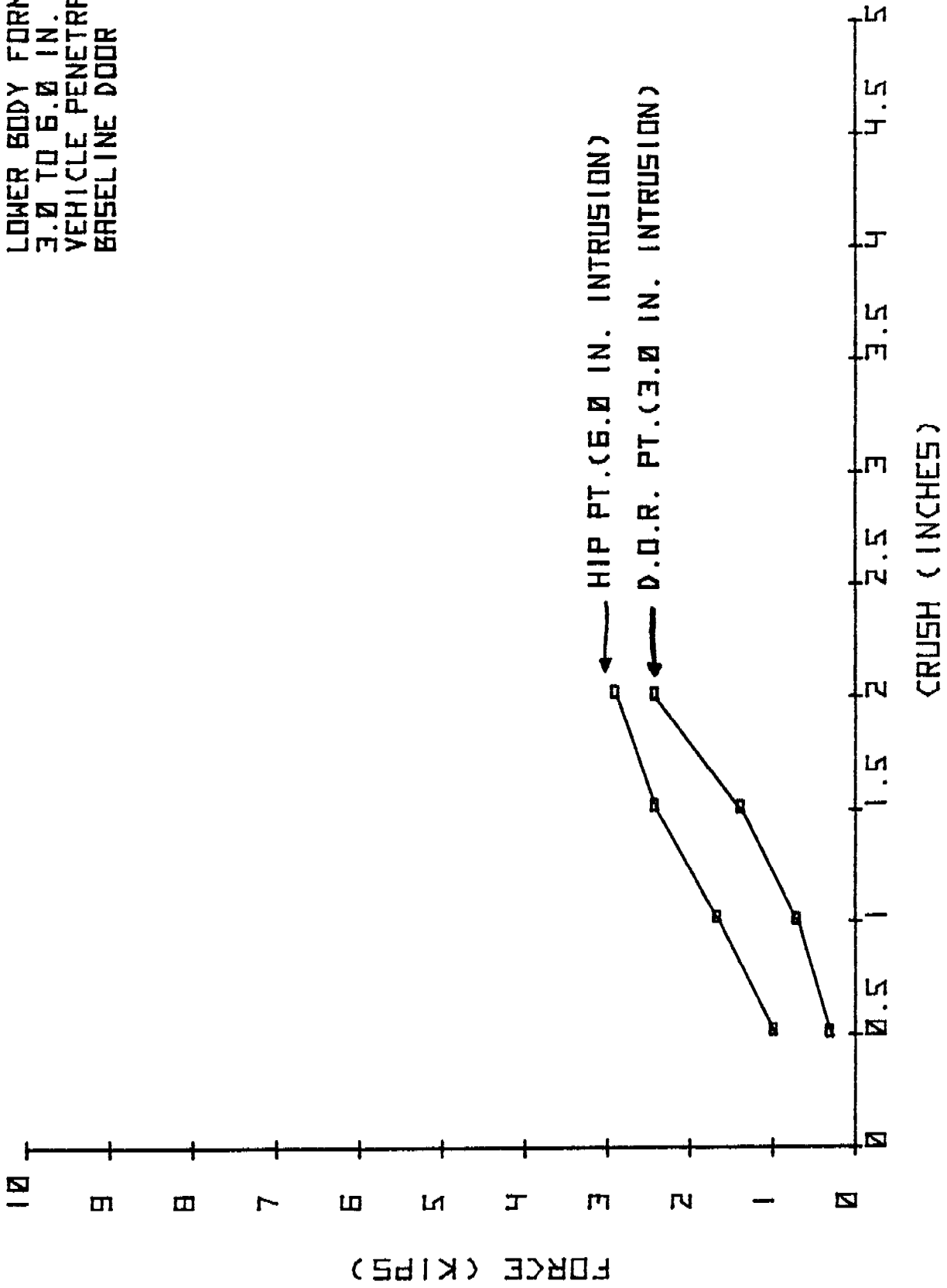
STATIC CRUSH PROPERTIES

D.O.R. PT. IMPACT
AT 3.0 IN. OF
VEHICLE PENETRATION
BASELINE DOOR



STATIC CRUSH PROPERTIES

LOWER BODY FORM
3.0 TO 6.0 IN. OF
VEHICLE PENETRATION
BASELINE DOOR



APPENDIX C

Discussion of Roller Tape Mechanisms

The Tape-Draw Force Limiter

A highly efficient way to utilize a given stroke distance by converting kinetic energy into strain energy of deformation is to design the deformable vehicle structure so as to exhibit a relatively constant force over the stroking distance. If this is done, the g-loads imparted to the vehicle(s) will be essentially constant over the stroke length, thereby eliminating spurious effects, such as instantaneously high deceleration loads that are potentially harmful to the vehicle occupant.

The idea of force limiting mechanism is not new and, in fact, much development work has taken place in an effort to develop a light-weight, low cost, reliable, force limiting mechanism. Although vehicles modified with such a force-limiter have exhibited significant improvements over unmodified vehicles, a large percentage of the solutions were expensive, heavy, and, unfortunately, not reliable. A case in point is the plastic hinge concept. Although, as mentioned, its use results in energy absorption improvements over an unmodified vehicle, it is heavy, rather costly, and due to its ever-changing moment arm during the stroking motion, does not have a constant force-deflection relationship.

To investigate these points a bit further, consider the weight. The plastic hinge concept, by definition, is plastic only at the hinge point, and during the stroking motion, only this section of the member is being utilized to its full potential, while the rest of the member merely goes along for the ride. It, therefore, has a high ratio of weight to absorbed energy.

Consider cost and reliability. The hinge is rather difficult to fabricate at low cost due to the high degree of manufacturing care required to ensure that it does not fail at the hinge joint in a brittle fashion rather than plastically as designed. In addition, the hinge concept has been shown to have erratic results even when tested on the component level under tightly controlled laboratory conditions. Sometimes cracks appear at the joints and on occasion the failure mode has been simply a buckling of the compression flange. These characteristics when coupled with the fact that the deforming force varies with stroke instead of being constant as would be desired, show the need for a more optimal energy management system.

between force and stroke is definitely not a constant force relationship, and in fact, is usually highly non-linear. However, by proper adjustment of the tape width and/or other parameters that will be discussed later, a substantially constant force during the stroking length could be realized. Thus, the roller-tape system exhibits a high degree of versatility in that the tape axis need not be co-linear with stroking direction.

Specific Applications

Let us now discuss some specific applications of the tape-roller system.

The writer is familiar with several applications in which the tape-roller system has been successfully used as an energy absorption device; however two stand out as prime examples of how such a device might be used.

Force limiting in belt systems has been accomplished by pulling a mild steel tape through a set of rollers as shown in Figure 1. Force limiting in impact sled decelerator design, has been accomplished in a similar method but with the tape draw axis at ninety degrees to the impact direction (Figure 2). The equations that describe the tension in the metal tape are identical for the two cases; however the force required to produce tape drawing is different since the direction of force application is different. In the following we will discuss the general operation of the device in some detail. After this discussion it will be apparent as to how the designer would proceed in each of the two general cases cited above.

Let us examine the type of application shown in Figure 1 in some

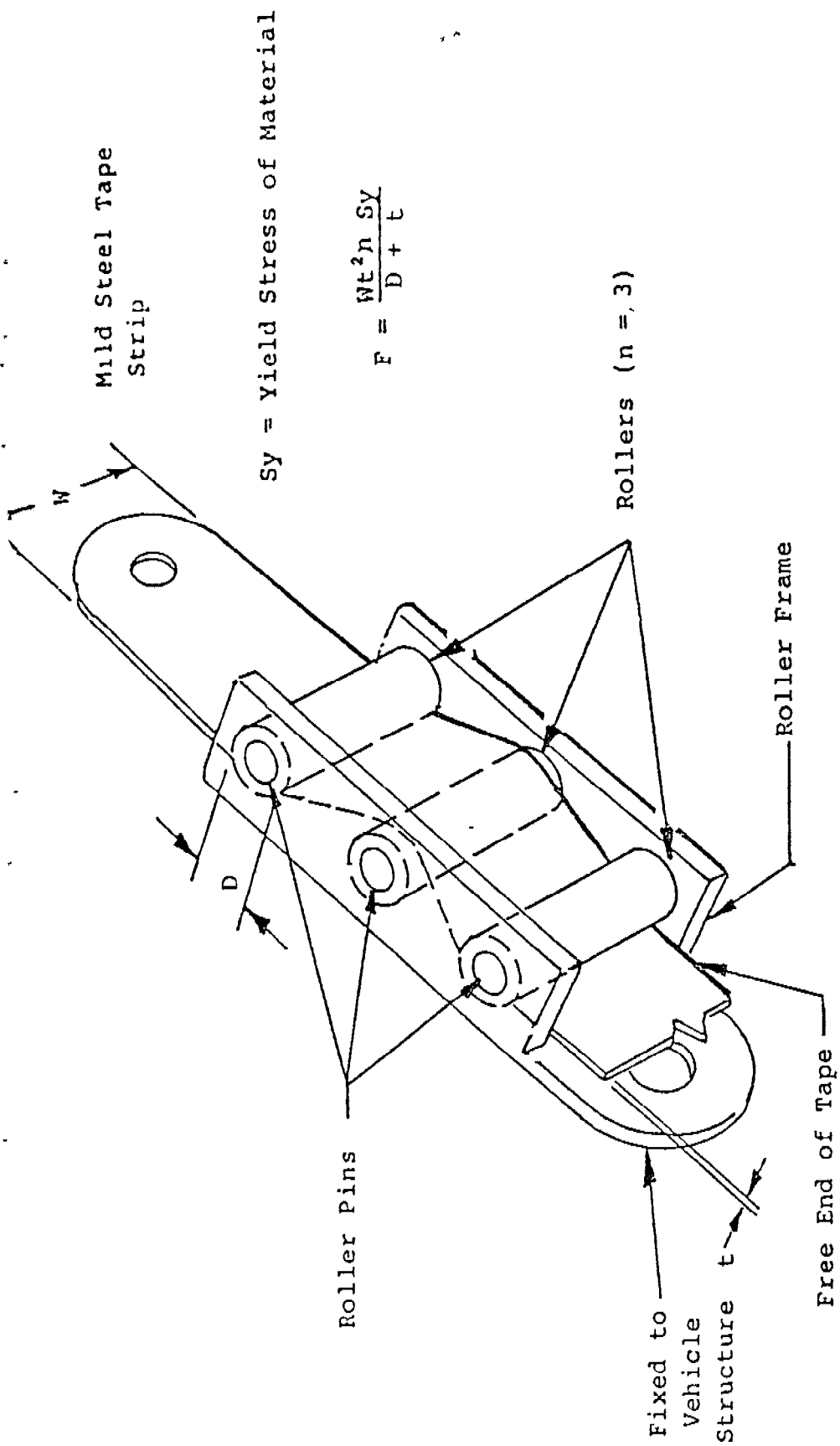
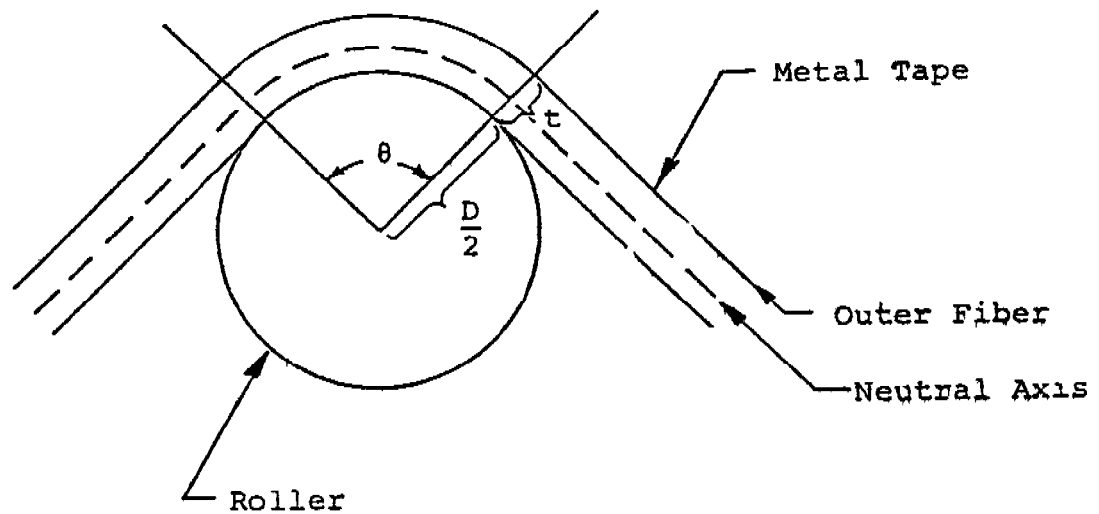


FIGURE 1 FORCE LIMITER



Strain (ϵ) = $\frac{\text{length of outer fiber} - \text{length of neutral axis}}{\text{length of neutral axis}}$

$$\epsilon = \frac{\theta \left(\frac{D}{2} + t \right) - \theta \left(\frac{D+t}{2} \right)}{\theta \frac{D+t}{2}}$$

$$\epsilon = \frac{t}{D+t} \quad \text{for one roller}$$

$$\epsilon = \frac{Nt}{D+t} \quad \text{where } N \text{ is the number of rollers}$$

STRAIN EQUATION

Figure 3

where t and D are in inches and dS_y in lbs/sq. in.. It should be noted that the equation is only valid up to a total stress, S_y plus dS_y = the ultimate strength of the material.

Friction can be assumed to be negligible in all true roller applications and, even when the roller is replaced with a non-rolling pin, the coefficient of friction is usually low varying from approximately 0.12 for completely unlubricated surfaces to 0.04 for lubricated surfaces (see Ref. 1, Appendix A).

Experience has shown that a good estimate on strain rate effects can be obtained by multiplying the basic equation by strain rate factor equal to:

$$(3) \quad \text{SRF} = 1 + 0.08 \cdot \log(V)$$

where V is the strain velocity in in/min. Using all the relationships previously derived, we end up with a general equation for the force required to pull the tape through the rollers equal to:

$$(4) \quad F = \frac{N W t^2 (S_y + dS_y) (\text{SRF})}{D + t}$$

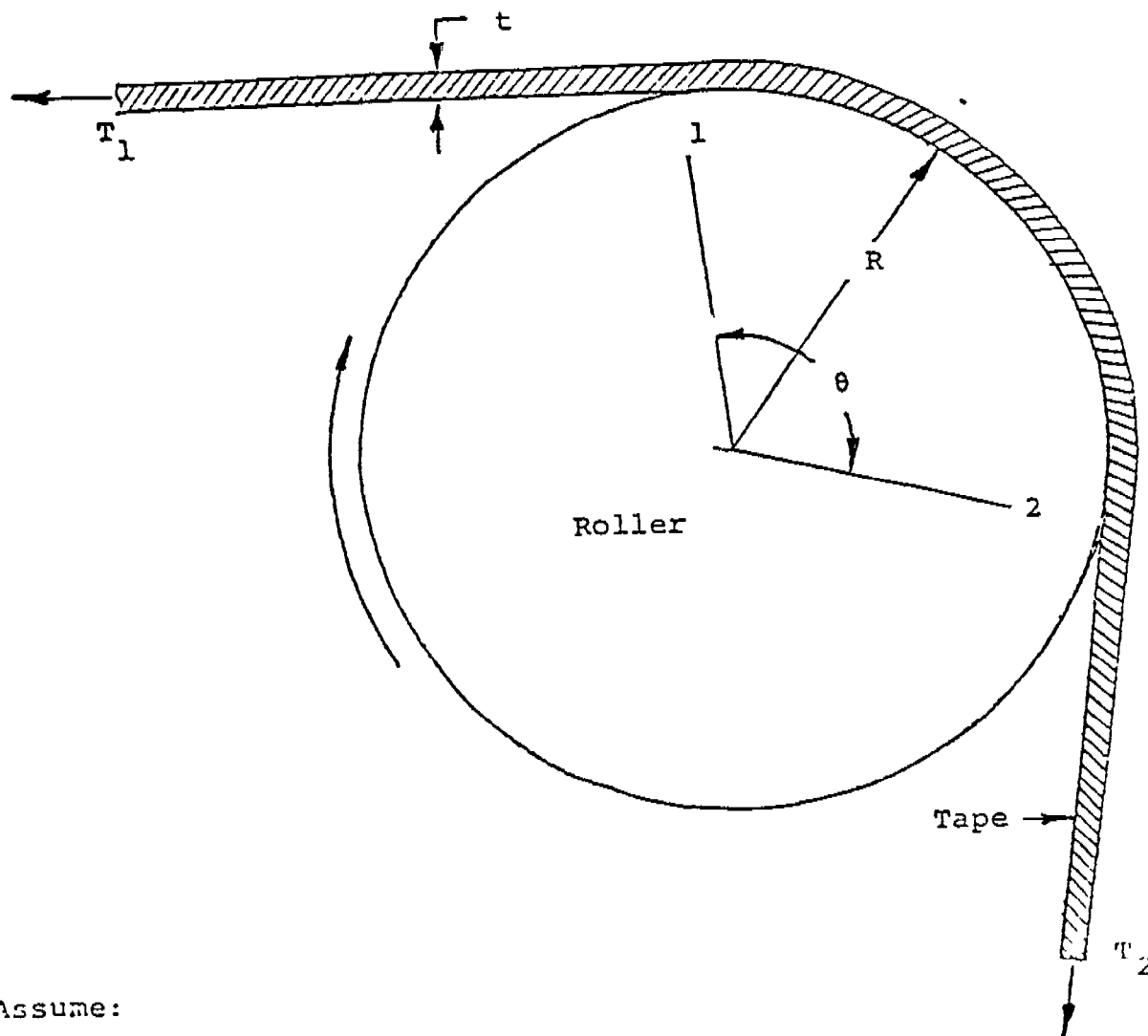
where all the values have been defined above.

This discussion completes a general description of how the tape-roller force limiter functions. With a little imagination the designer should be able to visualize many more applications. Figures 4 through 6 show a few more variations for belt restraint system applications.

ATTACHMENT A

Force Limited Tape/Roller Analysis

Prepared by: Michael Fitzpatrick



Assume:

1. No friction between tape and roller
2. Neutral axis of tape at $t/2$
3. Strain energy absorbed in exceeding elastic limit of material is negligible when compared to energy absorbed during plastic deformation.

Between Points 1 and 2, the strain in the tape is constant since the radius of curvature and stress condition is constant. After leaving Point 2, however, the tape must straighten so that more strain energy is absorbed by the tape. In the absence of strain hardening effects and for tape tensile stresses small compared with bending stresses this energy will be the same as that at Point 1.

Equating the work done in pulling the tape over the roller to the strain energy stored in the tape, we have:

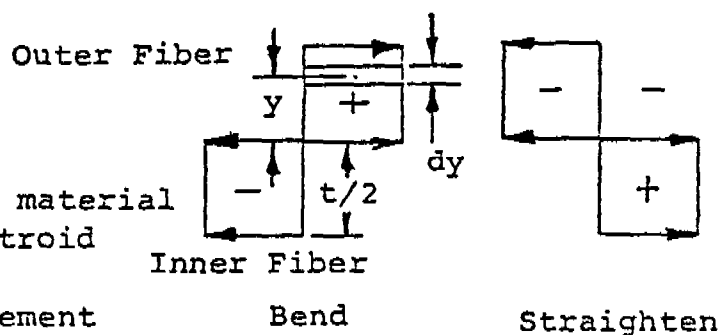
$$(T_2 - T_1)R\theta = 2M_p\theta \quad \text{or}$$

$$(2) \quad T_2 - T_1 = \frac{2M_p}{R} \quad \text{(The factor "2" comes from energy being absorbed at two places on the roller.)}$$

For a fully plastic section and the initial assumptions:

$$M_p = 2 \int_0^{t/2} WT_y y dy$$

Where: W = tape width
 T = yield stress of material
 y = distance to centroid of dy
 dy = thickness of element



$$(3) \quad M_p = 2WT_y \left[\frac{y^2}{2} \right]_0^{t/2} = \frac{WT_y t^2}{4}$$

Substituting (2) into (3)

$$(4) \quad T_2 - T_1 = \frac{T_y W t^2}{2R}$$

LIST OF REFERENCES

1. Swift, H.W., "Plastic Bending Under Tension", paper presented at the Seventh International Congress for Applied Mechanics, London, September 5-11, 1948.
2. Hayden, H.W., "The Structure and Properties of Materials", Volume III "Mechanical Behavior", John Wiley and Sons, Inc., New York. 1965.
3. Fitzpatrick, M.V., "Approximate Analysis of Plastic Deformation of Tape-Draw Mechanism", unpublished analysis for Minicars, Inc. 1972.

PROJECT

J & ORDER NO

CALCULATION SERIAL NO

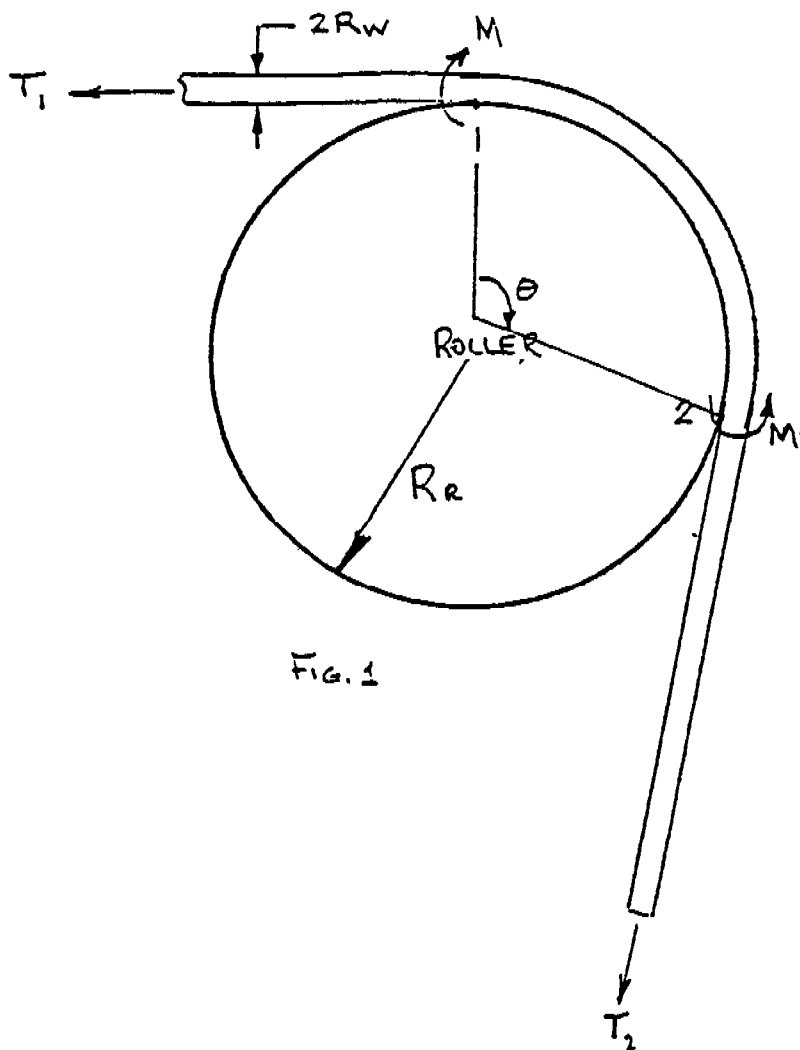


FIG. 1

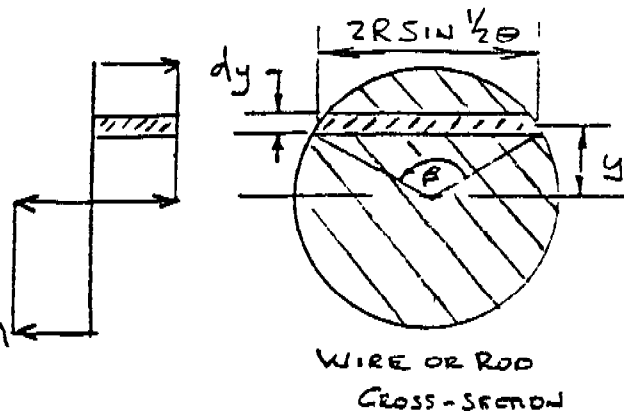


FIG. 2

AS THE WIRE APPROACHES THE ROLLER IT IS SUBJECTED TO A CONSTANTLY INCREASING BENDING MOMENT UNTIL AT SOME POINT THE STRESS IN THE OUTERMOST FIBERS REACHES THE YIELD POINT. THE RADIUS OF CURVATURE OF THE WIRE AT THIS POINT IS:

$$R = \frac{EI}{M_0}$$

PREPARED BY MICHAEL FITZPATRICK

DATE 11/ /19

CHECKED BY

DATE

PROJECT

JOB ORDER NO

CALCULATION SERIAL NO

THE WIRE FIRST CONFORMS TO THE ROLLER AND THEN AGAIN AS IT LEAVES THE ROLLER.

EQUATING THE WORK DONE IN PULLING THE WIRE OVER THE ROLLER TO THE STRAIN ENERGY STORED IN THE WIRE WE HAVE:

$$(T_2 - T_1) R_R \Theta = 2 M_P \Theta$$

WHERE M_P IS THE MOMENT IN THE WIRE FOR A FULLY PLASTIC CONDITION.

FOR A FULLY PLASTIC SECTION (SEE FIG. 2) WE HAVE

$$M_P = 2 T_{y.p.} \int_0^{R_w} y \, dA \quad \text{WHERE}$$

$$dA = 2 R_w \sin \frac{1}{2} \theta \, dy$$

WE MAY REWRITE $\frac{1}{2} \theta$ AS $\cos^{-1} y/R$ OR $\sin^{-1} \frac{\sqrt{R_w^2 - y^2}}{R_w}$

SO,

$$dA = 2 \sqrt{R_w^2 - y^2} \, dy \quad \text{SO THAT,}$$

$$M_P = 4 T_{y.p.} \int_0^{R_w} y \sqrt{R_w^2 - y^2} \, dy = 4 T_{y.p.} \left[-\frac{1}{3} (R_w^2 - y^2)^{3/2} \right]_0^{R_w}$$

$$M_P = \frac{4 T_{y.p.} R_w^3}{3}$$

SO,

$$(3) \quad T_2 - T_1 = \frac{8 T_{y.p.} R_w^3}{3 R_R} \quad \text{WHICH IS THE BASIC EQN (NEGLECTING STRAIN$$

HARDENING) FOR A ONE-ROLLER SYSTEM.

PREPARED BY

DATE

CHECKED BY

DATE

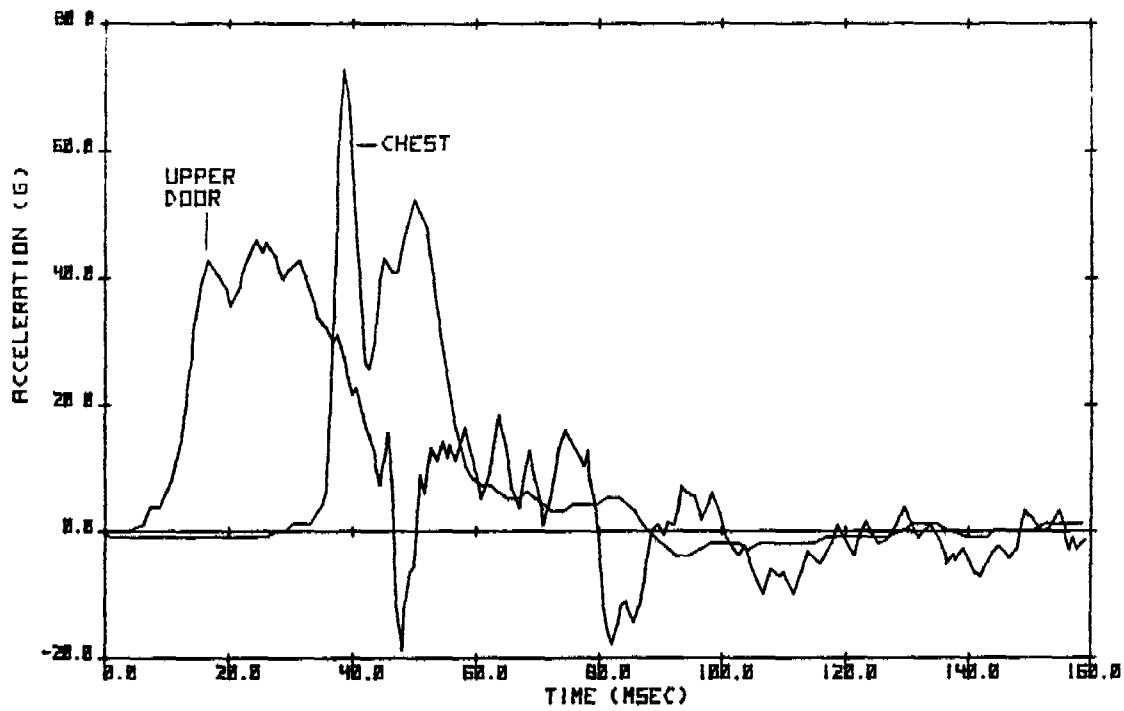
APPENDIX D

Occupant/Door Comparisons from Budd No. 11 Simulation

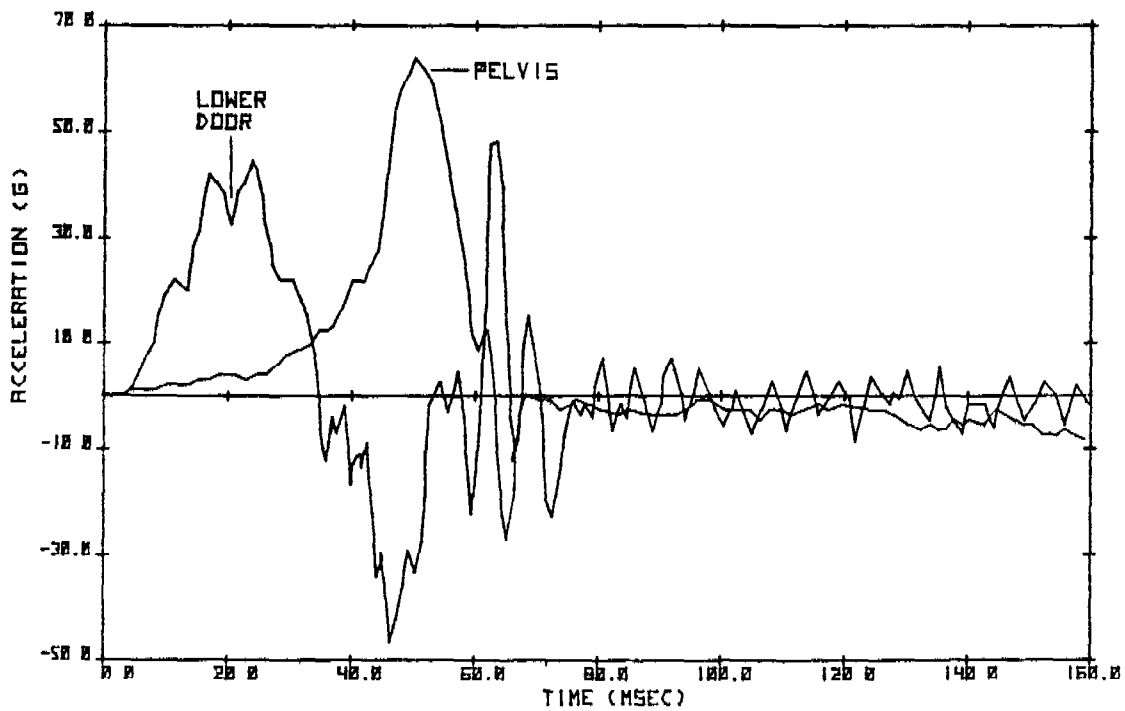
:

4

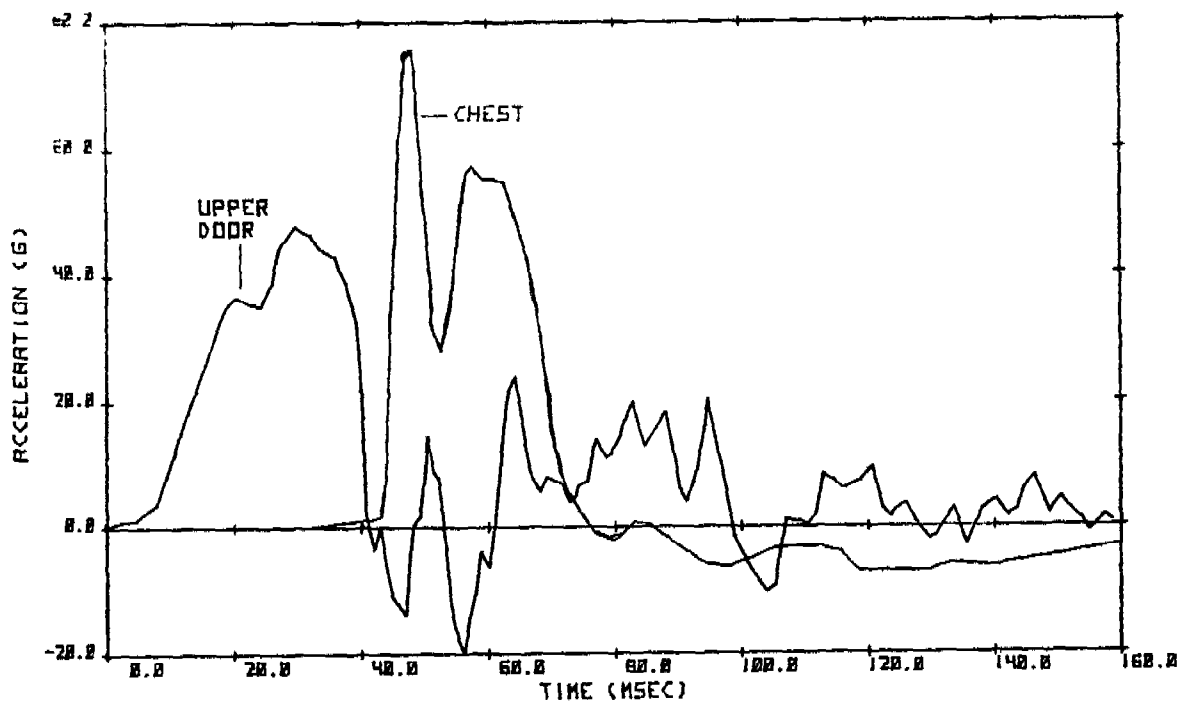
.



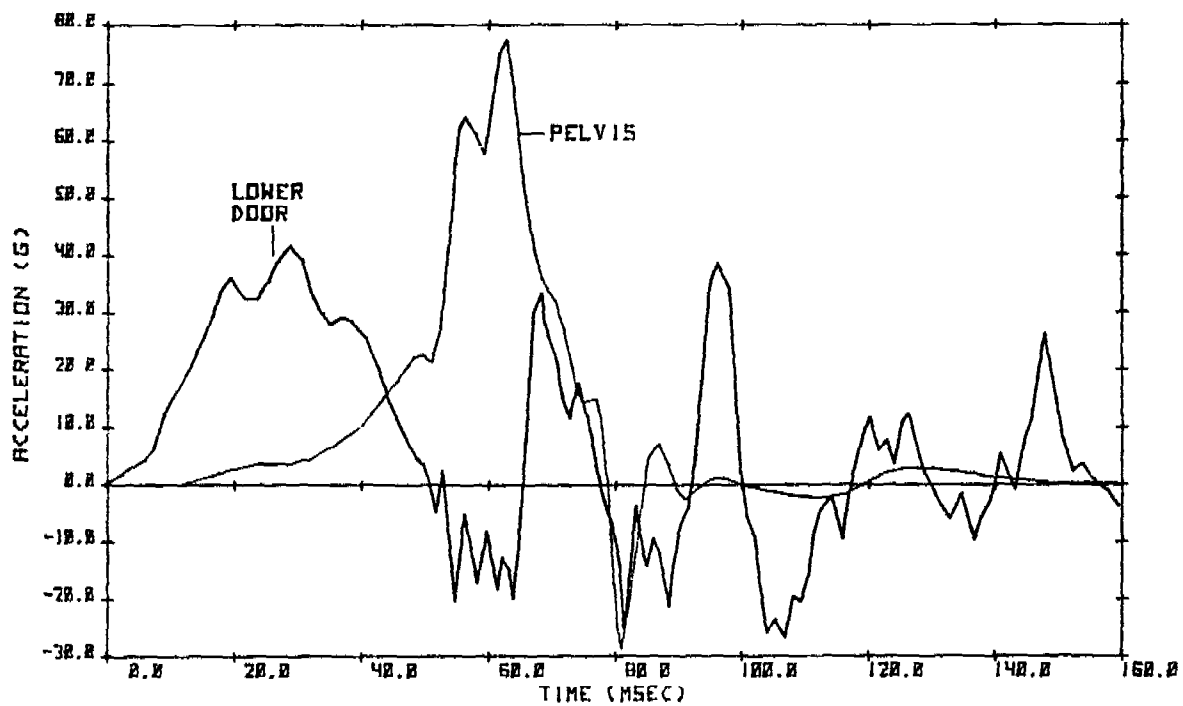
SRL 17-5 TEST #2 -VEHICLE/OCCUPANT-CHEST ACC



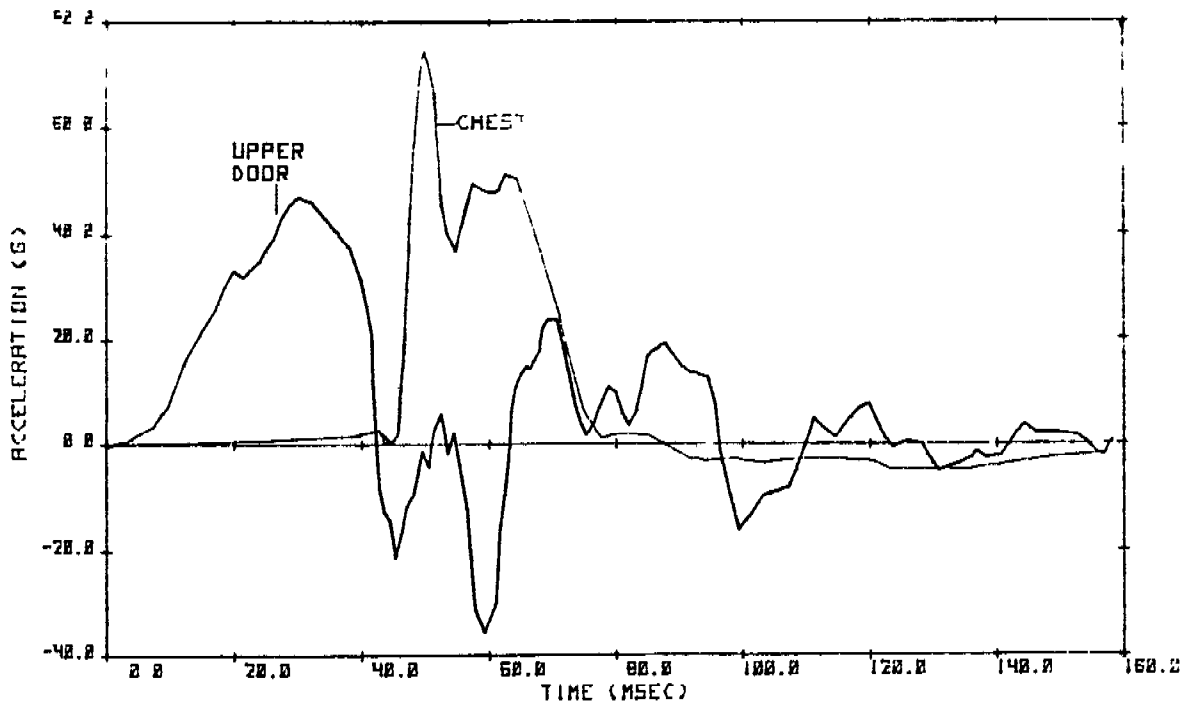
SRL 17-5 TEST #2 - VEHICLE/OCCUPANT-PELVIS ACC



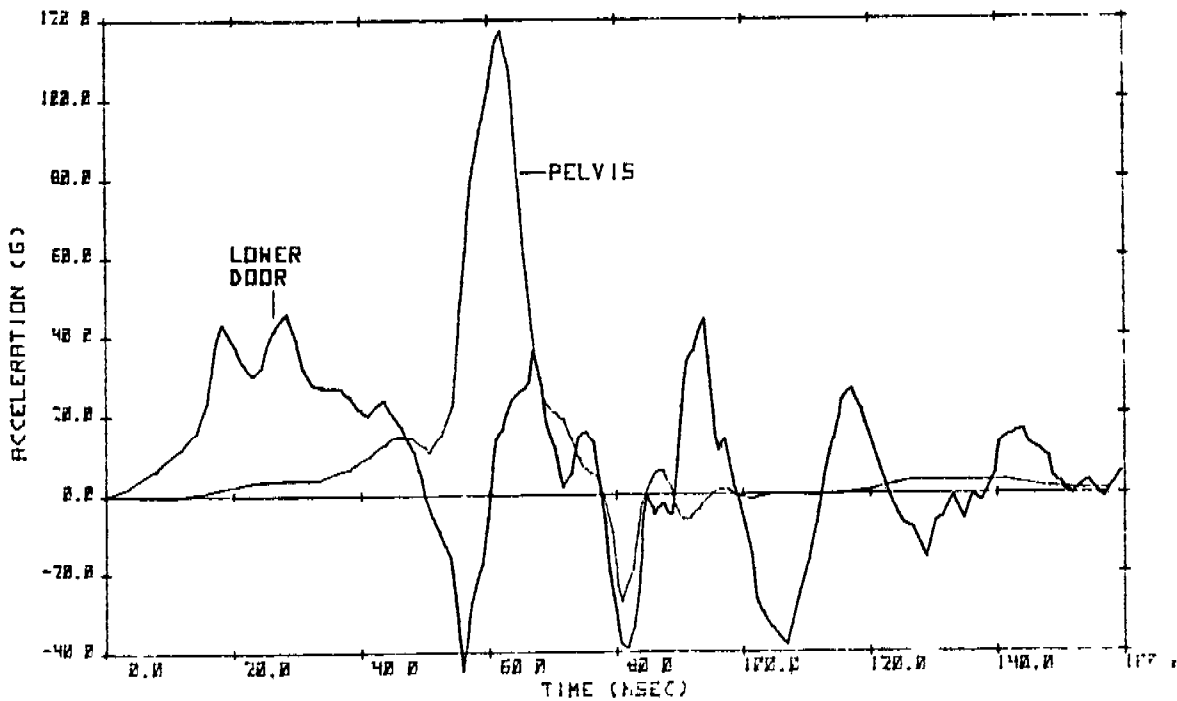
SRL 17-5 TEST #4-VEHICLE/OCCUPANT-CHEST ACC.



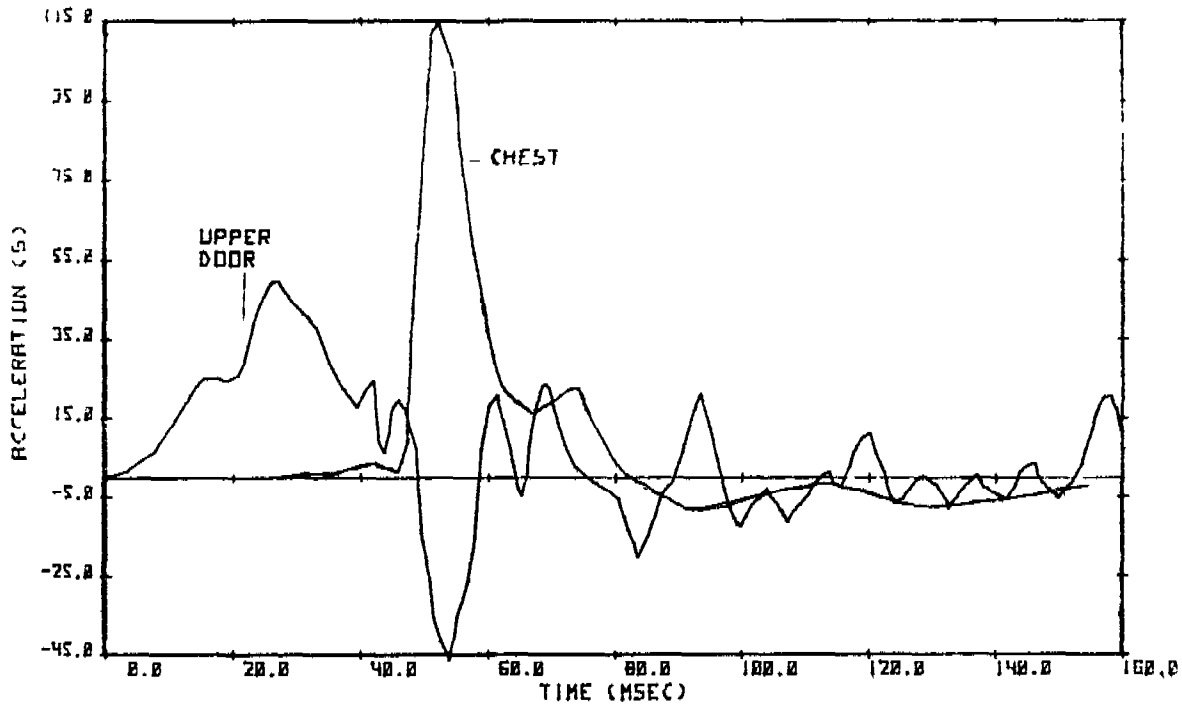
SRL 17-5 TEST #4-VEHICLE/OCCUPANT-PELVIS ACC



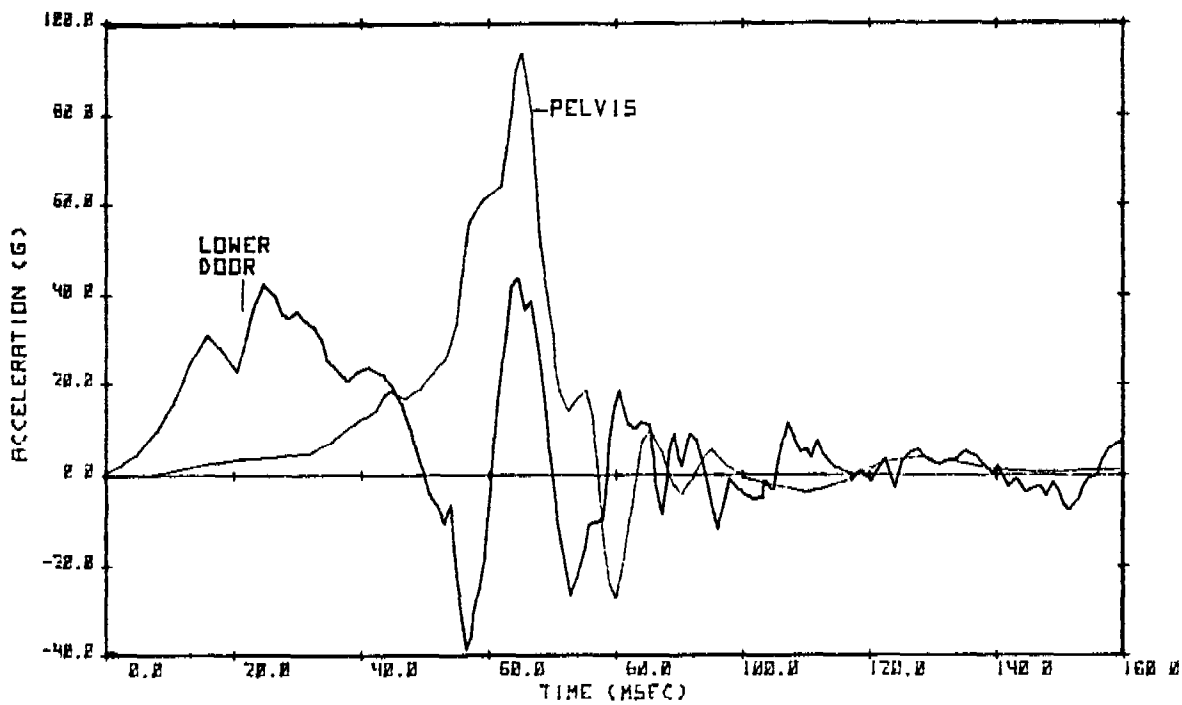
SRL 17-5 TEST #6-VEHICLE/OCCUPANT-CHEST ACC.



SRL 17-5 TEST #6-VEHICLE/OCCUPANT-PELVIS ACC.



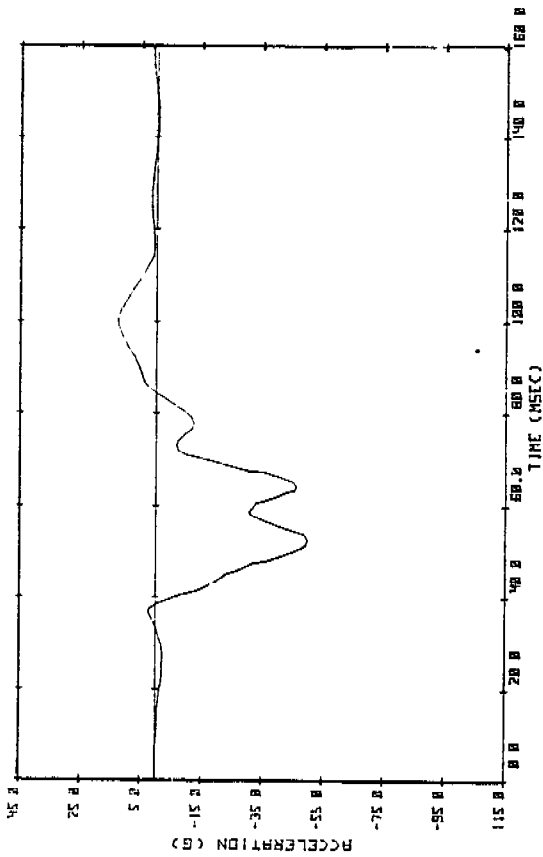
SRL 17-5 TEST #8-VEHICLE/OCCUPANT-CHEST ACC.



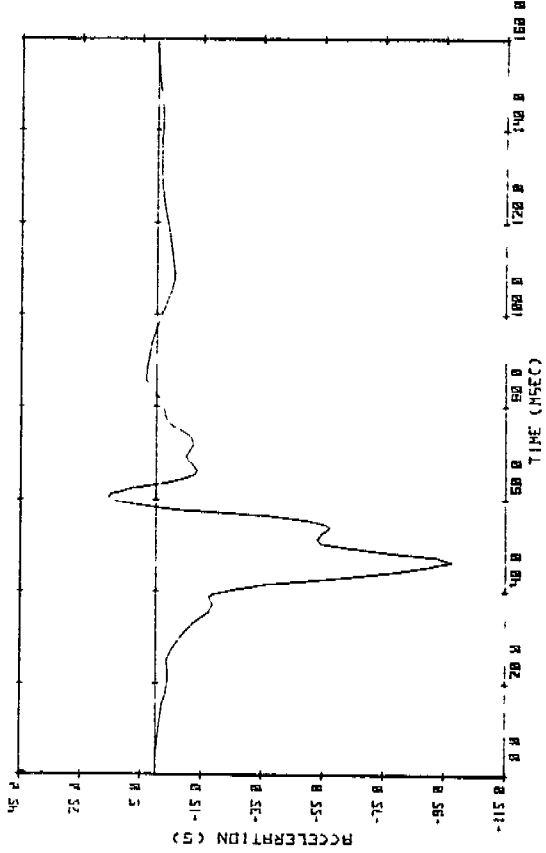
SRL 17-5 TEST #8-VEHICLE/OCCUPANT-PELVIS ACC

APPENDIX E

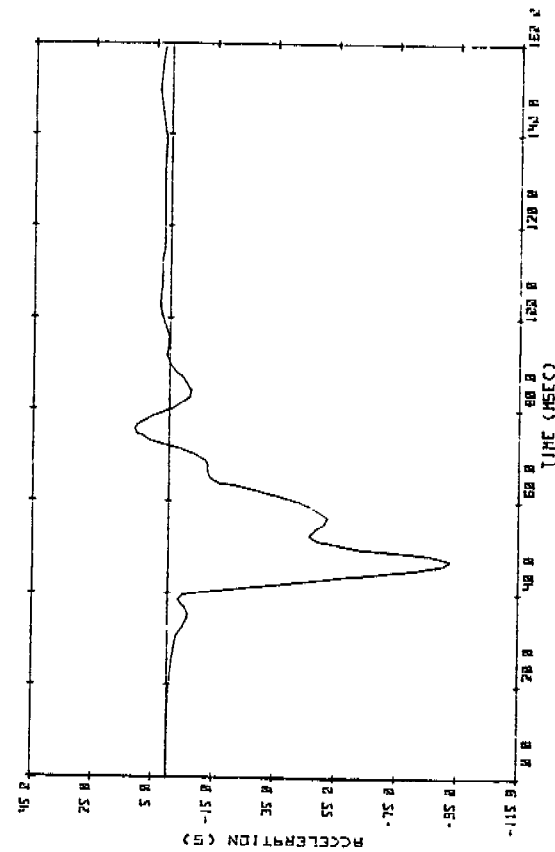
Body Form Responses from Dynamic
Science Test No. 8330-2 Simulation



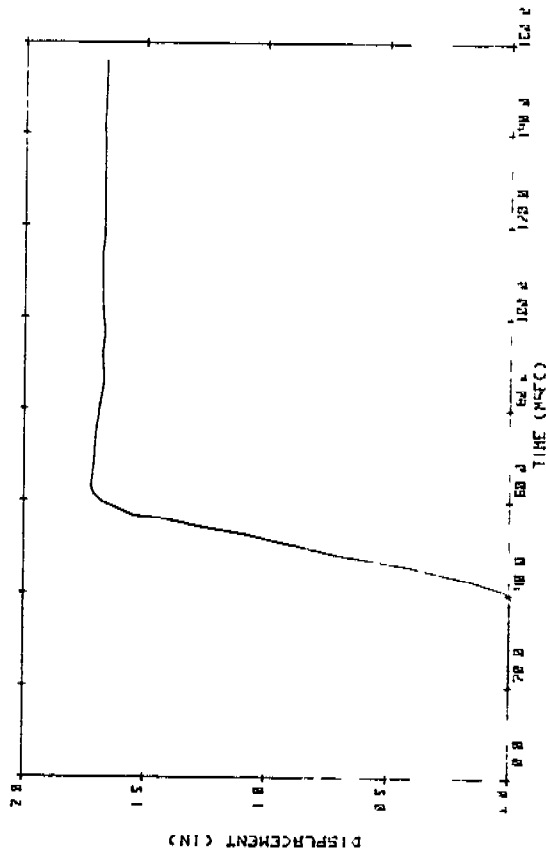
SRL 17-5 TEST #10 - UPPER SPINE



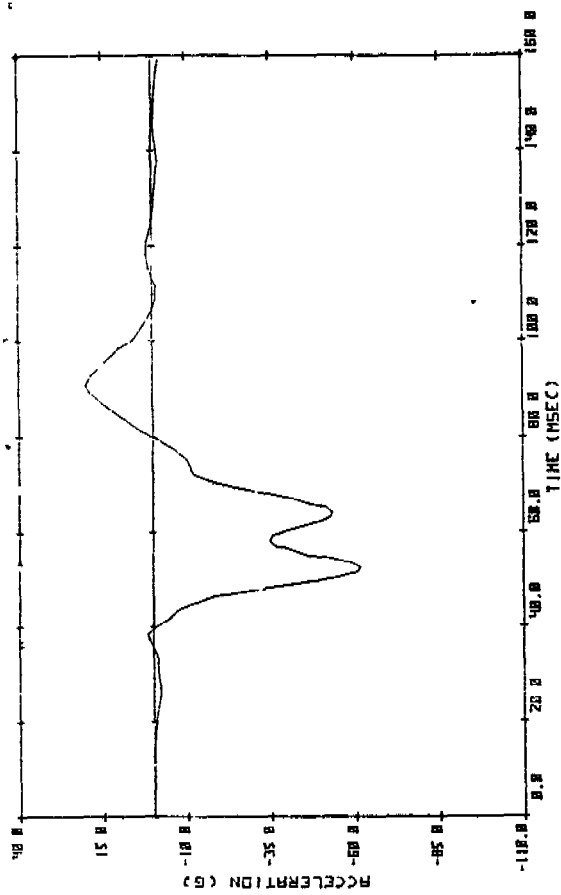
SRL 17-5 TEST #10 PELVIS



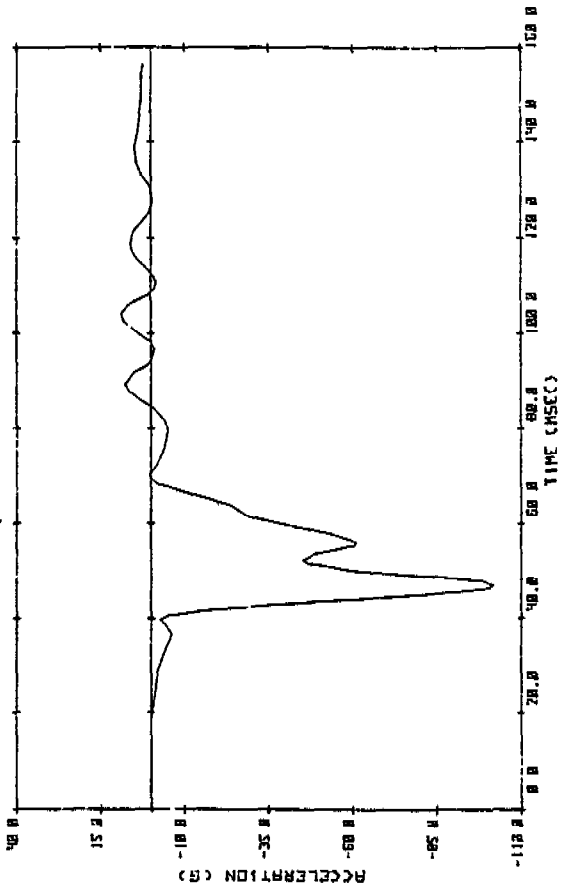
SPL 17-5 TEST #10 - LOWER SPINE



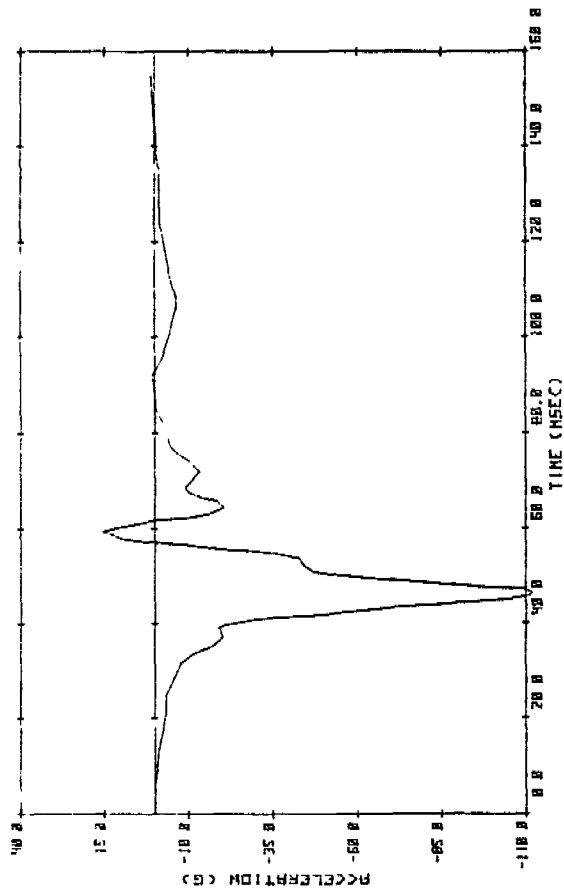
SPL 17-5 TEST #10 CHEST OUT



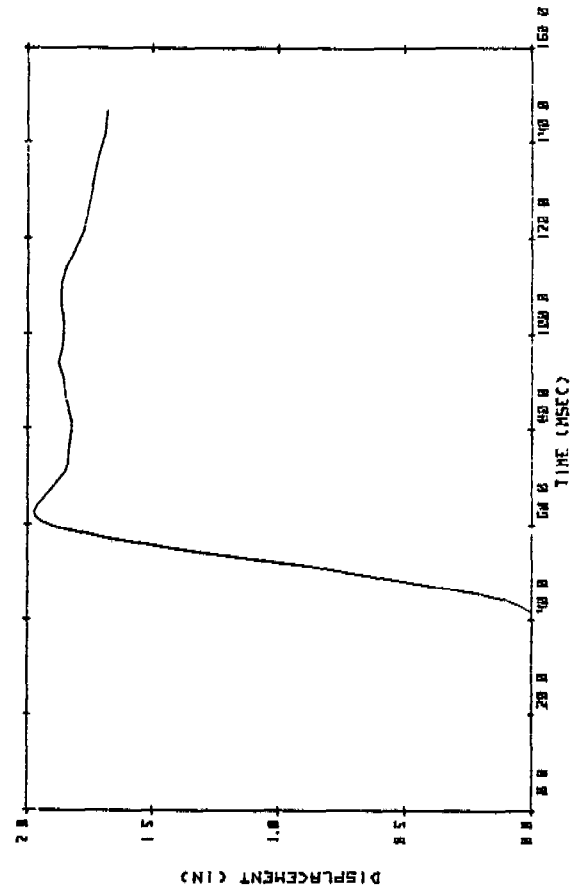
SRL 17-5 TEST #11 - UPPER SPINE



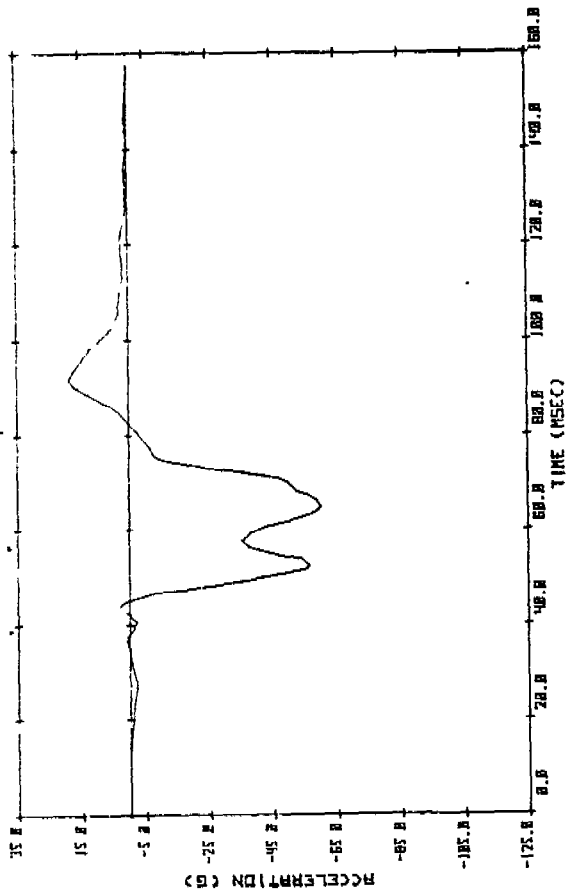
SRL 17-5 TEST #11 - LOWER SPINE



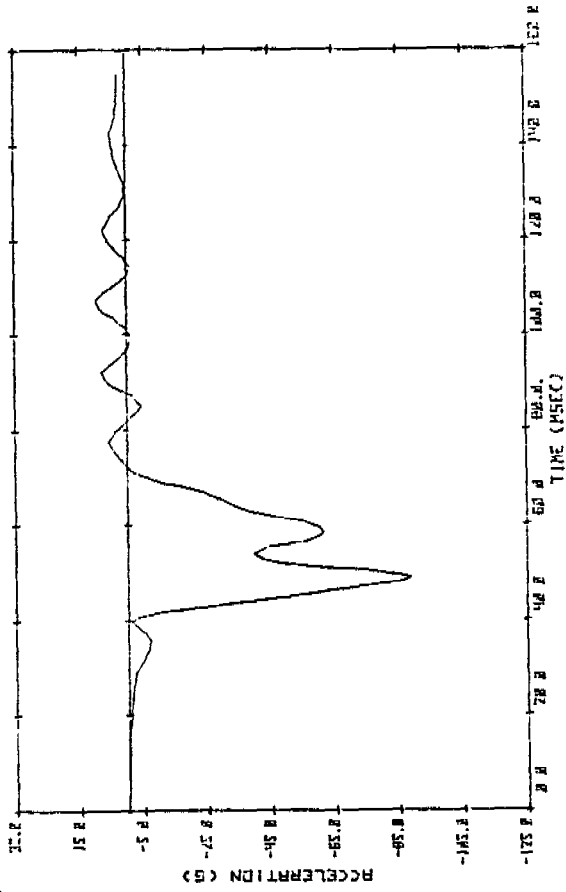
SRL 17-5 TEST #11 - PELVIS



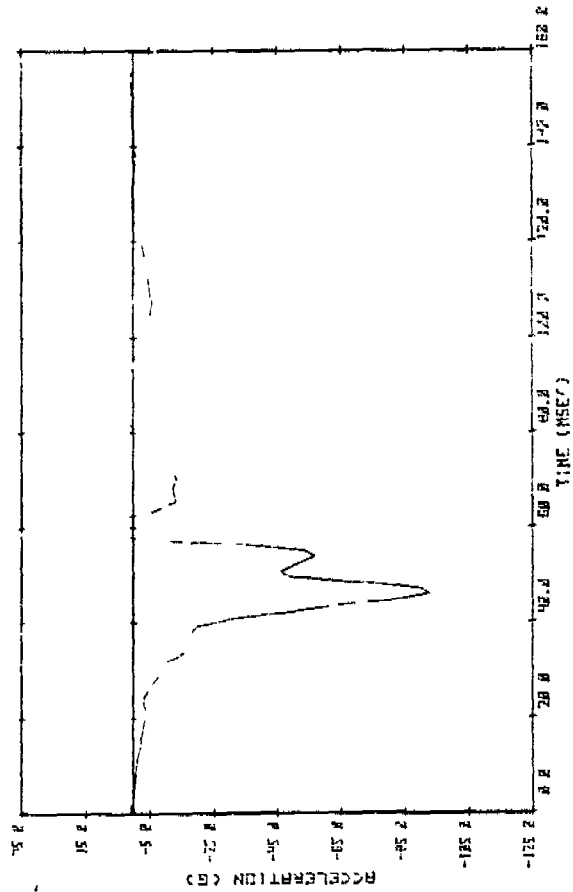
SRL 17-5 TEST #11 - CHEST DEFLECTION



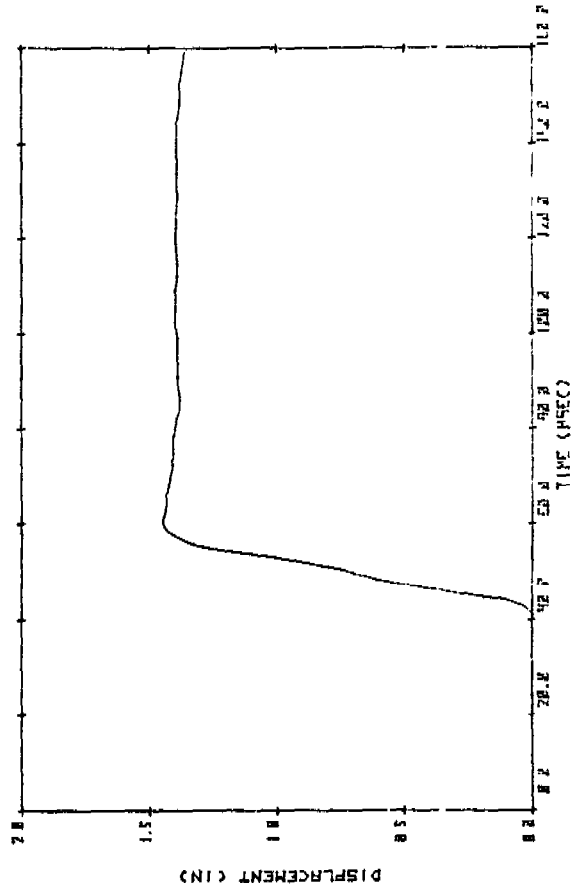
SRL 17-5 TEST #12 - UPPER SPINE



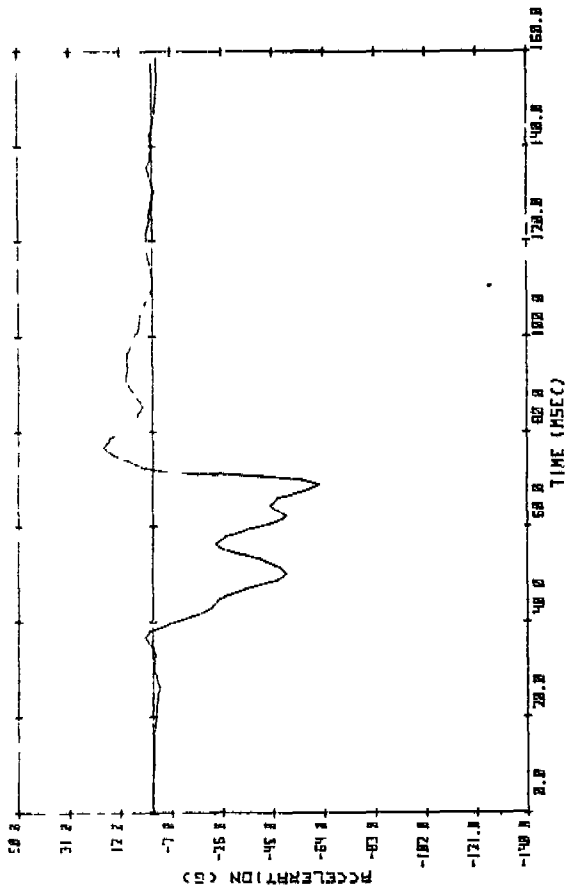
SRL 17-5 TEST #12 - LOWER SPINE



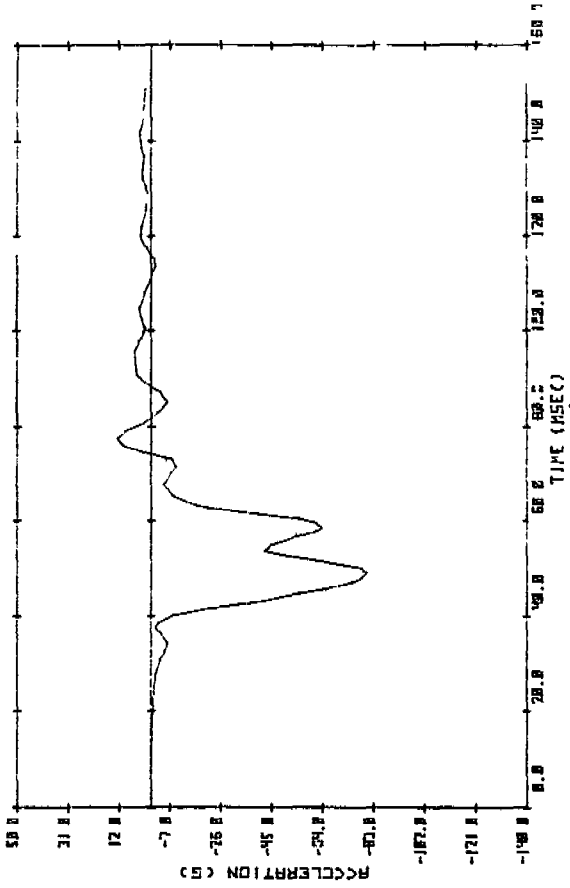
SRL 17-5 TEST #12 - CHEST DEFLECT



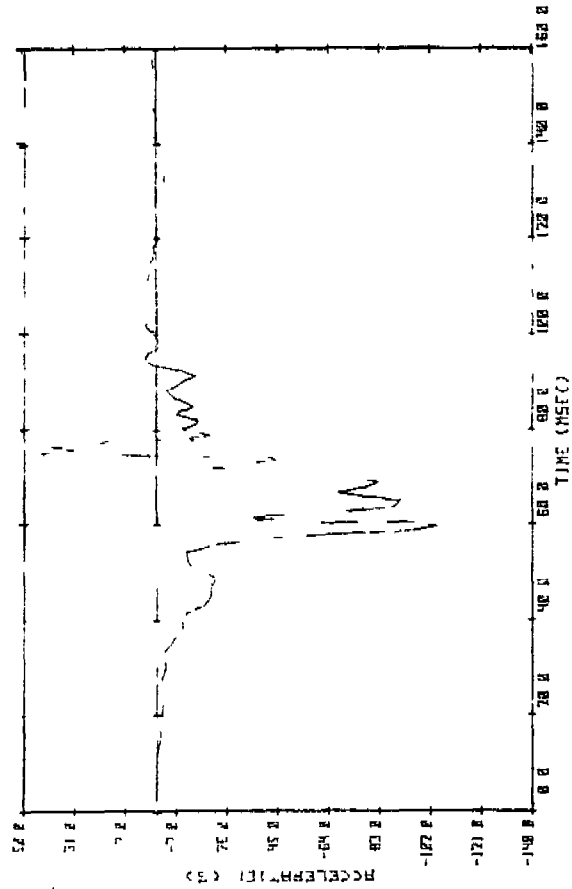
SRL 17-5 TEST #12 - CHEST DEFLECT



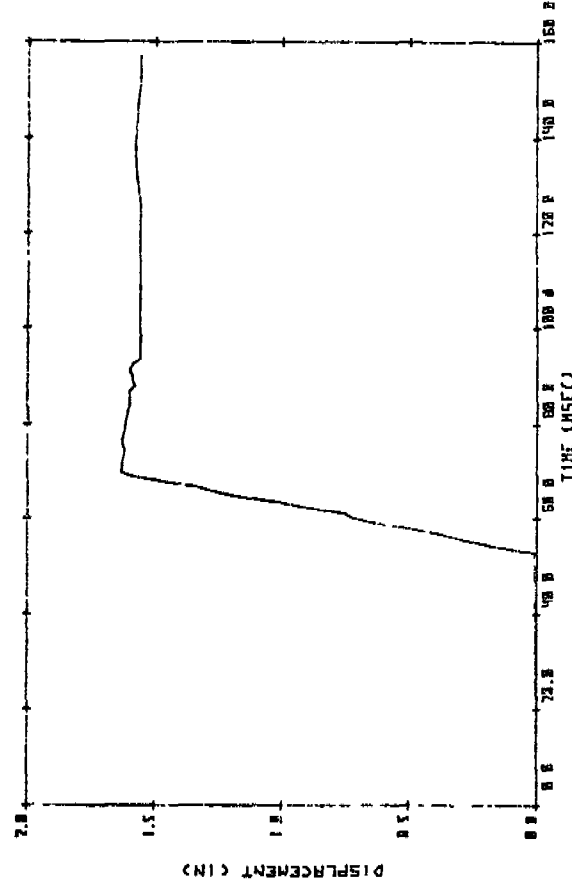
SRL 17-5 TEST #13 - UPPER SPINE



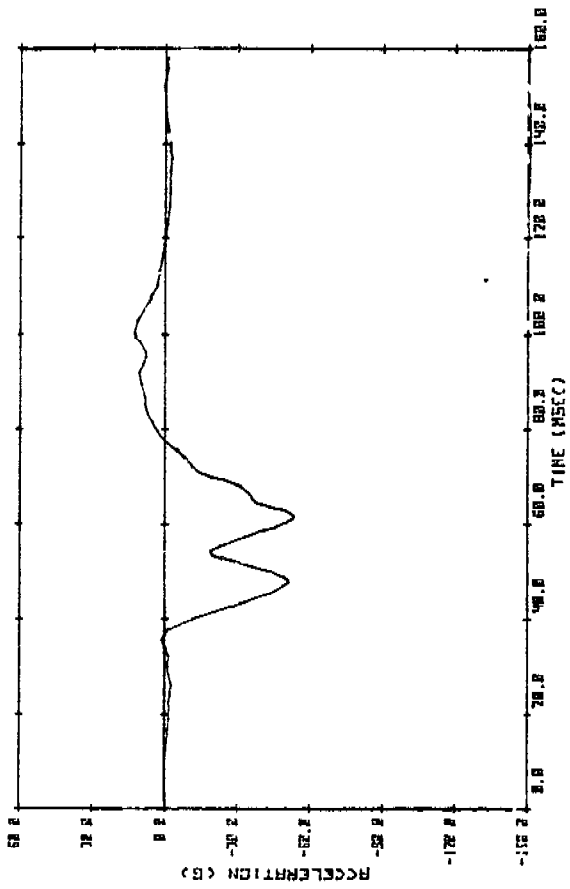
SRL 17-5 TEST #13 - LOWER SPINE



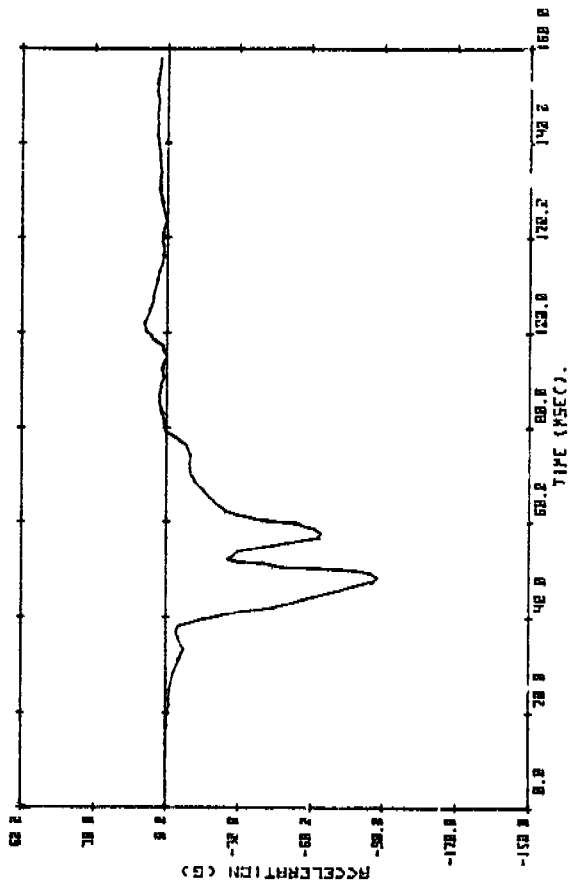
SRL 17-5 TEST #13 - PELVIS



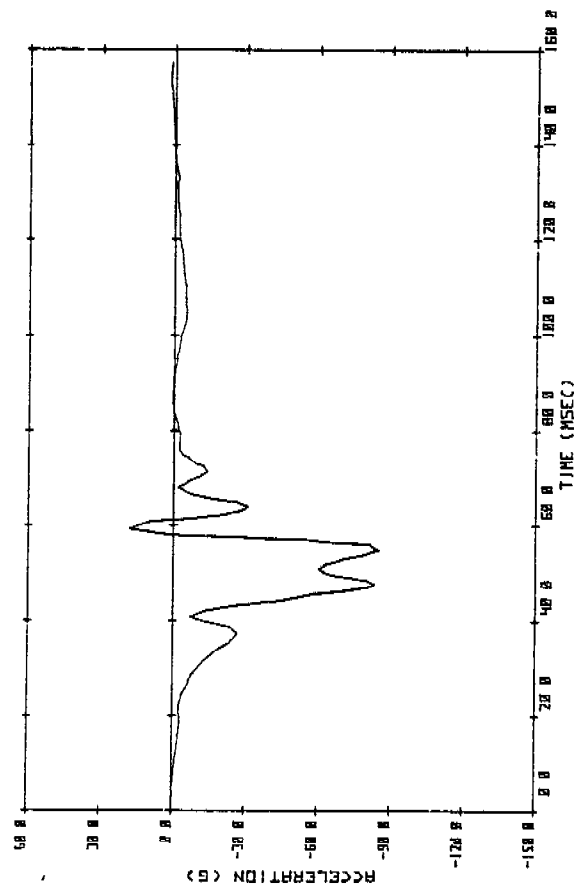
SRL 17-5 TEST #13 - CHEST DEFLECTION



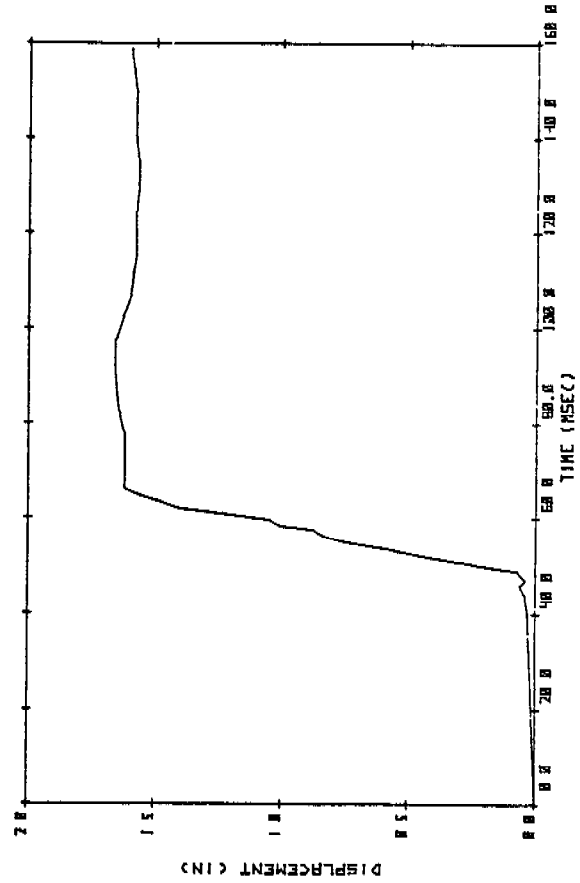
SRL 17-5 TEST #14 - UPPER SPINE



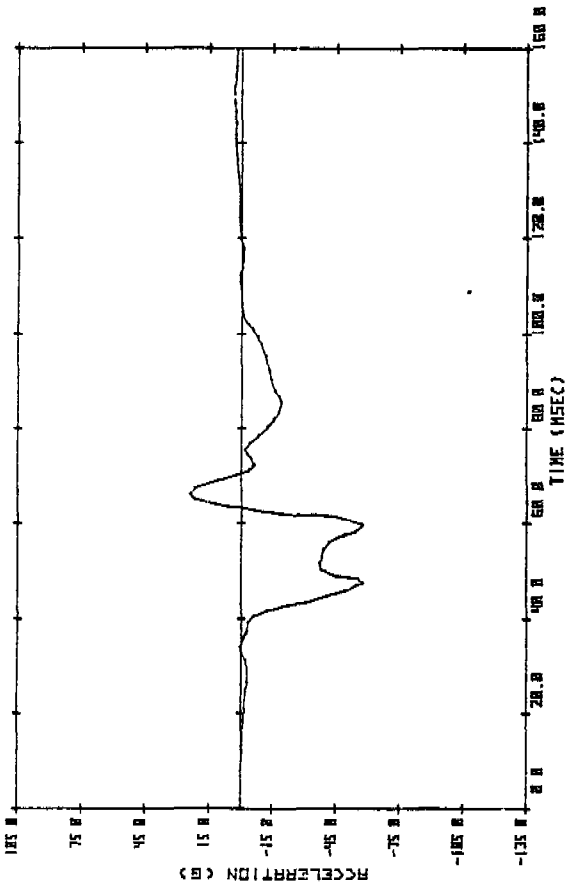
SRL 17-5 TEST #14 - LOWER SPINE



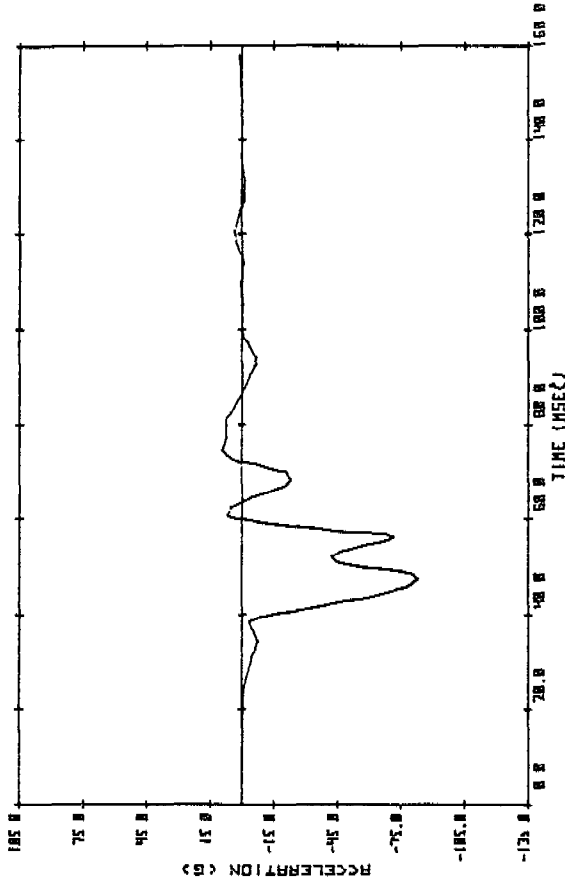
SRL 17-5 TEST #14 - PELVIS



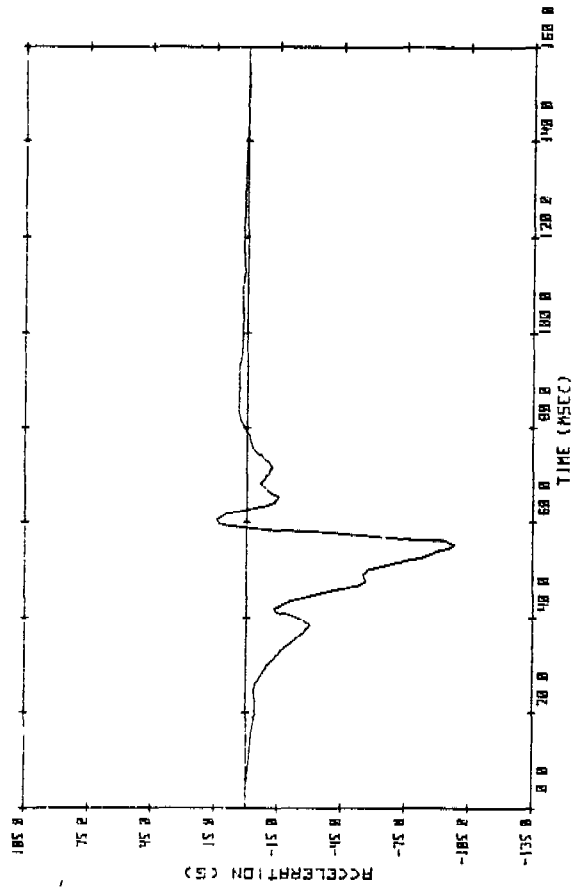
SRL 17-5 TEST #14 CHEST DEFLECTION



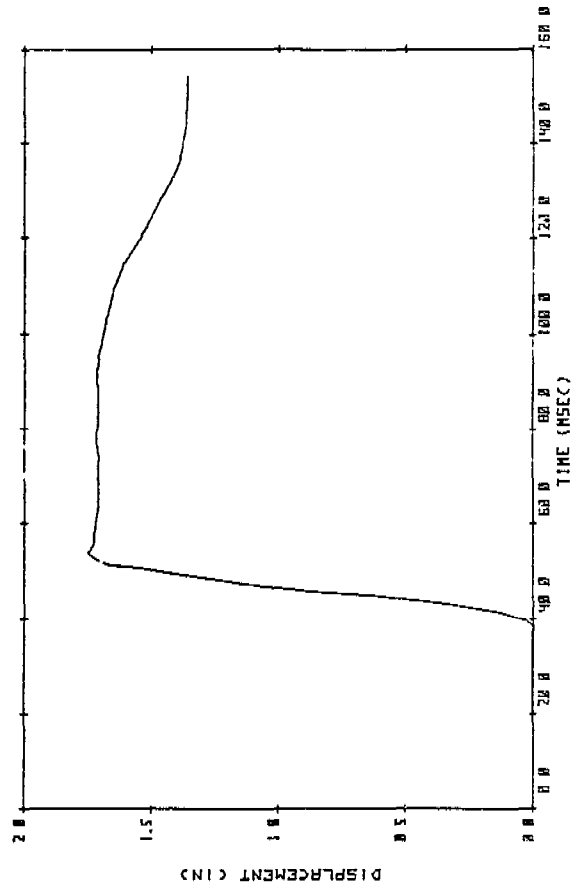
SRL 17-5 TEST #15 - UPPER SPINE



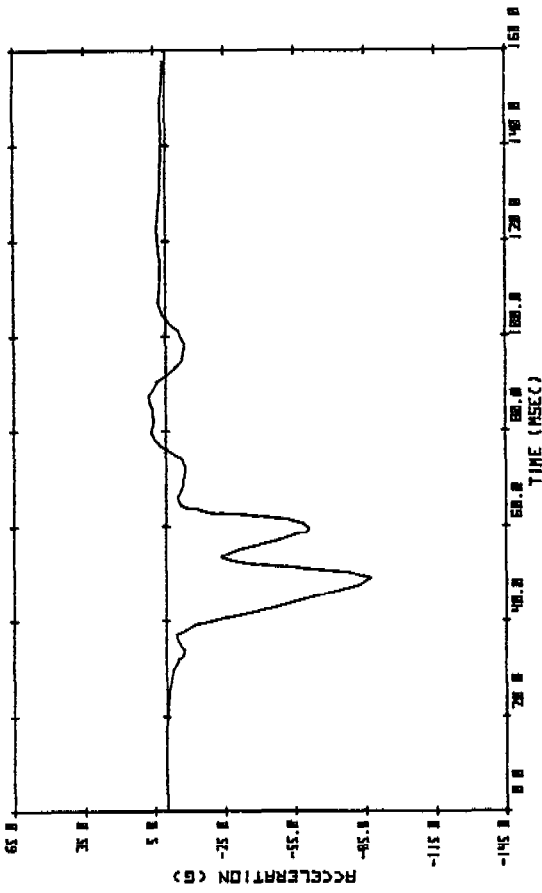
SRL 17-5 TEST #15 - LOWER SPINE



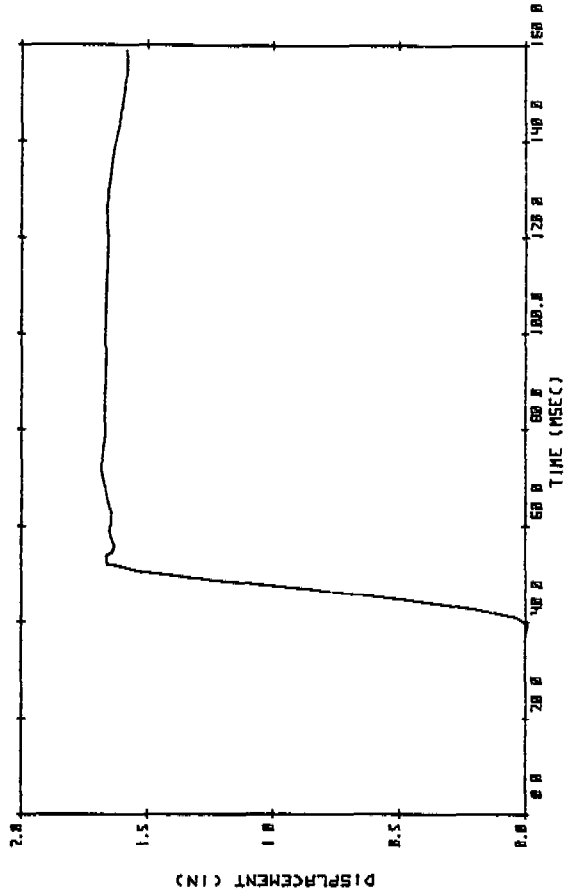
SRL 17-5 TEST #15 - PELVIS



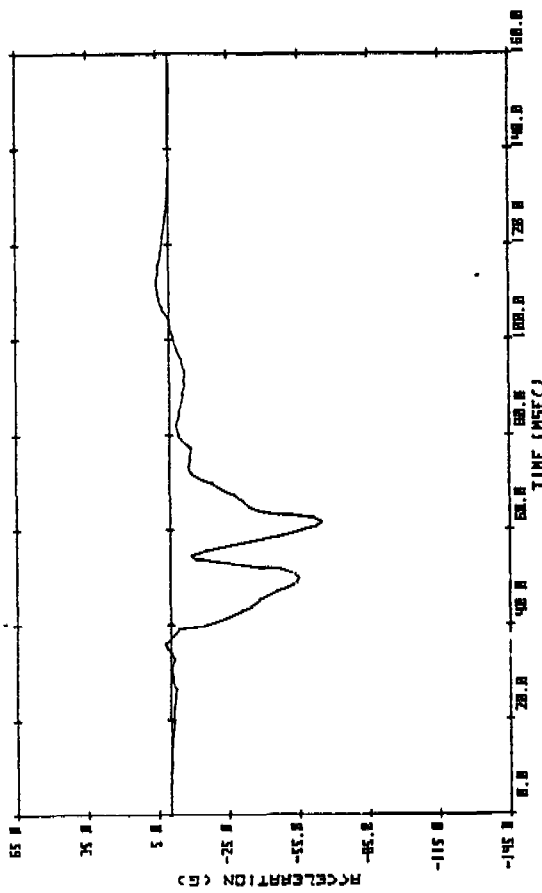
SRL 17-5 TEST #15 - CHEST DEFLECTION



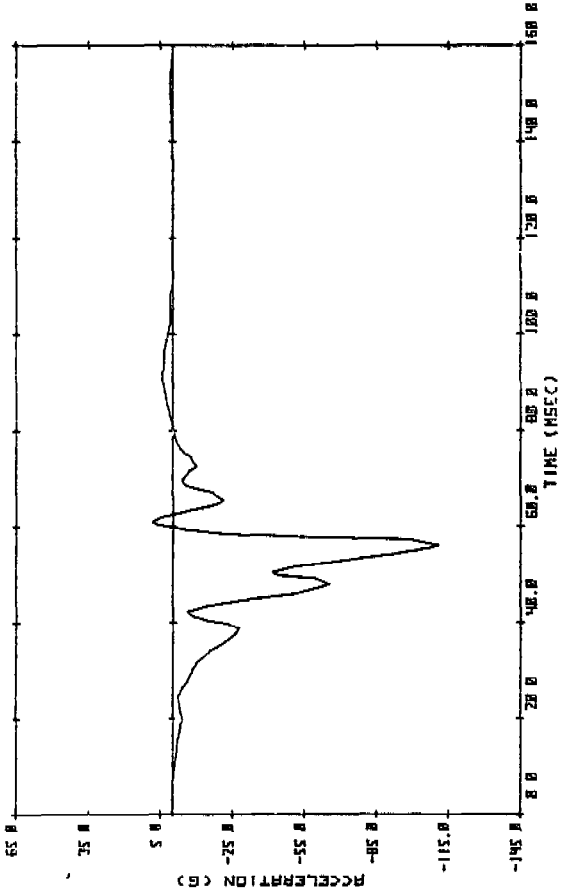
SRL 17-5 TEST #16 - LOWER SPINE



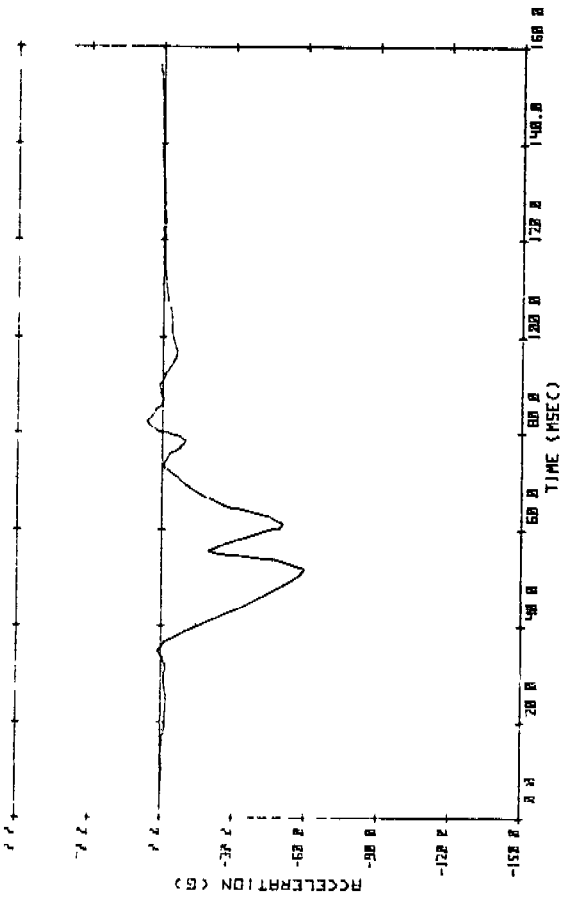
SRL 17-5 TEST #16 - CHEST DEFLECTION



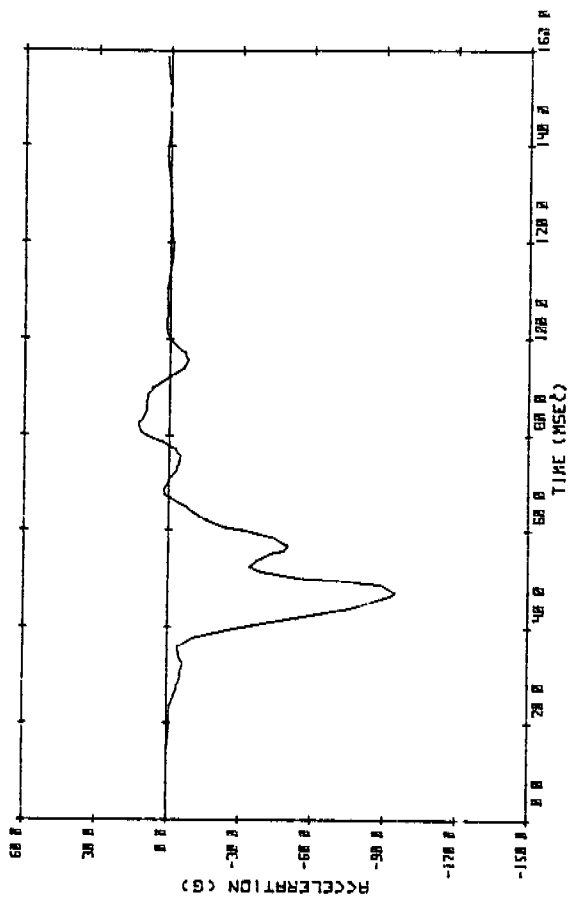
SRL 17-5 TEST #16 - UPPER SPINE



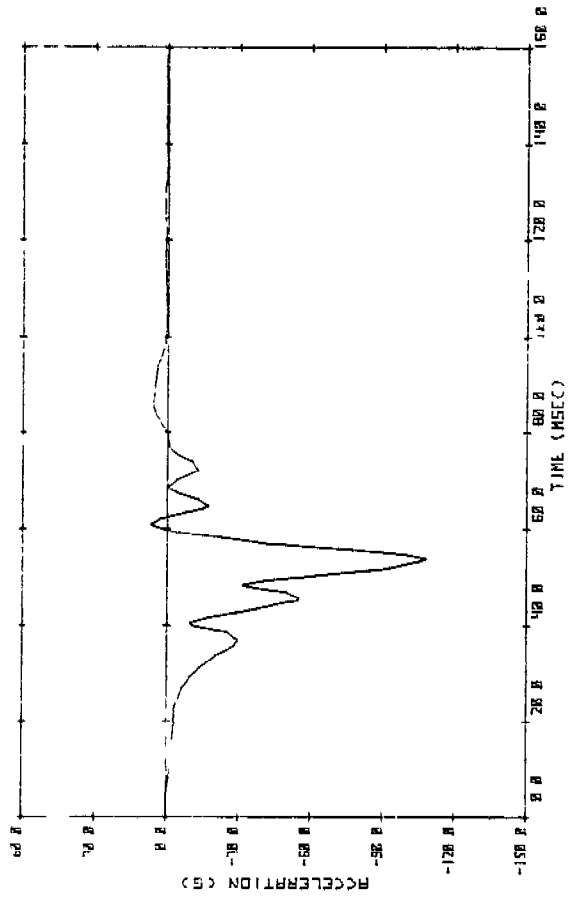
SRL 17-5 TEST #16 - PELVIS



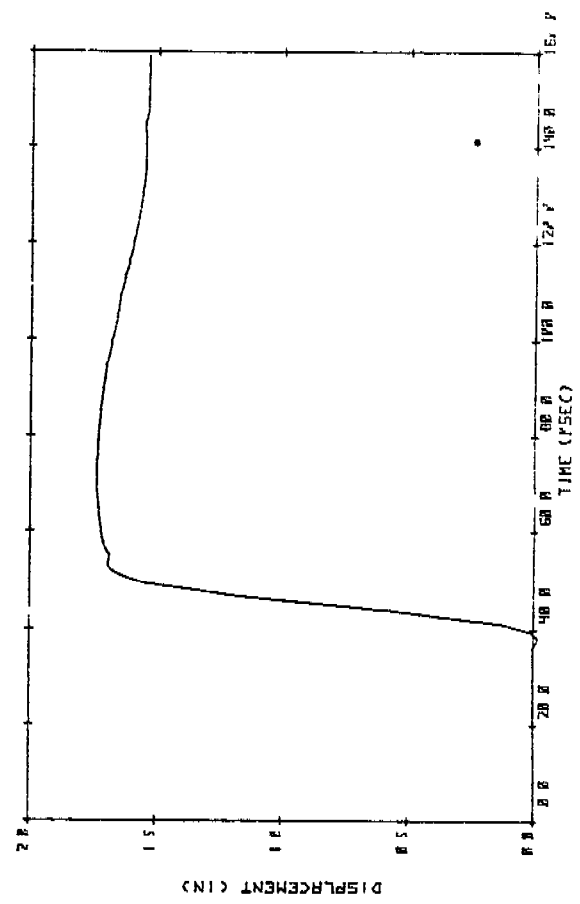
SRL 17-5 TEST #17 - UPPER SPINE



SRL 17-5 TEST #17 - LOWER SPINE



SRL 17-5 TEST #17 - PELVIS



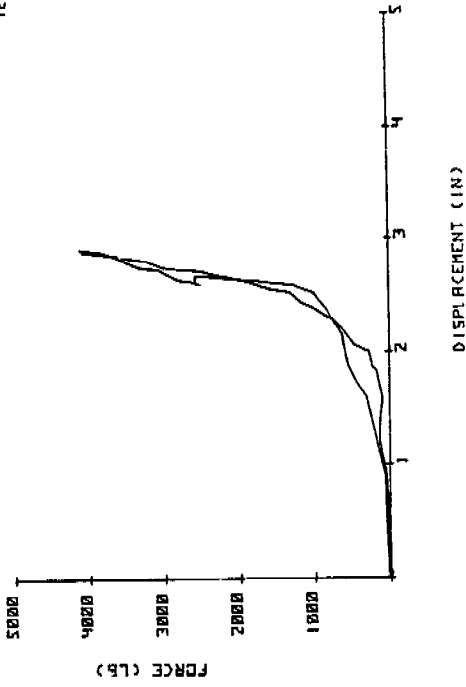
SRL 17-5 TEST #17 - CHEST REFLECTION

APPENDIX F

Force vs. Deflection Curves for Phase I
Padding Component Tests

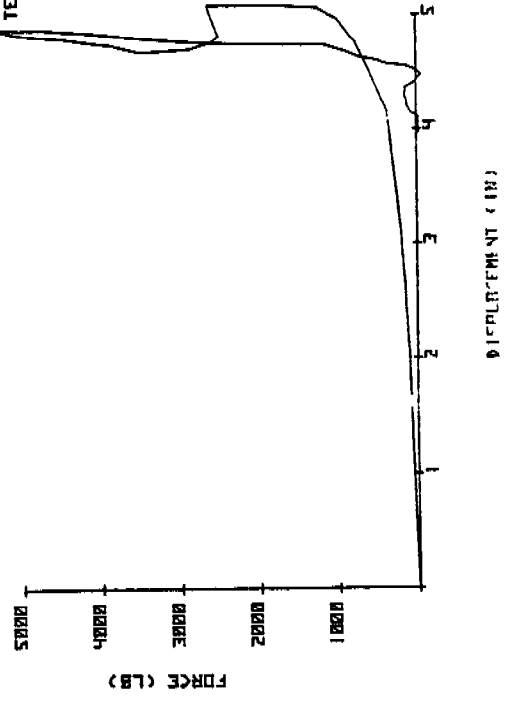
TEST NO 25 FIBERGLASS TYPE G

VELOCITY=14.99 MPH
THICKNESS=5.25 IN
TEMP=84 F



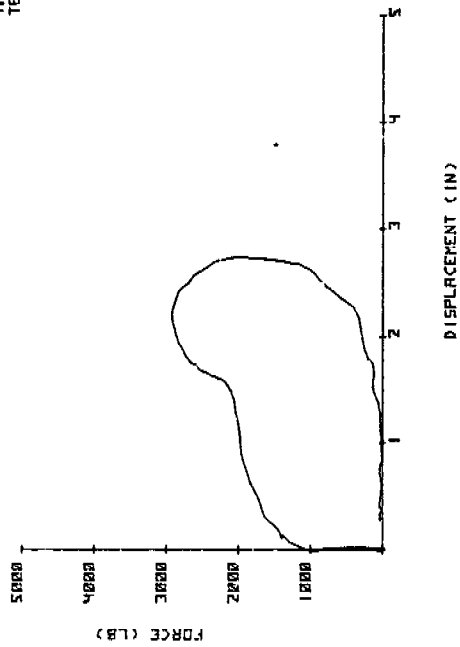
TEST NO 28 NEOPRENE UDRP

VELOCITY=15.15 MPH
THICKNESS=4.75 IN
TEMP=78 F



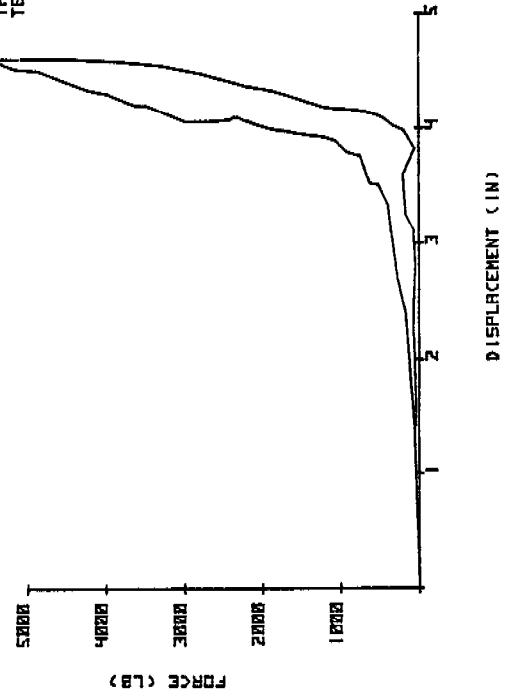
TEST NO 23 ENSOLITE HCR

VELOCITY=14.76 MPH
THICKNESS=5.5 IN
TEMP=84 F



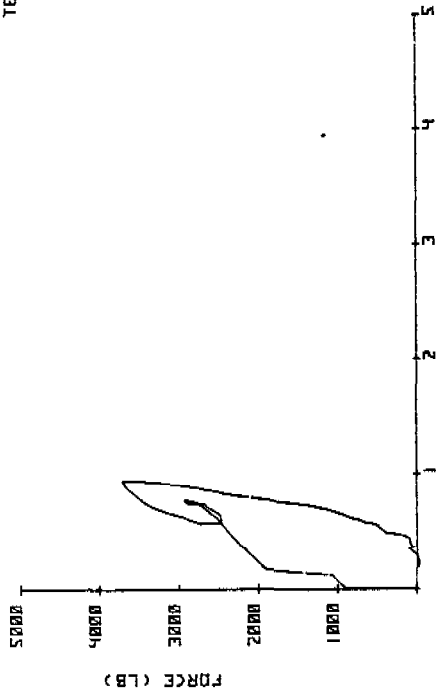
TEST NO 26 NEOPRENE LS ZR0

VELOCITY=14.82 MPH
THICKNESS=5.8 IN
TEMP=89 F



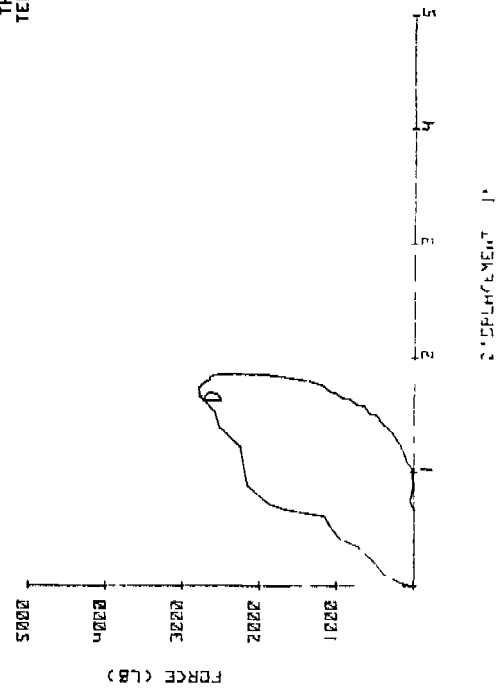
TEST NO 40 RUBATEX R8407-5

VELOCITY=15 15 MPH
THICKNESS=5 0 IN
TEMP=71 F



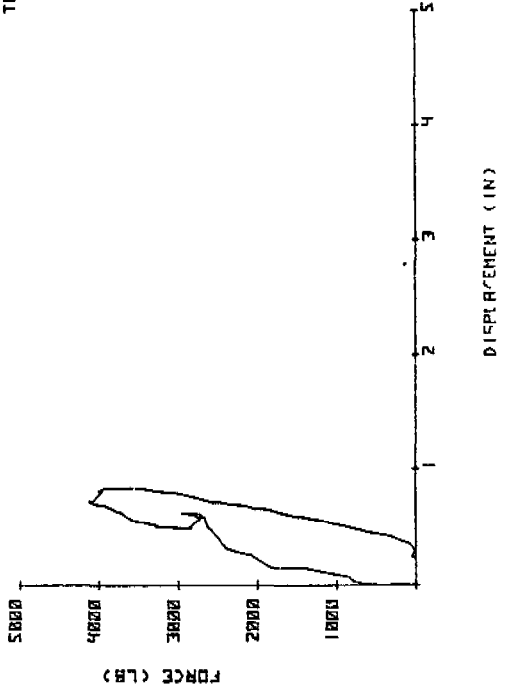
TEST NO 45 ENSOLITE BCR

VELOCITY = 15 25 MPH
THICKNESS = 5 125 IN
TEMP = 71 F



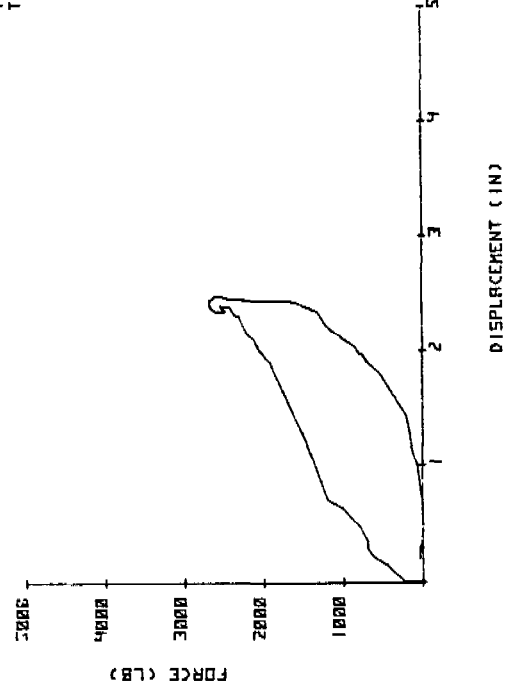
TEST NO.42 ETHAFORM 900

VELOCITY=15 15 MPH
THICKNESS=5 0625 IN
TEMP=71 F



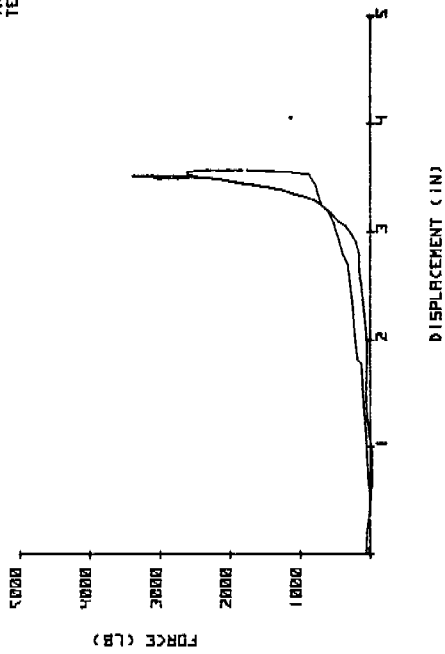
TEST NO 47 DURAFORM C 222 A

VELOCITY=15 25 MPH
THICKNESS=4 0625 IN
TEMP=70 F



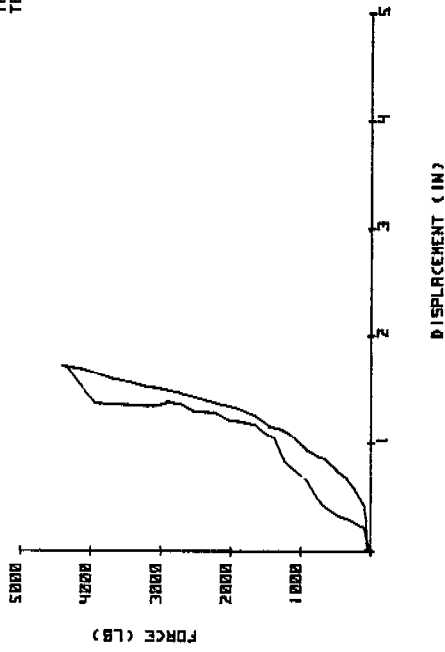
TEST NO 57 FIBERGLAS (D D)

VELOCITY = 14.20 MPH
THICKNESS = 4.25 IN
TEMP = 70 F



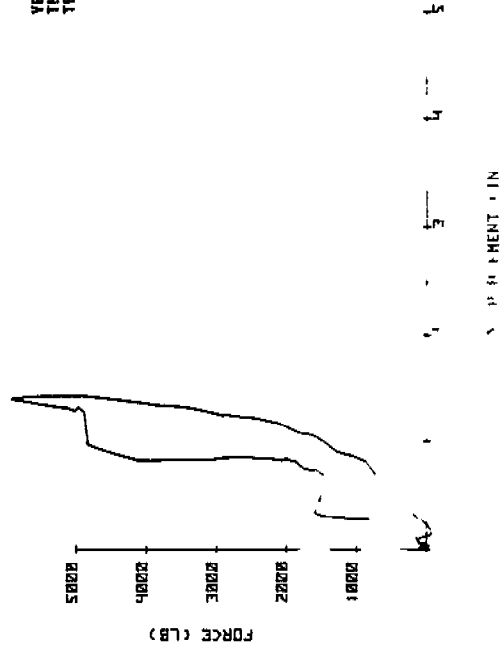
TEST NO 58 FIBERGLAS TYPE L

VELOCITY = 15.25 MPH
THICKNESS = 4.75 IN
TEMP = 59 F



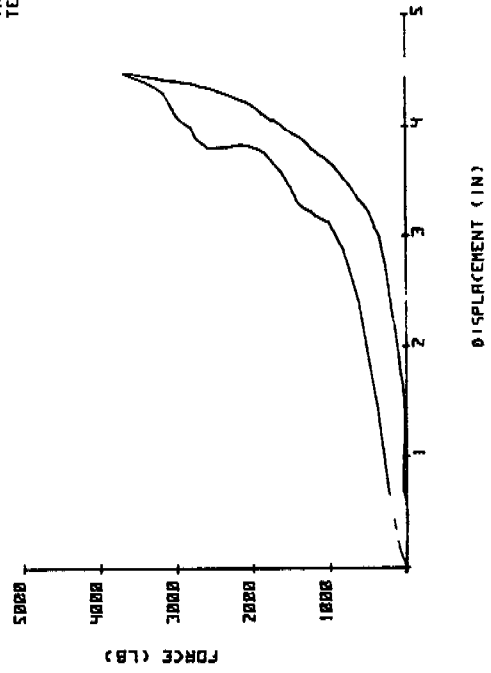
TEST NO 59 FIBERGLAS TYPE Q

VELOCITY = 15.25 MPH
THICKNESS = 4.625 IN
TEMP = 70 F



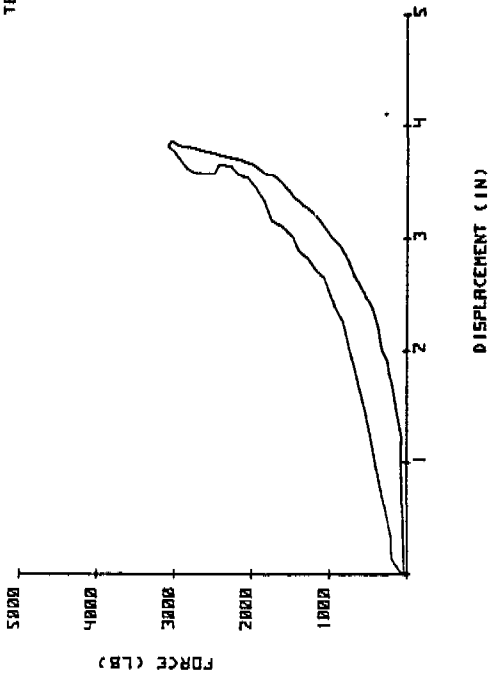
TEST NO 64 ENSOLITE MLC (WHT)

VELOCITY = 14.75 MPH
THICKNESS = 5.5 IN
TEMP = 70 F



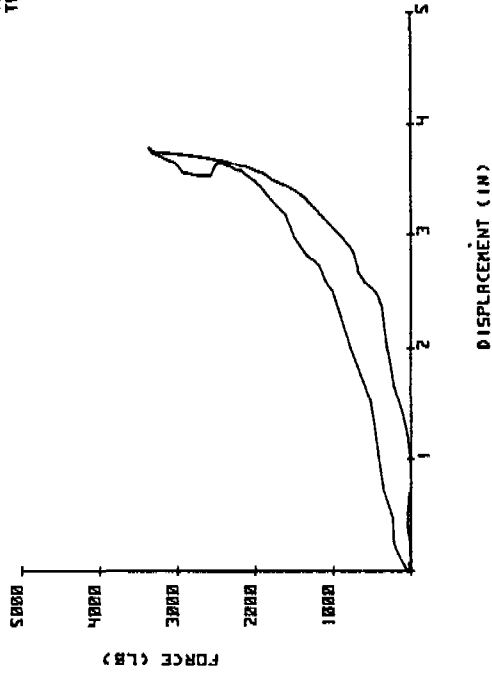
TEST NO 72 ENSOLITE LPC

VELOCITY = 15.37 MPH
THICKNESS = 5.25 IN
TEMP = 63 F



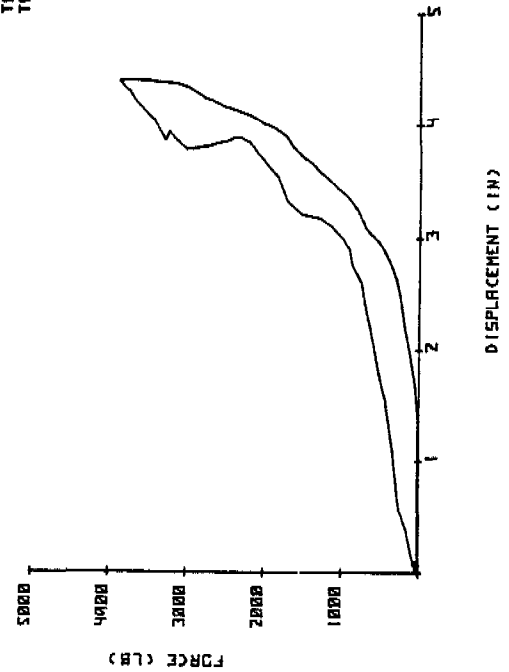
TEST NO 73 ENSOLITE LPC (20)

VELOCITY = 15.25 MPH
THICKNESS = 5.25 IN
TEMP = 66 F



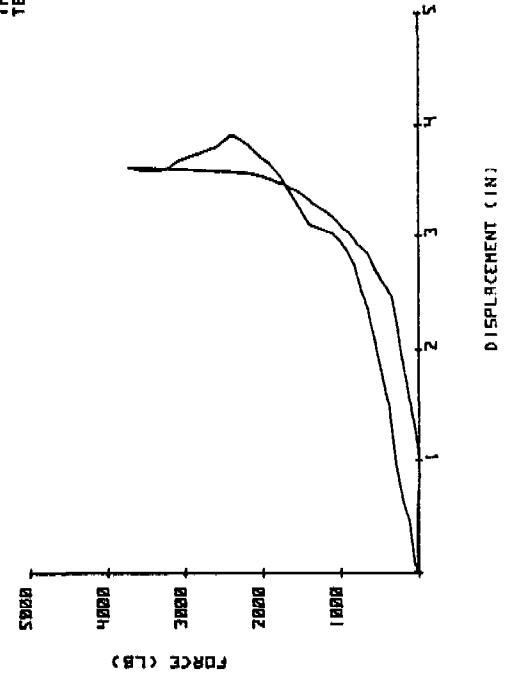
TEST NO 74 ENSOLITE FBC

VELOCITY = 15.25 MPH
THICKNESS = 5.25 IN
TEMP = 67 F



TEST NO 75 ENSOLITE FBC (20)

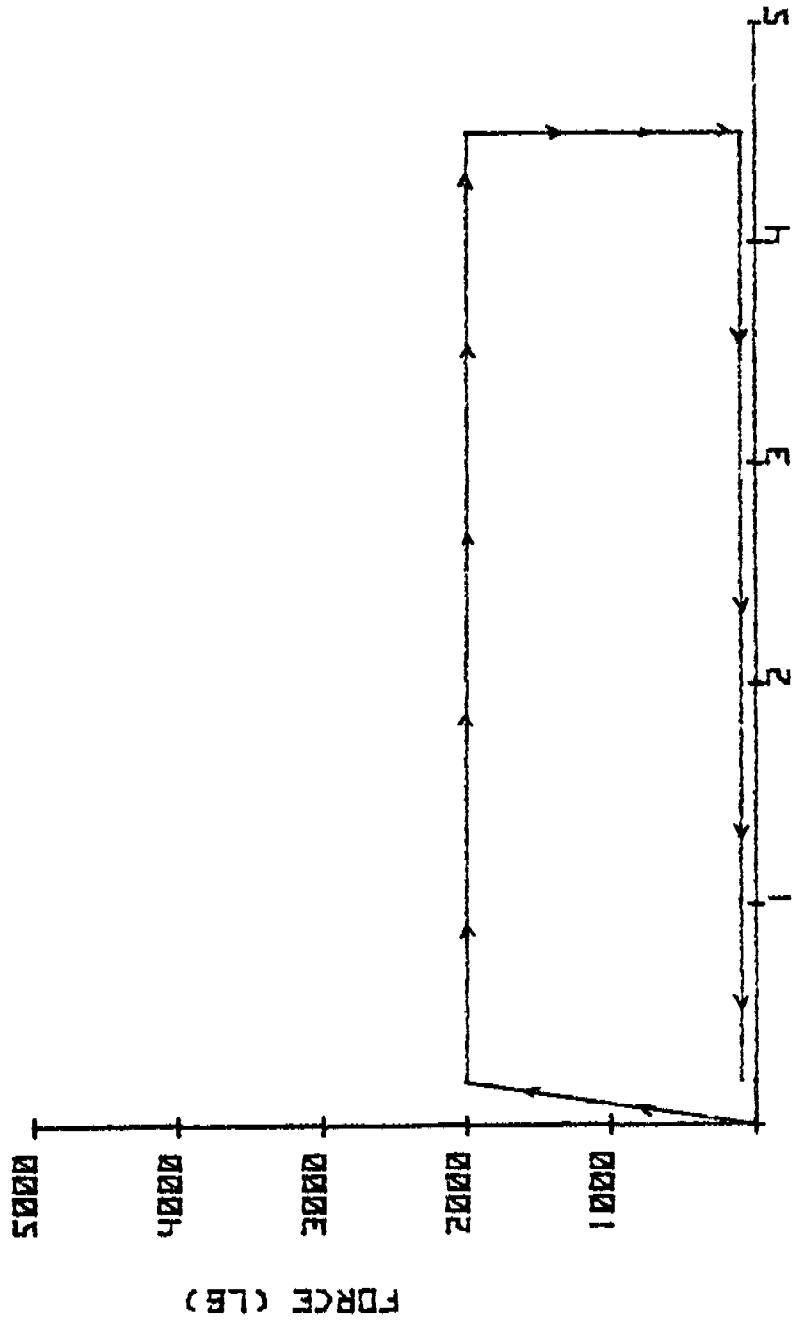
VELOCITY = 15.25 MPH
THICKNESS = 5.25 IN
TEMP = 67 F



APPENDIX G

Force vs. Deflection Curves for Phase II
Padding Component Tests

HYPOTHETICAL CASE IDEAL MATERIAL PROPERTY



DISPLACEMENT (IN)

FIGURE G-1

HYPOTHETICAL CASE SOFT MATERIAL

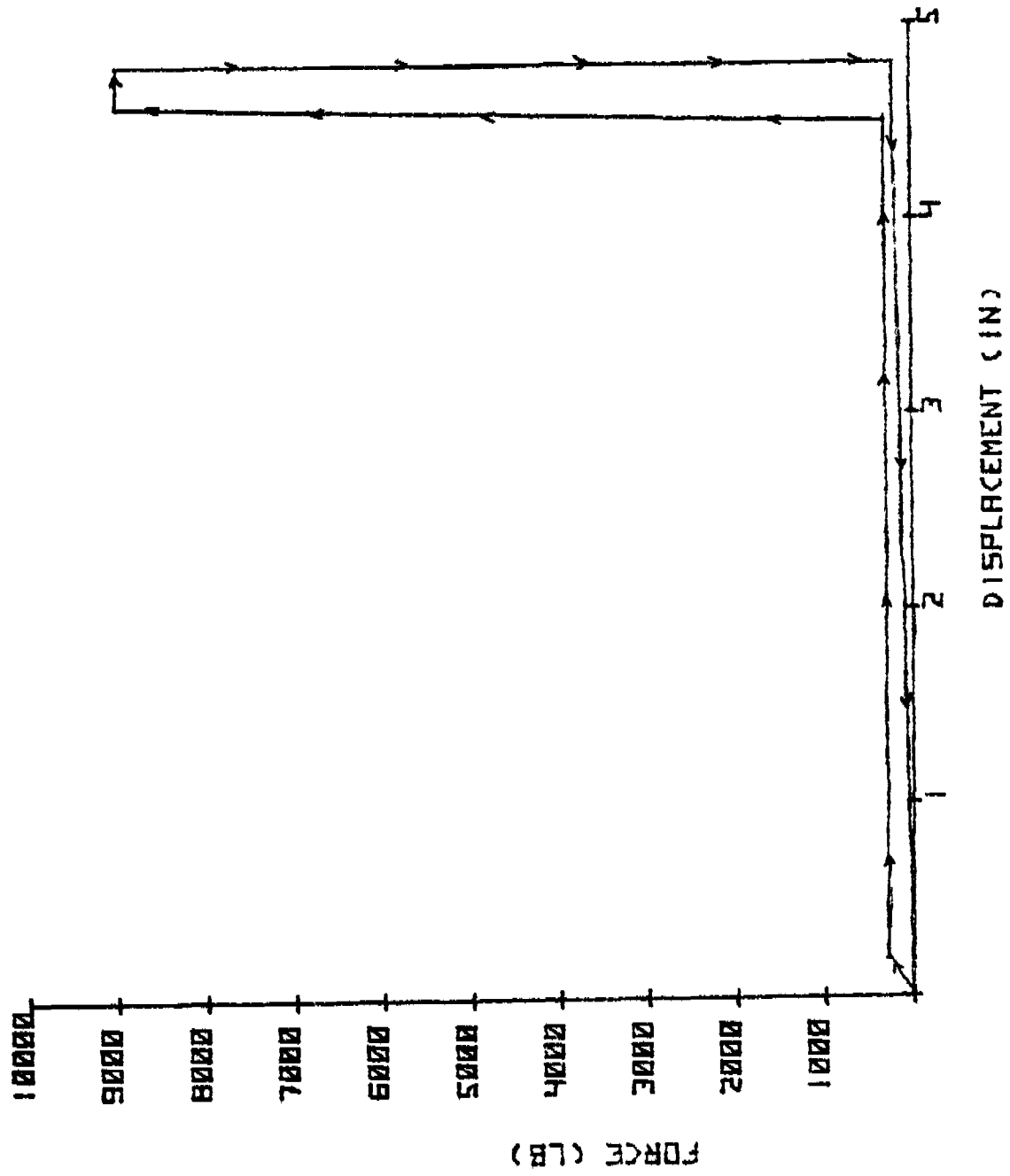
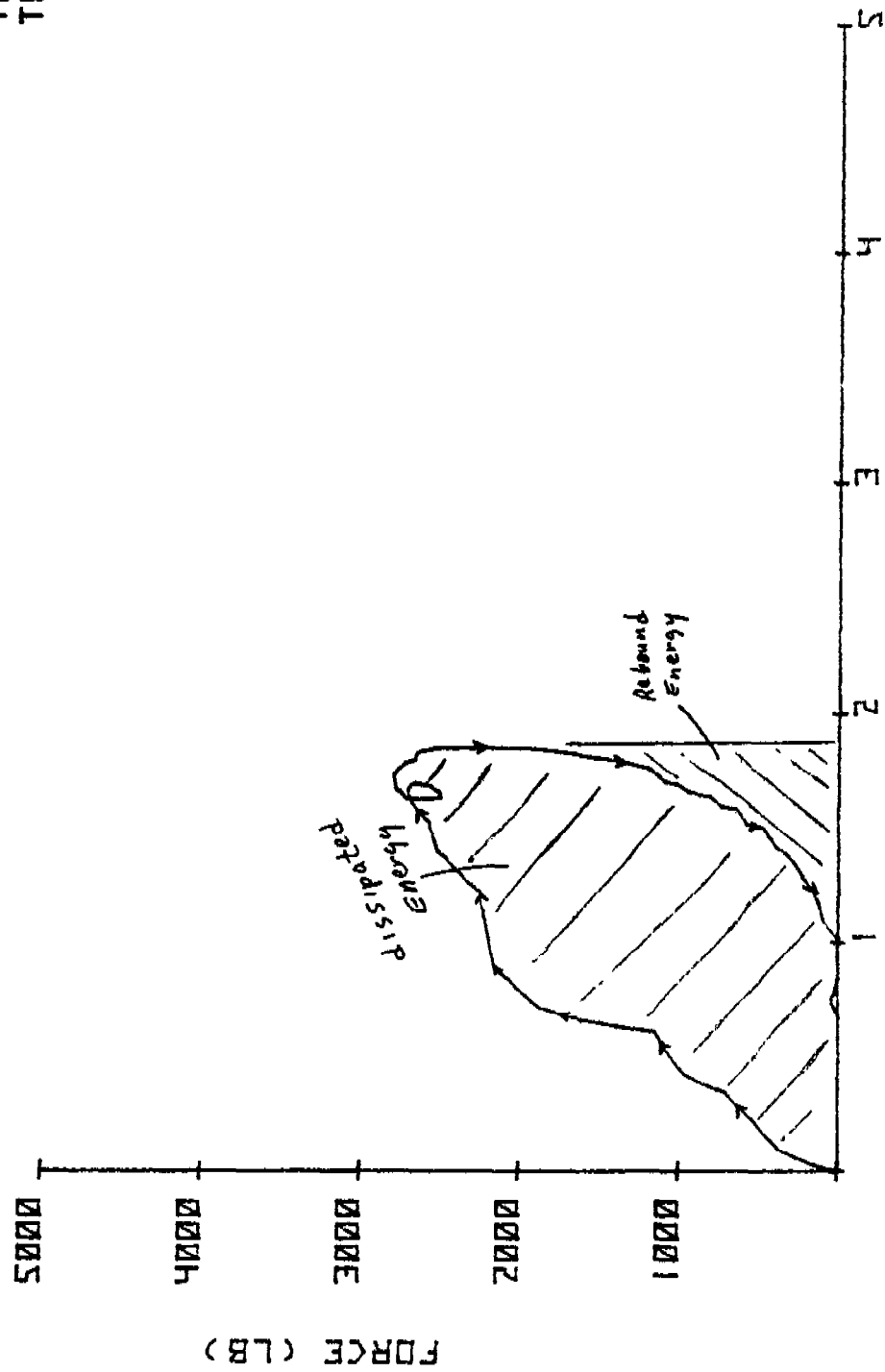


FIGURE G-3

TEST NO. 45 ENSOLITE BCR

VELOCITY=15.25 MPH
THICKNESS=5.125 IN
TEMP=71 F



DISPLACEMENT (IN)

FIGURE G-5

TEST NO 93 FIBERGLAS H3BC

VELOCITY = 14.82 MPH
THICKNESS = 3.5 IN
TEMP = 78 F

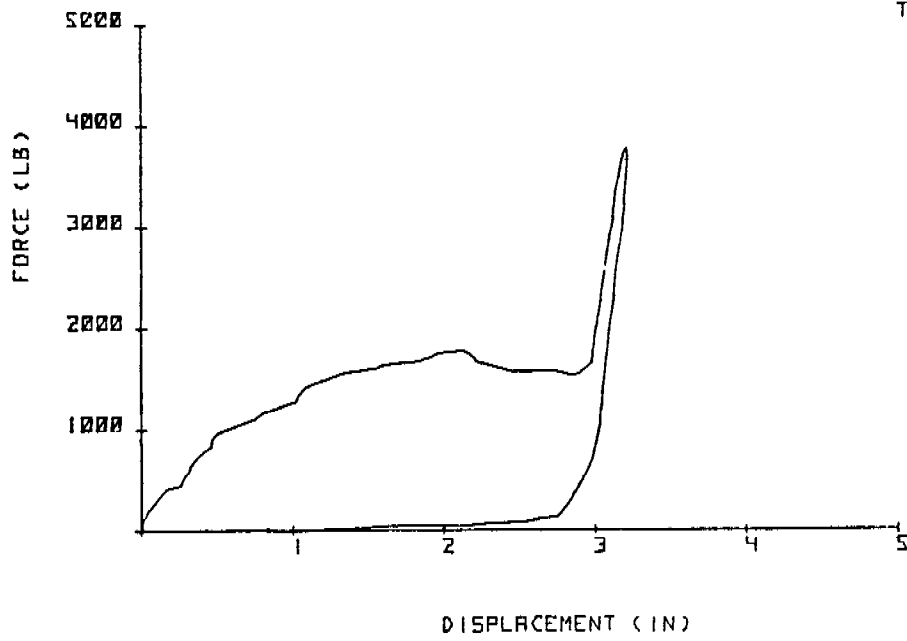


FIGURE G-24

VELOCITY = 15.15 MPH
THICKNESS = 3.5 IN
TEMP = 60 F

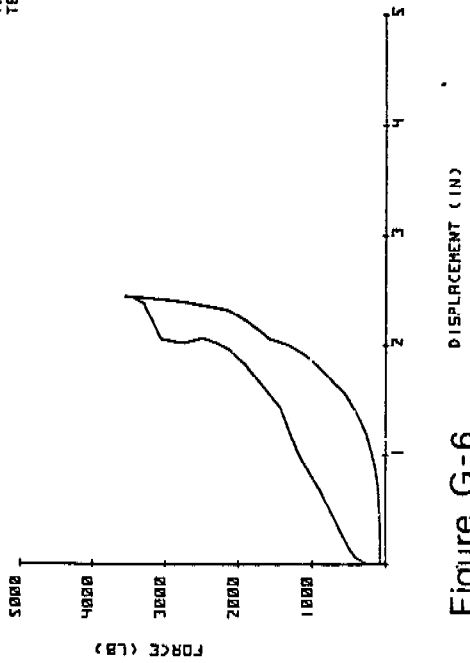


Figure G-6

TEST NO 62 ENSOLITE HCR

VELOCITY = 15.15 MPH
THICKNESS = 3.8125 IN
TEMP = 60 F

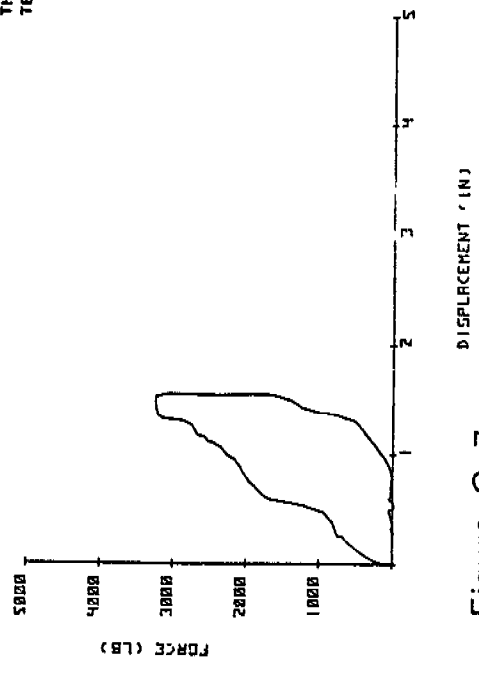


Figure G-7

TEST NO 63 ETHRFORM 600

VELOCITY = 15.15 MPH
THICKNESS = 3.375 IN
TEMP = 66 F

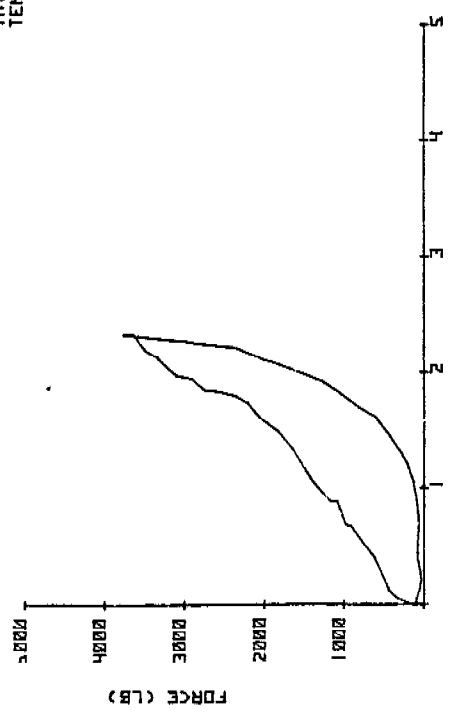


Figure G-8

VELOCITY = 15.32 MPH
THICKNESS = 3.0 IN
TEMP = 66 F

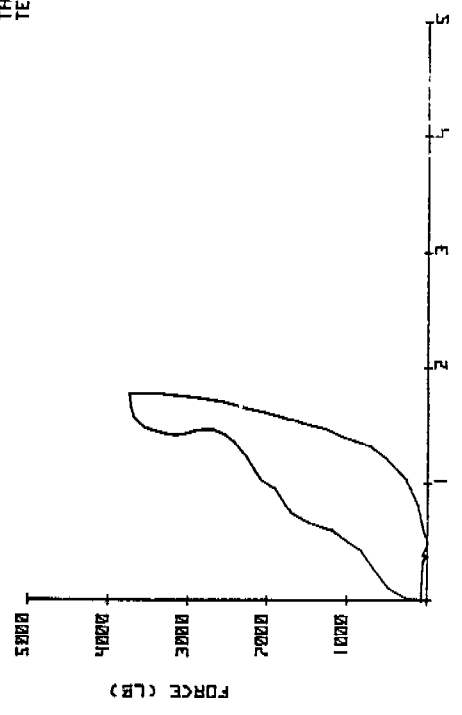


Figure G-9

VELOCITY = 15.88 MPH
THICKNESS = 3.8 IN
TEMP = 78 F

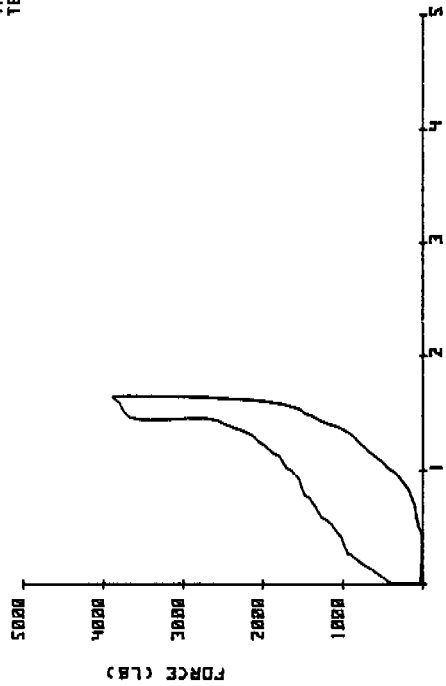


Figure G-14

TEST NO 82 FIBERGLAS HBC

VELOCITY = 15.15 MPH
THICKNESS = 3.5 IN
TEMP = 89 F

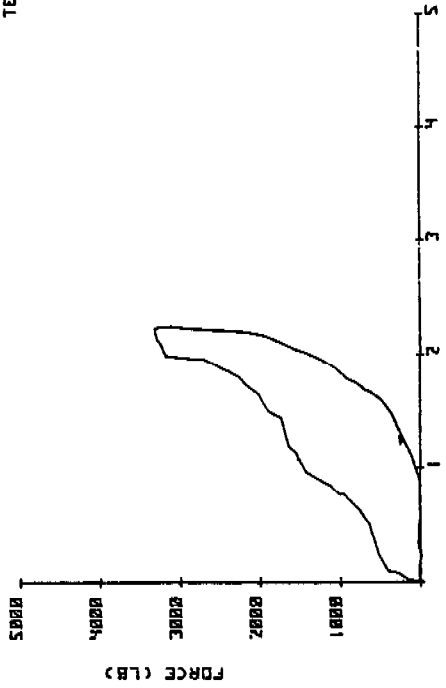


Figure G-15

TEST NO.86 FIBERGLAS HBC

VELOCITY = 15.45 MPH
THICKNESS = 3.75 IN
TEMP = 69 F

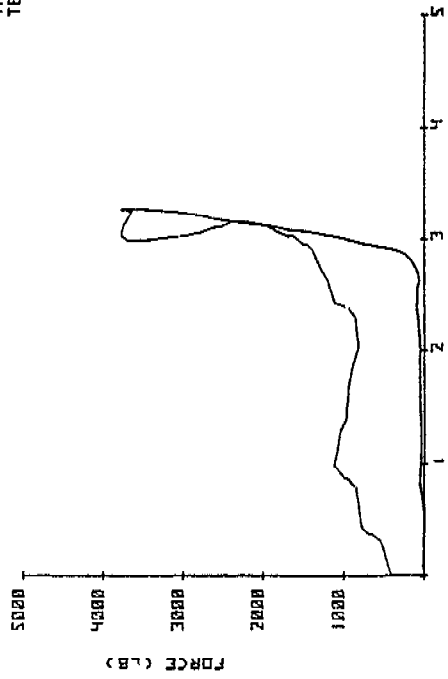


Figure G-16

VELOCITY = 15.72 MPH
THICKNESS = 3.19 IN
TEMP = 67 F

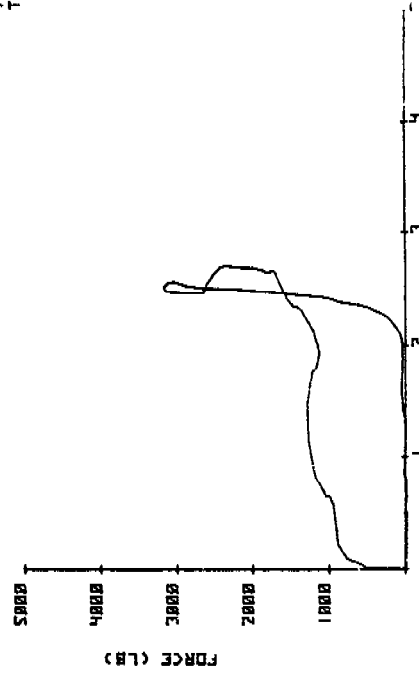


Figure G-17

TEST NO 91 AFR

VELOCITY = 15.22 MPH
THICKNESS = 3.0 IN
TEMP = 68 F

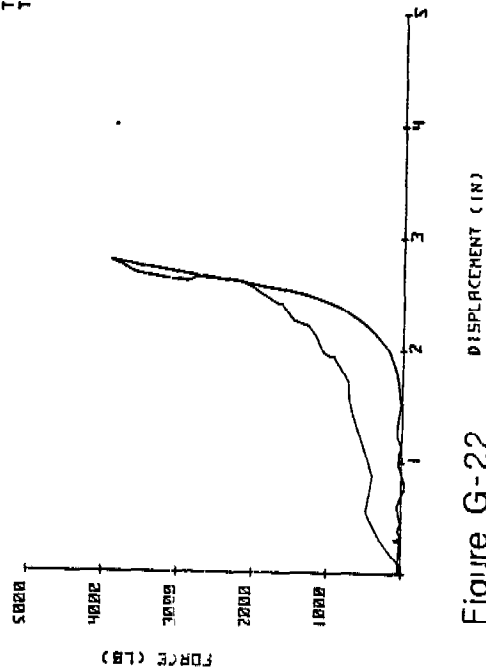


Figure G-22

TEST NO 92 RUBRTEX 2V5

VELOCITY = 15.15 MPH
THICKNESS = 3.0 IN
TEMP = 67 F

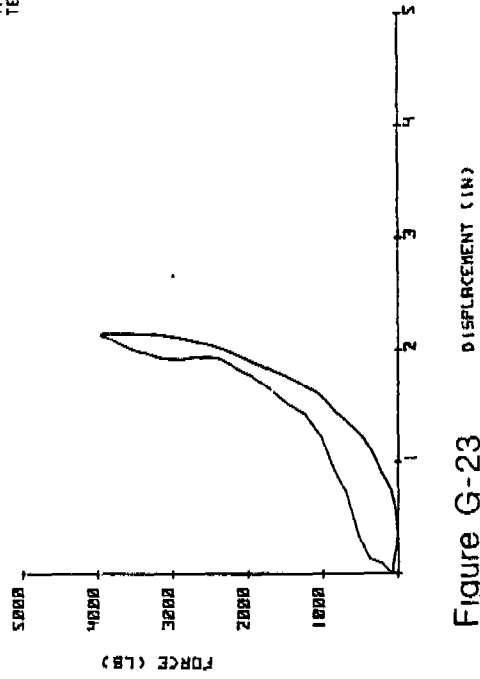
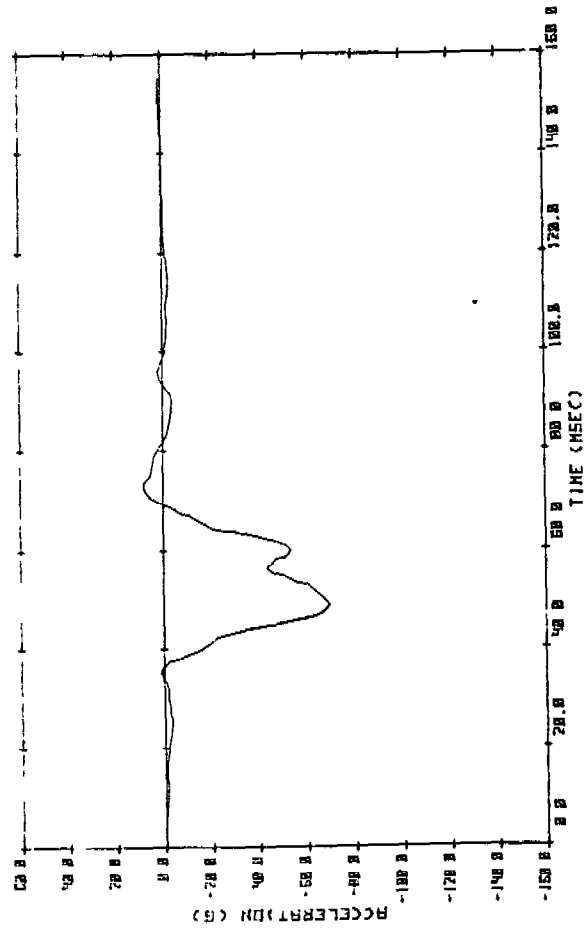


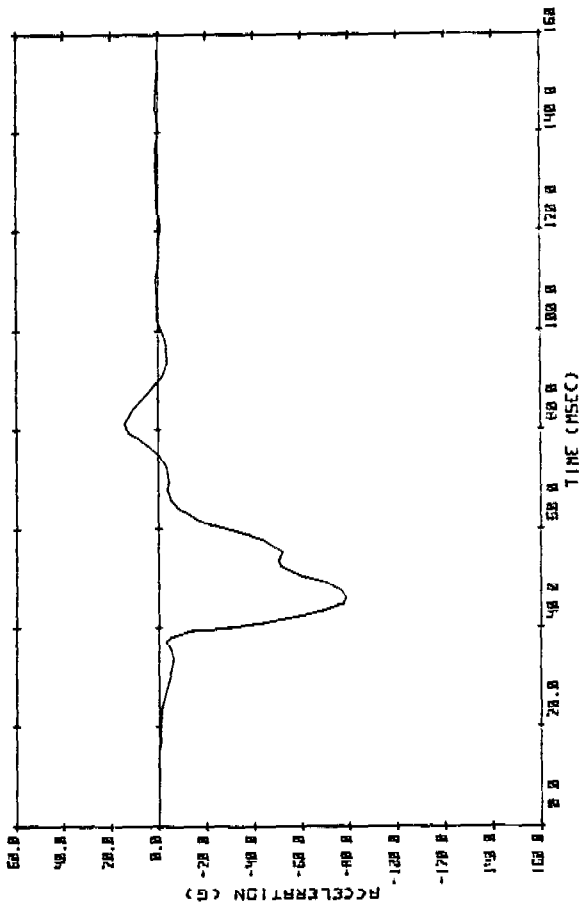
Figure G-23

APPENDIX H

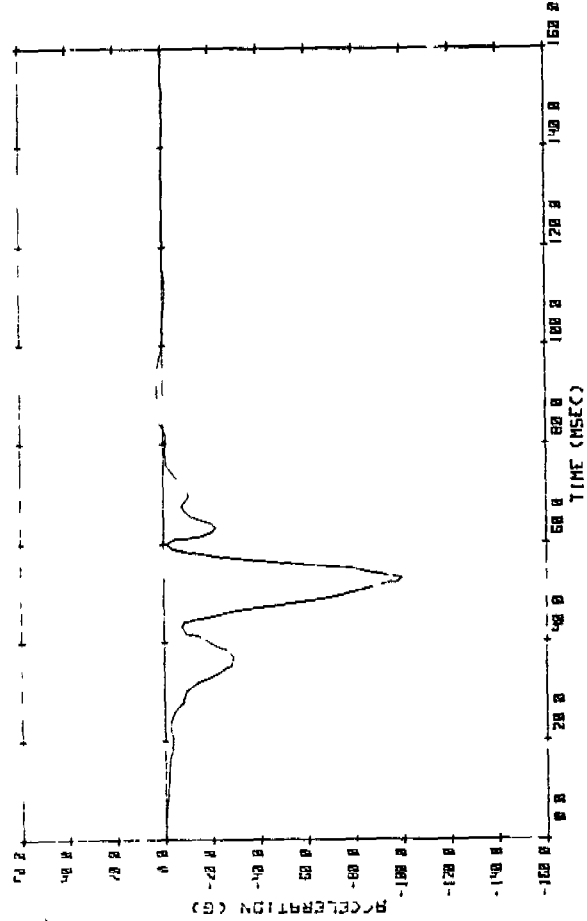
Body Form Responses from HYGE Sled
Padding Evaluation Tests



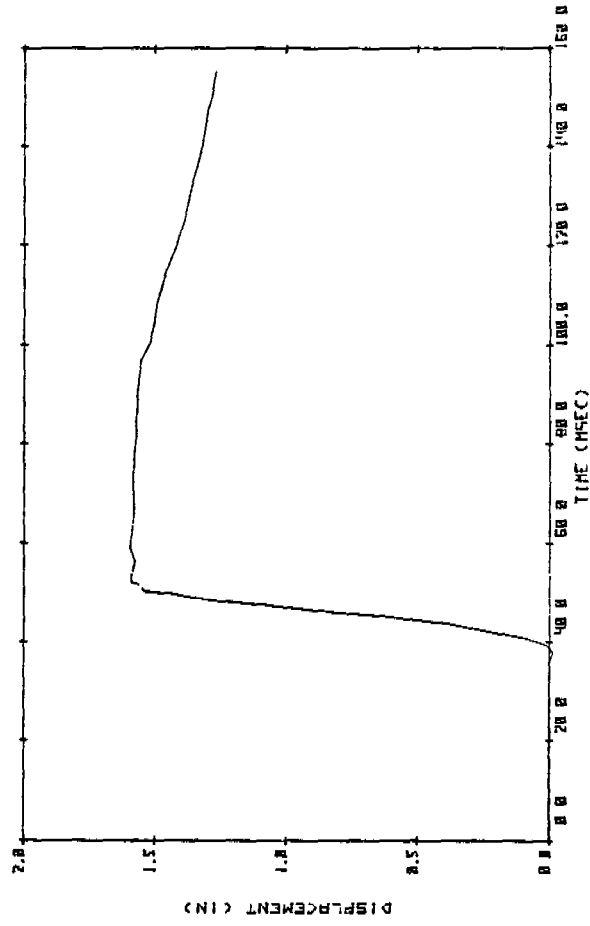
SRL 17-5 TEST #18 - UPPER SPINE



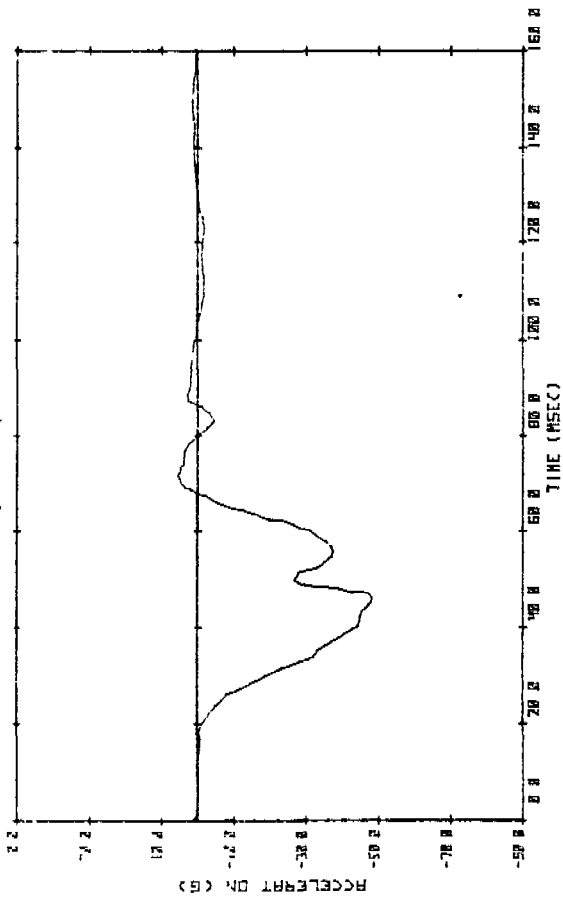
SRL 17-5 TEST #18 - LOWER SPINE



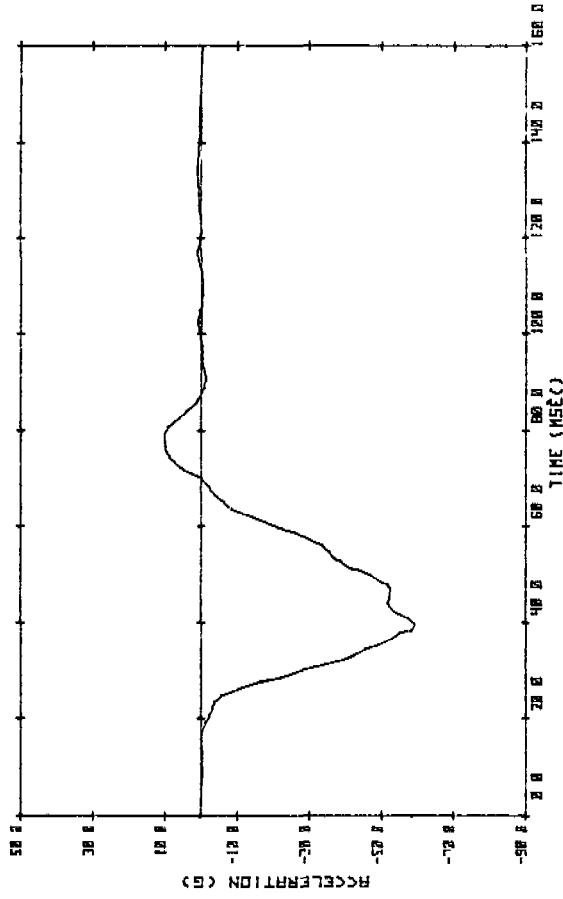
SRL 17-5 TEST #18 - PELVIS



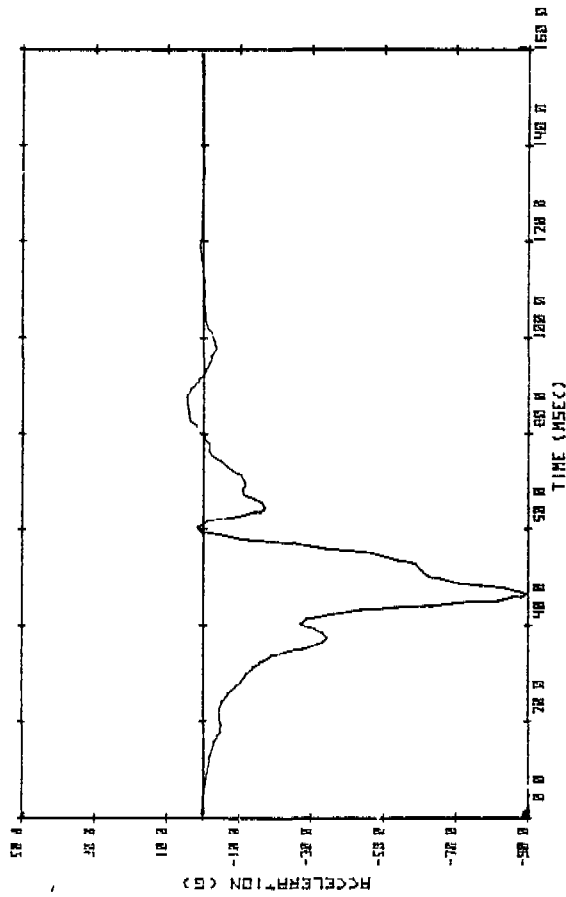
SRL 17 5 TEST #18 - CHEST DEFLECTION



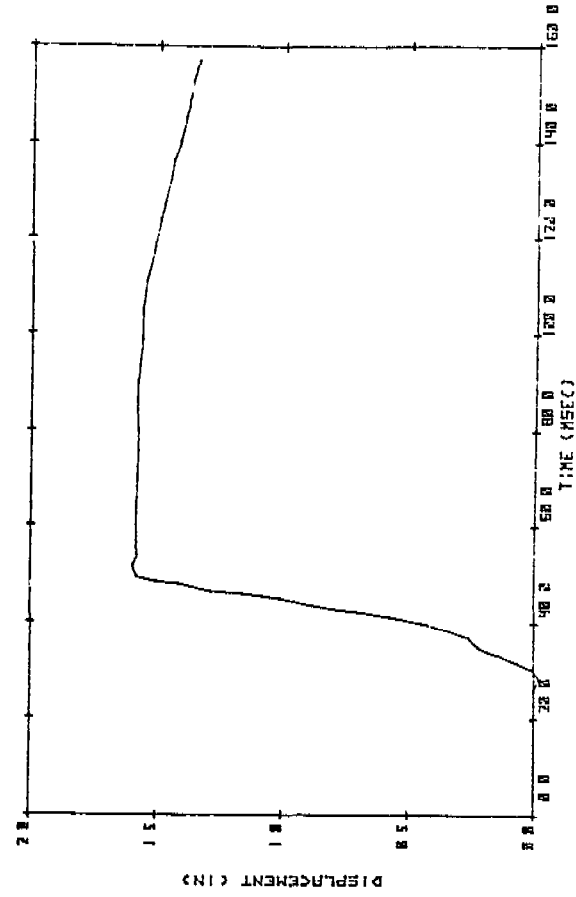
SRL 17-5 TEST #19 (ABC) - UPPER SPINE



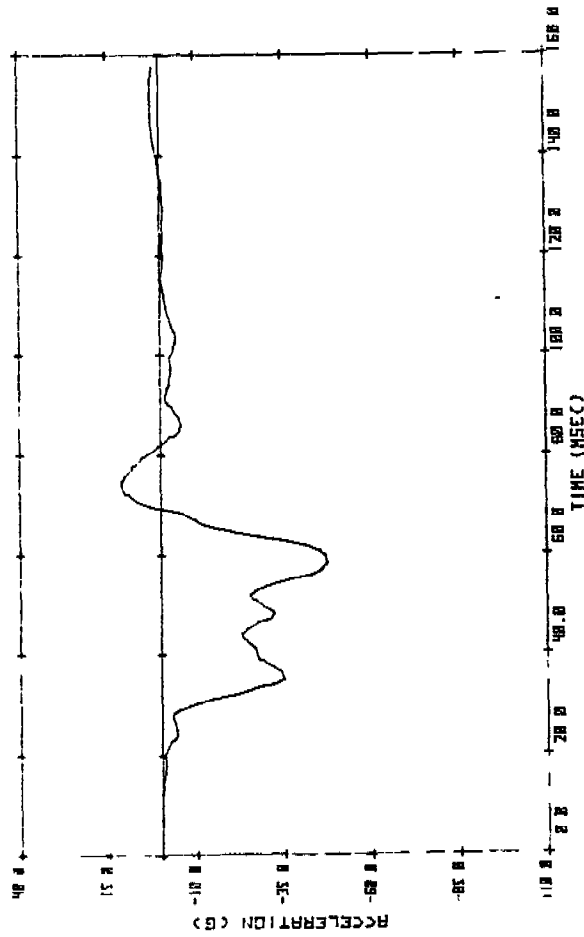
SRL 17-5 TEST #19 (ABC) - LOWER SPINE



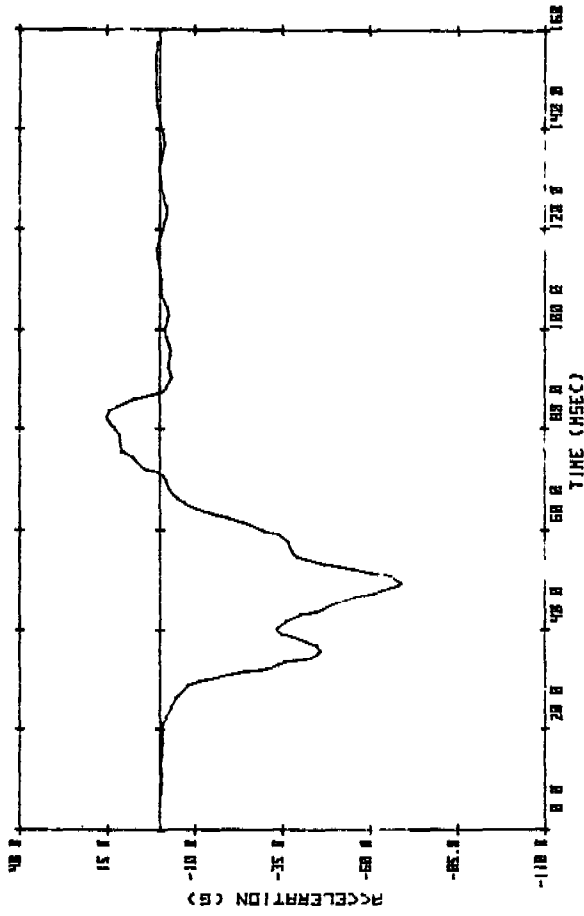
SRL 17-5 TEST #19 (ABC) - PELVIS



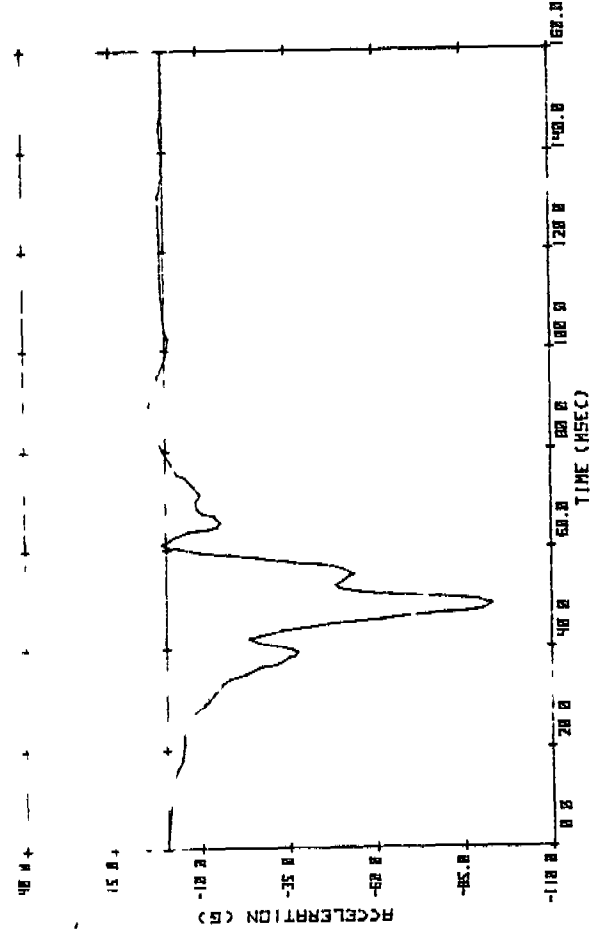
SRL 17-5 TEST #19 (ABC) - CHEST REFLECTOR



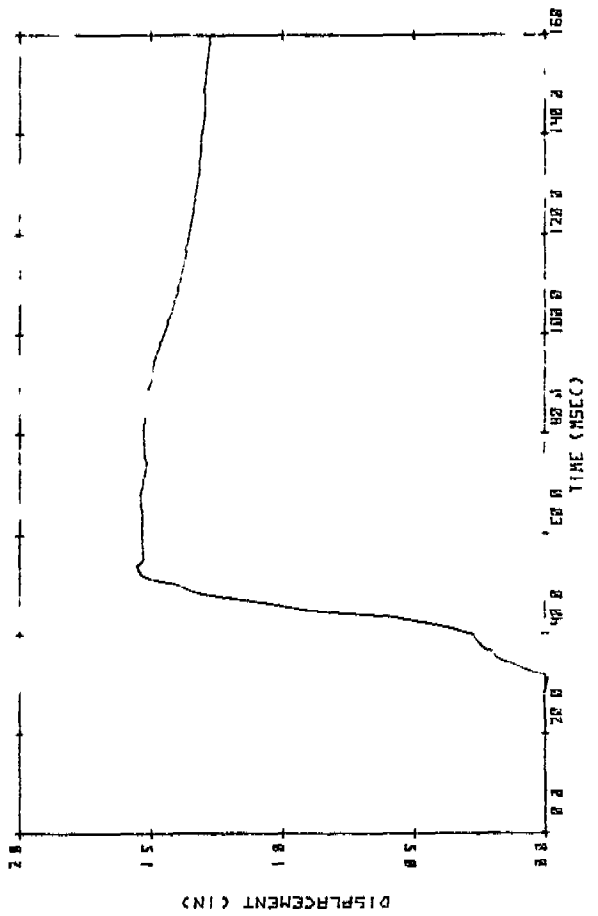
SRL 17-5 TEST #20 (H28C) - UPPER SPINE



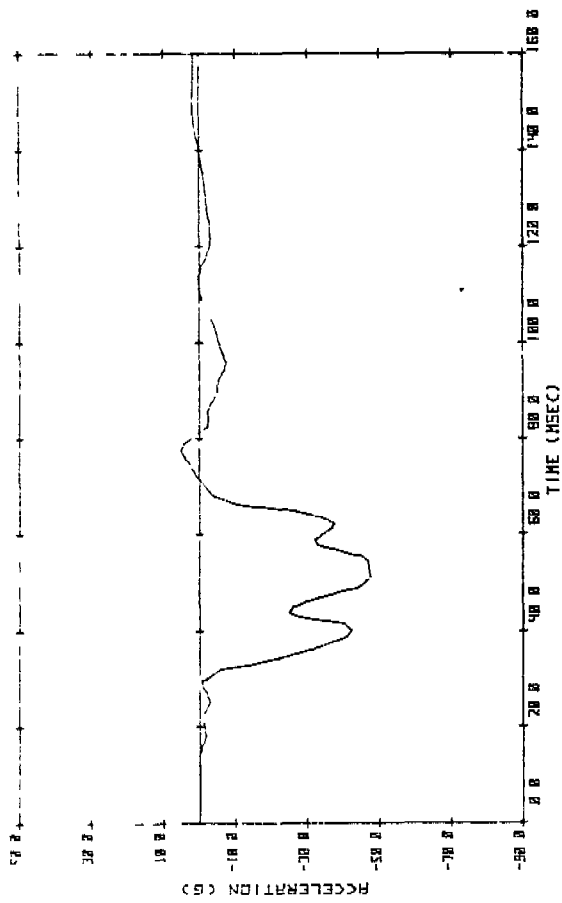
SRL 17-5 TEST #20 (H28C) - LOWER SPINE



SRL 17-5 TEST #20 (H28C) - PELVIS

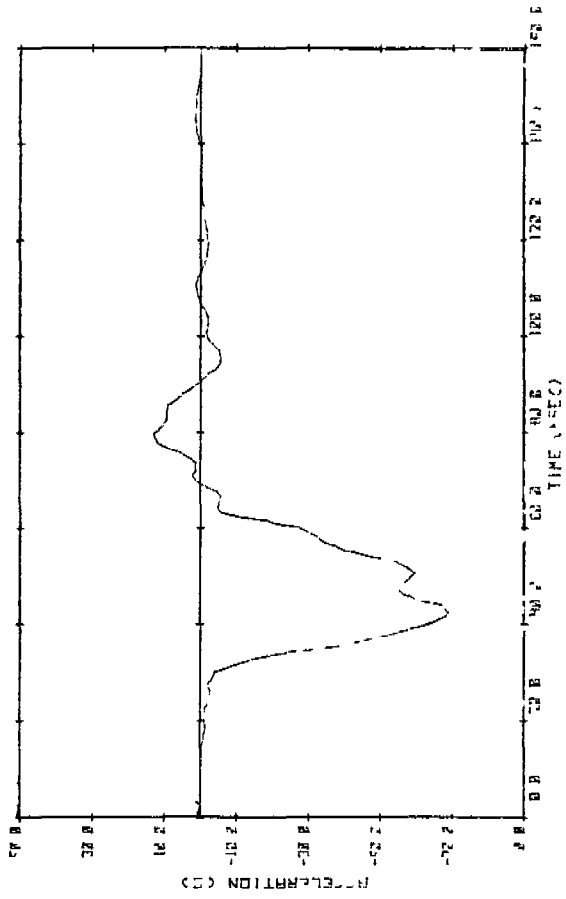


SRL 17-5 TEST #20 (H28C) - CHEST DEFLECT IN"

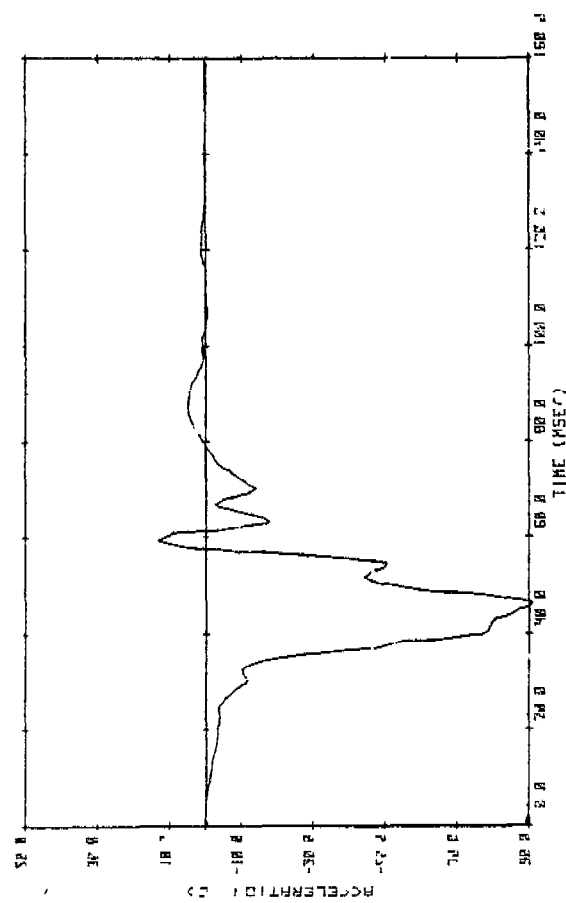


SRL 17-5 TEST #21 (GTREM) - UPPER SPINE

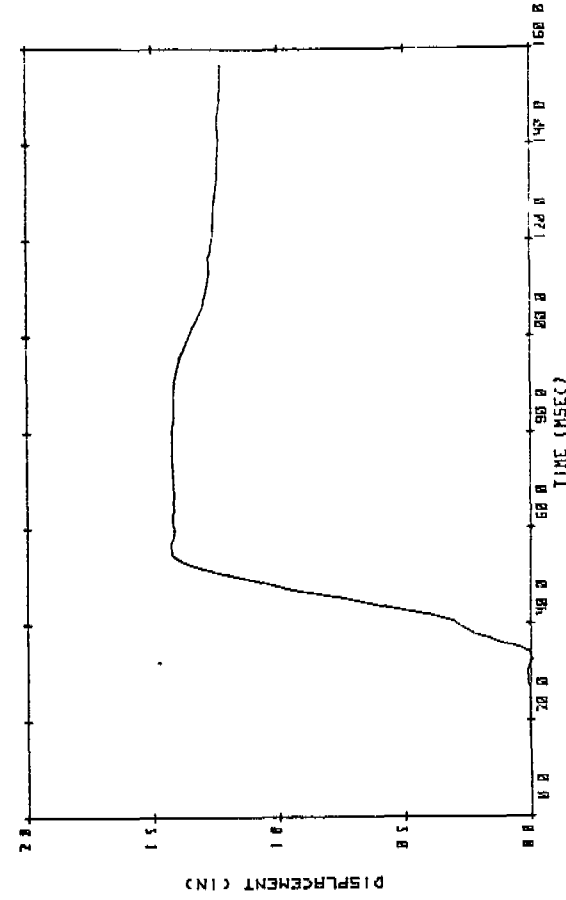
61



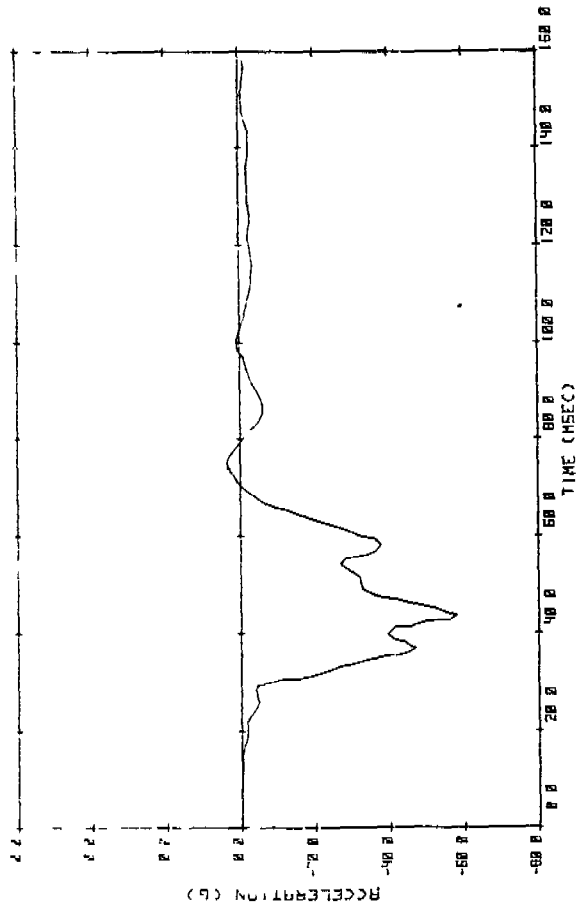
SRL 17-5 TEST #21 (GTREM) - LOWER SPINE



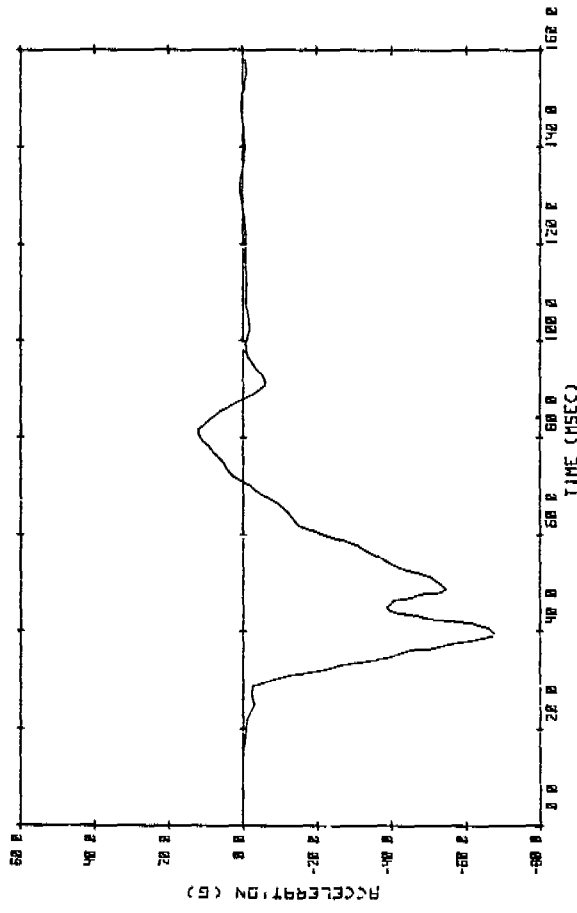
SRL 17-5 TEST #21 (GTREM) - PELVIS



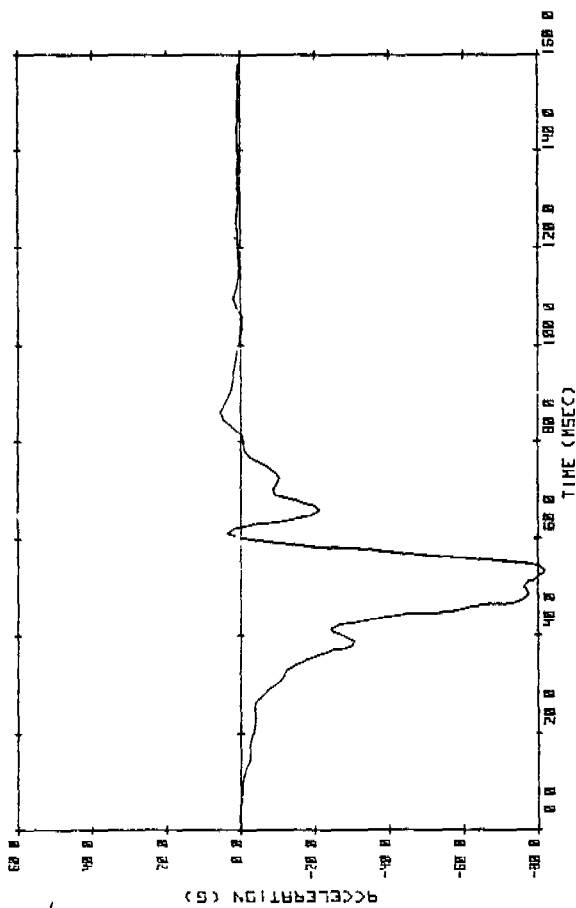
SRL 17-5 TEST #21 (GTREM) - CHEST



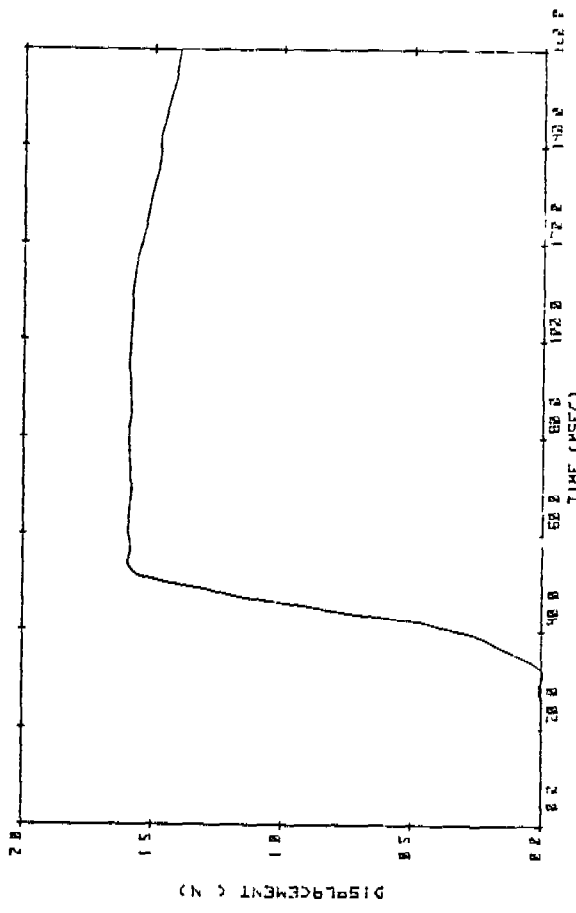
SRL 17-5 TEST #22 (2V5) - UPPER SPINE



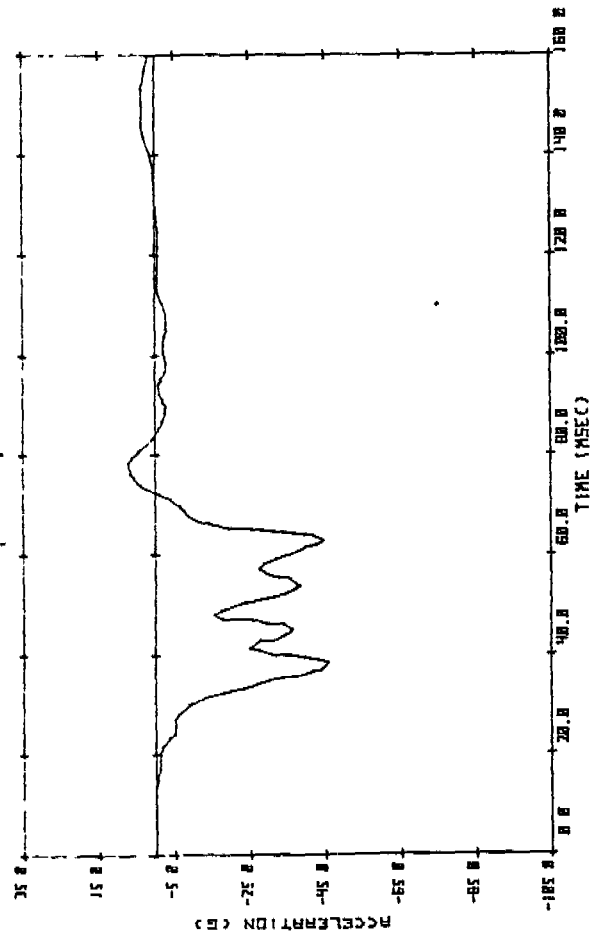
SRL 17-5 TEST #22 (2V5) - LOWER SPINE



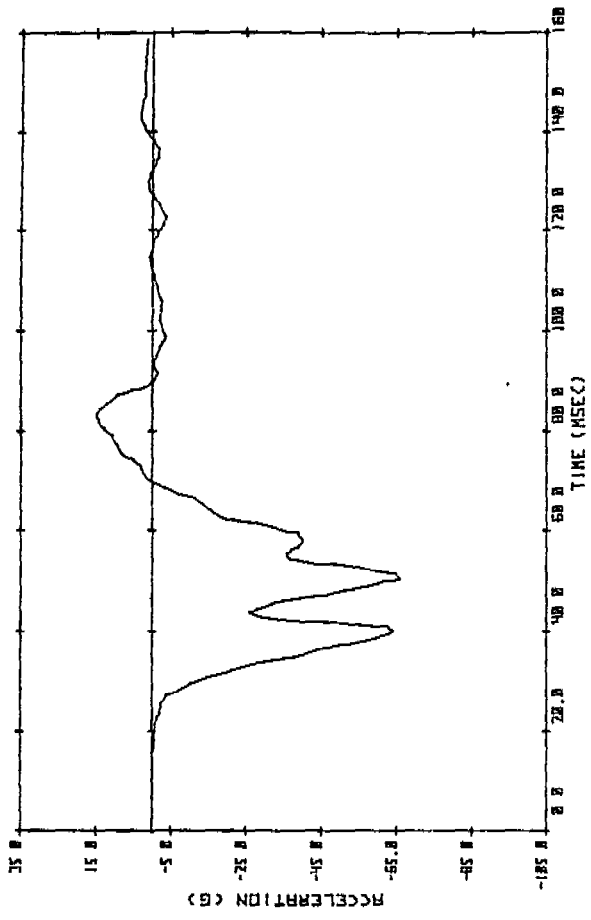
SRL 17-5 TEST #22 (2V5) - PELVIS



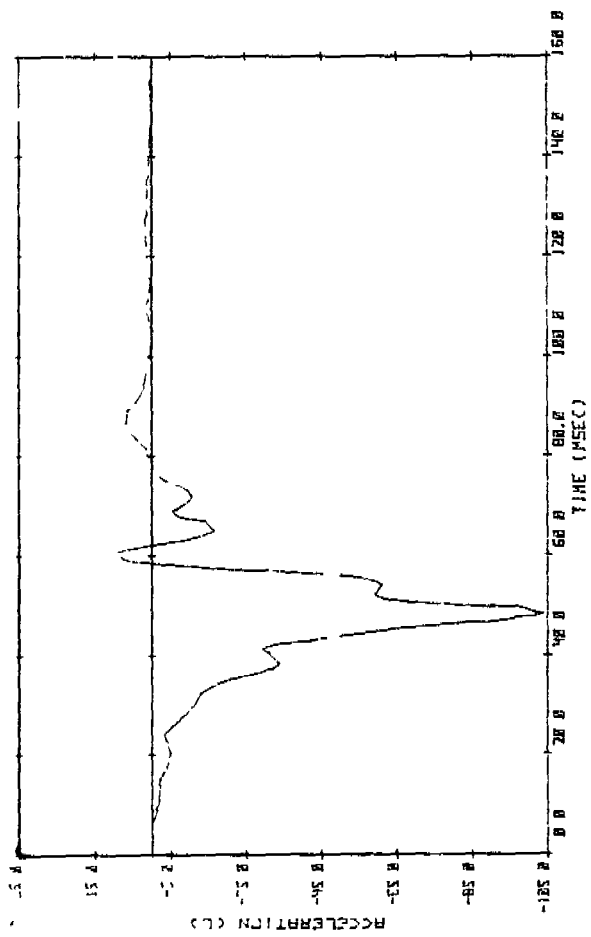
SRL 17-5 TEST #22 (2V5) - PELVIS (IN)



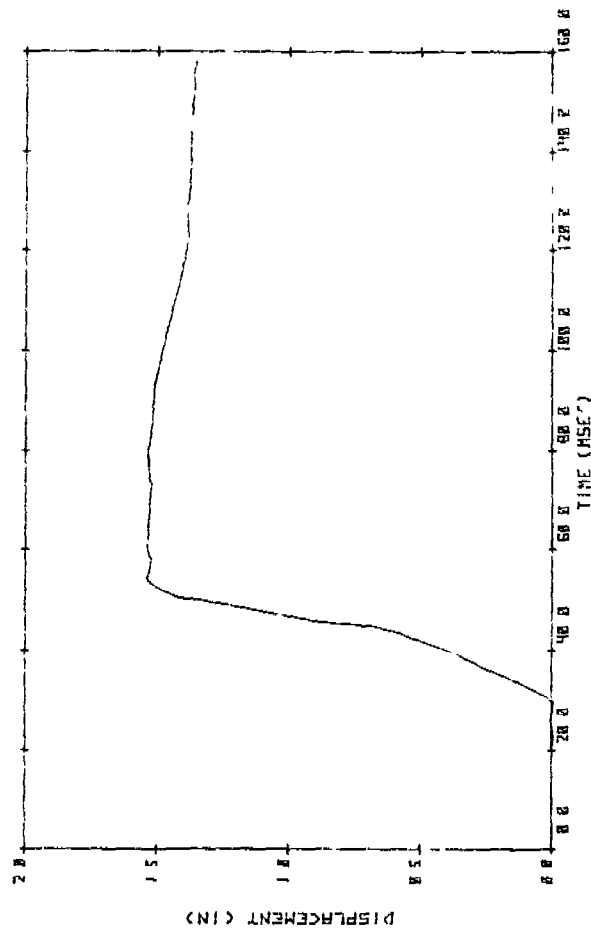
SRL 17-5 TEST #23 (H3BC) - UPPER SPINE



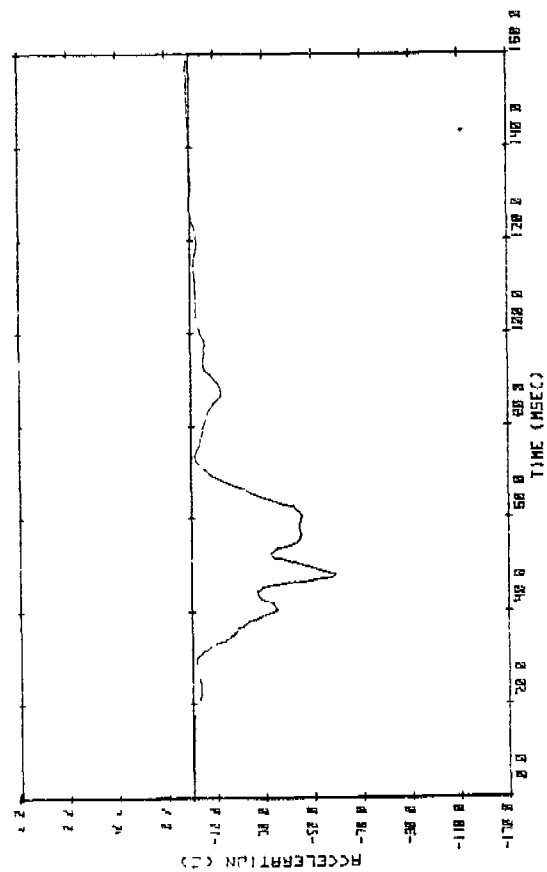
SRL 17-5 TEST #23 (H3BC) - LOWER SPINE



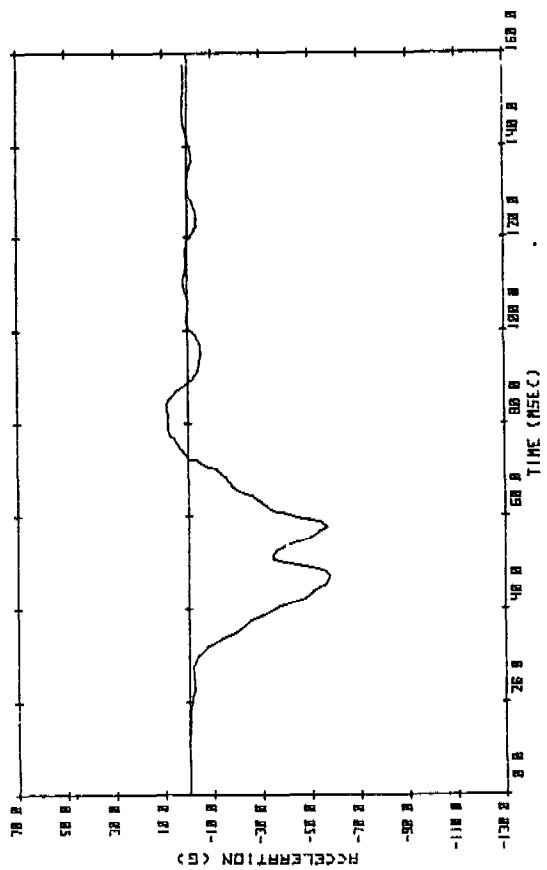
SRL 17-5 TEST #23 (H3BC) - PELVIS



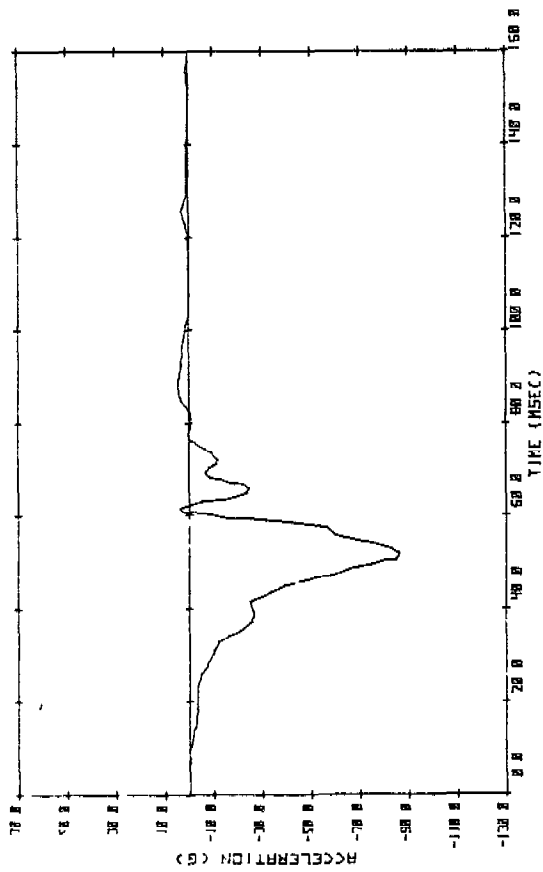
SRL 17-5 TEST #23 (H3BC) - CHEST DEFLECTION



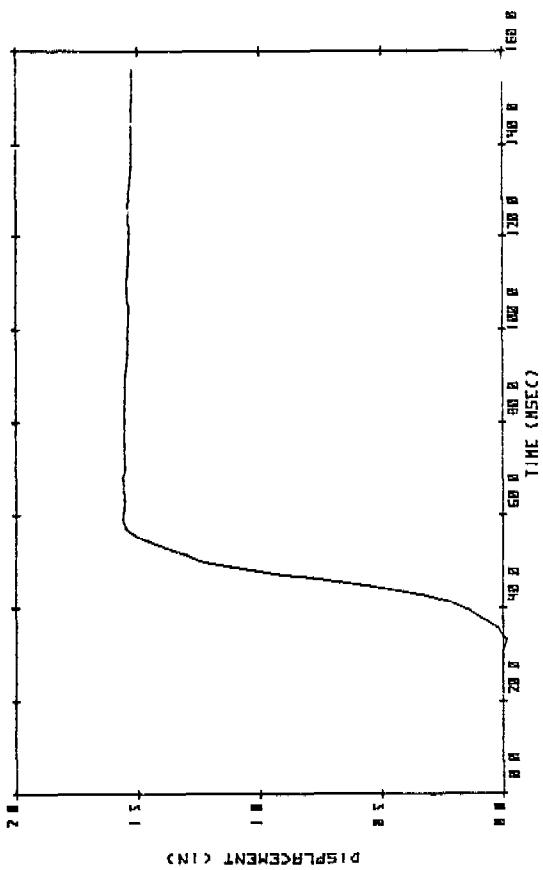
SRL 17-5 TEST #24 (C111A) - UPPER SPINE



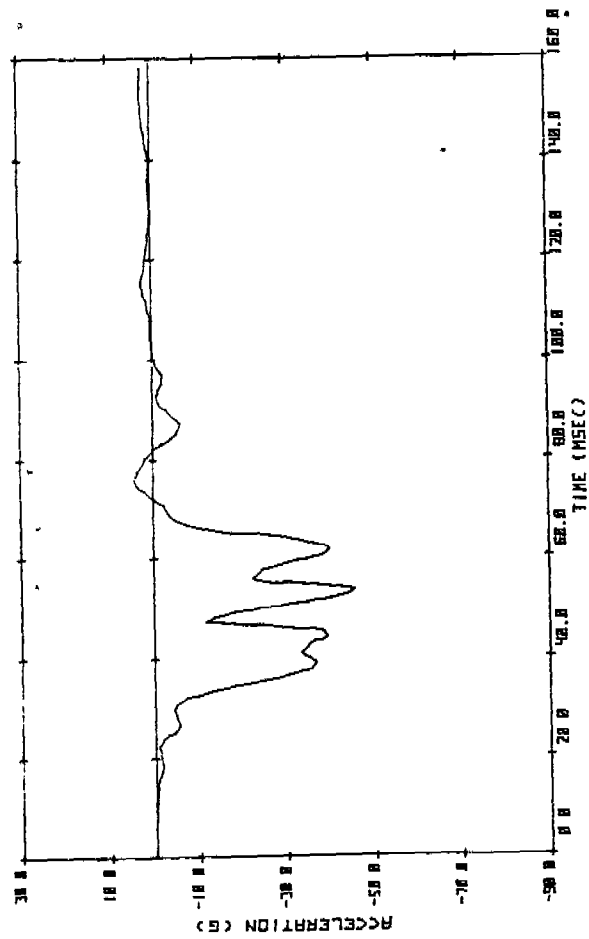
SRL 17-5 TEST #24 (C111A) - LOWER SPINE



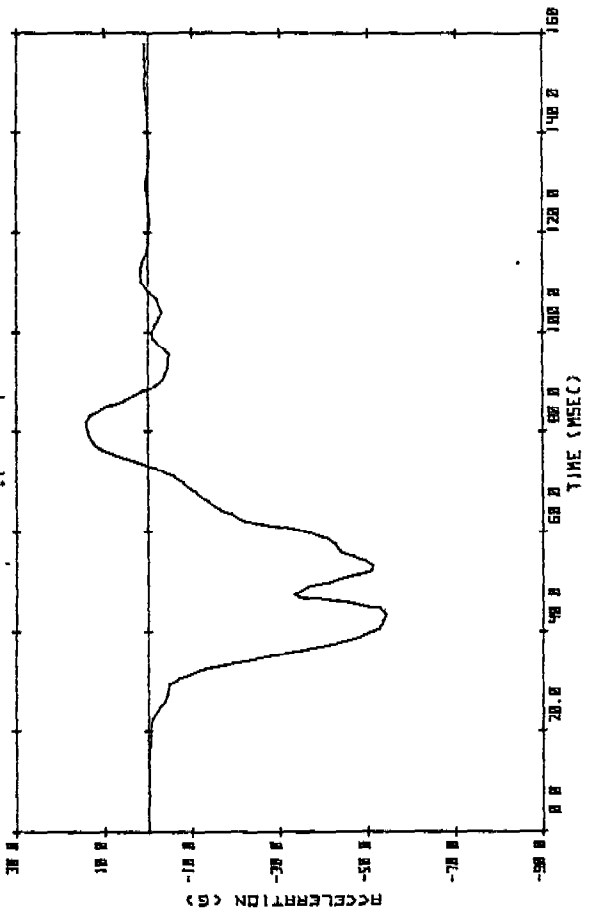
SRL 17-5 TEST #24 (C111A) - PELVIS



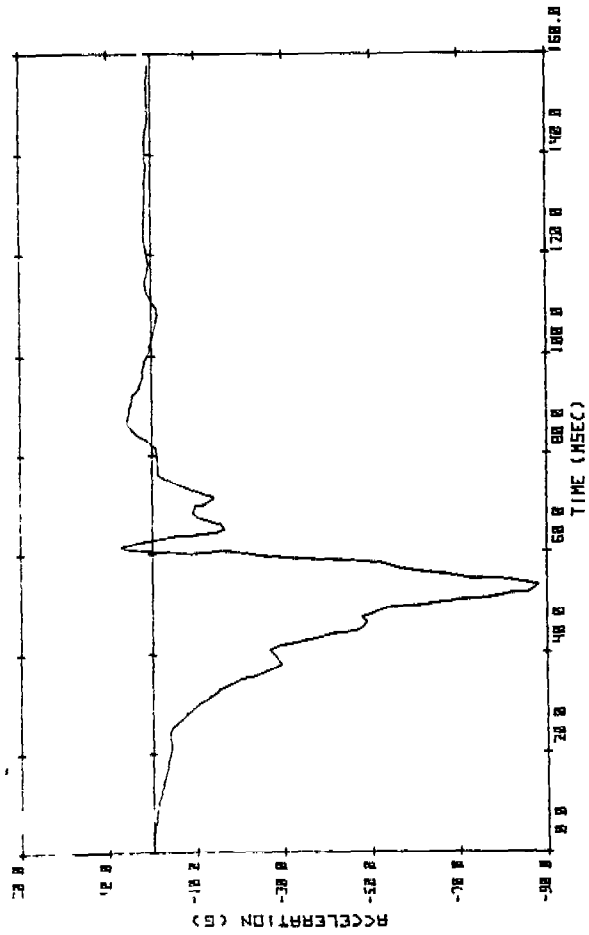
SRL 17-5 TEST #24 (C111A) - CHEST DEFLECTION



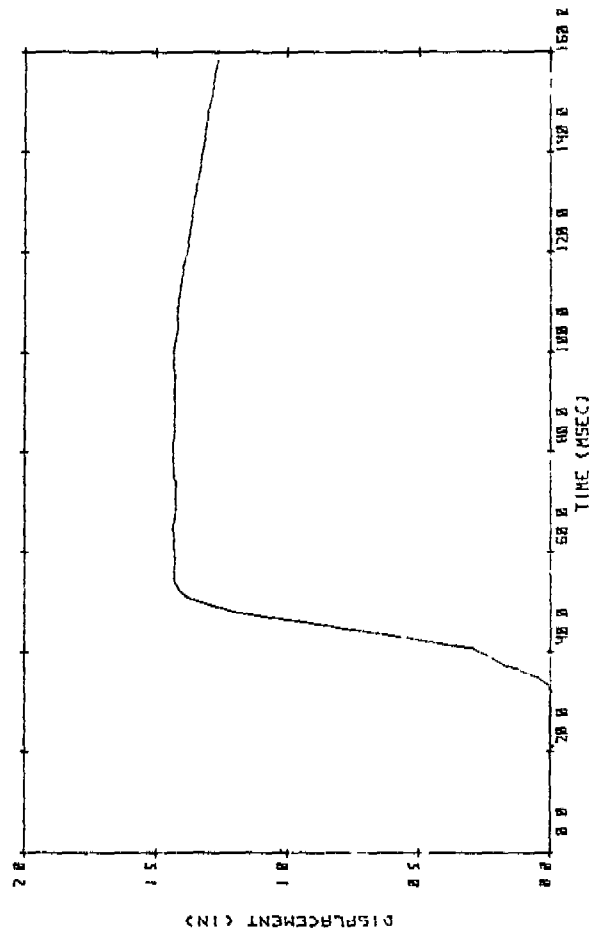
SRL 17-5 TEST #25 (C222A) - UPPER SPINE



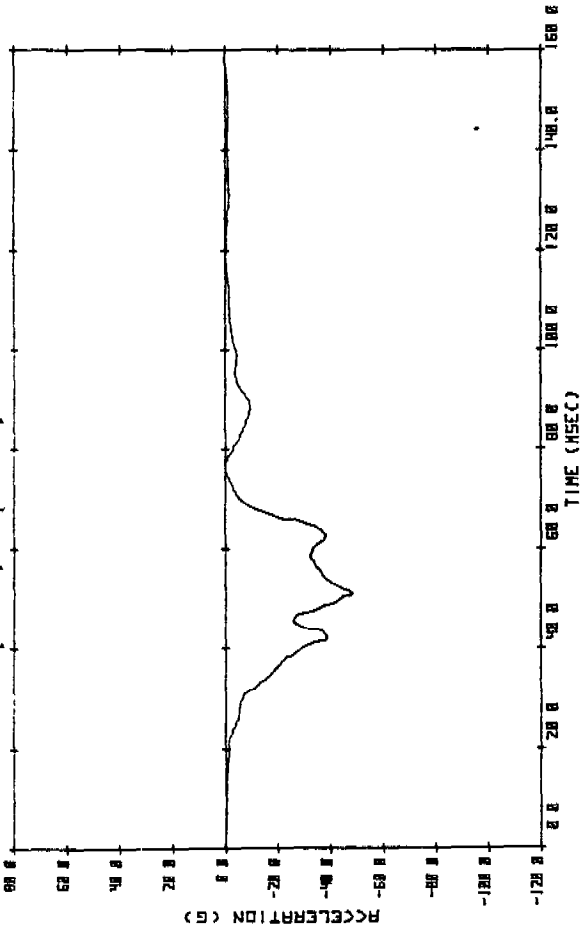
SRL 17-5 TEST #25 (C222A) - LOWER SPINE



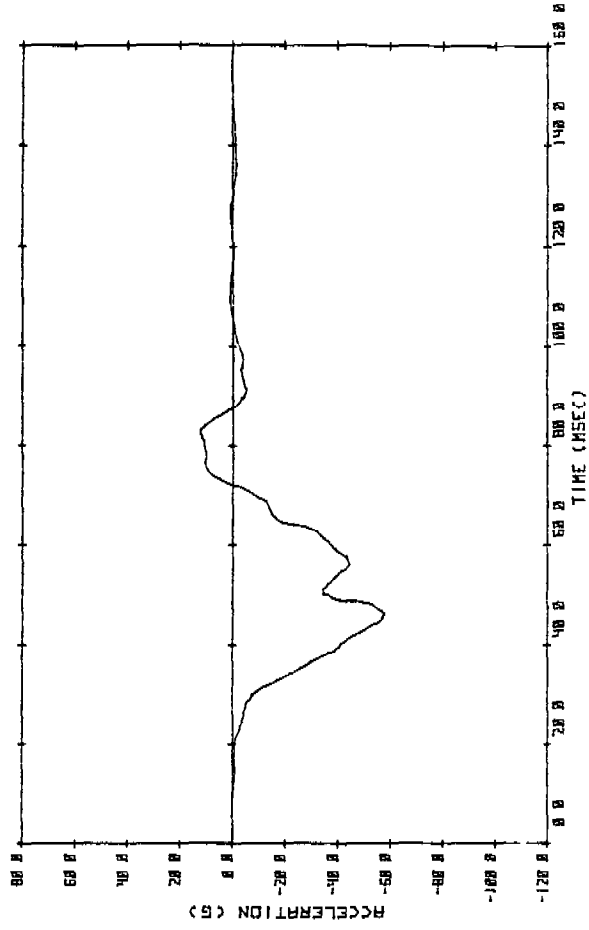
SRL 17-5 TEST #25 (C222A) - PELVIS



SRL 17-5 TEST #25 (C222A) - CHEST DEFLECTION

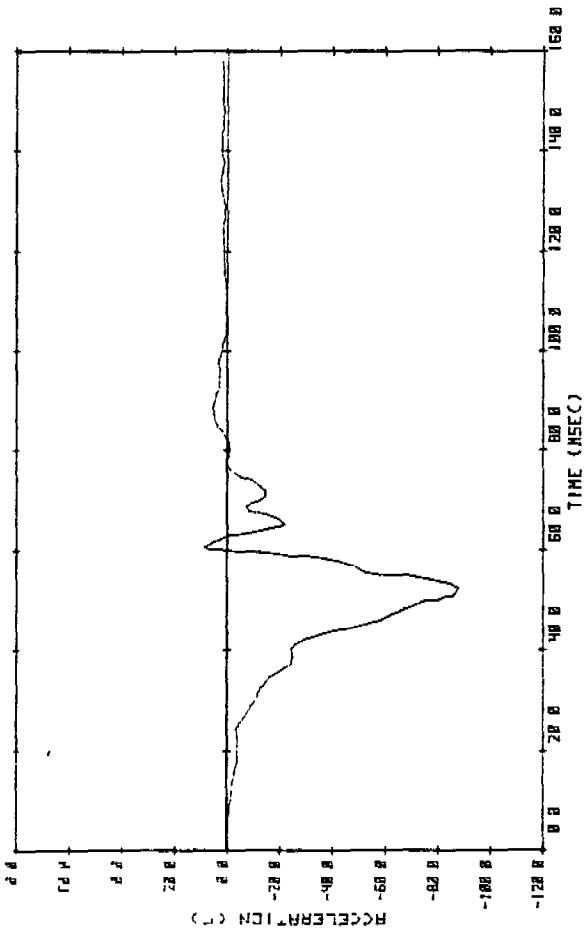


SRL 17-S TEST #26 (R-310-V) - UPPER SPINE

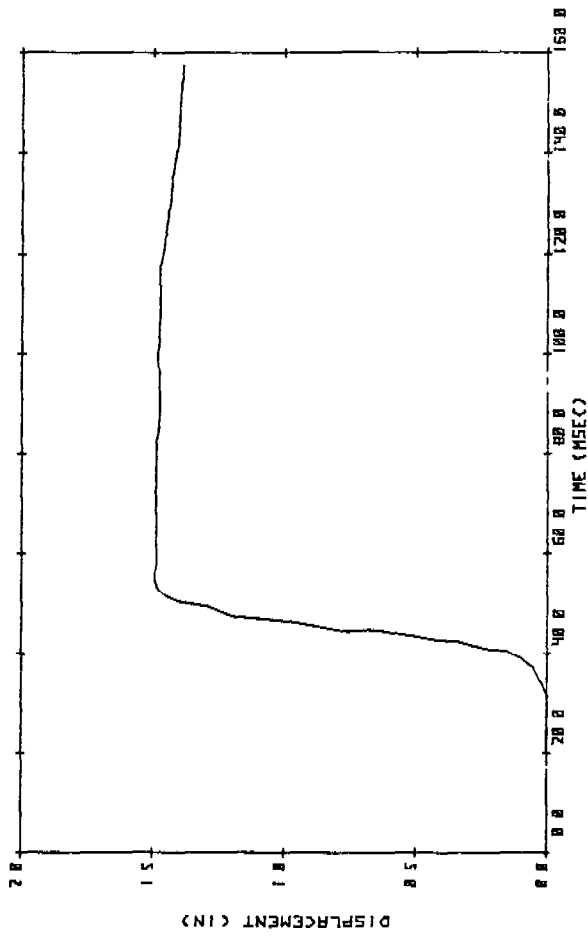


SRL 17 S TEST #26 (R-310-V) - LOWER SPINE

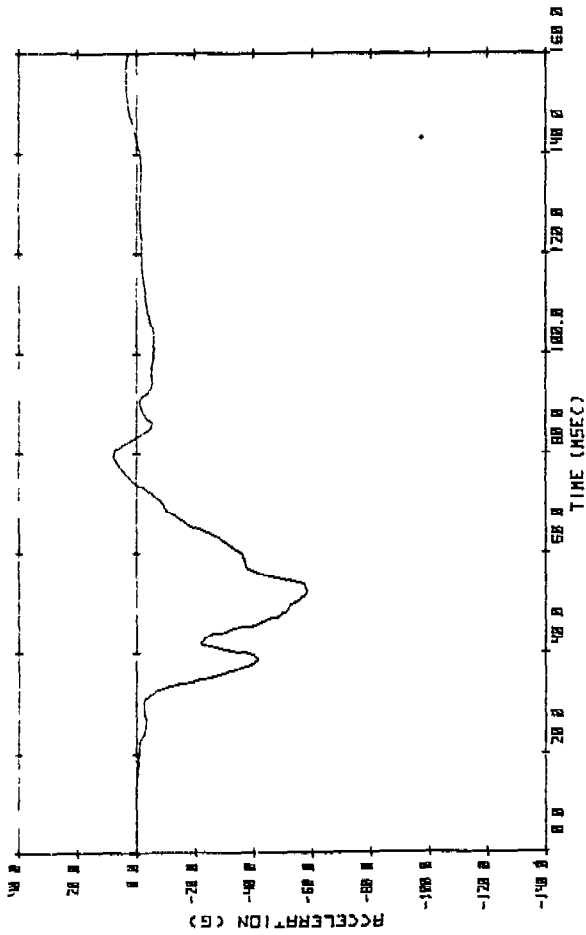
61-H



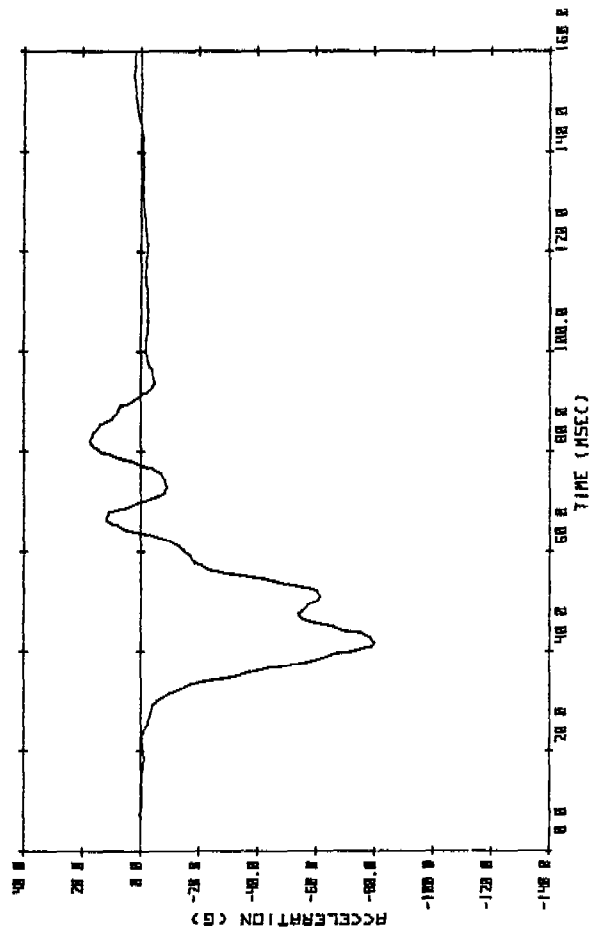
SRL 17-S TEST #26 (R-310-V) - PELVIS



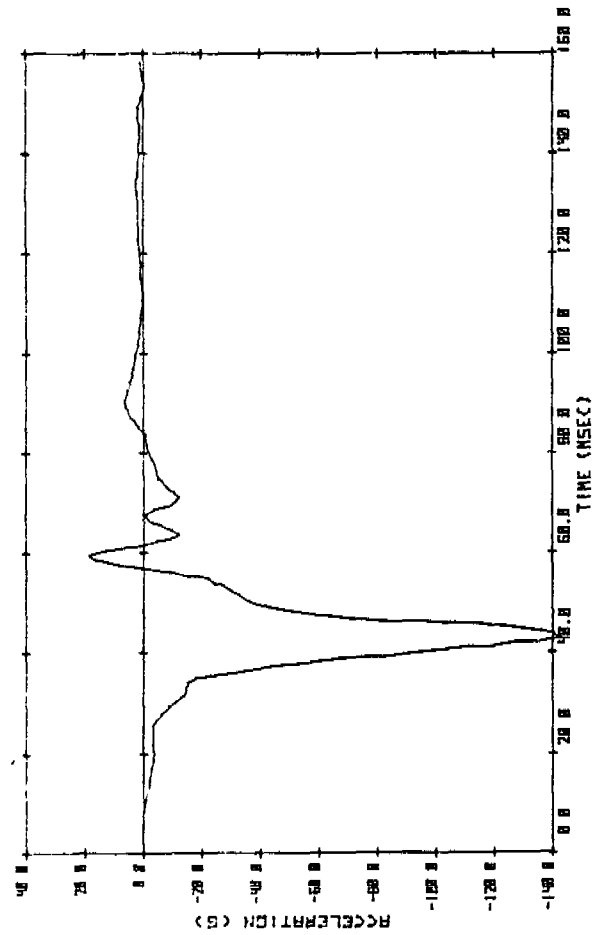
SRL 17-S TEST #26 (R-310-V) - CHEST DEFL'N



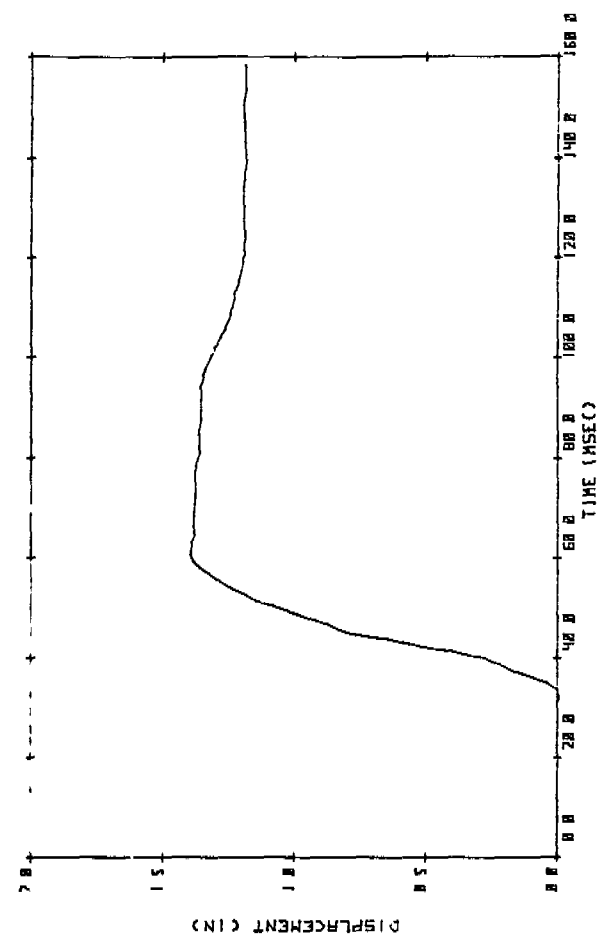
SRL 17-5 TEST #27 (GTREM) - UPPER SPINE



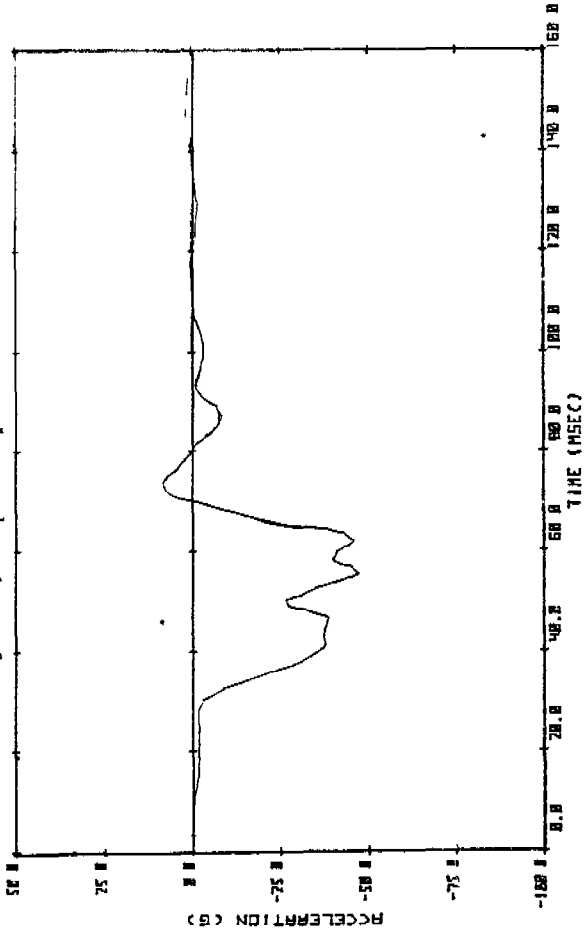
SRL 17-5 TEST #27 (GTREM) - LOWER SPINE



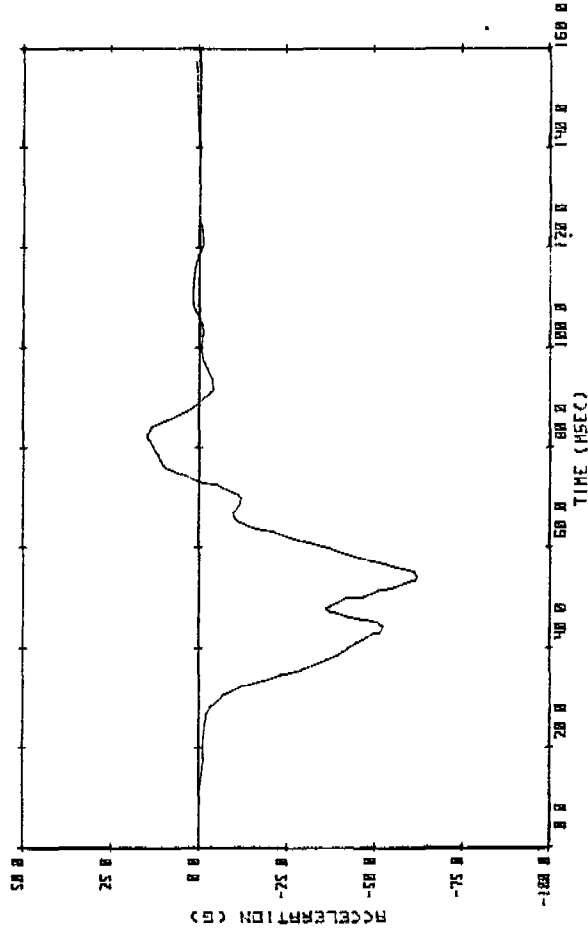
SRL 17-5 TEST #27 (GTREM) - PELVIS



SRL 17-5 TEST #27 (GTREM) - CHEST DEFLECTION

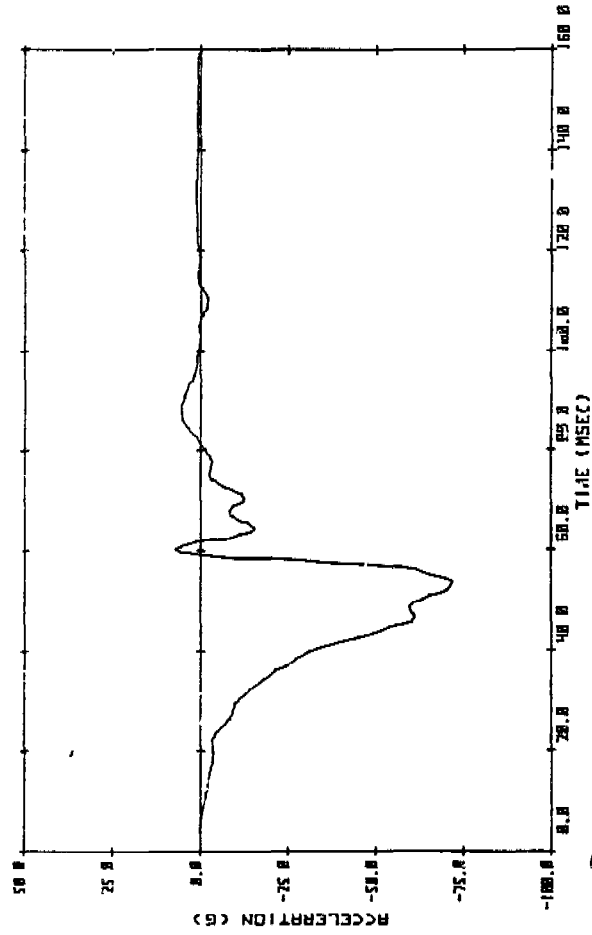


SRL 17-5 TEST #28 (APR) - UPPER SPINE

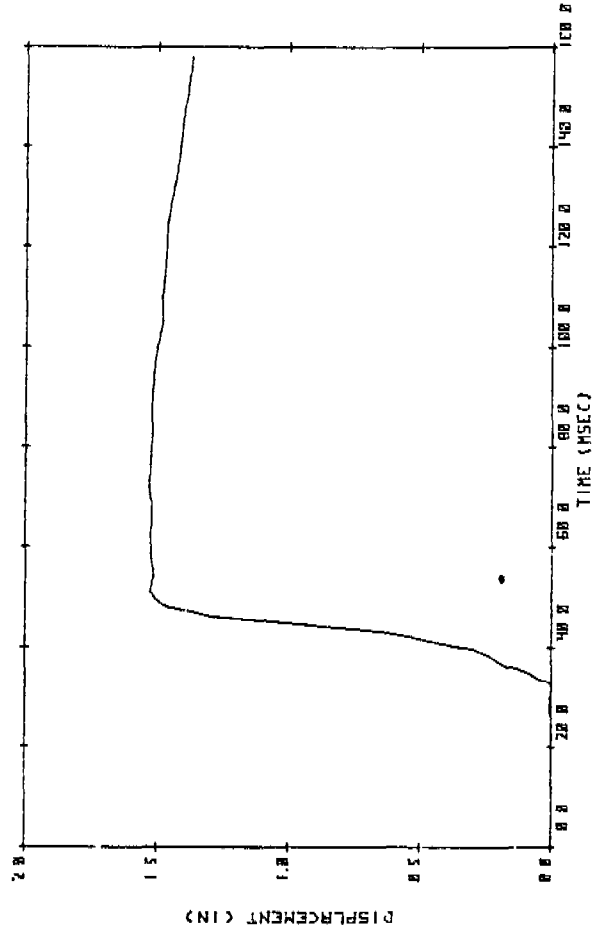


SRL 17-5 TEST #28 (APR) - LOWER SPINE

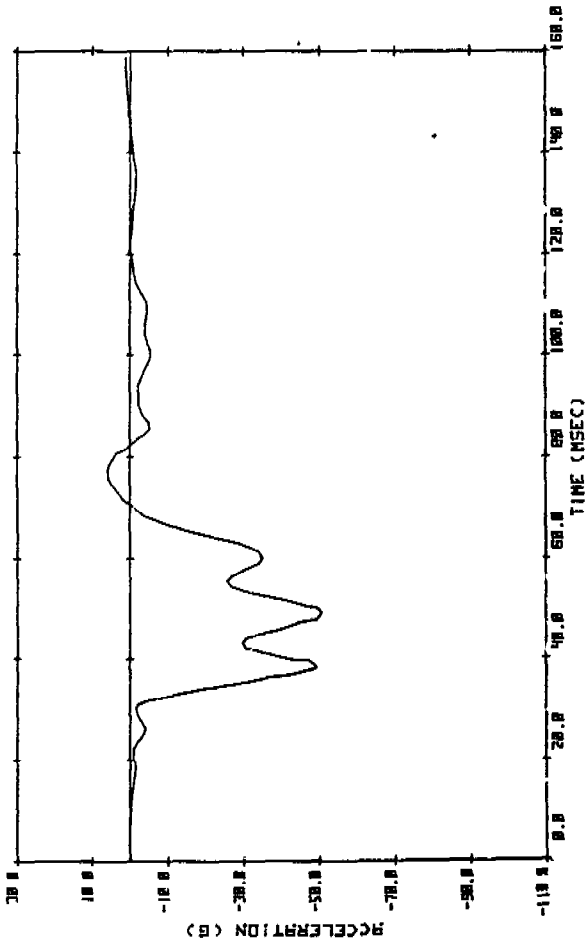
23



SRL 17-5 TEST #28 (APR) - PELVIS

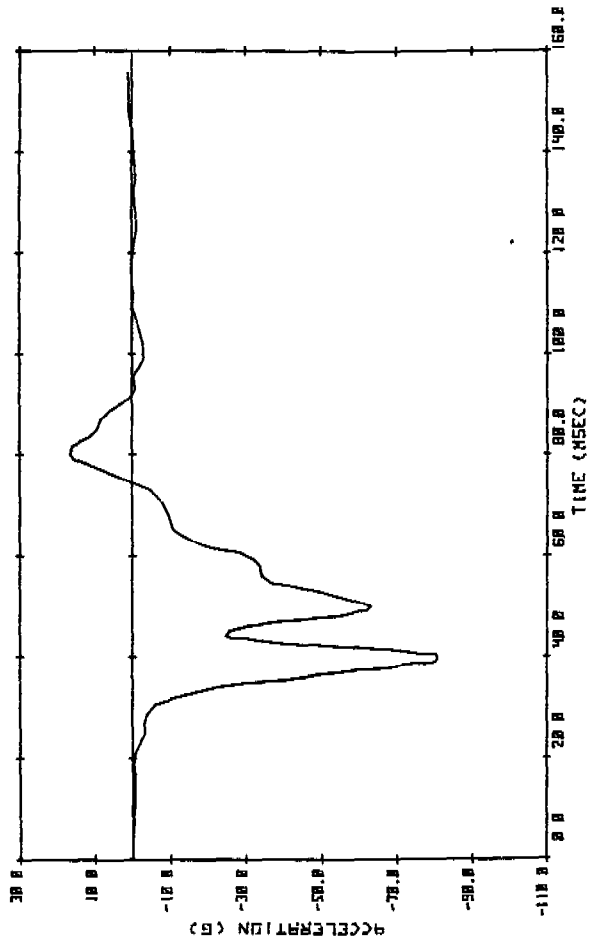


SRL 17-5 TEST #28 (APR) - CHEST DEFLECTION

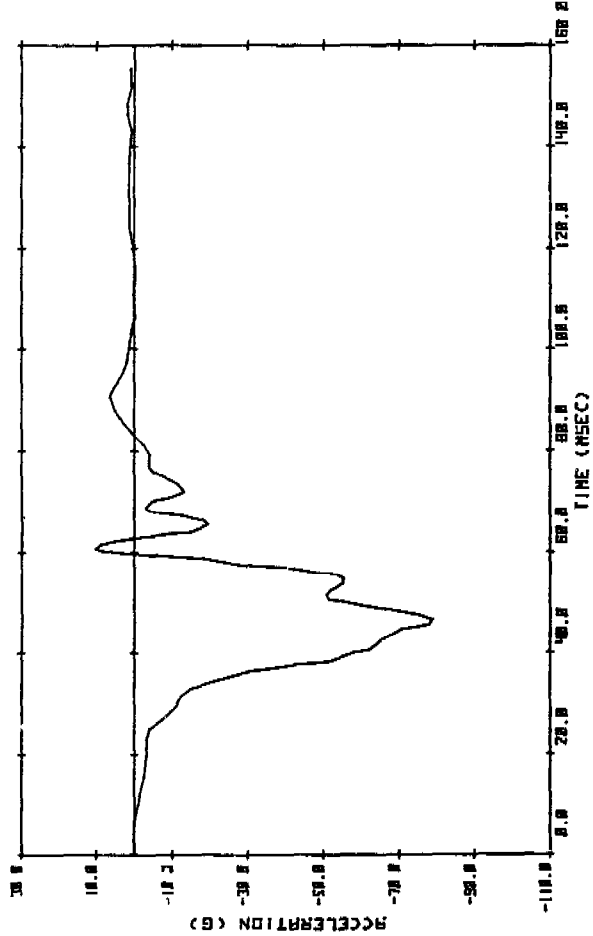


4-25

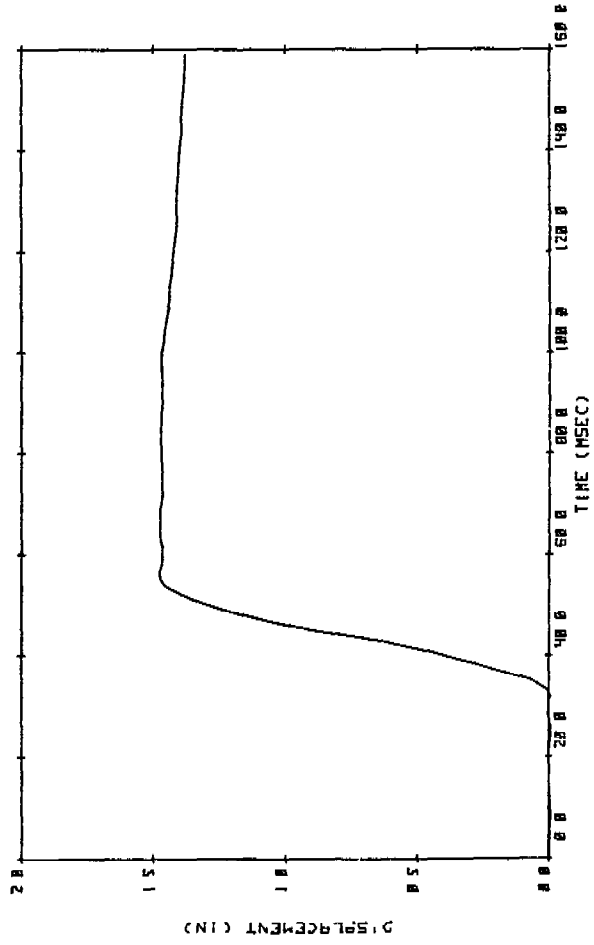
SRL 17-5 TEST #29 (C311A) - UPPER SPINE



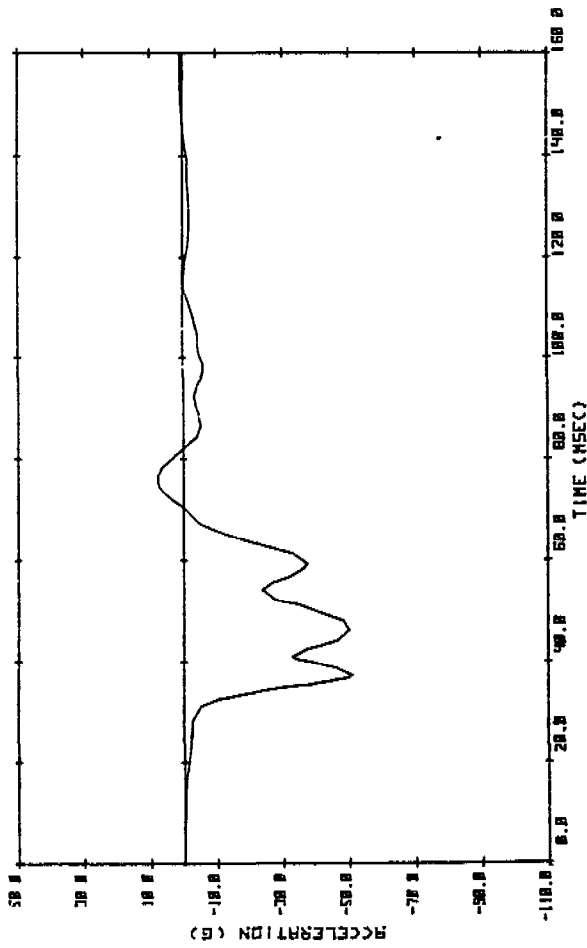
SRL 17-5 TEST #29 (C311A) - LOWER SPINE



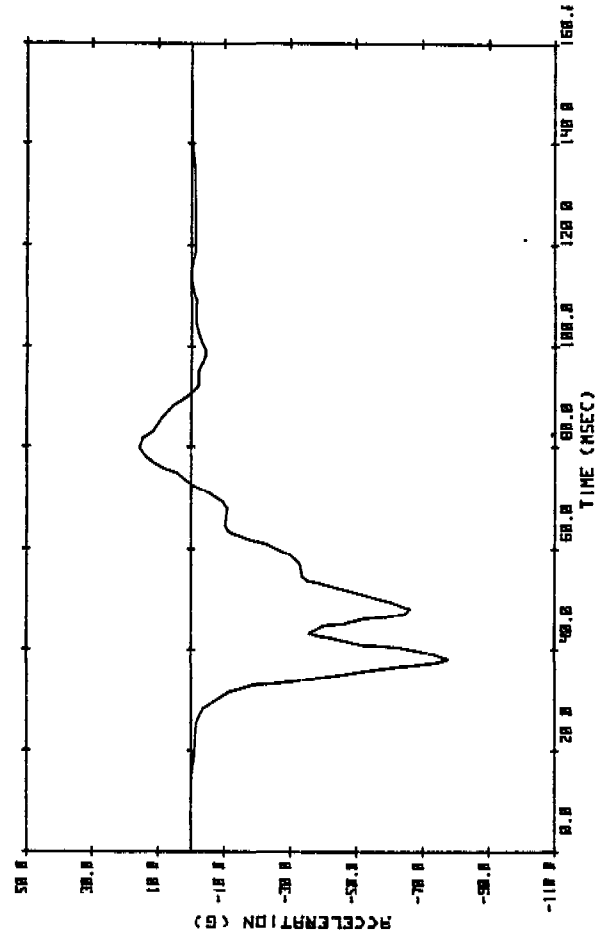
SRL 17-5 TEST #29 (C311A) - PELVIS



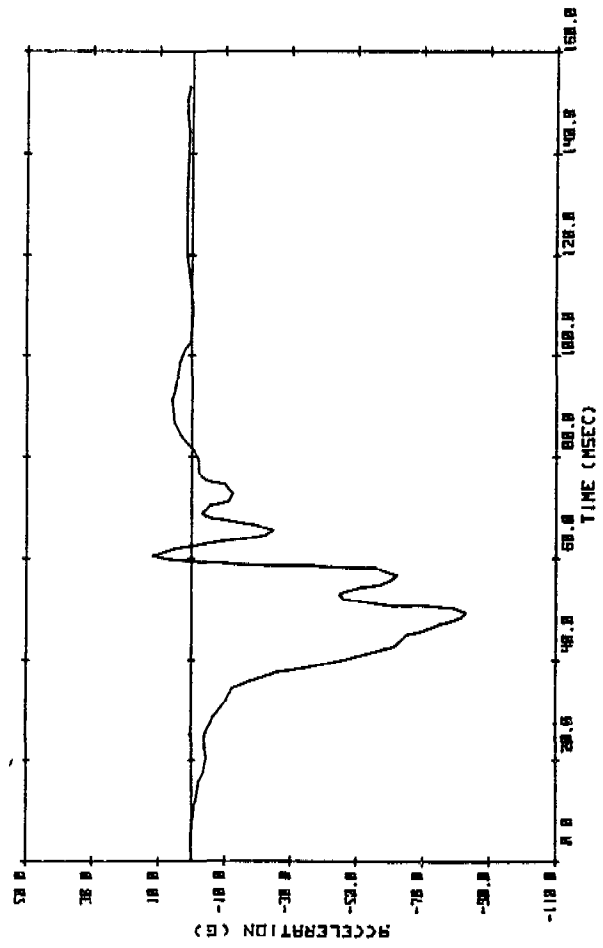
SRL 17-5 TEST #29 (C311A) - CHEST DEFLECTION



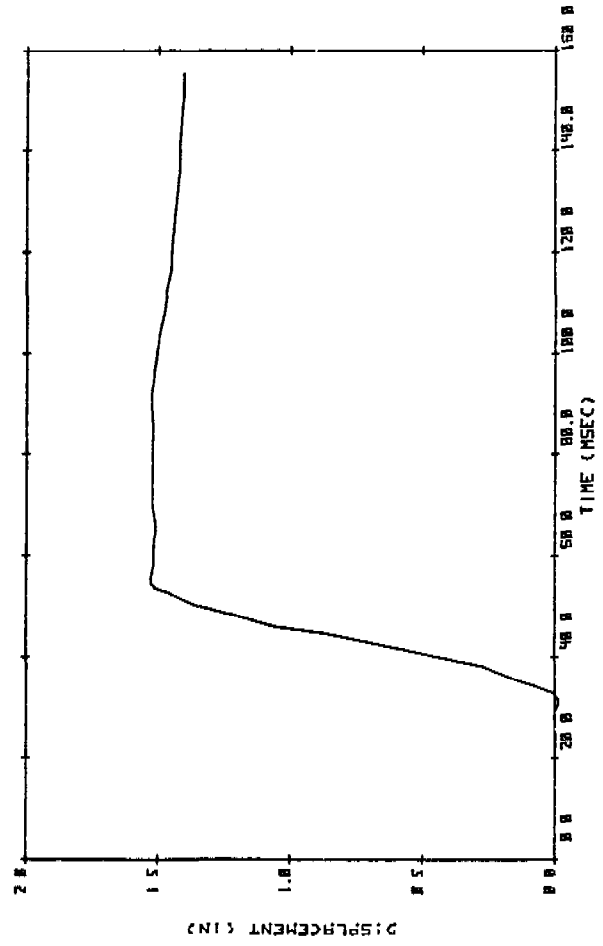
SRL 17-5 TEST #30 (ETH 600) - UPPER SPINE



SRL 17-5 TEST #30 (ETH 600) - LOWER SPINE

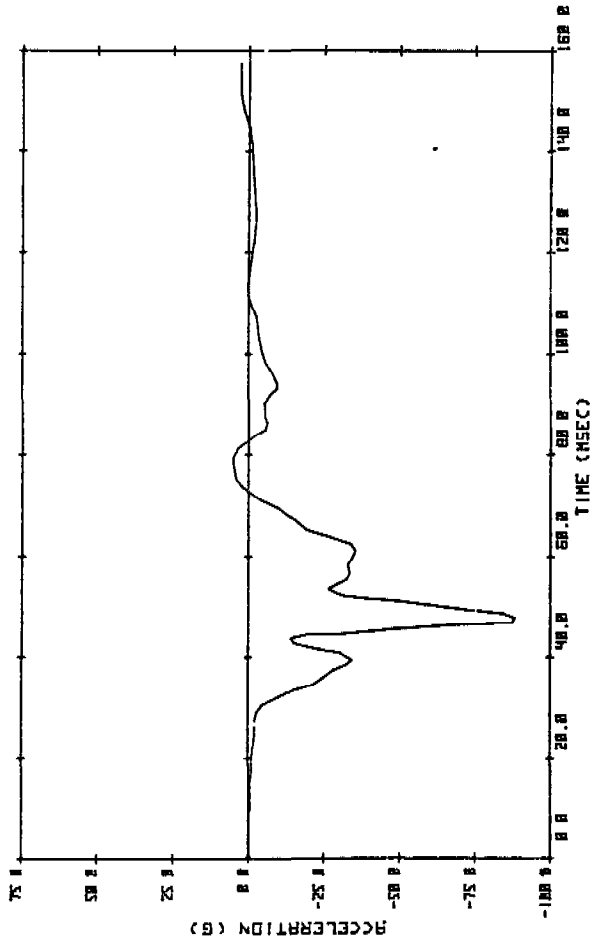


SRL 17-5 TEST #30 (ETH 600) - PELVIS

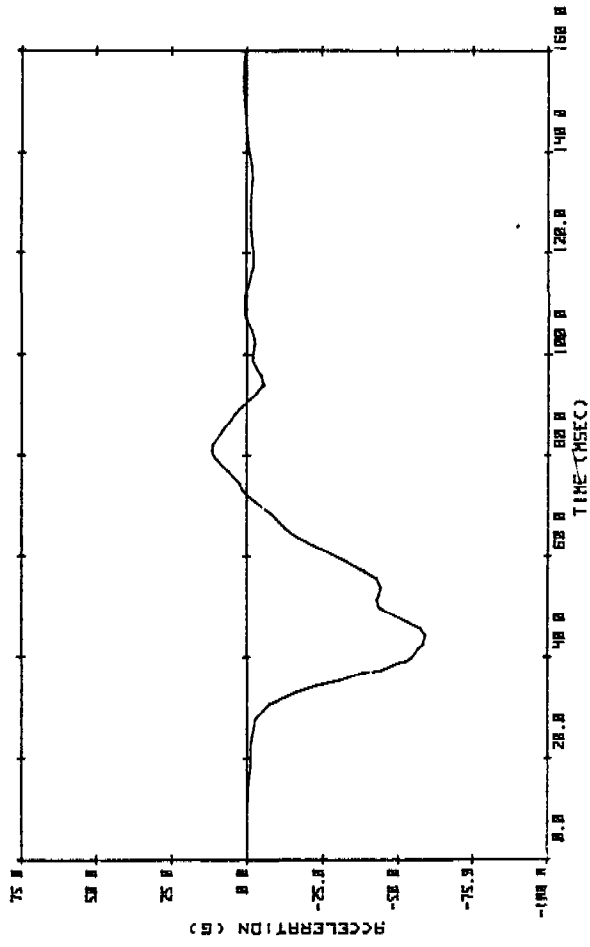


SRL 17-5 TEST #30 (ETH 600) - CHEST DEFL'N

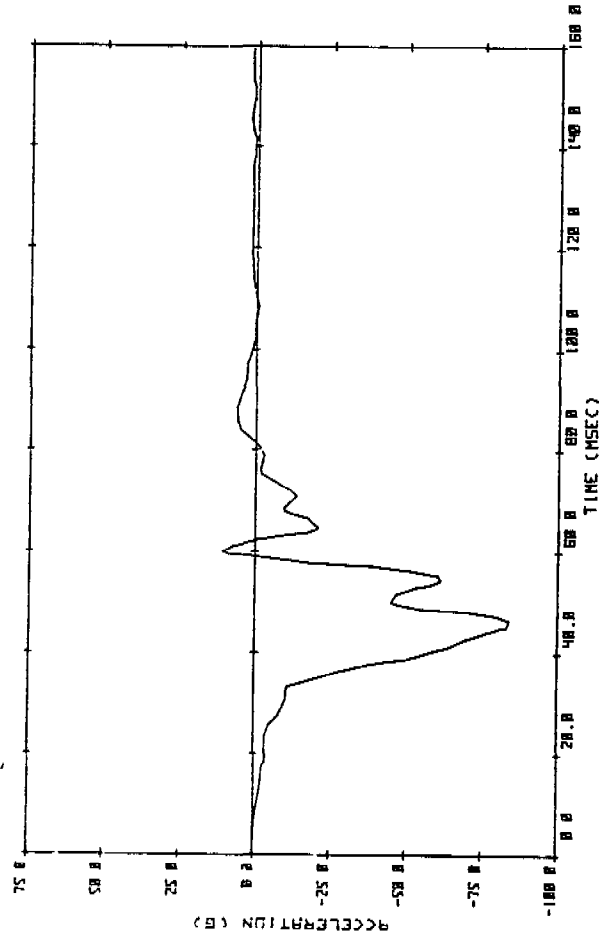
SRL 17-5 TEST #31 (R-310-V) - UPPER SPINE



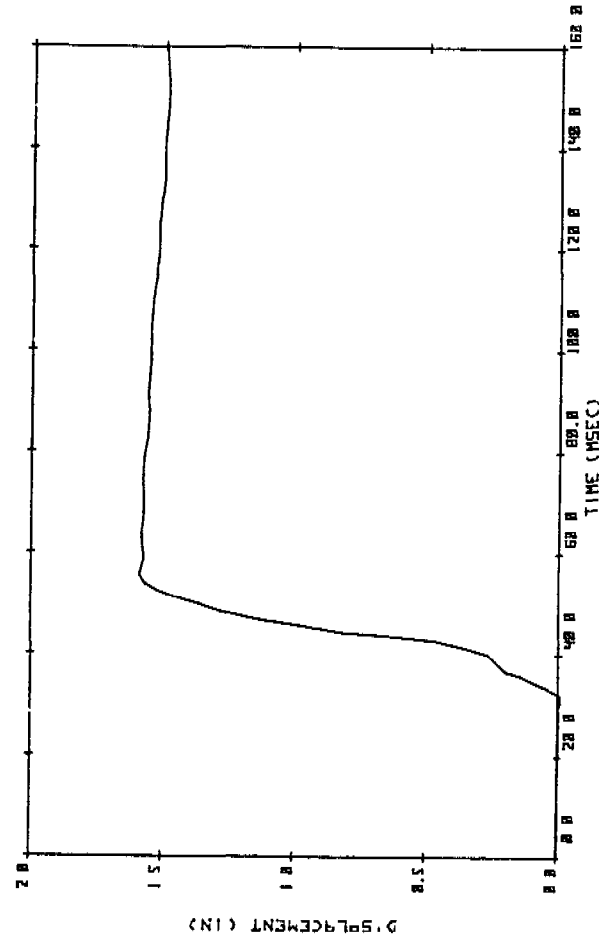
SRL 17-5 TEST #31 (R-310-V) - LOWER SPINE

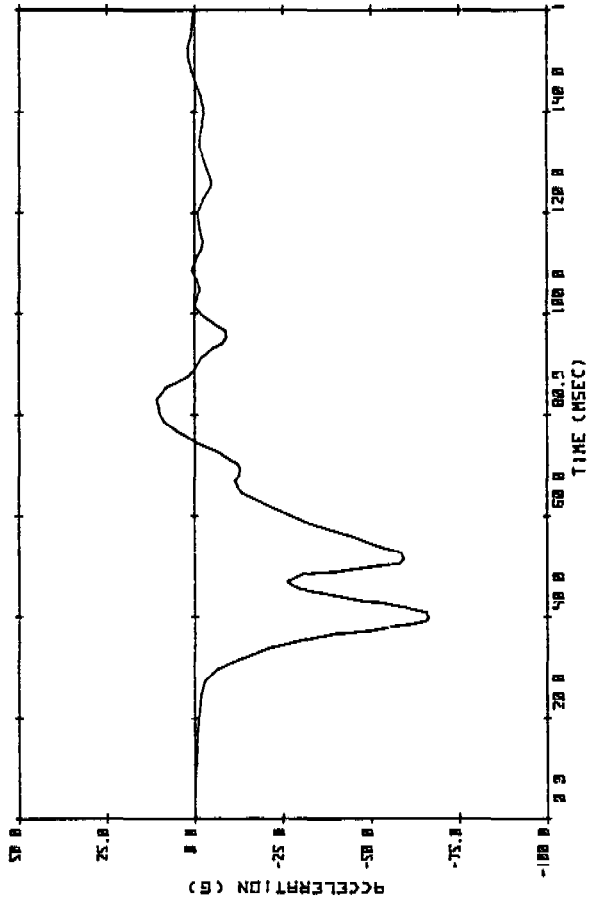


SRL 17-5 TEST #31 (R-310-V) - PELVIS

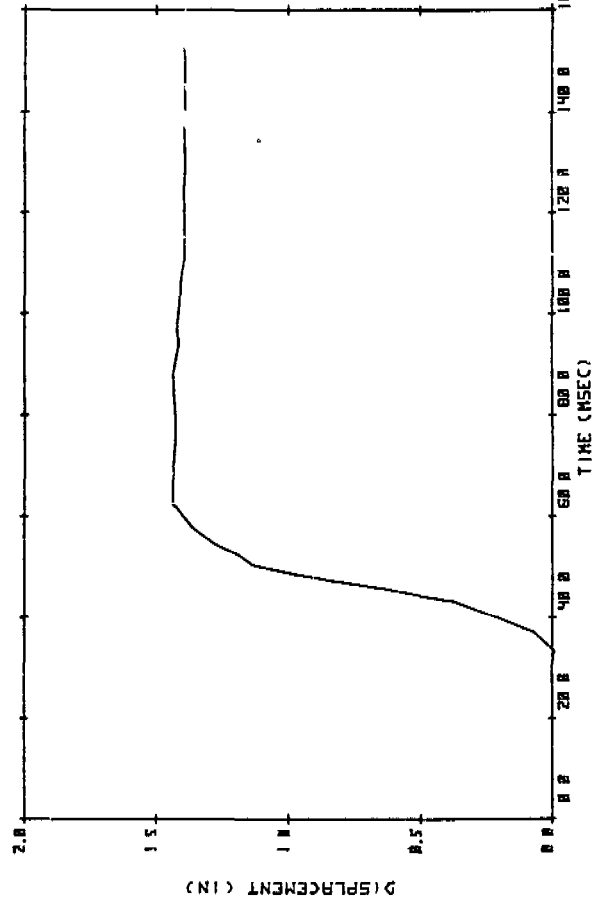


SRL 17-5 TEST #31 (R-310-V) - CHEST DEFLIN

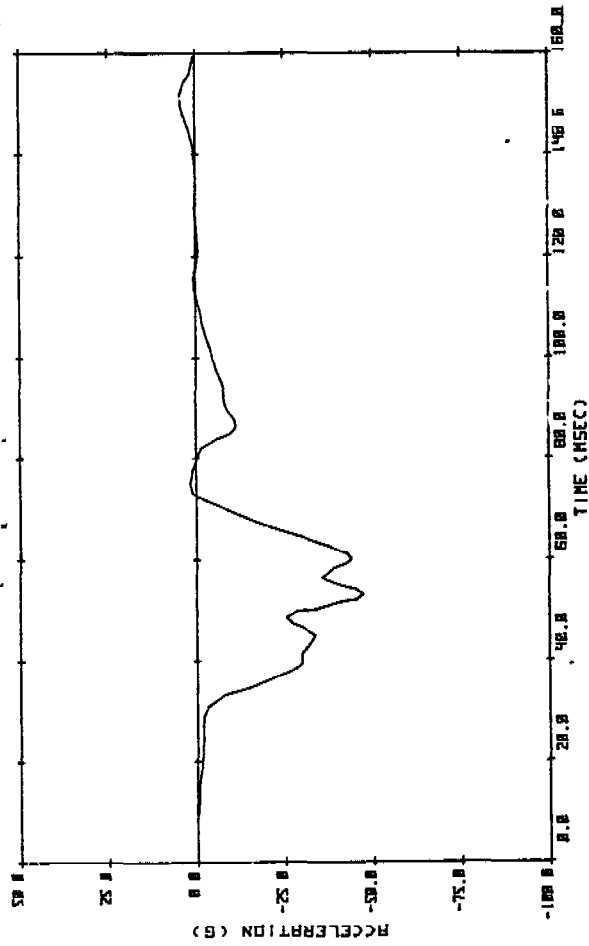




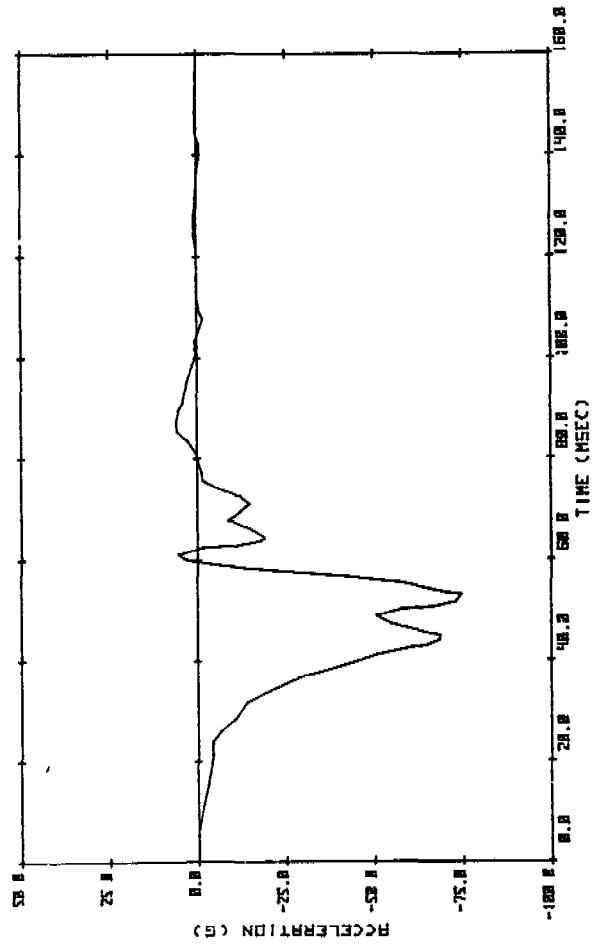
SRL 17-5 TEST #32 (ARC) - LOWER SPINE



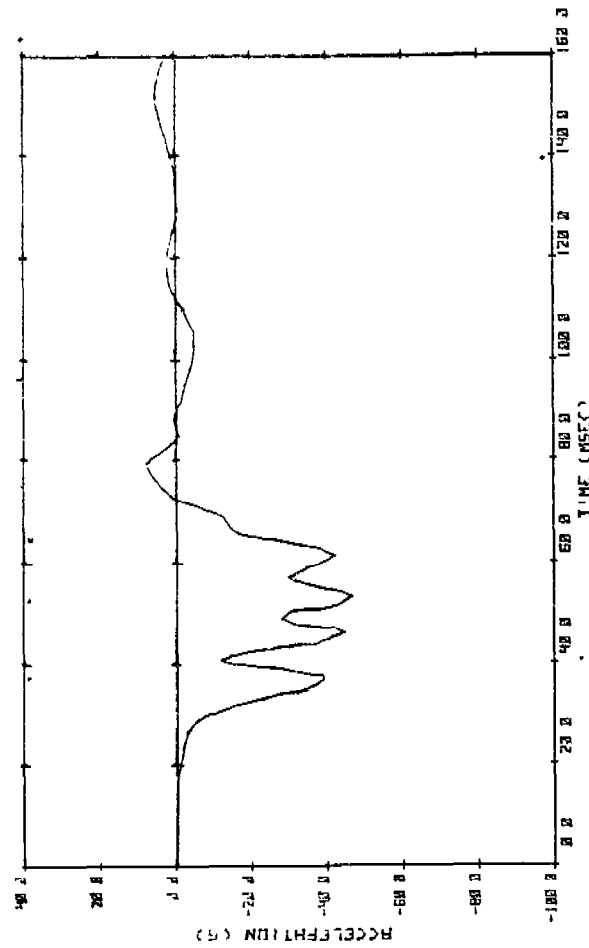
SRL 17-5 TEST #32 (ARC) - CHEST DEFLECTION



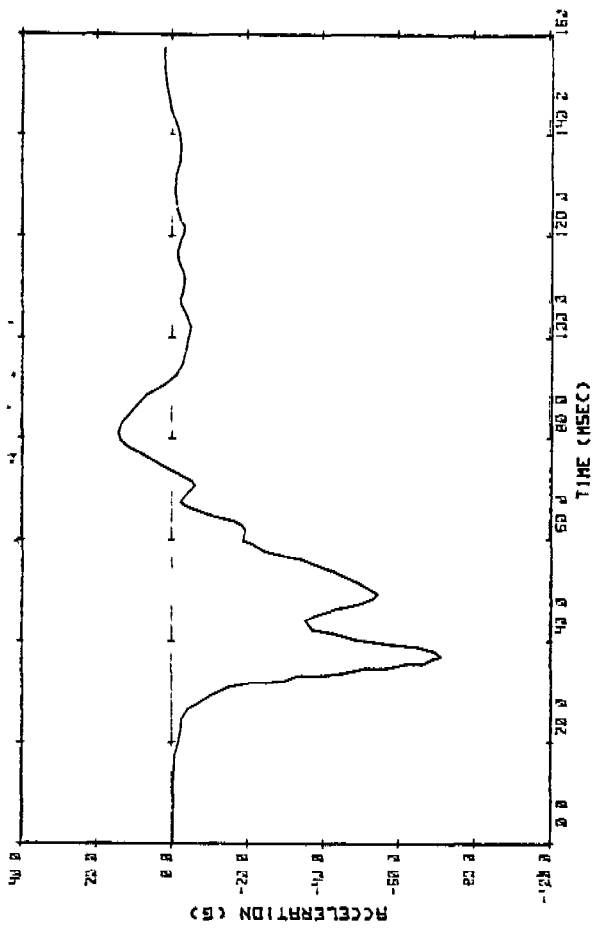
SRL 17-5 TEST #32 (ARC) - UPPER SPINE



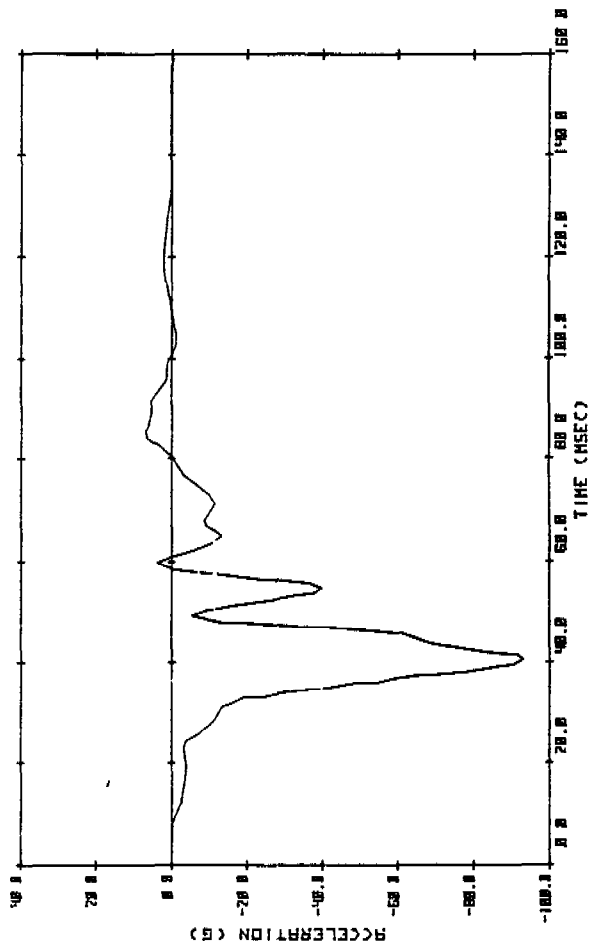
SRL 17-5 TEST #32 (ARC) - PELVIS



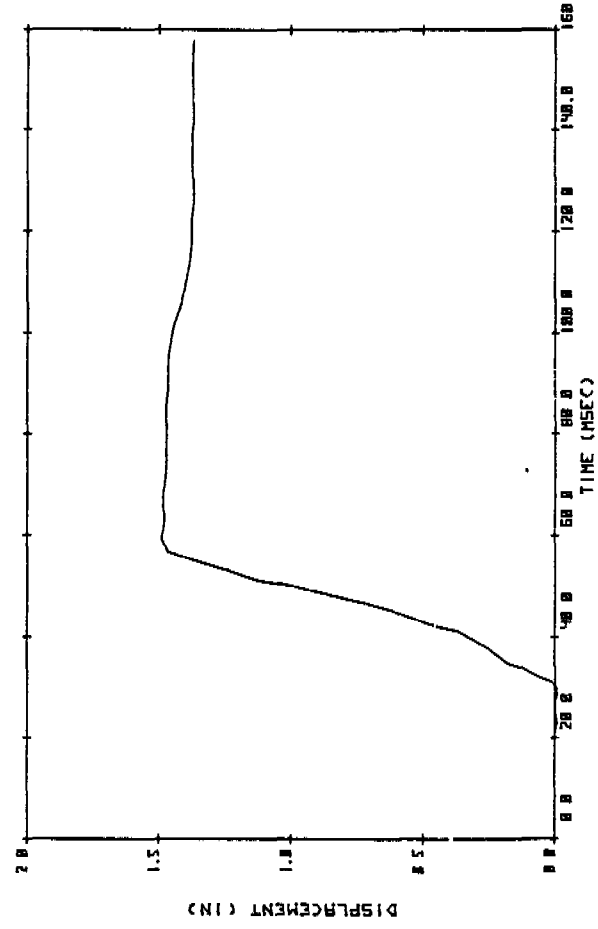
SRL 17-5 TEST #33 (H3BC) - UPPER SPINE



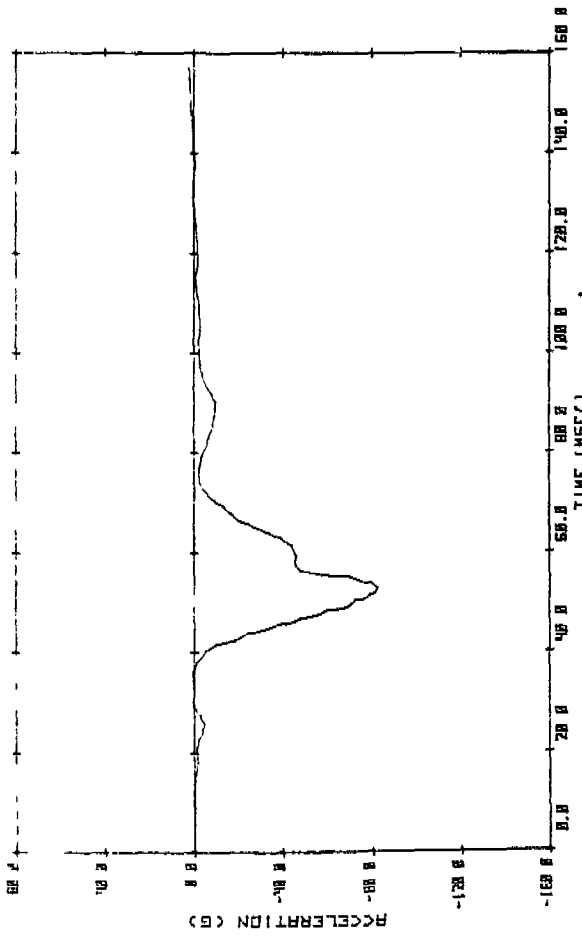
SRL 17-5 TEST #33 (H3BC) - LOWER FEMUR



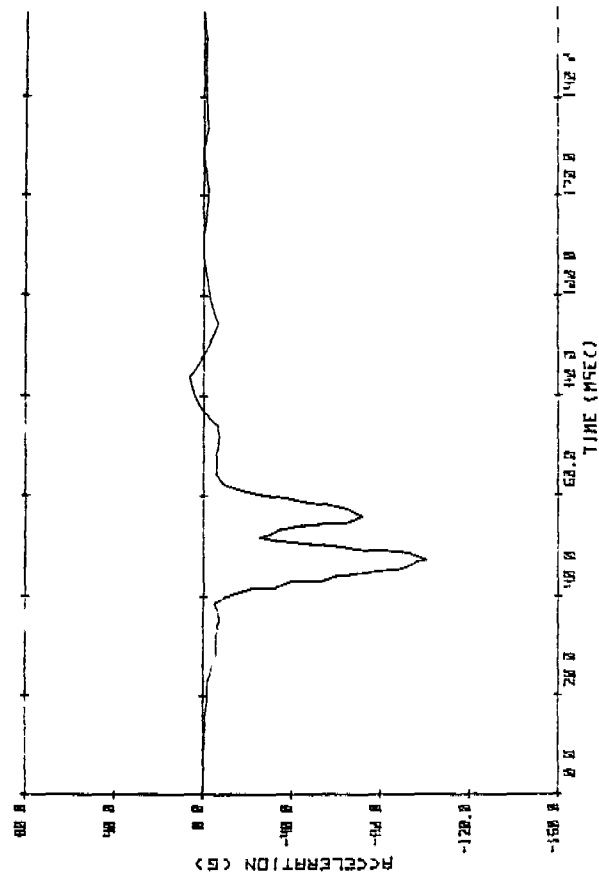
SRL 17-5 TEST #33 (H3BC) - PELVIS



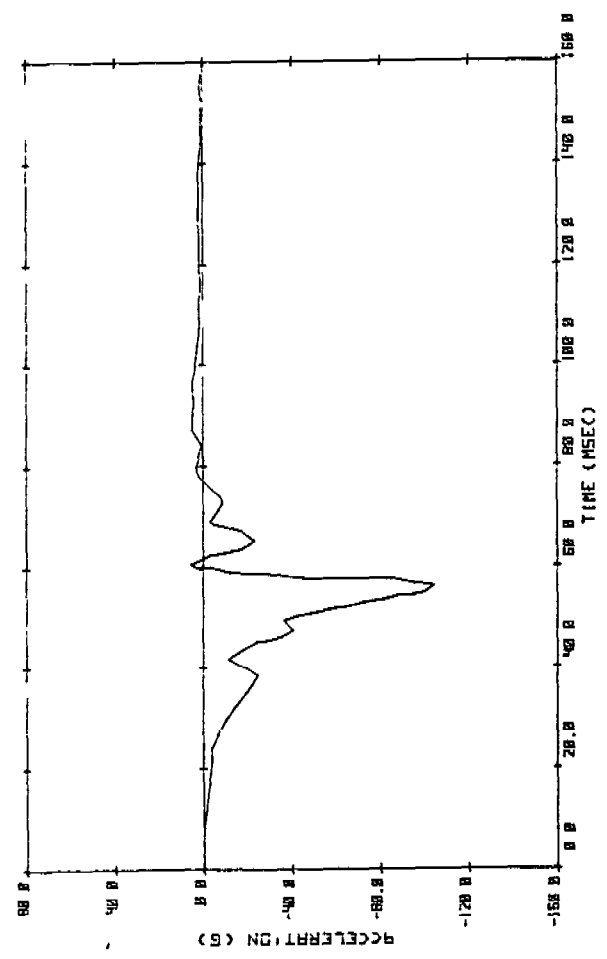
SRL 17-5 TEST #33 (H3BC) - CHEST DEFLECTION



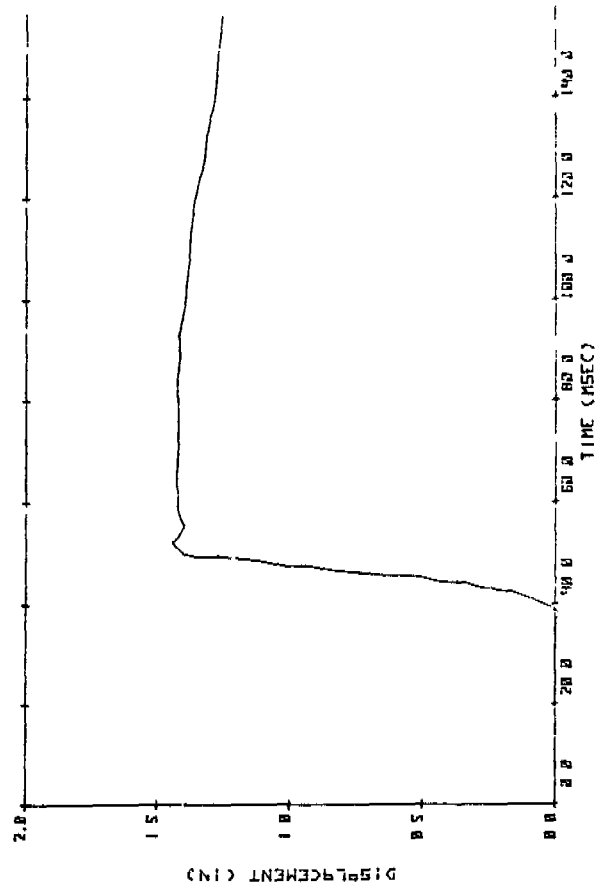
SRL 17-5 TEST #34 - UPPER SPINE



SRL 17-5 TEST #34 - LOWER SPINE



SRL 17-5 TEST #34 - PELVIS



SRL 17-5 TEST #34 - CHEST DEFLECT IN

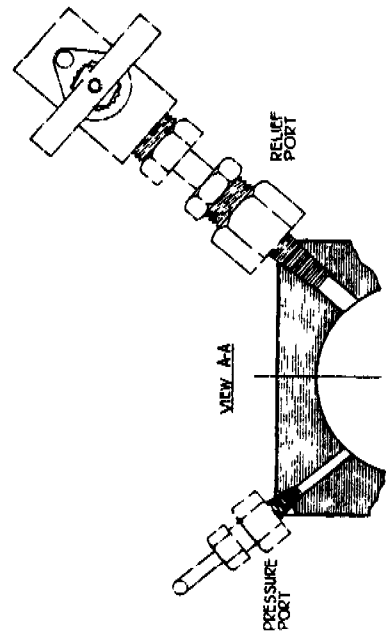
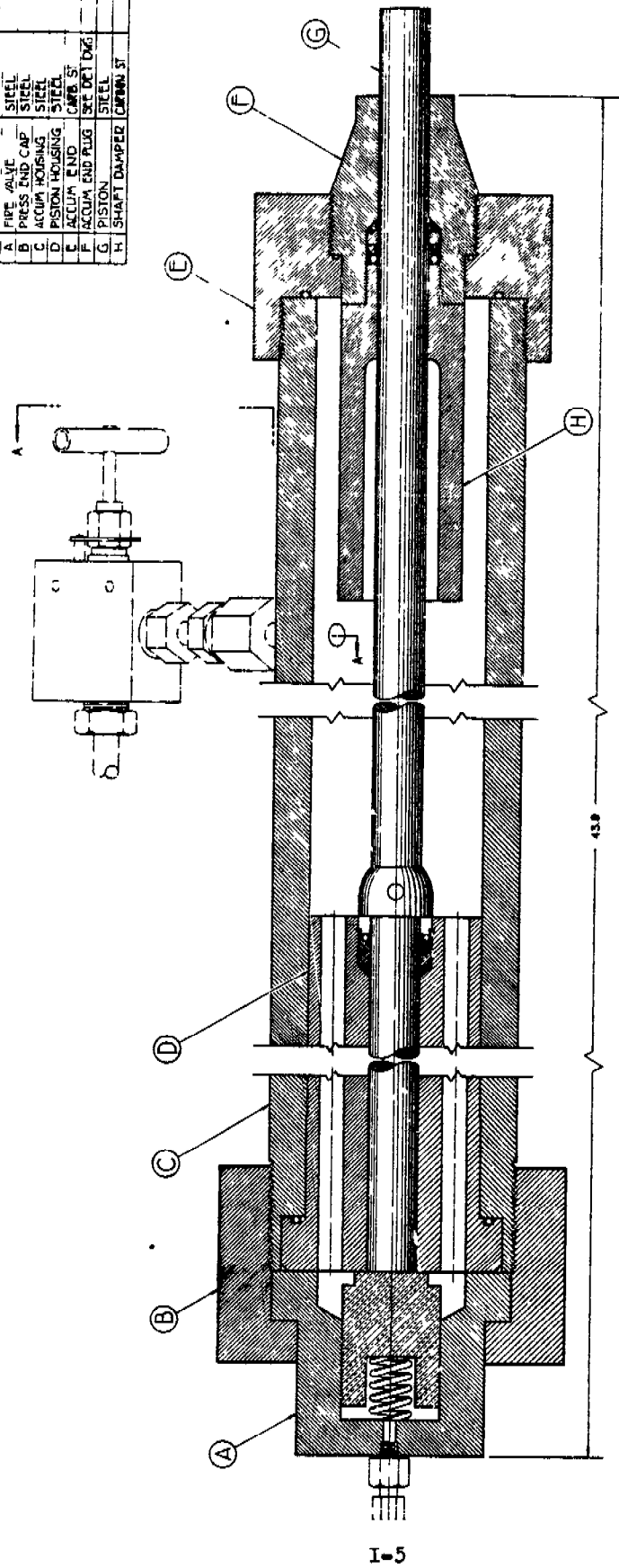
APPENDIX I

Drawing & Description of Fluid Impact Accelerator

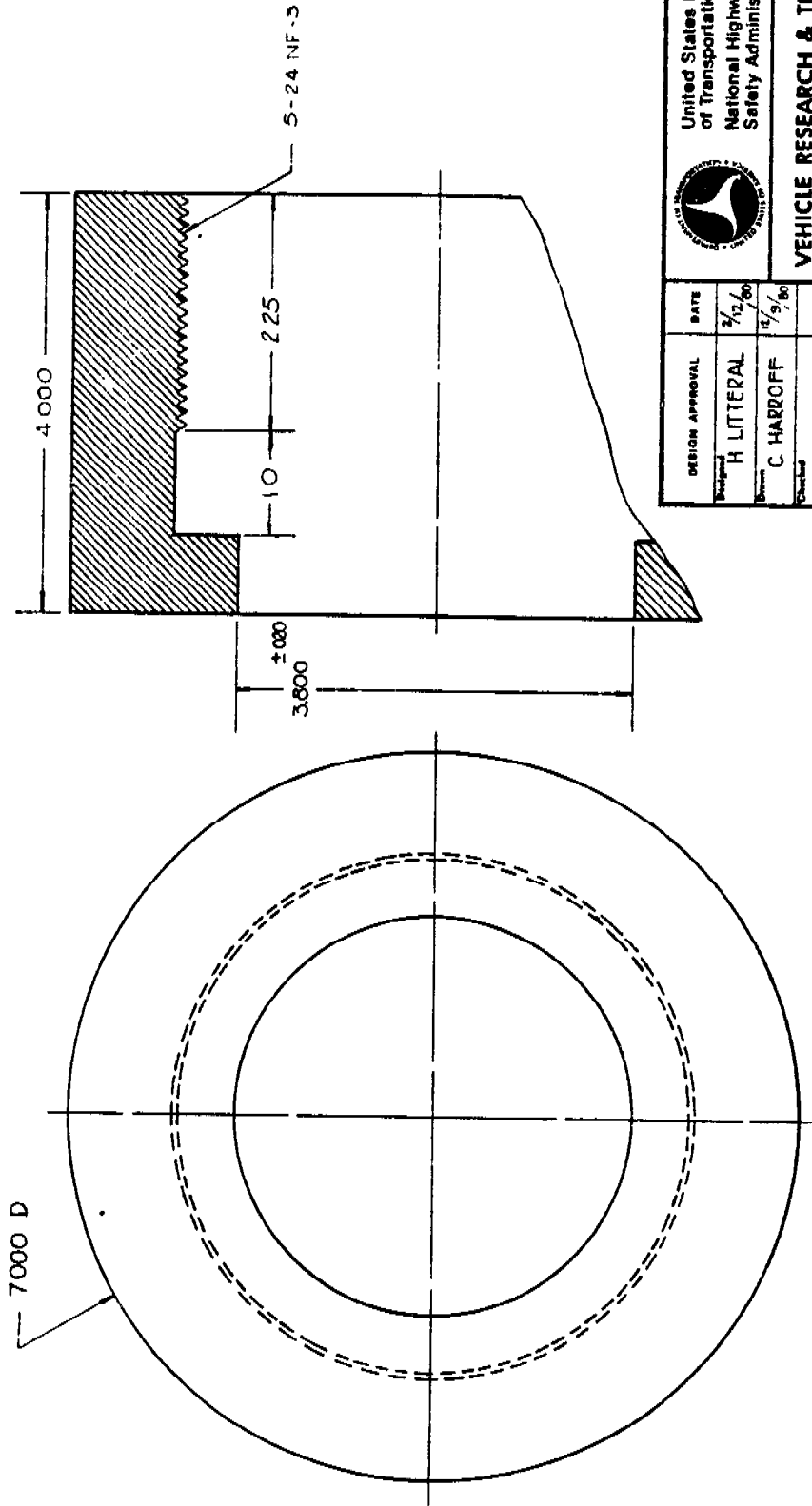
The device has many advantages over more commonly used pneumatic devices. Safety is a key factor. The hydraulic fluid only compresses to levels of less than 10%, so a fracture of the main casing should not throw fragments to the surrounding area. Compact size (5" x 5" x 36") and large capacity are also positive factors for the device.

The design drawings of the device are contained on the following pages.

PART LIST		N I	
NO.	NAME	MATL.	
A	FIRE VALVE	STEEL	
B	PRESS END CAP	STEEL	
C	ACCUM HOUSING	STEEL	
D	PISTON HOUSING	STEEL	
E	ACCUM END PLUG	CRK. ST.	
F	PISTON	STEEL	
G	SHAFT DAMPER	CRKBN. ST.	



DESIGNED BY	DATE	UNITED STATES DEPARTMENT OF COMMERCE
DRWING NO.	REV.	NATIONAL BUREAU OF STANDARDS
PROJECT NO.		SAFETY ADMINISTRATION
VEHICLE RESEARCH & TEST CENTER		
HYDRAULIC IMPACTOR		
JUL 7 1951	7	1-5



I-7



United States Department
of Transportation
National Highway Traffic
Safety Administration

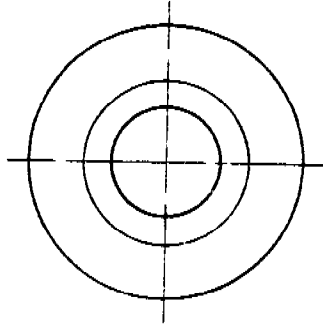
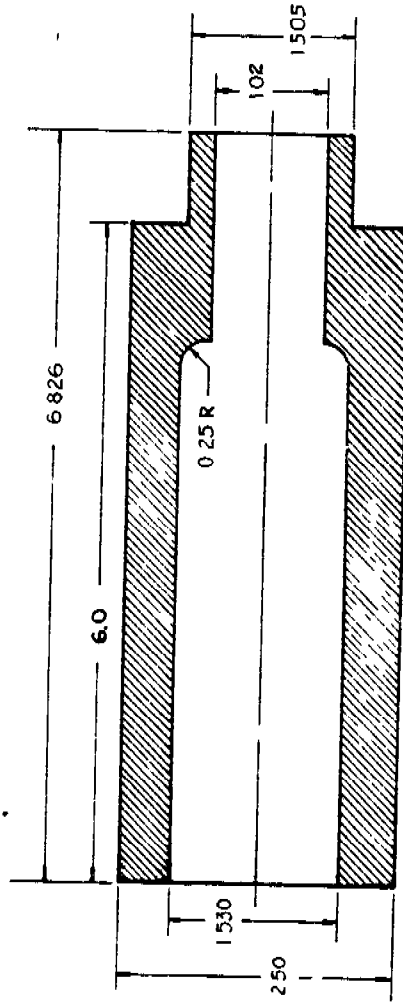
VEHICLE RESEARCH & TEST CENTER
EAST LIBERTY, OHIO 43319

TITLE
PRESSURE END CAP

Scale: Full
Drawing Number: SRL 17-B
File Number:

Sheet 5 of 9

DESIGN APPROVAL	DATE
Designed H LITTERAL	3/12/66
Checked C HARROFF	12/9/66
Approved	
Approved	
Approved	



I-13

MATERIAL CARBON STEEL

		United States Department of Transportation National Highway Traffic Safety Administration	
VEHICLE RESEARCH & TEST CENTER EAST LIBERTY, OHIO 43319		Title SHAFT DAMPER	
DESIGN APPROVAL Checked H LITTERAL By C HARROFF	DATE 7/9/60 11/9/60	Scale FULL	Drawing Number SRL 17-H
Checked Submitted Approved Approved Approved	Date Date Date Date Date	File Number	Sheet 9 of 9

APPENDIX J

Tarriere Drop Tests

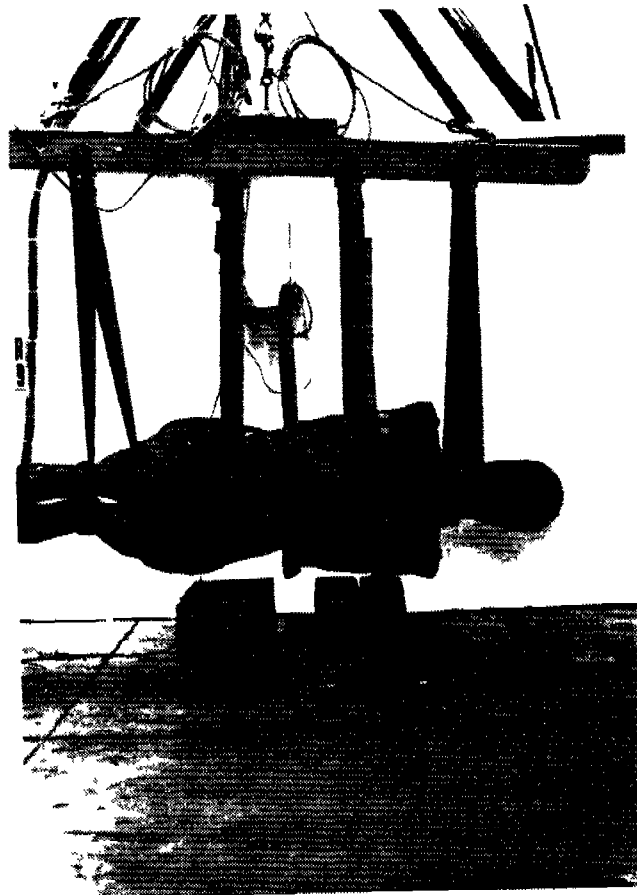


FIGURE J-1
Rigid Drop Test Set-up

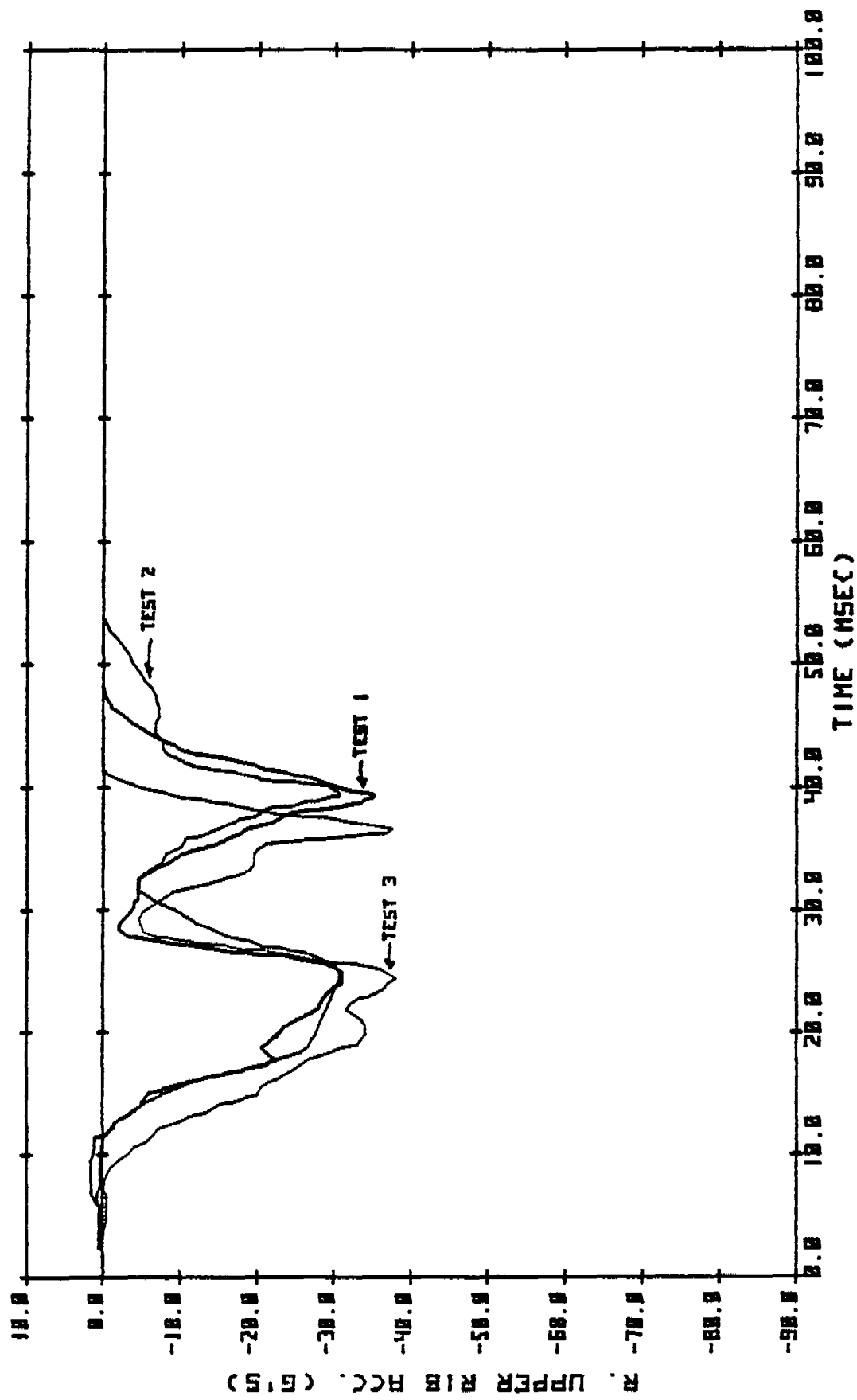


FIGURE J-3 RIGID DROP TESTS (1 METER)

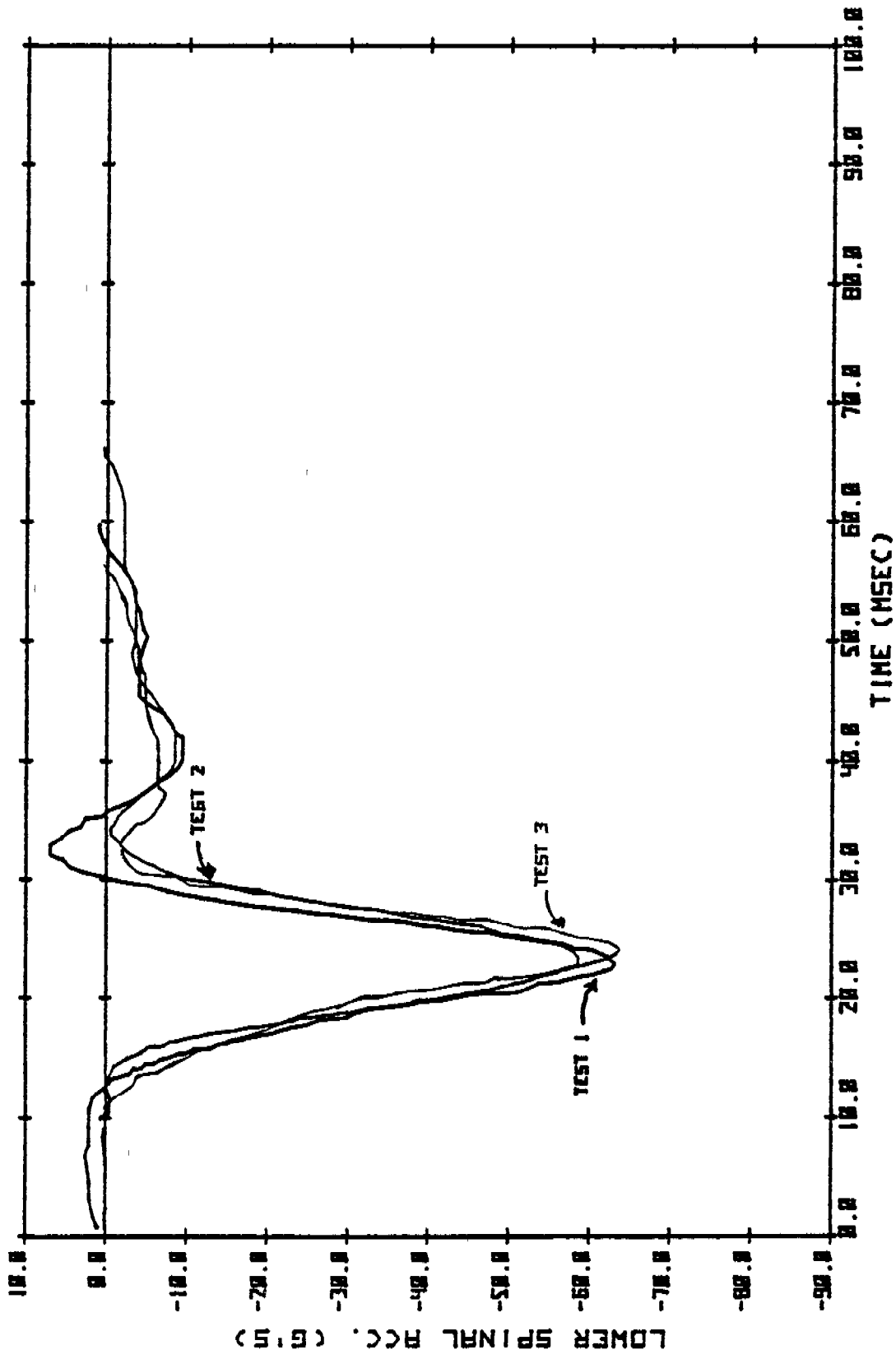


FIGURE J-5 RIGID DROP TESTS (1 METER)

TABLE J-1
 Tarrriere Drop Test Results

Test No.	Test Cond'n	Upper Spine Accel'n (G's)	Lower Spine Accel'n (G's)	Left Upper Rib (G's)	Half Chest Deflection (in)	AIS (HSRI)"Q"	AIS (HSRI)"B"	Rib Fracture (Burgett)
1	1 meter Rigid Drop	22.6	62.8	55.4	1.51	2.32	2.15	US Accel - 3.52 LS Accel - 13.17
2	1 meter Rigid Drop	32.4	58.8	54.9	1.51	2.48	2.45	US Accel - 5.87 LS Accel - 12.21
3	1 meter Rigid Drop	26.5	63.5	55.8	1.71	2.6	2.44	US Accel - 4.46 LS Accel - 13.34
4	2 meter 5 1/2" Padding	31.2	36.9	39.3	1.94	2.07	3.10	US Accel - 5.59 LS Accel - 6.95
5	2 meter 5 1/2" Padding	26.5	30.9	21.7	-	1.89	3.35	US Accel - 4.46 LS Accel - 5.52
6	2 meter 5 1/2" Padding No Skin on Thorax	32.9	32.0	39.8	-	2.07	2.89	US Accel - 5.99 LS Accel - 5.78
7	2 meter 3" Padding	37.6	45.8	52.6	-	2.43	2.95	US Accel - 7.12 LS Accel - 9.09

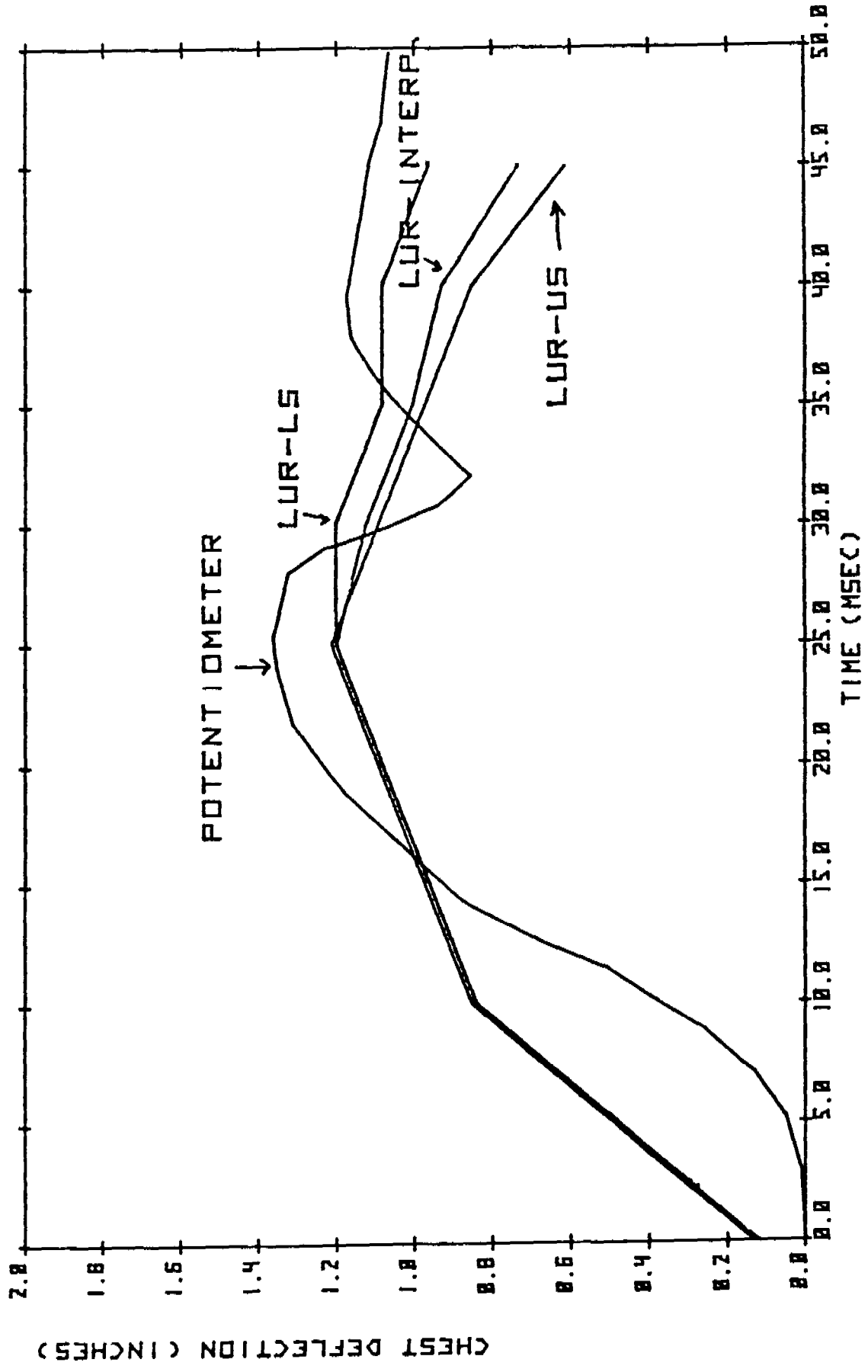


FIGURE J-7 CHEST DEFLECTION (PEND. #2)

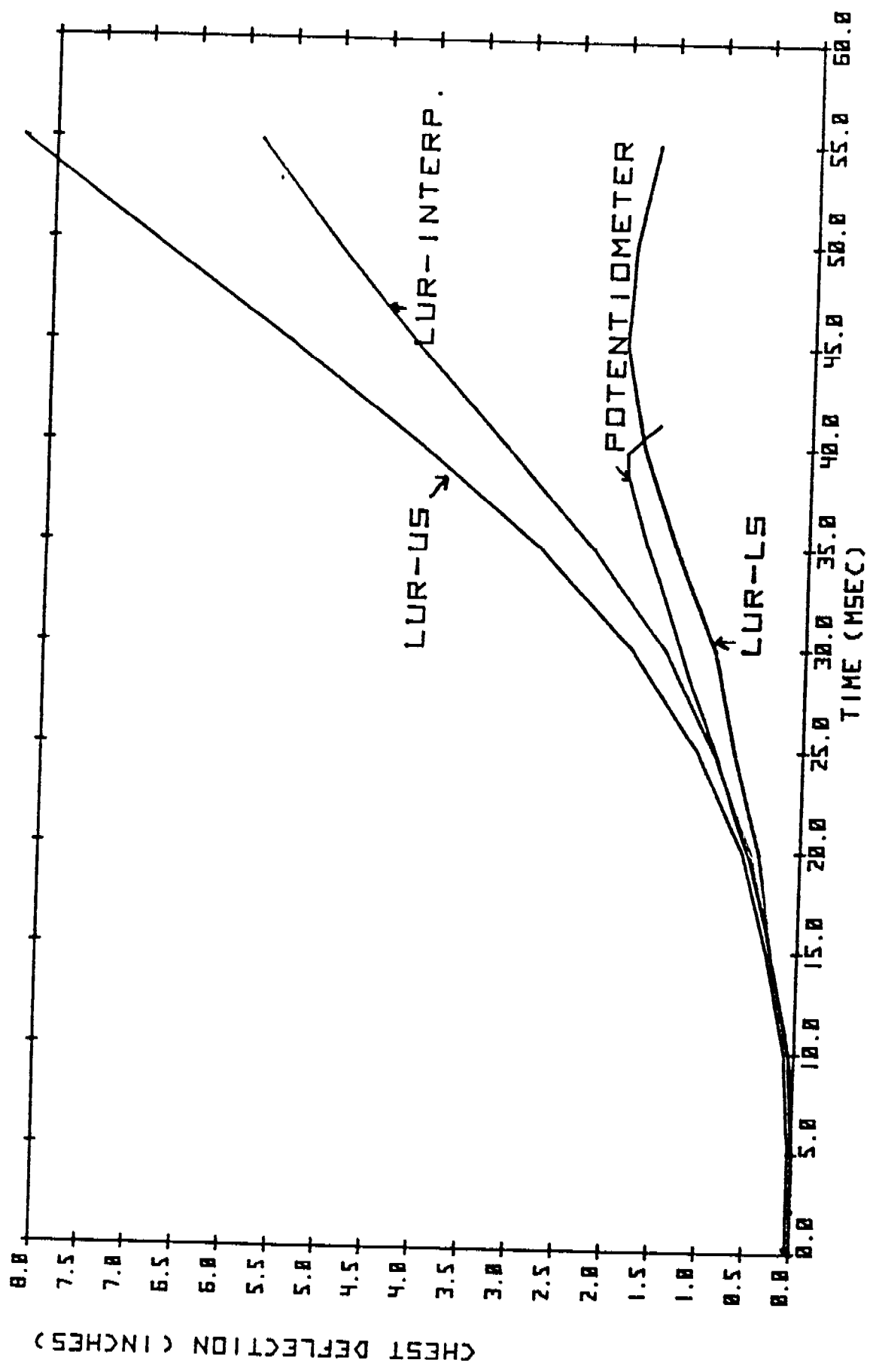


FIGURE J-9 CHEST DEFLECTION TEST #4